

# ORAC 6 User Manual

---

*Release 6.0*

## ORAC: A Molecular Dynamics Program to Simulate Complex Molecular Systems at the atomistic level

### **Authors and copyright holders:**

Piero Procacci

Massimo Marchi

### **Contributors:**

Simone Marsili

Tom Darden

Marc Souaille

Giorgio Federico Signorini

Riccardo Chelli

Emilio Gallicchio

# Contents

<b>1</b>	<b>Atomistic simulations: an introduction</b>	<b>4</b>
1.1	Multiple time steps integration schemes and electrostatic interactions in complex biomolecular systems	4
1.2	Enhanced sampling in atomistic simulations	6
<b>2</b>	<b>Symplectic and Reversible Integrators</b>	<b>9</b>
2.1	Canonical Transformation and Symplectic Conditions	9
2.2	Liouville Formalism: a Tool for Building Symplectic and Reversible Integrators	11
2.3	Potential Subdivision and Multiple Time Steps Integrators for NVE Simulations	12
2.4	Constraints and r-RESPA	15
2.5	Applications	15
<b>3</b>	<b>Multiple Time Steps Algorithms for the Isothermal-Isobaric Ensemble</b>	<b>19</b>
3.1	The Parrinello-Rahman-Nosé Extended Lagrangian	19
3.2	The Parrinello-Rahman-Nosé Hamiltonian and the Equations of Motion	20
3.3	Equivalence of Atomic and Molecular Pressure	23
3.4	Liouvillean Split and Multiple Time Step Algorithm for the <i>NPT</i> Ensemble	25
3.5	Group Scaling and Molecular Scaling	28
3.6	Switching to Other Ensembles	28
<b>4</b>	<b>Multiple Time Steps Algorithms For Large Size Flexible Systems with Strong Electrostatic Interactions</b>	
4.1	Subdivision of the “Bonded” Potential	30
4.2	The smooth particle mesh Ewald method	34
4.3	Subdivision the Non Bonded Potential	37
4.4	Electrostatic Corrections for the Multiple Time Step Simulation	38
<b>5</b>	<b>The Hamiltonian Replica Exchange Method</b>	<b>42</b>
5.1	Temperature REM	42
5.2	Hamiltonian REM	44
5.3	Calculating Ensemble Averages Using Configurations from All Ensembles (MBAR estimator)	47
<b>6</b>	<b>Serial generalized ensemble simulations</b>	<b>49</b>
6.1	Introduction	49
6.2	Fundamentals of serial generalized-ensemble methods	50
6.2.1	SGE simulations in temperature-space (simulated tempering) and its implementation in the ORAC program	
6.2.2	SGE simulations in $\lambda$ -space	52
6.3	The algorithm for optimal weights	52
6.3.1	Tackling free energy estimates	52
6.3.2	Implementation of adaptive free energy estimates in the ORAC program: the BAR-SGE method	54
6.3.3	Free energy evaluation from independent estimates and associated variances	56
<b>7</b>	<b>Metadynamics Simulation: history-dependent algorithms in Non-Boltzmann sampling</b>	<b>57</b>
7.1	Implementation in ORAC	58

<b>8</b>	<b>Steered Molecular Dynamics</b>	<b>61</b>
8.1	The Crooks theorem . . . . .	61
8.2	Determination of the potential of mean force via bidirectional non equilibrium techniques . . . . .	64
8.3	Implementation in ORAC . . . . .	65
<b>9</b>	<b>Alchemical Transformations</b>	<b>68</b>
9.0.1	Production of the MD trajectory with an externally driven alchemical process . . . . .	68
9.0.2	Calculation of the alchemical work . . . . .	72
9.0.3	Fast switching Double Annihilation method . . . . .	76
<b>10</b>	<b>Input to ORAC</b>	<b>77</b>
10.1	General Features . . . . .	77
10.2	Environments, Commands and Sub-commands . . . . .	77
10.2.1	&ANALYSIS . . . . .	79
10.2.2	&INOUT . . . . .	80
10.2.3	&INTEGRATOR . . . . .	86
10.2.4	&META . . . . .	89
10.2.5	&PARAMETERS . . . . .	93
10.2.6	&POTENTIAL . . . . .	99
10.2.7	&PROPERTIES . . . . .	113
10.2.8	&REM . . . . .	120
10.2.9	&RUN . . . . .	124
10.2.10	&SETUP . . . . .	129
10.2.11	&SGE . . . . .	134
10.2.12	&SIMULATION . . . . .	140
10.2.13	&SOLUTE . . . . .	148
10.2.14	&SOLVENT . . . . .	152
10.3	Input to ORAC : Force Field and Topology Files . . . . .	156
10.3.1	Force Field Parameters . . . . .	156
10.3.2	Topology . . . . .	160
<b>11</b>	<b>Compiling and Running ORAC</b>	<b>167</b>
11.1	Compiling the Program . . . . .	167
11.1.1	Serial version . . . . .	167
11.1.2	Parallel version . . . . .	168
11.2	How to set dimensions in ORAC : The config.h file . . . . .	169

## Preface

This manual is for release 6.0 of the program ORAC .<sup>1</sup>

In release 6.0 ORAC has been equipped with a hybrid Open Multi-Processing(OpenMP)/Message Passing Interface (MPI) multilevel parallelism tailored for generalized ensemble (GE) and fast switching double annihilation (FS-DAM) nonequilibrium (NE) technology[1] for evaluating the binding free energy in drug-receptors system on High Performance Computing platforms. The production of the GE or FS-DAM trajectories is handled using a weak scaling parallel approach on the MPI level only, while a strong scaling force domain decomposition scheme is implemented for intranode computations with shared memory access at the OpenMP level. The present manual is organized as follows: The first seven chapters constitute the ORAC theoretical background. Chapter 1) contains general and introductory remarks. Chapter 2) deals with symplectic and reversible integrators and introduces to the Liouvillean formalism, Chapter 3) extends the Liouvillean formalism to the extended Lagrangian methods and Chapter 4) describes how to deal with long range electrostatic interactions and how to combine the SPME method with the multilevel integration of the equations of motion in order to obtain efficient simulation algorithms. Chapter for 5 to 7 have been added in the release 5. Chapter 5) contains an introduction to replica exchange techniques and a description on how such a technique has been implemented in the ORAC program. Chapter 6) deals with metadynamics simulations. Chapter 7) treats steered molecular dynamics simulation and the theory of non equilibrium processes. Chapter 8) is the command reference of the ORAC program. Chapter 9) contains instructions on how to compile and run ORAC in a serial and parallel environment.

---

<sup>1</sup>The ORAC program has been copyrighted (C) by Massimo Marchi and Piero Procacci 1995-2008. This program is free software; you can redistribute it and/or modify it under the terms of the **GNU General Public License** as published by the Free Software Foundation; either version 2 of the License, or (at your option) any later version.

This program is distributed in the hope that it will be useful, but **WITHOUT ANY WARRANTY**; without even the implied warranty of MERCHANTABILITY or FITNESS FOR A PARTICULAR PURPOSE. See the GNU for more details. A general version of the GPL may be requested at: Free Software Foundation, Inc., 59 Temple Place - Suite 330, Boston, MA 02111-1307, USA.

## Contributors to ORAC

Main contributors and license holders:

**Piero Procacci<sup>2</sup>**

Dipartimento di Chimica, Università di Firenze, Via della Lastruccia 3, I-50019 Sesto Fiorentino, Italy  
E-mail: piero.procacci@unifi.it

**Massimo Marchi**

Commissariat à l'Énergie Atomique DSV/IBITEC-S/SB2SM Centre d'Études de Saclay, 91191 Gif sur Yvette Cedex, France  
E-mail: massimo.marchi@cea.fr

Other contributors:

**Simone Marsili**

Dipartimento di Chimica, Università di Firenze, Via della Lastruccia 3, I-50019 Sesto Fiorentino, Italy  
E-mail: simone.marsili@unifi.it  
Role in development: Replica Exchange Method and Metadynamics.

**Giorgio Federico Signorini**

Dipartimento di Chimica, Università di Firenze, Via della Lastruccia 3, I-50019 Sesto Fiorentino, Italy  
E-mail: giorgio.signorini@unifi.it  
Role in development: Tests; tools; package, distribution, and version management.

**Riccardo Chelli**

Dipartimento di Chimica, Università di Firenze, Via della Lastruccia 3, I-50019 Sesto Fiorentino, Italy  
E-mail: riccardo.chelli@unifi.it  
Role in development: Serial Generalized Ensemble simulations.

**Marc Souaille**

Medit SA, 2 rue du Belvédère 91120 Palaiseau, France  
Role in development: linked cell neighbor listing routines.

---

<sup>2</sup>Author to whom comments and bug reports should be sent.

## Literature citation

The current version of ORAC represents a further development of the release published in 1997[2]. The required citations are

P. Procacci, T. A. Darden, E. Paci, M. Marchi

ORAC: a molecular dynamics program to simulate complex molecular systems with realistic electrostatic interactions

J. Comput. Chem. 1997, Volume:18, Pages:1848-1862

S. Marsili, G. F. Signorini, R. Chelli, M. Marchi, P. Procacci

ORAC: a molecular dynamics simulation program to explore free energy surfaces in biomolecular systems at the atomistic level

J. Comput. Chem. 2010, Volume:31, Pages:1106-1116

In general, in addition to the above citations, we recommend citing the original references describing the theoretical methods used when reporting results obtained from ORAC calculations. These references are given in the description of the theory through the user guide as well as in the description of the relevant keywords.

# Chapter 1

## Atomistic simulations: an introduction

In this manual we describe ORAC , a program for the molecular dynamics (MD) simulation of atomistic models of complex molecular systems. In atomistic models the coordinates of all atomic nuclei including hydrogen are treated explicitly and interactions between distant atoms are represented by a pairwise additive dispersive-repulsive potential and a Coulomb contribution due to the atomic charges. Furthermore, nearby atoms interact through special two body, three body and four body functions representing the valence bonds, bending and torsional interaction energies surfaces.

The validity of such an approach as well as the reliability of the various potential models proposed in the literature [3, 4, 5, 6] is not the object of the present book. For reading on this topic, we refer to the extensive and ever growing literature [4, 7, 8, 9]. Here, we want only to stress the general concept that atomistic simulations usually have more predictive power than simplified models, but are also very expensive with respect to the latter from a computational standpoint. This predictive power stems from the fact that, in principle, simulations at the atomistic level do not introduce any uncontrolled approximation besides the obvious assumptions inherent in the definition of the potential model and do not assume any *a priori* knowledge of the system, except of course its chemical composition and topology. Therefore, the failure in predicting specific properties of the system for an atomistic simulation is due only to the inadequacy of the adopted interaction potential. We may define this statement as the *brute force postulate*. In practice, however, in order to reduce the computational burden, severe and essentially uncontrolled approximations such as neglect of long range interactions, suppression of degrees of freedom, dubious thermostating or constant pressure schemes are often undertaken. These approximations, however, lessen the predictive power of the atomistic approach and incorrect results may follow due to the inadequacy in the potential model, baseless approximations or combinations of the two. Also, due to their cost, the predictive capability of atomistic level simulations might often only be on paper, since in practice only a very limited phase space region can be accessed in an affordable way, thereby providing only biased and unreliable statistics for determining the macroscopic and microscopic behavior of the system. It is therefore of paramount importance in atomistic simulations to use computational techniques that do not introduced uncontrolled approximations and at the same time are efficient in the sampling of the complex and rugged conformational space of biological systems. Regarding this last issue, many progresses has been done recently by devising new both non-Boltzmann and Boltzmann techniques for extended sampling of complex systems. Chapter 6 and Chapter 7 are devoted to these aspects of atomistic molecular simulations.

### 1.1 Multiple time steps integration schemes and electrostatic interactions in complex biomolecular systems

As stated above, simulations of complex systems at the atomistic level, unlike simplified models, have the advantage of representing with realistic detail the full flexibility of the system and the potential energy surface according to which the atoms move. Both these physically significant ingredients of the atomistic approach unfortunately pose severe computational problems: on one hand the inclusion of full flexibility

necessarily implies the selection of small step size thereby reducing in a MD simulation the sampling power of the phase space. On the other hand, especially the evaluation of inter-particle long range interactions is an extremely expensive task using conventional methods, its computational cost scaling typically like  $N^2$  (with  $N$  being the number of particles) quickly exceeding any reasonable limit. In this book we shall devote our attention to the methods, within the framework of classical MD simulations, that partially overcome the difficulties related to the presence of flexibility and long range interactions when simulating complex systems at the atomistic level.

Complex systems experience different kind of motions with different time scales: Intramolecular vibrations have a period not exceeding few hundreds of femtoseconds while reorientational motions and conformational changes have much longer time scales ranging from few picoseconds to hundreds of nanoseconds. In the intra-molecular dynamics one may also distinguish between fast stretching involving hydrogen with period smaller than 10 fs, stretching between heavy atoms and bending involving hydrogen with double period or more, slow bending and torsional movements and so on. In a similar manner in the diffusional regime many different contributions can be identified.

In a standard integration of Newtonian equations, all these motions, irrespectively of their time scales, are advanced using *the same* time step whose size is inversely proportional to the frequency of the *fastest* degree of freedom present in the system, therefore on the order of the femtosecond or even less. This constraint on the step size severely limits the accessible simulation time. One common way to alleviate the problem of the small step size is to freeze some supposedly irrelevant and fast degrees of freedom in the system. This procedure relies on the so-called SHAKE algorithm [10, 11, 12] that implements holonomic constraints while advancing the *Cartesian* coordinates. Typically, bonds and/or bending are kept rigid thus removing most of the high frequency density of states and allowing a moderate increase of the step size. The SHAKE procedure changes the input potential and therefore the output density of the states. Freezing degrees of freedom, therefore, requires in principle an *a priori* knowledge of the dynamical behavior of the system. SHAKE is in fact fully justified when the suppressed degrees of freedom do not mix with the “relevant” degrees of freedom. This might be “almost” true for fast stretching involving hydrogen which approximately defines an independent subspace of internal coordinates in almost all complex molecular systems [13] but may turn to be wrong in certain cases even for fast stretching between heavy atoms. In any case the degree of mixing of the various degrees of freedom of a complex system is not known *a priori* and should be on the contrary considered one of the targets of atomistic simulations. The SHAKE algorithm allows only a moderate increase of the step size while introducing, if used without caution, essentially uncontrolled approximations. In other words indiscriminate use of constraints violates the brute-force postulate. A more fruitful approach to the multiple time scale problem is to devise a more efficient “multiple time step” integration of the equation of motion. Multiple time step integration in MD is a relatively old idea [14, 15, 16, 17, 18, 19] but only in recent times, due to the work of Tuckerman, Martyna and Berne and coworkers [20, 21, 22, 23, 24, 25] is finding widespread application. These authors introduced a very effective formalism for devising multilevel integrators based on the symmetric factorization of the Liouvillean classical time propagator. The multiple time step approach allows integration of all degrees of freedom at an affordable computational cost. In the simulation of complex systems, for a well tuned multilevel integrator, the speed up can be sensibly larger than that obtained imposing bond constraints. Besides its efficiency, the multiple time steps approach has the advantage of not introducing any *a priori* assumption that may modify part of the density of the state of the system.

The Liouvillean approach to multiple time steps integrator lends itself to the straightforward, albeit tedious, application to extended Lagrangian systems for the simulation in the canonical and isobaric ensembles: once the equations of motions are known, the Liouvillean and hence the scheme, is *de facto* available. Many efficient multilevel schemes for constant pressure or constant temperature simulation are available in the literature [26, 25, 27].

As already outlined, long range interactions are the other stumbling block in the atomistic MD simulation of complex systems. The problem is particularly acute in biopolymers where the presence of distributed net charges makes the local potential oscillate wildly while summing, e.g. onto spherical non neutral shells. The conditionally convergent nature of the electrostatic energy series for a periodic system such as the MD box in periodic boundary conditions (PBC) makes any straightforward truncation method essentially unreliable [28, 12, 29].

The reaction field [30, 31] is in principle a physically appealing method that correctly accounts for long range effects and requires only limited computational effort. The technique assumes explicit electrostatic



interactions within a cutoff sphere surrounded by a dielectric medium which exerts back in the sphere a “polarization” or reaction field. The dielectric medium has a dielectric constant that matches that of the inner sphere. The technique has been proved to give results identical to those obtained with the *exact* Ewald method in Monte Carlo simulation of dipolar spherocylinders where the dielectric constant that enters in the reaction field is updated periodically according to the value found in the sphere. The reaction field method does however suffer of two major disadvantages that strongly limits its use in MD simulations of complex systems at the atomistic level: during time integration the system may experience instabilities related to the circulating dielectric constant of the reaction field and to the jumps into the dielectric of molecules in the sphere with explicit interactions. The other problem, maybe more serious, is that again the method requires an *a priori* knowledge of the system, that is the dielectric constant. In pure phases this might not be a great problem but in inhomogeneous systems such as solvated protein, the knowledge of the dielectric constant might be not easily available. Even with the circulating technique, an initial unreliable guess of the unknown dielectric constant, can strongly affect the dielectric behavior of the system and in turn its dynamical and structural state.

The electrostatic series can be computed in principle *exactly* using the Ewald re-summation technique [32, 33]. The Ewald method rewrites the electrostatic sum for the periodic system in terms of two absolutely convergent series, one in the direct lattice and the other in reciprocal lattice. This method, in its standard implementation, is extremely CPU demanding and scales like  $N^2$  with  $N$  being the number of charges with the unfortunate consequence that even moderately large size simulations of inhomogeneous biological systems are not within its reach. The rigorous Ewald method, which does not suffers of none of the inconveniences experienced by the reaction field approach, has however regained resurgent interest very recently after publication by Darden, York and Pedersen [34] of the Particle Mesh technique and later on by Essmann, Darden *et al.* [35] of the variant termed Smooth Particle Mesh Ewald (SPME). SPME is based on older idea of Hockney [36] and is essentially an interpolation technique with a charge smearing onto a regular grid and evaluation via fast Fourier Transform (FFT) of the interpolated reciprocal lattice energy sums. The performances of this techniques, both in accuracy and efficiency, are astonishing. Most important, the computational cost scales like  $N \log N$ , that is essentially *linearly* for any practical application. Other algorithm like the Fast Multipole Method (FMM) [37, 38, 39, 40] scales exactly like  $N$ , even better than SPME. However FMM has a very large prefactor and the break even point with SPME is on the order of several hundred thousand of particles, that is, as up to now, beyond any reasonable practical limit.

The combination of the multiple time step algorithm and of the SPME [13] makes the simulation of large size complex molecular systems such as biopolymers, polar mesogenic molecules, organic molecules in solution etc., extremely efficient and therefore affordable even for long time spans. Further, this technique do not involve any uncontrolled approximation<sup>1</sup> and is perfectly consistent with standard PBC.

## 1.2 Enhanced sampling in atomistic simulations

Standard *equilibrium* simulations of complex biosystems are usually done on a single solvated biomolecule in PBC due to computational bounds.<sup>2</sup>

In these conditions the only mean to measure, e.g., the free energy differences between two given protein conformations, is to record the number of times the protein molecule in the MD cell is observed in each of the two conformations. Swaps between these conformers can take, in (time) average, as long as 0.1-1 microseconds [41] even for small proteins. One then needs to do extremely long equilibrium simulations in order to have a sufficient number of swaps between conformational states so as to determine with good accuracy a stationary (equilibrium) ratio of the conformational probability and hence the free energy

<sup>1</sup>Of course SPME *is* itself an approximation of the true electrostatic energy. This approximation is however totally under control since the energy can be determined to any given accuracy and the effect of finite accuracy can be easily controlled on any computed property of the system. The approximation *is not* uncontrolled.

<sup>2</sup>The explicit (i.e. atomistic) solvent introduced in the MD cell is in fact the minimum amount required such that the distance between any two portion of *different* solute replicas is sufficiently large so as to assume negligible interprotein interactions. Also the shape of the MD cell is usually chosen so as to minimize the amount of explicit solvent whose sole role, at an extremely demanding computational cost, is to provide the correct dielectric medium for the biomolecule (including microsolvation effects). For example, globular (i.e. quasi-spherical) proteins are usually simulated in a dodecahedral box. Such a system, single solvated protein in PBC, is thus representative of *dilute* solution of biomolecules since the solute molecules in the periodic systems can never come close to each other, thereby *interacting*

difference. To give just a faint idea of the computational cost involved, for the simple system of decaalanine *in vacuo*, 1.0 microseconds of *serial* simulation takes about 10 days on 2.5 MH processor. Due to this computational bounds, standard molecular dynamics simulation of even small biological systems are in general not ergodic in the accessible simulation time. Typically, the system remains trapped during the whole simulation time span in a local minimum and the rare event of escaping the trap surmounting a free energy barrier never happens.

In order to overcome such severe sampling problem, many recent MD techniques has been devised. The Replica Exchange Method (REM)[42, 43, 44, 45] provides an elegant and simple solution to quasi-ergodic sampling. In REM, several independent trajectories, called replicas, are simultaneously generated in different thermodynamic conditions. The production of these simultaneous trajectories usually occurs on an array of parallel processors. The thermodynamics conditions of these replicas are chosen so as to span homogeneously the thermodynamic space from the ensemble of interest to a different ensemble with enhanced transition rates, where the sampling is ergodic. During the simulation, neighbouring replicas are allowed to exchange their configurations, subject to specific acceptance criteria. In this fashion, a trajectory is no longer bound to an unique given equilibrium ensemble but can randomly walk in a thermodynamic space of different equilibrium conditions, visiting ensembles where an ergodic sampling is possible, and then going back to the quasi-ergodic ensemble of interest. Therefore, REM is an algorithm which employs an extended ensemble formalism in order to overcome slow relaxation. The gain in sampling efficiency with respect to a series of uncoupled parallel trajectories comes from the exchange of information between trajectories, and the replica exchange process is the tool by which “information” (e.g. a particular configuration) is carried, for example, from an high to a low temperature. The REM algorithm can be used in principle without prior knowledge of the “important” reaction coordinates of the system, i.e., in the case of biological systems, those that defines the accessible conformational space in the target thermodynamics conditions. The REM algorithm is described in detail in Chapter 5.

A class of simulation algorithms closely related to REM are the so-called *serial generalized-ensemble* (SGE) methods[46]. The basic difference between SGE methods and REM is that in the former no pairs of replicas are necessary to make a trajectory in temperature space and more generally in the generalized ensemble space. In SGE methods only one replica can undergo ensemble transitions which are realized on the basis of a Monte Carlo like criterion. The most known example of SGE algorithm is the simulated tempering technique[44, 47], where weighted sampling is used to produce a random walk in temperature space. An important limitation of SGE approaches is that an evaluation of free energy differences between ensembles is needed as input to ensure equal visitation of the ensembles, and eventually a faster convergence of structural properties[48]. REM was just developed to eliminate the need to know a priori such free energy differences. On the other side, several studies[48, 49, 50] have reported that SGE in general and simulated tempering in particular consistently gives a higher rate of delivering the system between high temperature states and low temperature states, as well as a higher rate of transversing the potential energy space. Moreover SGE methods are well-suited to distributed computing environments because synchronization and communication between replicas/processors can be avoided. The potential of mean force[51, 52] along a chosen collective coordinate can be computed a posteriori in REM and SGE simulations using multiple-histogram reweighting techniques[53, 54]. The potential of mean force can also be determined by performing SGE and REM simulations directly in the space of the collective coordinate[55]. In the ORAC program we have implemented SGE simulations, either in a simulated-tempering like fashion or in the space of bond, bending, and torsion coordinates. These simulations exploit the adaptive method to calculate weight factors (*i.e.* free energies) proposed in Ref. [56]. The method is described in Chapter 6.

The *a priori* identification of the unknown coordinates, along with their underlying free energy surface, are actually one of the outputs of the REM and SGE approaches. However, once these important coordinates are known, one can use less expensive techniques to study the associated *essential* free energy surface. Canonical reweighting or Umbrella Sampling methods[57], for example, modify (bias) the interaction Hamiltonian of the system in such a way to facilitate barrier crossing between conformational basins. The canonical average of the unperturbed systems are then reconstructed by appropriately reweighting the biased averaged.

Quasi-equilibrium techniques[58, 59, 60, 61] builds such biasing potential that favours barrier crossing by periodically adding a small perturbation to the system Hamiltonian so as to progressively flatten the free energy surfaces along selected reaction coordinates. For example, in the so-called standard “metadynamics” simulation method[58], a history-dependent potential, made of accumulated Gaussian functions deposited

continuously at the instantaneous values of the given reaction coordinates, is imposed to the system. The history-dependent potential disfavors configurations in the space of the reaction coordinates that have already been visited, and it has been shown, by appropriately adjusting system dependent parameters, to numerically converge to the inverse of the free energy surface.[62] In the present version of ORAC the metadynamics technique has been implemented in the parallel version whereby multiple metadynamics simulation (walkers) are run in parallel cooperatively building a common history dependent potential which is passed among all processes. The history dependent potential is generally defined over a multidimensional domain involving several reaction coordinates. Metadynamics can be used, e.g., to identify the minimum free energy path between two metastable protein states defining the reactants and products of an elementary chemical reaction. Quasi-equilibrium techniques in biological systems converge rather slowly since the convergence rate depends crucially on the inherent slow diffusion along the conformational coordinates. So even if the potential is relatively flattened, the diffusion along a nearly free reaction coordinates can still be slow due to the friction of the orthogonal coordinates. The metadynamics algorithm is described in detail in Chapter 6.3.3

Non equilibrium techniques[63, 64, 65, 66] uses an additional driving potential acting on an appropriate reaction coordinates to *fast* steer the system from a given equilibrium initial state to a given final state, and *viceversa* producing a series of forward and reverse non equilibrium trajectories. The driven coordinate is strictly mono-dimensional but can be defined as a trajectory in a multidimensional reaction coordinate space. The free energy differences between the initial and final states (the reactants and the products) is connected, through the Crooks fluctuation theorem[64], to the ratio of distribution functions of the work spent in these trajectories. Free energy reconstruction, using non equilibrium steered molecular dynamics, of the potential of mean force[67] along one arbitrary reaction coordinate is described in detail in Chapter 7.1.

## Chapter 2

# Symplectic and Reversible Integrators

In an Hamiltonian problem, the symplectic condition and microscopic reversibility are inherent properties of the true time trajectories which, in turn, are the exact solution of Hamilton's equation. A stepwise integration defines a  $t$ -flow mapping which may or may not retain these properties. Non symplectic and/or non reversible integrators are generally believed [68, 69, 70, 71] to be less stable in the long-time integration of Hamiltonian systems. In this section we shall illustrate the concept of reversible and symplectic mapping in relation to the numerical integration of the equations of motion.

### 2.1 Canonical Transformation and Symplectic Conditions

Given a system with  $n$  generalized coordinates  $q$ ,  $n$  conjugated momenta  $p$  and Hamiltonian  $H$ , the corresponding Hamilton's equations of motion are

$$\begin{aligned}\dot{q}_i &= \frac{\partial H}{\partial p_i} \\ \dot{p}_i &= -\frac{\partial H}{\partial q_i} \quad i = 1, 2, \dots, n\end{aligned}\tag{2.1}$$

These equations can be written in a more compact form by defining a column matrix with  $2n$  elements such that

$$\mathbf{x} = \begin{pmatrix} \mathbf{q} \\ \mathbf{p} \end{pmatrix}.\tag{2.2}$$

In this notation the Hamilton's equations (2.1) can be compactly written as

$$\dot{\mathbf{x}} = \mathbf{J} \frac{\partial H}{\partial \mathbf{x}} \quad \mathbf{J} = \begin{pmatrix} \mathbf{0} & \mathbf{1} \\ -\mathbf{1} & \mathbf{0} \end{pmatrix}\tag{2.3}$$

where  $\mathbf{J}$  is a  $2n \times 2n$  matrix,  $\mathbf{1}$  is an  $n \times n$  identity matrix and  $\mathbf{0}$  is a  $n \times n$  matrix of zeroes. Eq. (2.3) is the so-called symplectic notation for the Hamilton's equations.<sup>1</sup>

Using the same notation we now may define a transformation of variables from  $\mathbf{x} \equiv \{q, p\}$  to  $\mathbf{y} \equiv \{Q, P\}$  as

$$\mathbf{y} = \mathbf{y}(\mathbf{x})\tag{2.4}$$

For a restricted canonical transformation [72, 73] we know that the function  $H(\mathbf{x})$  expressed in the new coordinates  $\mathbf{y}$  serves as the Hamiltonian function for the new coordinates  $\mathbf{y}$ , that is the Hamilton's equations

---

<sup>1</sup>Symplectic means "intertwined" in Greek and refers to the interlaced role of coordinate and momenta in Hamilton's equations.

of motion in the  $\mathbf{y}$  basis have exactly the same form as in Eq. (2.3):

$$\dot{\mathbf{y}} = \mathbf{J} \frac{\partial H}{\partial \mathbf{y}} \quad (2.5)$$

If we now take the time derivative of Eq. (2.4), use the chain rule relating  $\mathbf{x}$  and  $\mathbf{y}$  derivatives and use Eq. (2.5), we arrive at

$$\dot{\mathbf{y}} = \mathbf{M} \mathbf{J} \mathbf{M}^t \frac{\partial H}{\partial \mathbf{y}}. \quad (2.6)$$

Here  $\mathbf{M}$  is the Jacobian matrix with elements

$$M_{ij} = \partial y_i / \partial x_j, \quad (2.7)$$

and  $\mathbf{M}^t$  is its transpose. By comparing Eqs. (2.5) and (2.6), we arrive at the conclusion that a transformation is canonical if, and only if, the Jacobian matrix  $\mathbf{M}$  of the transformation Eq. 2.4 satisfies the condition

$$\mathbf{M} \mathbf{J} \mathbf{M}^t = \mathbf{J}. \quad (2.8)$$

Eq. (2.8) is known as the symplectic condition for canonical transformations and represents an effective tool to test whether a generic transformation is canonical. Canonical transformations play a key role in Hamiltonian dynamics. For example, consider transformation  $\phi$

$$\mathbf{z}(t) = \phi(t, \mathbf{z}(0)) \quad (2.9)$$

where  $\{p_0 q_0\} \equiv \mathbf{z}(0)$  and  $\{P, Q\} \equiv \mathbf{z}(t)$ , i.e. one writes the coordinates and momenta at time  $t$ , obtained from the solution of the Hamiltonian equation of motion, *as a function* of the coordinates and momenta at the initial time zero. This transformation, which depends on the scalar parameter  $t$ , is trivially canonical since both  $\{p_0 q_0\}$  and  $\{P, Q\}$  satisfies the Hamilton equations of motion. Hence the above transformation defines the  $t$ -flow mapping of the systems and, being canonical, its Jacobian matrix obeys the symplectic condition (2.8). An important consequence of the symplectic condition, is the invariance under canonical (or symplectic) transformations of many properties of the phase space. These invariant properties are known as ‘‘Poincare invariants’’ or canonical invariants. For example transformations or  $t$ -flow’s mapping obeying Eq. (2.8) preserve the phase space volume. This is easy to see, since the infinitesimal volume elements in the  $\mathbf{y}$  and  $\mathbf{x}$  bases are related by

$$d\mathbf{y} = |\det \mathbf{M}| d\mathbf{x} \quad (2.10)$$

where  $|\det \mathbf{M}|$  is the Jacobian of the transformation. Taking the determinant of the symplectic condition Eq. (2.8) we see that  $|\det \mathbf{M}| = 1$  and therefore

$$d\mathbf{y} = d\mathbf{x}. \quad (2.11)$$

For a canonical or symplectic  $t$ -flow mapping this means that the phase total space volume is invariant and therefore Liouville theorem is automatically satisfied.

A stepwise numerical integration scheme defines a  $\Delta t$ -flow mapping or equivalently a coordinates transformation, that is

$$\begin{aligned} Q(\Delta t) &= Q(q(0), p(0), \Delta t) \\ P(\Delta t) &= P(q(0), p(0), \Delta t) \end{aligned} \quad \mathbf{y}(\Delta t) = \mathbf{y}(\mathbf{x}(0)). \quad (2.12)$$

We have seen that exact solution of the Hamilton equations has  $t$ -flow mapping satisfying the symplectic conditions (2.8). If the Jacobian matrix of the transformation (2.12) satisfies the symplectic condition then the integrator is termed to be symplectic. The resulting integrator, therefore, exhibits properties identical to those of the exact solution, in particular it satisfies Eq. (2.11). Symplectic algorithms have also been proved to be robust, i.e resistant to time step increase, and generate stable long time trajectory, i.e. they do not show drifts of the total energy. Popular MD algorithms like Verlet, leap frog and velocity Verlet are all symplectic and their robustness is now understood to be due in part to this property. [70, 20, 23, 71]

## 2.2 Liouville Formalism: a Tool for Building Symplectic and Reversible Integrators

In the previous paragraphs we have seen that it is highly beneficial for an integrator to be symplectic. We may now wonder if there exists a general way for obtaining symplectic and possibly, reversible integrators from “first principles”. To this end, we start by noting that for any property which depends on time implicitly through  $p, q \equiv \mathbf{x}$  we have

$$\begin{aligned} \frac{dA(p, q)}{dt} &= \sum_{q, p} \left( \dot{q} \frac{\partial A}{\partial q} + \dot{p} \frac{\partial A}{\partial p} \right) = \sum_{q, p} \left( \frac{\partial H}{\partial p} \frac{\partial A}{\partial q} - \frac{\partial H}{\partial q} \frac{\partial A}{\partial p} \right) \\ &= iLA \end{aligned} \quad (2.13)$$

where the sum is extended to all  $n$  degrees of freedom in the system.  $L$  is the Liouvillean operator defined by

$$iL \equiv \sum_{q, p} \left( \dot{q} \frac{\partial}{\partial q} + \dot{p} \frac{\partial}{\partial p} \right) = \sum_{q, p} \left( \frac{\partial H}{\partial p} \frac{\partial}{\partial q} - \frac{\partial H}{\partial q} \frac{\partial}{\partial p} \right). \quad (2.14)$$

Eq. (2.13) can be integrated to yield

$$A(t) = e^{iLt} A(0). \quad (2.15)$$

If  $A$  is the state vector itself we can use Eq. (2.15) to integrate Hamilton’s equations:

$$\begin{bmatrix} q(t) \\ p(t) \end{bmatrix} = e^{iLt} \begin{bmatrix} q(0) \\ p(0) \end{bmatrix}. \quad (2.16)$$

The above equation is a formal solution of Hamilton’s equations of motion. The exponential operator  $e^{iLt}$  times the state vector defines the  $t$ -flow of the Hamiltonian system which brings the system phase space point from the initial state  $q_0, p_0$  to the state  $p(t), q(t)$  at a later time  $t$ . We already know that this transformation obeys Eq. (2.8). We may also note that the adjoint of the exponential operator corresponds to the inverse, that is  $e^{iLt}$  is unitary. This implies that the trajectory is exactly time reversible. In order to build our integrator, we now define the *discrete time propagator*  $e^{iL\Delta t}$  as

$$e^{iLt} = \left[ e^{iLt/n} \right]^n; \quad \Delta t = t/n \quad (2.17)$$

$$e^{iL\Delta t} = e^{\sum_{q, p} (\dot{q} \frac{\partial}{\partial q} + \dot{p} \frac{\partial}{\partial p}) \Delta t}. \quad (2.18)$$

In principle, to evaluate the action of  $e^{iL\Delta t}$  on the state vector  $p, q$  one should know the derivatives of all orders of the potential  $V$ . This can be easily seen by Taylor expanding the discrete time propagator  $e^{iL\Delta t}$  and noting that the operator  $\dot{q} \partial / \partial q$  does not commute with  $-\partial V / \partial q (\partial / \partial p)$  when the coordinates and momenta refer to *same* degree of freedom. We seek therefore approximate expressions of the discrete time propagator that retain both the symplectic and the reversibility property. For any two linear operators  $A, B$  the Trotter formula [74] holds:

$$e^{(A+B)t} = \lim_{n \rightarrow \infty} (e^{At/n} e^{Bt/n})^n \quad (2.19)$$

We recognize that the propagator Eq. (2.18) has the same structure as the left hand side of Eq. (2.19); hence, using Eq. (2.19), we may write for  $\Delta t$  sufficiently small

$$e^{iL\Delta t} = e^{(\dot{q} \frac{\partial}{\partial q} + \dot{p} \frac{\partial}{\partial p}) \Delta t} \simeq e^{\dot{q} \frac{\partial}{\partial q} \Delta t} e^{\dot{p} \frac{\partial}{\partial p} \Delta t} + O(\Delta t^2) \quad (2.20)$$

Where, for simplicity of discussion, we have omitted the sum over  $q$  and  $p$  in the exponential. Eq. (2.20) is exact in the limit that  $\Delta t \rightarrow 0$  and is first order for finite step size. Using Eq. (2.8) it is easy to show that the  $t$ -flow defined in Eq. (2.20) is symplectic, being the product of two successive symplectic transformations. Unfortunately, the propagator Eq. (2.20) is not unitary and therefore the corresponding algorithm is not

time reversible. Again the non unitarity is due to the fact that the two factorized exponential operators are non commuting. We can overcome this problem by halving the time step and using the approximant:

$$e^{(A+B)t} \simeq e^{At/2} e^{Bt/2} e^{Bt/2} e^{At/2} = e^{At/2} e^{Bt} e^{At/2}. \quad (2.21)$$

The resulting propagator is clearly unitary, therefore time reversible, and is also correct to the second order [75]. Thus, requiring that the product of the exponential operator be unitary, automatically leads to more accurate approximations of the true discrete time propagator [76, 75]. Applying the same argument to the propagator (2.18) we have

$$e^{iL\Delta t} = e^{(\dot{q}\frac{\partial}{\partial q} + \dot{p}\frac{\partial}{\partial p})\Delta t} \simeq e^{\dot{p}\frac{\partial}{\partial p}\Delta t/2} e^{\dot{q}\frac{\partial}{\partial q}\Delta t} e^{\dot{p}\frac{\partial}{\partial p}\Delta t/2} + O(\Delta t^3). \quad (2.22)$$

The action of an exponential operator  $e^{(a\partial/\partial x)}$  on a generic function  $f(x)$  trivially corresponds to the Taylor expansion of  $f(x)$  around the point  $x$  at the point  $x + a$ , that is

$$e^{a\partial/\partial x} f(x) = f(x + a). \quad (2.23)$$

Using Eq. (2.23), the time reversible and symplectic integration algorithm can now be derived by acting with our Hermitian operator Eq. (2.22) onto the state vector at  $t = 0$  to produce updated coordinate and momenta at a later time  $\Delta t$ . The resulting algorithm is completely equivalent to the well known velocity Verlet:

$$\begin{aligned} p(\Delta t/2) &= p(0) + F(0)\Delta t/2 \\ q(\Delta t) &= q(0) + \left(\frac{p(\Delta t/2)}{m}\right)\Delta t \\ p(\Delta t) &= p(\Delta t/2) + F(\Delta t)\Delta t/2. \end{aligned} \quad (2.24)$$

We first notice that each of the three transformations obeys the symplectic condition Eq. (2.8) and has a Jacobian determinant equal to one. The product of the three transformation is also symplectic and, thus, phase volume preserving. Finally, since the discrete time propagator (2.22) is unitary, the algorithm is time reversible.

One may wonder what it is obtained if the operators  $\dot{q}\partial/\partial q$  and  $-\partial V/\partial q(\partial/\partial p)$  are exchanged in the definition of the discrete time propagator (2.22). If we do so, the new integrator is

$$\begin{aligned} q(\Delta t/2) &= q(0) + \frac{p(0)}{m}\Delta t/2 \\ p(\Delta t) &= p(0) + F[q(\Delta t/2)]\Delta t \\ q(\Delta t) &= q(\Delta t/2) + \frac{p(\Delta t)}{m}\Delta t/2. \end{aligned} \quad (2.25)$$

This algorithm has been proved to be equivalent to the so-called Leap-frog algorithm [77]. Tuckerman *et al.* [20] called this algorithm *position Verlet* which is certainly a more appropriate name in the light of the exchanged role of positions and velocities with respect to the velocity Verlet. Also, Eq. (2.21) clearly shows that the position Verlet is essentially identical to the Velocity Verlet. A shift of a time origin by  $\Delta t/2$  of either Eq. (2.25) or Eq. (2.24) would actually make both integrator perfectly equivalent. However, as pointed out in Ref. [21], half time steps are not formally defined, being the right hand side of Eq. (2.21) an approximation of the discrete time propagator for the *full* step  $\Delta t$ . Velocity Verlet and Position Verlet, therefore, do not generate numerically identical trajectories although of course the trajectories are similar.

We conclude this section by saying that is indeed noticeable that using the same Liouville formalism different long-time known schemes can be derived. The Liouville approach represent therefore a unifying treatment for understanding the properties and relationships between stepwise integrators.

## 2.3 Potential Subdivision and Multiple Time Steps Integrators for NVE Simulations

The ideas developed in the preceding sections can be used to build multiple time step integrators. Multiple time step integration is based on the concept of reference system. Let us now assume that the system



potential  $V$  be subdivided in  $n$  terms such that

$$V = V_0 + V_1 + \dots + V_n. \quad (2.26)$$

Additionally, we suppose that the corresponding average values of the square modulus of the forces  $F_k = |\partial V_k / \partial \mathbf{x}|$  and of their time derivatives  $\dot{F}_k = |d/dt(\partial V_k / \partial \mathbf{x})|$  satisfy the following condition:

$$\begin{aligned} F_0^2 &>> F_1^2 >> \dots >> F_n^2 \\ \dot{F}_0^2 &>> \dot{F}_1^2 >> \dots >> \dot{F}_n^2. \end{aligned} \quad (2.27)$$

These equations express the situation where different time scales of the system correspond to different pieces of the potential. Thus, the Hamiltonian of the  $k$ -th *reference system* is defined as

$$H = T + V_0 + \dots + V_k, \quad (2.28)$$

with a perturbation given by:

$$P = V_{k+1} + V_{k+2} + \dots + V_n. \quad (2.29)$$

For a general subdivision of the kind given in Eq. (2.26) there exist  $n$  reference *nested* systems. In the general case of a flexible molecular systems, we have fast degrees of freedom which are governed by the stretching, bending and torsional potentials and by slow intermolecular motions driven by the intermolecular potential. As we shall discuss with greater detail in section 4, in real systems there is no clear cut condition between intra and intermolecular motions since their time scales may well overlap in many cases. The conditions Eq. (2.27) are, hence, never fully met for any of all possible potential subdivisions.

Given a potential subdivision Eq. (2.26), we now show how a multi-step scheme can be built with the methods described in section 2.2. For the sake of simplicity, we subdivide the interaction potential of a molecular system into two components only: One intra molecular,  $V_0$ , generating mostly “fast” motions and the other intermolecular,  $V_1$ , driving slower degrees of freedom. Generalization of the forthcoming discussion to a  $n$ -fold subdivision, Eq. (2.26), is then straightforward.

For the 2-fold inter/intra subdivision, the system with Hamiltonian  $H = T + V_0$  is called the intra-molecular reference system whereas  $V_1$  is the intermolecular perturbation to the reference system. Correspondingly, the Liouvillean may be split as

$$\begin{aligned} iL_0 &= \dot{q} \frac{\partial}{\partial q} - \frac{\partial V_0}{\partial q} \frac{\partial}{\partial p} \\ iL_1 &= - \frac{\partial V_1}{\partial q} \frac{\partial}{\partial p}. \end{aligned} \quad (2.30)$$

Here  $L_0$  is the Liouvillean of the 0-th reference system with Hamiltonian  $T + V_0$ , while  $L_1$  is a perturbation Liouvillean. Let us now suppose now that  $\Delta t_1$  is a good time discretization for the time evolution of the perturbation, that is for the slowly varying intermolecular potential. The discrete  $e^{iL\Delta t_1} \equiv e^{(iL_0 + iL_1)\Delta t_1}$  time propagator can be factorized as

$$\begin{aligned} e^{iL\Delta t_1} &= e^{iL_1\Delta t_1/2} (e^{iL_0\Delta t_1/n})^n e^{iL_1\Delta t_1/2} \\ &= e^{iL_1\Delta t_1/2} (e^{iL_0\Delta t_0})^n e^{iL_1\Delta t_1/2}, \end{aligned} \quad (2.31)$$

where we have used Eq. (2.21) and we have defined

$$\Delta t_0 = \frac{\Delta t_1}{n} \quad (2.32)$$

as the time step for the “fast” reference system with Hamiltonian  $T + V_0$ . The propagator (2.31) is unitary and hence time reversible. The external propagators depending on the Liouvillean  $L_1$  acting on the state vectors define a symplectic mapping, as it can be easily proved by using Eq. (2.8). The full factorized propagator is therefore symplectic as long as the inner propagator is symplectic. The Liouvillean  $iL_0 \equiv \dot{q} \partial / \partial q - \partial V_0 / \partial q \partial / \partial p$  can be factorized according to the Verlet symplectic and reversible breakup



described in the preceding section, but with an Hamiltonian  $T + V_0$ . Inserting the result into Eq. (2.31) and using the definition (2.30), the resulting double time step propagator is then

$$e^{iL\Delta t_1} = e^{\frac{-\partial V_1}{\partial q} \frac{\partial}{\partial p} \Delta t_1/2} \left( e^{\frac{-\partial V_0}{\partial q} \frac{\partial}{\partial p} \Delta t_0/2} e^{i\dot{q} \frac{\partial}{\partial q} \Delta t_0} e^{\frac{-\partial V_0}{\partial q} \frac{\partial}{\partial p} \Delta t_0/2} \right)^n e^{\frac{-\partial V_1}{\partial q} \frac{\partial}{\partial p} \Delta t_1/2} \quad (2.33)$$

This propagator is unfolded straightforwardly using the rule (2.23) generating the following symplectic and reversible integrator from step  $t = 0$  to  $t = \Delta t_1$ :

$$\begin{aligned} p \left( \frac{\Delta t_1}{2} \right) &= p(0) + F_1(0) \frac{\Delta t_1}{2} \\ \text{DO} \quad i=1, n & \\ p \left( \frac{\Delta t_1}{2} + i \frac{\Delta t_0}{2} \right) &= p \left( \frac{\Delta t_1}{2} + [i-1] \frac{\Delta t_0}{2} \right) + F_0 \left( [i-1] \frac{\Delta t_0}{2} \right) \frac{\Delta t_0}{2} \\ q(i\Delta t_0) &= q([i-1]\Delta t_0) + p \left( \frac{\Delta t_1}{2} + i \frac{\Delta t_0}{2} \right) \frac{\Delta t_0}{m} \\ p \left( \frac{\Delta t_1}{2} + i\Delta t_0 \right) &= p \left( \frac{\Delta t_1}{2} + i \frac{\Delta t_0}{2} \right) + F_0(i\Delta t_0) \frac{\Delta t_0}{2} \\ \text{ENDDO} & \\ p(\Delta t_1) &= p' \left( \frac{\Delta t_1}{2} \right) + F_1(n\Delta t_0) \frac{\Delta t_1}{2} \end{aligned} \quad (2.34)$$

Note that the slowly varying forces  $F_1$  are felt only at the beginning and the end of the macro-step<sup>2</sup>  $\Delta t_1$ . In the inner  $n$  steps loop the system moves only according to the Hamiltonian of the reference system  $H = T + V_0$ . When using the potential breakup, the inner reference system is rigorously conservative and the total energy of the reference system (i.e.  $T + V_0 + \dots + V_k$ ) is conserved during the  $P$  micro-steps.<sup>3</sup>

The integration algorithm given an arbitrary subdivision of the interaction potential is now straightforward. For the general subdivision (2.26) the corresponding Liouvillean split is

$$iL_0 = \dot{q} \frac{\partial}{\partial q} - \frac{\partial V_i}{\partial q} \frac{\partial}{\partial p}; \quad iL_1 = -\frac{\partial V_1}{\partial q} \frac{\partial}{\partial p} \quad \dots; \quad iL_n = -\frac{\partial V_k}{\partial q} \frac{\partial}{\partial p}. \quad (2.35)$$

We write the discrete time operator for the Liouville operator  $iL = L_0 + \dots L_n$  and use repeatedly the Hermitian approximant and Trotter formula to get a hierarchy of *nested* reference systems propagator, viz.

$$e^{i(\sum_{i=0}^n L_i)\Delta t_n} = e^{iL_n \frac{\Delta t_n}{2}} \left( e^{i(\sum_{i=0}^{n-1} L_i)\Delta t_{n-1}} \right)^{P_{n-1}} e^{iL_n \frac{\Delta t_n}{2}} \quad (2.36)$$

$$\begin{aligned} \Delta t_n &= \Delta t_{n-1} P_{n-1} \\ e^{i(\sum_{i=0}^{n-1} L_i)\Delta t_{n-1}} &= e^{iL_{n-1} \frac{\Delta t_{n-1}}{2}} \left( e^{i(\sum_{i=0}^{n-2} L_i)\Delta t_{n-2}} \right)^{P_{n-2}} e^{iL_{n-1} \frac{\Delta t_{n-1}}{2}} \end{aligned} \quad (2.37)$$

$$\begin{aligned} \Delta t_{n-1} &= \Delta t_{n-2} P_{n-2} \\ &\dots \\ e^{i(L_0+L_1+L_2)\Delta t_2} &= e^{iL_2 \frac{\Delta t_2}{2}} \left( e^{i(L_1+L_0)\Delta t_1} \right)^{P_1} e^{iL_2 \frac{\Delta t_2}{2}} \end{aligned} \quad (2.38)$$

$$\begin{aligned} \Delta t_2 &= \Delta t_1 P_1 \\ e^{i(L_0+L_1)\Delta t_1} &= e^{iL_1 \frac{\Delta t_1}{2}} \left( e^{iL_0\Delta t_0} \right)^{P_0} e^{iL_1 \frac{\Delta t_1}{2}} \\ \Delta t_1 &= \Delta t_0 P_0 \end{aligned} \quad (2.39)$$

where  $\Delta t_i$  is the generic integration time steps selected according to the time scale of the  $i$ -th force  $F_i$ . We now substitute Eq. (2.39) into Eq. (2.38) and so on climbing the whole hierarchy until Eq. (2.36). The resulting multiple time steps symplectic and reversible propagator is then

$$\begin{aligned} e^{iL\Delta t_n} &= e^{F_n \frac{\partial}{\partial p} \Delta t_n} \left( e^{F_{n-1} \frac{\partial}{\partial p} \frac{\Delta t_{n-1}}{2}} \dots \right. \\ &\dots \left( e^{F_0 \frac{\partial}{\partial p} \frac{\Delta t_0}{2}} e^{i\dot{q} \frac{\partial}{\partial q} \Delta t_0} e^{F_0 \frac{\partial}{\partial p} \frac{\Delta t_0}{2}} \right)^{P_0} \dots e^{F_{n-1} \frac{\partial}{\partial p} \frac{\Delta t_{n-1}}{2}} \left. \right)^{P_{n-1}} e^{F_n \frac{\partial}{\partial p} \frac{\Delta t_n}{2}} \end{aligned} \quad (2.40)$$

<sup>2</sup>When the large step size at which the intermittent impulses are computed matches the period of natural oscillations in the system, one can detect instabilities of the numerical integration due to resonance effects. Resonances occurs for pathological systems such as fast harmonic oscillators in presence of strong, albeit slowly varying, forces [70] and can be cured easily by tuning the time steps in the multilevel integration. However, for large and complex molecules it is unlikely that an artificial resonance could sustain for any length of time [70]

<sup>3</sup>In the original *force* breakup [19, 20], the energy is not generally conserved during the unperturbed motion of the inner reference systems but only at the end of the full macro-step. Force breakup and potential breakup have been proved to produce identical trajectories [23]. With respect to the force the breakup, implementation of the potential breakup is slightly more complicated when dealing with intermolecular potential separation, but the energy conservation requirement in any defined reference system makes the debugging process easier.

The integration algorithm that can be derived from the above propagator was first proposed by Tuckerman, Martyna and Berne and called r-RESPA, reversible reference system propagation algorithm [20]

## 2.4 Constraints and r-RESPA

The r-RESPA approach makes unnecessary to resort to the SHAKE procedure [10, 11] to freeze some fast degrees of freedom. However the SHAKE and r-RESPA algorithms are not mutually exclusive and sometimes it might be convenient to freeze some degrees of freedom while simultaneously using a multi-step integration for all other freely evolving degrees of freedom. Since r-RESPA consists in a series of nested velocity Verlet like algorithms, the constraint technique RATTLE [78] used in the past for single time step velocity Verlet integrator can be straightforwardly applied. In RATTLE both the constraint conditions on the coordinates and their time derivatives must be satisfied. The resulting coordinate constraints is upheld by a SHAKE iterative procedure which corrects the positions exactly as in a standard Verlet integration, while a similar iterative procedure is applied to the velocities at the half time step.

In a multi time step integration, whenever velocities are updated, using part of the overall forces (e.g. the intermolecular forces), they must also be corrected for the corresponding constraints forces with a call to RATTLE. This combined RATTLE-r-RESPA procedure has been described for the first time by Tuckerman and Parrinello [79] in the framework of the Car-Parrinello simulation method. To illustrate the combined RATTLE-r-RESPA technique in a multi-step integration, we assume a separation of the potential into two components deriving from intramolecular and intermolecular interactions. In addition, some of the covalent bonds are supposed rigid, i.e.

$$d_a = d_a^{(0)} \quad (2.41)$$

$$\dot{d}_a = 0 \quad (2.42)$$

equation where  $a$  runs over all constrained bonds and  $d_a^{(0)}$  are constants. In the double time integration (2.34), velocities are updated four times, i.e. two times in the inner loop and two times in the outer loop. To satisfy (2.41), SHAKE must be called to correct the position in the inner loop. To satisfy (2.42), RATTLE must be called twice, once in the inner loop and the second time in the outer loop according to the following scheme

$$\begin{aligned} p' \left( \frac{\Delta t_1}{2} \right) &= p(0) + F_1(0) \frac{\Delta t_1}{2} \\ p \left( \Delta t_1 \right) &= RATTLE_p \{ p' \left( \frac{\Delta t_1}{2} \right) \} \\ \text{DO} \quad i=1, n & \\ p' \left( \frac{\Delta t_1}{2} + i \frac{\Delta t_0}{2} \right) &= p \left( \frac{\Delta t_1}{2} + [i-1] \frac{\Delta t_0}{2} \right) + F_0 \left( [i-1] \frac{\Delta t_0}{2} \right) \frac{\Delta t_0}{2} \\ p \left( \frac{\Delta t_1}{2} + i \frac{\Delta t_0}{2} \right) &= RATTLE_p \{ p' \left( \frac{\Delta t_1}{2} + i \frac{\Delta t_0}{2} \right) \} \\ q' (i \Delta t_0) &= q \left( [i-1] \Delta t_0 \right) + p \left( \frac{\Delta t_1}{2} + i \frac{\Delta t_0}{2} \right) \frac{\Delta t_0}{m} \\ q (i \Delta t_0) &= RATTLE_q \{ q' (i \Delta t_0) \} \\ p \left( \frac{\Delta t_1}{2} + i \Delta t_0 \right) &= p \left( \frac{\Delta t_1}{2} + i \frac{\Delta t_0}{2} \right) + F_0 (i \Delta t_0) \frac{\Delta t_0}{2} \\ \text{ENDDO} & \\ p \left( \Delta t_1 \right) &= p' \left( \frac{\Delta t_1}{2} \right) + F_1(n \Delta t_0) \frac{\Delta t_1}{2}. \end{aligned} \quad (2.43)$$

Where  $RATTLE_p$  and  $RATTLE_q$  represent the constraint procedure on velocity and coordinates, respectively.

## 2.5 Applications

As a first simple example we apply the double time integrator (2.34) to the NVE simulation of flexible nitrogen at 100 K.

The overall interaction potential is given by

$$V = V_{intra} + V_{inter}$$

Where  $V_{inter}$  is the intermolecular potential described by a Lennard-Jones model between all nitrogen atoms on different molecules [80].  $V_{intra}$  is instead the intramolecular stretching potential holding together

Table 2.1: Energy conservation ratio  $R$  for various integrators (see text). The last three entries refer to a velocity Verlet with bond constraints.  $\langle V_i \rangle$  and  $\langle V_m \rangle$  are the average value of the intra-molecular and intermolecular energies (in KJ/mole), respectively. CPU is given in seconds per picoseconds of simulation and  $\Delta t$  in  $fs$ . Single time step velocity Verlet with  $\Delta t = 4.5 fs$  is unstable.

$\Delta t$	$n$	$R$	CPU	$\langle V_i \rangle$	$\langle V_m \rangle$
<b>0.3</b>	<b>1</b>	<b>0.005</b>	<b>119</b>	<b>0.1912</b>	<b>-4.75</b>
0.6	1	0.018	62	0.1937	-4.75
1.5	1	0.121	26	0.2142	-4.75
4.5	1	-	-	-	-
0.6	2	0.004	59	0.1912	-4.75
1.5	5	0.004	28	0.1912	-4.75
3.0	10	0.005	18	0.1912	-4.75
4.5	15	0.006	15	0.1912	-4.75
6.0	20	0.008	12	0.1912	-4.74
9.0	30	0.012	10	0.1911	-4.74
3.0	-	0.001	14	-	-4.74
6.0	-	0.004	8	-	-4.75
9.0	-	0.008	6	-	-4.74

the two nitrogen atoms of each given molecule. We use here a simple harmonic spring depending on the molecular bond length  $r_m$ , namely:

$$V_i = \frac{1}{2} \sum_m k(r - r_0)^2,$$

with  $r_0$  and  $r$  the equilibrium and instantaneous distance between the nitrogen atoms, and  $k$  the force constant tuned to reproduce the experimental gas-phase stretching frequency [81].

As a measure of the accuracy of the numerical integration we use the adimensional energy conservation ratio [23, 82, 24, 13]

$$R = \frac{\langle E^2 \rangle - \langle E \rangle^2}{\langle K^2 \rangle - \langle K \rangle^2} \quad (2.44)$$

where  $E$  and  $K$  are the total and kinetic energy of the system, respectively. In table 1 we show the energy conservation ratio  $R$  and CPU timings on a IBM-43P/160MH/RS6000 obtained for flexible nitrogen at 100 K with the r-RESPA integrator as a function of  $n$  and  $\Delta t_1$  in Eq. (2.34) and also for single time step integrators. Results of integrators for rigid nitrogen using SHAKE are also shown for comparison. The data in Table 1 refer to a 3.0 ps run without velocity rescaling. They were obtained starting all runs from coordinates corresponding to the experimental  $Pa3$  structure [83, 84] of solid nitrogen and from velocities taken randomly according to the Boltzmann distribution at 100 K.

The entry in bold refers to the “exact” result, obtained with a single time step integrator with a very small step size of 0.3 fs. Note that  $R$  increases quadratically with the time step for single time step integrators whereas r-RESPA is remarkably resistant to outer time step size increase. For example r-RESPA with  $\Delta t_1 = 9.0 fs$  and  $P = 30$  (i.e.  $\Delta t_0 = 0.3 fs$ ) yields better accuracy on energy conservation than single time step Velocity Verlet with  $\Delta t = 0.6 fs$  does, while being more than six times faster. Moreover, r-RESPA integrates all degrees of freedom of the systems and is almost as efficient as Velocity Verlet with constraints on bonds. It is also worth pointing out that energy averages for all r-RESPA integrators is equal to the exact value, while at single time step even a moderate step size increase results in sensibly different averages intra-molecular energies. As a more complex example we now study a cluster of eight single chain alkanes  $C_{24}H_{50}$ . In this case the potential contains stretching, bending and torsional contributions plus the intermolecular Van-der-Waals interactions between non bonded atoms. The parameter are chosen according to the AMBER protocol [4] by assigning the carbon and hydrogen atoms to the AMBER types **ct** and **hc**, respectively. For various dynamical and structural properties we compare three integrators, namely a triple time step r-RESPA (R3) a single time step integrator with bond constraints on  $X-H$  (S1) and a single time step integrator with all bonds kept rigid (S). These three integrators are tested, starting

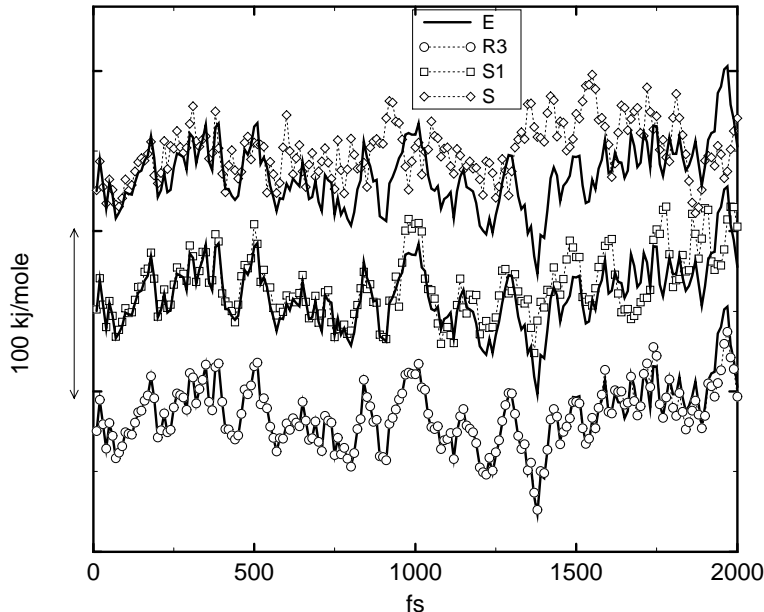


Figure 2.1: Time record of the torsional potential energy at about 300 K for a cluster of eight molecules of  $C_{24}H_{50}$  obtained using three integrators: solid line integrator E; circles integrator R3; squares integrator S1; diamonds integrator S (see text)

from the same phase space point, against a single time step integrator (E) with a very small time step generating the “exact” trajectory. In Fig. 2.1 we show the time record of the torsional potential energy. The R3 integrator generates a trajectory practically coincident with the “exact” trajectory for as long as 1.5 ps. The single time step with rigid  $X-H$  bonds also produces a fairly accurate trajectory, whereas the trajectory generated by S quickly drifts away from the exact time record. In Fig. 2.2 we show the power spectrum of the velocity auto-correlation function obtained with R3, S1 and S. The spectra are compared to the exact spectrum computed using the trajectories generated by the accurate integrator E. We see that R3 and S1 generates the same spectral profile within statistical error. In contrast, especially in the region above 800 wavenumbers, S generates a spectrum which differs appreciably from the exact one. This does not mean, of course, that S is unreliable for the “relevant” torsional degrees of freedom. Simply, we cannot *a priori* exclude that keeping all bonds rigid will not have an impact on the equilibrium structure of the alkanes molecules and on torsional dynamics. Actually, in the present case, as long as torsional motions are concerned all three integrators produce essentially identical results. In 20 picoseconds of simulation, R3 S1 and S predicted 60, 61, 60 torsional jumps, respectively, against the 59 jumps obtained with the exact integrator E. According to prescription of Ref. [85], in order to avoid period doubling, we compute the power spectrum of torsional motion from the auto-correlation function of the vector product of two normalized vector perpendicular to the dihedral planes. Rare events such as torsional jumps produce large amplitudes long time scale oscillations in the time auto-correlation function and therefore their contribution overwhelms the spectrum which appears as a single broaden peak around zero frequency. For this reason all torsions that did undergo a barrier crossing were discarded in the computation of the power spectrum. The power spectrum of the torsional motions is identical for all integrators within statistical error when evaluated over 20 ps of simulations.

From these results it can be concluded that S1 and R3 are very likely to produce essentially the same dynamics for all “relevant” degrees of freedom. We are forced to state that also the integrator S appears to accurately predict the structure and overall dynamics of the torsional degrees of freedom at least for the 20 ps time span of this specific system.<sup>4</sup> Since torsions *are not* normal coordinates and couple to higher

<sup>4</sup>For example, our conclusions on the effect of SHAKE onto torsional motions for highly flexible systems differs from the

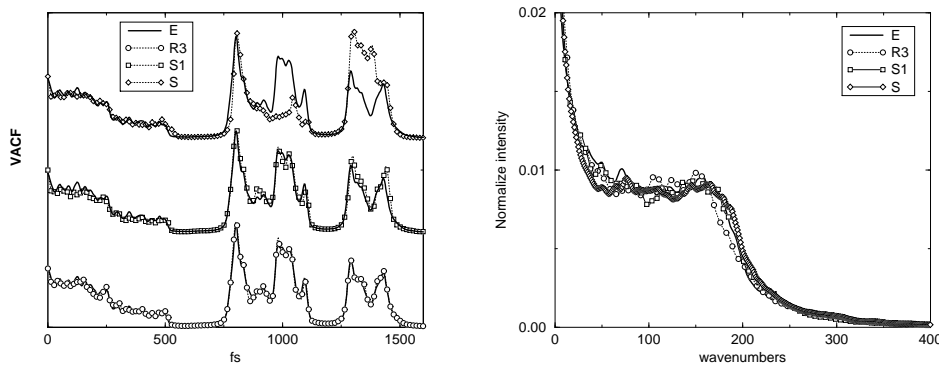


Figure 2.2: Power spectra of the velocity auto-correlation function (left) and of the torsional internal coordinates (right) at 300 K for a cluster of 8  $C_{24}H_{50}$  molecules calculated with integrators E, R3, S1 and S (see text) starting from the same phase space point

frequency internal coordinates such as bending and stretching, the ability of the efficient S integrator of correctly predicting low frequency dynamics and structural properties *cannot* be assumed *a priori* and must be, in principle, verified for each specific case. We also do not know how the individual eigenvectors are affected by the integrators and, although the overall density for S and S1 appears to be the same, there might be considerable changes in the torsional dynamics. R3 does not require any assumption, is accurate everywhere in the spectrum (see Fig. 2.2) and is as efficient as S. For these reasons R3, or a multi-step version of the equally accurate S1, must be the natural choice for the simulation of complex systems using *all-atoms* models

---

results published by Watanabe and Karplus [82] for another flexible system. i.e. met-enkephalin *in vacuo*. They compared SHAKE on  $X-H$  against full flexibility and found that the power spectrum of torsional degrees of freedom differs significantly. For met-enkephalin their spectrum, evaluated on a 10 ps time span, shows a single strong peak at 10 or 40 wavenumbers, with and without constraints, respectively. The different behavior of the constrained and totally flexible system might be ascribed in their case to the the specificity of the system and/or the potential, although this seems unlikely [24]. In their study, on the other hand, we must remark the unusual shape of the spectral torsional profile with virtually no frequencies above 100 wavenumbers and with strong peaks suspiciously close the minimum detectable frequency according to their spectral resolution.

## Chapter 3

# Multiple Time Steps Algorithms for the Isothermal-Isobaric Ensemble

The integrators developed in the previous section generates dynamics in the microcanonical ensemble where total energy, number of particles and volume are conserved. The derivation based on the Liouvillean and the corresponding propagator, however lends itself to a straightforward generalization to non microcanonical ensembles. Simulations of this kind are based on the concept of extended system and generate trajectories that sample the phase space according to a target distribution function. The extended system method is reviewed in many excellent textbooks and papers [12, 86, 87, 88, 89, 90, 91, 25] to which we refer for a complete and detailed description. Here it suffices to say that the technique relies on the clever definition of a modified or *extended* Lagrangian which includes extra degrees of freedom related to the intensive properties (e.g. pressure or temperature) one wishes to sample with a well defined distribution function. The dynamics of the extended system is generated in the *microcanonical* ensemble with the true  $n$  degrees of freedom and, additionally, the extra degrees of freedom related to the macroscopic thermodynamic variables. With an appropriate choice, the equations of motion of the extended system will produce trajectories in the *extended* phase space generating the desired equilibrium distribution function upon integration over the extra (extended) variables. There are several extended system techniques corresponding to various ensembles, e.g. constant pressure in the NPH ensemble simulation with isotropic [92] and anisotropic [93] stress, constant temperature simulation [94] in the NVT ensemble and isothermal–isobaric simulation [95] in the NPT ensemble. As we shall see, the dynamic of the *real* system generated by the extended system method is never Hamiltonian. Hence, symplecticness is no longer an inherent property of the equations of motion. Nonetheless, the Liouvillean formalism developed in the preceding section, turns out to be very useful for the derivation of multiple time step reversible integrators for a general isothermal–isobaric ensemble with anisotropic stress, or **NPT**<sup>1</sup>. This extended system is the most general among all non microcanonical simulations: The NPT, NPH the NVT and even NVE ensemble may be derived from this Lagrangian by imposing special constraints and/or choosing appropriate parameters [25, 27]

### 3.1 The Parrinello-Rahman-Nosé Extended Lagrangian

The starting point of our derivation of the multilevel integrator for the NPT ensemble is the Parrinello-Rahman-Nosé Lagrangian for a molecular system with  $N$  molecules or groups <sup>2</sup> each containing  $n_i$  atoms and subject to a potential  $V$ . In order to construct the Lagrangian we define a coordinate scaling and a

---

<sup>1</sup>When P is not in boldface, we imply that the stress is *isotropic*

<sup>2</sup>For large molecules it may be convenient to further subdivide the molecule into groups. A group, therefore encompasses a conveniently chosen subset of the atoms of the molecule

velocity scaling, i.e.

$$r_{ik\alpha} = R_{i\alpha} + l_{ik\alpha} = \sum_{\beta} h_{\alpha\beta} S_{i\beta} + l_{ik\alpha} \quad (3.1)$$

$$\begin{aligned} \dot{R}_{i\alpha}' &= \dot{R}_{i\alpha} s \\ \dot{l}_{ik\alpha}' &= \dot{l}_{ik\alpha} s \end{aligned} \quad (3.2)$$

Here, the indices  $i$  and  $k$  refer to molecules and atoms, respectively, while Greek letters are used to label the Cartesian components.  $r_{ik\alpha}$  is the  $\alpha$  component of the coordinates of the  $k$ -th atom belonging to the  $i$ -th molecule;  $R_{i\alpha}$  is the center of mass coordinates;  $S_{i\beta}$  is the scaled coordinate of the  $i$ -th molecular center of mass.  $l_{ik\alpha}$  is the coordinate of the  $k$ -th atom belonging to the  $i$ -th molecule expressed in a frame parallel at any instant to the fixed laboratory frame, but with origin on the instantaneous molecular center of mass. The set of  $l_{ik\alpha}$  coordinates satisfies  $3N$  constraints of the type  $\sum_{k=1}^{n_i} l_{ik\alpha} = 0$ .

The matrix  $\mathbf{h}$  and the variable  $s$  control the pressure and temperature of the extended system, respectively. The columns of the matrix  $\mathbf{h}$  are the Cartesian components of the cell edges with respect to a fixed frame. The elements of this matrix allow the simulation cell to change shape and size and are sometimes called the “barostat” coordinates. The volume of the MD cell is related to  $\mathbf{h}$  through the relation

$$\Omega = \det(\mathbf{h}). \quad (3.3)$$

$s$  is the coordinates of the so-called “Nosé thermostat” and is coupled to the intramolecular and center of mass velocities,

We define the “potentials” depending on the thermodynamic variables  $P$  and  $T$

$$\begin{aligned} V_P &= P \det(\mathbf{h}) \\ V_T &= \frac{g}{\beta} \ln s. \end{aligned} \quad (3.4)$$

Where  $P$  is the *external* pressure of the system,  $\beta = k_B T$ , and  $g$  is a constant related to total the number of degrees of freedom in the system. This constant is chosen to correctly sample the *NPT* distribution function.

The extended *NPT* Lagrangian is then defined as

$$\mathcal{L} = \frac{1}{2} \sum_i^N M_i s^2 \dot{\mathbf{S}}_i^t \mathbf{h}^t \mathbf{h} \dot{\mathbf{S}}_i + \frac{1}{2} \sum_{ik} m_{ik} s^2 \dot{\mathbf{l}}_{ik}^t \mathbf{l}_{ik} + \frac{1}{2} W s^2 \text{tr}(\dot{\mathbf{h}}^t \dot{\mathbf{h}}) \quad (3.5)$$

$$+ \frac{1}{2} Q \dot{s}^2 - V - P_{ext} \Omega - \frac{g}{\beta} \ln s \quad (3.6)$$

The arbitrary parameters  $W$  and  $Q$  are the “masses” of the barostat and of the thermostats, respectively<sup>3</sup>. They do not affect the sampled distribution function but only the sampling efficiency [26, 94, 95]. For a detailed discussion of the sampling properties of this Lagrangian the reader is referred to Refs. [91, 27].

### 3.2 The Parrinello-Rahman-Nosé Hamiltonian and the Equations of Motion

In order to derive the multiple time step integration algorithm using the Liouville formalism described in the preceding sections we must switch to the Hamiltonian formalism. Thus, we evaluate the conjugate momenta of the coordinates  $S_{i\alpha}$ ,  $l_{ik\alpha}$ ,  $h_{\alpha\beta}$  and  $s$  by taking the derivatives of the Lagrangian in Eq. (3.6) with respect to corresponding velocities, i.e.

$$\mathbf{T}_i = M_i \mathbf{G} s^2 \dot{\mathbf{S}}_i \quad (3.7)$$

$$\mathbf{p}_{ik} = m_{ik} s^2 \dot{\mathbf{l}}_{ik} \quad (3.8)$$

$$\mathbf{P}_h = s^2 W \dot{\mathbf{h}} \quad (3.9)$$

$$p_s = Q \dot{s}. \quad (3.10)$$

---

<sup>3</sup> $W$  has actually the dimension of a mass, while  $Q$  has the dimension of a mass time a length squared



Where we have defined the symmetric matrix

$$\mathbf{G} = \mathbf{h}^t \mathbf{h} \quad (3.11)$$

The Hamiltonian of the system is obtained using the usual Legendre transformation [72]

$$H(p, q) = \sum \dot{q}p - \mathcal{L}(q, \dot{q}). \quad (3.12)$$

One obtains

$$\begin{aligned} H = & \frac{1}{2} \sum_i^N \frac{\dot{\mathbf{T}}_i \mathbf{G}^{-1} \dot{\mathbf{T}}_i}{M s^2} + \frac{1}{2} \sum_{ik} \frac{\mathbf{p}_{ik}^t \mathbf{p}_{ik}}{m_{ik} s^2} + \frac{1}{2} \frac{tr(\mathbf{P}_h^t \mathbf{P}_h)}{s^2 W} + \frac{p_s^2}{2Q} \\ & + V + P\Omega + \frac{g \ln s}{\beta} \end{aligned} \quad (3.13)$$

In the extended systems formulation we always deal with real and *virtual* variables. The virtual variables in the Hamiltonian (3.13) are the scaled coordinates and momenta while the unscaled variables (e.g  $\mathbf{R}_i = \mathbf{h} \mathbf{S}_i$  or  $p'_{ik\alpha} = p_{ik\alpha}/s$  are the real counterpart. The variable  $s$  in the Nosé formulation plays the role of a time scaling [86, 80, 94]. The above Hamiltonian is given in terms of *virtual variables* and in term of a virtual time and is indeed a *true* Hamiltonian function and has corresponding equation of motions that can be obtained applying Eq. (2.3) with  $\mathbf{x} \equiv S_{i\alpha}, l_{ik\alpha}, h_{\alpha\beta}, s, T_{i\alpha}, p_{ik\alpha}, \pi_{\alpha\beta}, p_s$  in a standard fashion. Nonetheless, the equations of motions in terms of these virtual variable are inadequate for several reasons since for example one would deal with a fluctuating time step [86, 94]. It is therefore convenient to work in terms of real momenta and real time. The real momenta are related to the virtual counterpart through the relations

$$T_{i\alpha} \rightarrow T_{i\alpha}/s \quad (3.14)$$

$$p_{ik\alpha} \rightarrow p_{ik\alpha}/s \quad (3.15)$$

$$(\mathbf{P}_h)_{\alpha\beta} \rightarrow (\mathbf{P}_h)_{\alpha\beta}/s \quad (3.16)$$

$$p_s \rightarrow p_s/s \quad (3.17)$$

$$(3.18)$$

It is also convenient [26] to introduce new center of mass momenta as

$$\mathbf{P}_i \equiv \mathbf{G}^{-1} \mathbf{T}_i. \quad (3.19)$$

such that the corresponding velocities may be obtained directly without the knowledge of the “coordinates”  $\mathbf{h}$  in  $\mathbf{G}^4$ , namely

$$\dot{\mathbf{S}}_i = \frac{\mathbf{P}_i}{M}. \quad (3.20)$$

Finally, a real time formulation and a new dynamical variable  $\eta$  are adopted:

$$t \rightarrow t/s \quad (3.21)$$

$$\eta \equiv \ln s \quad (3.22)$$

The equations of motions for the newly adopted set of dynamical variables are easily obtained from the true Hamiltonian in Eq. (3.13) and then using Eqs. (3.14-3.22) to rewrite the resulting equations in terms of the new momenta. In so doing, we obtain:

$$\dot{l}_{ik} = \frac{\mathbf{p}_{ik}}{m_{ik}}, \quad \dot{\mathbf{S}}_i = \frac{\mathbf{P}_i}{M_i}, \quad \dot{\mathbf{h}} = \frac{\mathbf{P}_h}{W}, \quad \dot{\eta} = \frac{p_\eta}{Q} \quad (3.23)$$

$$\dot{\mathbf{p}}_{ik} = \mathbf{f}_{ik}^c - \frac{p_\eta}{Q} \mathbf{p}_{ik}, \quad (3.24)$$

$$\dot{\mathbf{P}}_i = \mathbf{h}^{-1} \mathbf{F}_i - \overleftrightarrow{\mathbf{G}}^{-1} \overleftrightarrow{\mathbf{G}} \mathbf{P}_i - \frac{p_\eta}{Q} \mathbf{P}_i, \quad (3.25)$$

$$\overleftrightarrow{\mathbf{P}}_h = \left( \overleftrightarrow{\mathbf{V}} + \overleftrightarrow{\mathbf{K}} - \mathbf{h}^{-1} P_{ext} \det \mathbf{h} \right) - \frac{p_\eta}{Q} \mathbf{P}_h, \quad (3.26)$$

$$\dot{p}_\eta = \mathcal{F}_\eta, \quad (3.27)$$

---

<sup>4</sup>This allows to maintain Verlet-like breakup while integrating the equation of motions [26].



It can be verified that the conserved quantity  $\mathcal{H}$  is associated with the above equations of motion, namely

$$\begin{aligned}\mathcal{H} &= \frac{1}{2} \sum_{i=1}^N \frac{\mathbf{P}_i^t \overleftrightarrow{\mathbf{G}} \mathbf{P}_i}{M_i} + \frac{1}{2} \sum_{i=1}^N \sum_{k=1}^{n_i} \frac{\mathbf{P}_{ik}^t \mathbf{P}_{ik}}{m_{ik}} + \frac{1}{2} \frac{\text{tr}(\mathbf{P}_h^t \mathbf{P}_h)}{W} + \\ &+ \frac{1}{2} \frac{p_\eta p_\eta}{Q} + V + P_{ext} \det \mathbf{h} + g k_B T \eta.\end{aligned}\quad (3.28)$$

The atomic force  $\mathbf{f}_{ik}^c = \frac{\partial V}{\partial \mathbf{r}_{ik\alpha}} - \frac{m_{ik}}{M_i} \mathbf{F}_i$  includes a constraint force contribution which guarantees that the center of mass in the intramolecular frame of the  $l_{ik\alpha}$  coordinates remains at the origin.  $\overleftarrow{\mathbf{V}}$  and  $\overleftarrow{\mathbf{K}}$  are the virial and ideal gas contribution to the internal pressure tensor  $\mathbf{P}_{int} = \overleftarrow{\mathbf{V}} + \overleftarrow{\mathbf{K}}$  and they are defined as<sup>5</sup>

$$\begin{aligned}\overleftarrow{\mathbf{V}} &= \sum_{i=1}^N \mathbf{F}_i \mathbf{S}_i^t \\ \overleftarrow{\mathbf{K}} &= \sum_{i=1}^N M_i (\mathbf{h} \dot{\mathbf{S}}_i) \dot{\mathbf{S}}_i^t.\end{aligned}\quad (3.29)$$

Finally  $\mathcal{F}_\eta$  is the force driving the Nosé thermostat

$$\mathcal{F}_\eta = \frac{1}{2} \sum_{i=1}^N M_i \dot{\mathbf{S}}_i^t \overleftrightarrow{\mathbf{G}} \dot{\mathbf{S}}_i + \frac{1}{2} \sum_{i=1}^N \sum_{k=1}^{n_i} \frac{\mathbf{P}_{ik}^t \mathbf{P}_{ik}}{m_{ik}} - g k_B T, \quad (3.30)$$

with  $g$  equal to the number of all degrees of freedom  $N_f$  including those of the barostat<sup>6</sup>.

Eqs. (3.14-3.21) define a generalized coordinates transformation of the kind of Eq. (2.4). This transformation is non canonical, i.e. the Jacobian matrix of the transformation from the virtual coordinates does not obey Eq. (2.8). This means that  $\mathcal{H}$  in terms of the new coordinates Eq. (3.28) is “only” a constant of motion, but is no longer a true Hamiltonian: application of Eq. (2.1) does not lead to Eqs. (3.23-3.27). Simulations using the real variables are not Hamiltonian in nature in the sense that the phase space of the real variables is compressible [96] and that Liouville theorem is not satisfied [91]. This “strangeness” in the dynamics of the real variables in the extended systems does not of course imply that the sampling of the configurational *real* space is incorrect. To show this, it suffices to evaluate the partition function for a microcanonical distribution of the kind  $\delta(\mathcal{H} - E)$ , with  $\mathcal{H}$  being given by Eq. (3.28). The Jacobian of the transformation of Eqs. (3.14-3.22) must be included in the integration with respect to the real coordinates when evaluating the partition function for the extended system. If the equations of motion in terms of the transformed coordinates are known, this Jacobian,  $\mathcal{J}$ , can be readily computed from the relation [73]:

$$\frac{d\mathcal{J}}{dt} = -\mathcal{J} \left( \frac{\partial}{\partial \mathbf{y}} \cdot \dot{\mathbf{y}} \right). \quad (3.31)$$

Where  $\mathbf{y}$  has the usual meaning of phase space vector containing all independent coordinates and momenta of the systems. Inserting the equations of motion of Eq. (3.27) into Eq. (3.31) and integrating by separation of variables yields

$$\mathcal{J} = e^{N_f \eta} [\det \mathbf{h}]^{6N}. \quad (3.32)$$

Using (3.32) and integrating out the thermostat degrees of freedom, the partition function can be easily shown [91, 97] to be equivalent to that of  $NPT$  ensemble, i.e.

$$\Delta_{NPT} \propto \int d\mathbf{h} e^{-\beta P_{ext} \det(\mathbf{h})} Q(\mathbf{h}) \quad (3.33)$$

<sup>5</sup> In presence of bond constraints and if the scaling is group-based instead of molecular based, these expression should contain a contribution from the constraints forces. Complications due to the constraints can be avoided altogether by defining groups so that no two groups are connected through a constrained bond [27]. In that case  $\overleftarrow{\mathbf{V}}$  does not include any constraint contribution.

<sup>6</sup> The thermostat degree of freedom must be included [86, 91] in the count when working in *virtual* coordinates. Indeed in Eq. (3.13) we have  $g = N_f + 1$

with  $Q(\mathbf{h})$  being the canonical distribution of a system with cell of shape and size define by the columns of  $\mathbf{h}$ .<sup>7</sup>

### 3.3 Equivalence of Atomic and Molecular Pressure

The volume scaling defined in Eq. (3.1) is not unique. Note that only the equation of motion for the center of mass momentum, Eq. (3.25), has a velocity dependent term that depends on the coordinates of the barostat through the matrix  $\mathbf{G}$  defined in Eq. (3.11). The atomic momenta, Eq. (3.24), on the contrary, are not coupled to the barostat. This fact is also reflected in the equations of motion for the barostat momenta, Eq. (3.26), which is driven by the internal pressure due only to the molecular or group center of masses. In defining the extended Lagrangian one could as well have defined an *atomic* scaling of the form

$$r_{ik\alpha} = \sum_{\beta} h_{\alpha\beta} s_{i\alpha k}. \quad (3.34)$$

Atomic scaling might be trivially implemented by eliminating the kinetic energy, which depends on the  $l_{ik\alpha}$  velocities, from the starting Lagrangian (3.6) and replacing the term  $\frac{1}{2} \sum_i^N M_i s^2 \dot{\mathbf{S}}_i^t \mathbf{h}^t \mathbf{h} \dot{\mathbf{S}}_i$  with  $\frac{1}{2} \sum_{ik} m_{ik} s^2 \dot{\mathbf{s}}_{ik}^t \mathbf{h}^t \mathbf{h} \dot{\mathbf{s}}_{ik}$ . The corresponding equations of motions for atomic scaling are then

$$\dot{\mathbf{r}}_{ik} = \frac{\mathbf{p}_{ik}}{m_{ik}}, \quad \dot{\mathbf{h}} = \frac{\mathbf{P}_h}{W}, \quad \dot{\eta} = \frac{p_\eta}{Q} \quad (3.35)$$

$$\dot{\mathbf{p}}_{ik} = \mathbf{h}^{-1} \dot{\mathbf{p}}_{ik} - \overleftrightarrow{\mathbf{G}}^{-1} \overleftrightarrow{\mathbf{G}} \dot{\mathbf{p}}_{ik} - \frac{p_\eta}{Q} \dot{\mathbf{p}}_{ik}, \quad (3.36)$$

$$\overleftrightarrow{\mathbf{P}}_h = \left( \overleftrightarrow{\mathcal{V}} + \overleftrightarrow{\mathcal{K}} - \mathbf{h}^{-1} P_{ext} \det \mathbf{h} \right) - \frac{p_\eta}{Q} \mathbf{P}_h, \quad (3.37)$$

$$\dot{p}_\eta = \mathcal{F}_\eta \quad (3.38)$$

where the quantities  $\mathcal{V}, \mathcal{K}, \mathcal{F}_\eta$  depend now on the *atomic* coordinates

$$\begin{aligned} \overleftrightarrow{\mathcal{V}} &= \sum_{i=1}^N \mathbf{f}_{ik} \mathbf{s}_{ik}^t \\ \overleftrightarrow{\mathcal{K}} &= \sum_{i=1}^N M_i (\mathbf{h} \mathbf{s}_{ik}) \mathbf{s}_{ik}^t \end{aligned} \quad (3.39)$$

$$\mathcal{F}_\eta = \frac{1}{2} \sum_{i=1}^N \sum_{k=1}^{n_i} \frac{\mathbf{p}_{ik}^t \mathbf{p}_{ik}}{m_{ik}} - g k_B T. \quad (3.40)$$

In case of atomic, Eq. (3.34), or molecular scaling, Eq. (3.1), the internal pressure entering in Eqs. (3.26, 3.37) is then

$$P_{int} = \langle P_{atom} \rangle = \left\langle \frac{1}{3V} \sum_i \sum_k \left( \frac{\mathbf{p}_{ik}^2}{m_{ik}} + \mathbf{r}_{ik} \cdot \mathbf{f}_{ik} \right) \right\rangle \quad (3.41)$$

$$P_{int} = \langle P_{mol} \rangle = \left\langle \frac{1}{3V} \sum_i \left( \frac{\mathbf{P}_i^2}{M_i} + \mathbf{R}_i \cdot \mathbf{F}_i \right) \right\rangle \quad (3.42)$$

---

<sup>7</sup> Actually in ref. [91, 27] is pointed out that the virial theorem implied by the distribution (3.33) is slightly different from the exact virial in the NPT ensemble. Martyna *et al.* [91] proposed an improved set of equations of motion that generates a distribution satisfying exactly the virial theorem.

respectively. Where the molecular quantities can be written in term of the atomic counterpart according to:

$$\mathbf{R}_i = \frac{1}{M_i} \sum_k m_{ik} \mathbf{r}_{ik} \quad (3.43)$$

$$\mathbf{P}_i = \sum_k \mathbf{p}_{ik} \quad (3.44)$$

$$\mathbf{F}_i = \sum_k \mathbf{f}_{ik} \quad (3.45)$$

The equation of motion for the barostat in the two cases, Eqs.(3.37, 3.26), has the same form whether atomic or molecular scaling is adopted. The internal pressure in the former case is given by Eq. (3.41) and in the latter is given by Eq. (3.42). The two pressures, Eqs. (3.41,3.42), differ instantaneously. Should the difference persist after averaging, then it would be obvious that the equilibrium thermodynamic state in the *NPT* ensemble depends on the scaling method. The two formulas (3.41,3.42) are fortunately equivalent. To prove this statement, we closely follow the route proposed by H. Berendsen and reported by Ciccotti and Ryckaert [98] and use Eqs. (3.43-3.45) to rearrange Eq. (3.42). We obtain

$$\sum_i \langle \mathbf{R}_i \bullet \mathbf{F}_i \rangle = \sum_i \frac{1}{M_i} \sum_{kl} \langle m_{ik} \mathbf{r}_{ik} \bullet \mathbf{f}_{il} \rangle. \quad (3.46)$$

Adding and subtracting  $m_{ik} \mathbf{r}_{il} \bullet \mathbf{f}_{il}$ , we get

$$= \sum_i \frac{1}{M_i} \sum_{kl} \langle m_{ik} (\mathbf{r}_{ik} - \mathbf{r}_{il}) \bullet \mathbf{f}_{il} + m_{ik} \mathbf{r}_{il} \bullet \mathbf{f}_{il} \rangle \quad (3.47)$$

which can be rearranged as

$$= \sum_i \frac{1}{M_i} \left\{ \sum_{kl} \left[ \frac{1}{2} \langle (\mathbf{r}_{ik} - \mathbf{r}_{il}) \bullet (m_i \mathbf{f}_{il} - m_j \mathbf{f}_{ik}) \rangle \right] + \sum_l \langle \mathbf{r}_{il} \bullet \mathbf{f}_{il} \rangle \right\} \quad (3.48)$$

using the newton law  $\mathbf{f}_{ik} = m_{ik} \mathbf{a}_{ik}$ , where  $\mathbf{a}_{ik}$  is the acceleration, we obtain

$$= \sum_i \frac{1}{M_i} \left\{ \sum_{kl} \left[ \frac{1}{2} \langle m_j m_i (\mathbf{r}_{ik} - \mathbf{r}_{il}) \bullet (\mathbf{a}_{il} - \mathbf{a}_{ik}) \rangle \right] + \sum_l \langle \mathbf{r}_{il} \bullet \mathbf{f}_{il} \rangle \right\}. \quad (3.49)$$

The first term in the above equation can be decomposed according to:

$$(\mathbf{r}_{ik} - \mathbf{r}_{il}) \bullet (\mathbf{a}_{il} - \mathbf{a}_{ik}) = \frac{d}{dt} [(\mathbf{r}_{ik} - \mathbf{r}_{il}) \bullet (\mathbf{v}_{il} - \mathbf{v}_{ik})] + (\mathbf{v}_{il} - \mathbf{v}_{ik})^2 \quad (3.50)$$

The first derivative term on the right hand side is zero rigorously for rigid molecules or rigid group and is zero on average for flexible molecules or groups, assuming that the flexible molecules or groups do not dissociate. This can be readily seen in case of ergodic systems, by evaluating directly the average of this derivatives as

$$\left\langle \frac{d}{dt} [(\mathbf{r}_{ik} - \mathbf{r}_{il}) \bullet (\mathbf{v}_{il} - \mathbf{v}_{ik})] \right\rangle = \lim_{\tau \rightarrow \infty} \frac{1}{\tau} \int_0^\tau \frac{d}{dt} [(\mathbf{r}_{ik} - \mathbf{r}_{il}) \bullet (\mathbf{v}_{il} - \mathbf{v}_{ik})] dt \quad (3.51)$$

$$= \lim_{\tau \rightarrow \infty} \frac{1}{\tau} [(\mathbf{r}_{ik}(\tau) - \mathbf{r}_{il}(\tau)) \bullet (\mathbf{v}_{il}(\tau) - \mathbf{v}_{ik}(\tau)) + C] \quad (3.52)$$

So if the quantity  $\mathbf{r}_{ikl}(\tau) \bullet \mathbf{v}_{ilk}(\tau)$  remains bounded (which is true if the potential is not dissociative, since  $k, l$  refers to the same molecule  $i$ ), the average in Eq. (3.52) is zero<sup>8</sup>. Thus, we can rewrite the average of Eq. (3.49) as

$$\left\langle \sum_i \mathbf{R}_i \bullet \mathbf{F}_i \right\rangle = \sum_i \frac{1}{2M_i} \sum_{kl} m_{ik} m_{il} \langle (\mathbf{v}_{il} - \mathbf{v}_{ik})^2 \rangle + \sum_{ik} \langle \mathbf{r}_{ik} \bullet \mathbf{f}_{ik} \rangle. \quad (3.53)$$

---

<sup>8</sup>The statement *the molecule of group does not dissociate* is even too restrictive. It is enough to say that the quantity (3.52) remains bound.

The first term on the right hand side of the above equation can be further developed obtaining the trivial identity:

$$\begin{aligned} \sum_{kl} m_{ik} m_{il} \langle (\mathbf{v}_{il} - \mathbf{v}_{ik})^2 \rangle &= \sum_{kl} m_{ik} m_{il} \langle \mathbf{v}_{ik}^2 \rangle + \sum_{kl} m_{ik} m_{il} \langle \mathbf{v}_{il}^2 \rangle - \\ &- \sum_{kl} 2m_{ik} m_{il} \langle \mathbf{v}_{il} \bullet \mathbf{v}_{ik} \rangle \end{aligned} \quad (3.54)$$

$$= 2M_i \sum_k m_{ik} \langle \mathbf{v}_{ik}^2 \rangle - 2\langle \mathbf{P}_i^2 \rangle \quad (3.55)$$

Substituting Eq. (3.55) in Eq. (3.53) we get

$$\langle \sum_i \mathbf{R}_i \bullet \mathbf{F}_i \rangle = \sum_{ik} m_{ik} \langle \mathbf{v}_{ik}^2 \rangle - \frac{1}{M_i} \langle \mathbf{P}_i^2 \rangle + \sum_{ik} \langle \mathbf{r}_{ik} \bullet \mathbf{f}_{ik} \rangle \quad (3.56)$$

Substituting Eq. (3.56) into Eq. (3.42) leads speedily to (3.41) which completes the proof. As a consequence of the above discussion, it seems likely that both the equilibrium and non equilibrium properties of the MD system are not affected by coordinate scaling. We shall see later that this is actually the case.

### 3.4 Liouvillean Split and Multiple Time Step Algorithm for the *NPT* Ensemble

We have seen in section 2.2 that the knowledge of the Liouvillean allows us to straightforwardly derive a multi-step integration algorithm. Thus, for simulation in the *NPT* ensemble, the Liouvillean  $iL = \dot{\mathbf{y}} \nabla_{\mathbf{y}}$  is readily available from the equations of motion in (3.23-3.27). For sake of simplicity, to build our *NPT* multiple time step integrator we assume that the system potential contains only a fast *intramolecular*  $V_0$  term and a slow *intermolecular* term  $V_1$ , as discussed in Sec. 2.3. Generalization to multiple intra and inter-molecular components is straightforward.

We define the following components of the *NPT* Liouvillean

$$iL_x = - \sum_i \mathbf{P}_i \frac{p_\eta}{Q} \nabla_{\mathbf{P}_i} - \sum_{ik} \mathbf{p}_{ik} \frac{p_\eta}{Q} \nabla_{\mathbf{p}_{ik}} - \sum_{\alpha\beta} (\mathbf{P}_h)_{\alpha\beta} \frac{p_\eta}{Q} (\nabla_{\mathbf{P}_h})_{\alpha\beta} \quad (3.57)$$

$$iL_y = \mathcal{F}_\eta \nabla_{p_\eta} \quad (3.58)$$

$$iL_z = \sum_i \overleftrightarrow{\mathbf{G}}^{-1} \overleftrightarrow{\mathbf{G}} \mathbf{P}_i \nabla_{\mathbf{P}_i} \quad (3.59)$$

$$iL_u = \sum_{\alpha\beta} \left( \overleftrightarrow{\mathbf{K}} - \mathbf{h}^{-1} P_{ext} \det \mathbf{h} \right)_{\alpha\beta} (\nabla_{\mathbf{P}_h})_{\alpha\beta} \quad (3.60)$$

$$iL_s = \sum_i \mathbf{J}_i \nabla_{\mathbf{P}_i} + \sum_{ik} \mathbf{f}_{ik}^c \nabla_{\mathbf{p}_{ik}} + \sum_{\alpha\beta} \left( \overleftrightarrow{\mathbf{V}} \right)_{\alpha\beta} (\nabla_{\mathbf{P}_h})_{\alpha\beta} \quad (3.61)$$

$$\begin{aligned} iG_0 &= \sum_i \frac{\mathbf{P}_i}{M_i} \nabla_{\mathbf{s}_i} + \sum_{ik} \frac{\mathbf{p}_{ik}}{m_{ik}} \nabla_{\mathbf{l}_{ik}} + \sum_{\alpha\beta} \frac{(\mathbf{P}_h)_{\alpha\beta}}{W} (\nabla_{\mathbf{h}})_{\alpha\beta} + \\ &+ \frac{p_\eta}{Q} \nabla_\eta - \nabla_{\mathbf{l}_{ik}} V_0 \nabla_{\mathbf{p}_{ik}}, \end{aligned} \quad (3.62)$$

where in Eq. (3.61) the scaled forces  $\mathbf{F}_i$  have been replaced by its real space counterparts, i.e.  $\mathbf{J}_i = \mathbf{h}^{-1} \mathbf{F}_i$ .

The atomic scaling version of this Liouvillean breakup is derived on the basis of Eqs. (3.38). One

obtains

$$iL_x = -\sum_{ik} \mathbf{p}_{ik} \frac{p_\eta}{Q} \nabla_{\mathbf{p}_{ik}} - \sum_{\alpha\beta} (\mathbf{P}_h)_{\alpha\beta} \frac{p_\eta}{Q} (\nabla_{\mathbf{P}_h})_{\alpha\beta} \quad (3.63)$$

$$iL_y = \mathcal{F}_\eta \nabla_{p_\eta} \quad (3.64)$$

$$iL_z = \sum_{ik} \overleftrightarrow{\mathbf{G}}^{-1} \overleftrightarrow{\mathbf{G}} \mathbf{p}_{ik} \nabla_{\mathbf{p}_{ik}} \quad (3.65)$$

$$iL_u = \sum_{\alpha\beta} \left( \overleftrightarrow{\mathcal{K}} - \mathbf{h}^{-1} P_{ext} \det \mathbf{h} \right)_{\alpha\beta} (\nabla_{\mathbf{P}_h})_{\alpha\beta} \quad (3.66)$$

$$iL_s = \sum_{ik} \mathbf{j}_{ik} \nabla_{\mathbf{p}_{ik}} + \sum_{\alpha\beta} \left( \overleftrightarrow{\mathcal{V}} \right)_{\alpha\beta} (\nabla_{\mathbf{P}_h})_{\alpha\beta} \quad (3.67)$$

$$\begin{aligned} iG_0 &= \sum_{ik} \frac{\mathbf{p}_{ik}}{m_{ik}} \nabla_{\mathbf{l}_{ik}} + \sum_{\alpha\beta} \frac{(\mathbf{P}_h)_{\alpha\beta}}{W} (\nabla_{\mathbf{h}})_{\alpha\beta} + \\ &+ \frac{p_\eta}{Q} \nabla_\eta - \nabla_{lik} V_0 \nabla_{\mathbf{p}_{ik}}, \end{aligned} \quad (3.68)$$

where  $\mathbf{j}_{ik} = \mathbf{h}^{-1} \mathbf{f}_{ik}$  and  $\mathcal{V}, \mathcal{K}, \mathcal{F}_\eta$  are given in Eqs. (3.39,3.40). For the time scale breakup in the *NPT* ensemble we have the complication of the extra degrees of freedom whose time scale dynamics can be controlled by varying the parameter  $Q$  and  $W$ . Large values of  $Q$  and  $W$  slow down the time dynamics of the barostat and thermostat coordinates. The potential  $V$  determines the time scale of the  $iG_0$  term (the fast component) and of the  $iL_s$  contribution (the slow component). All other sub-Liouvillians either handle the coupling of the true coordinates to the extra degrees of freedom ( $iL_x$  expresses the coupling of all momenta (including barostat momenta) to the thermostat momentum, while  $iL_z$  is a coupling term between the center of mass momenta and the barostat momentum), or drive the evolution of the extra coordinates of the barostat and thermostat ( $iL_y$  and  $iL_u$ ). The time scale dynamics of these terms depends not only on the potential subdivision and on the parameters  $W$  and  $Q$ , but also on the type of scaling [27]. When the molecular scaling is adopted the dynamics of the virial term  $\overleftrightarrow{\mathcal{V}}$  contains contributions only from the intermolecular potential since the barostat is coupled only to the center of mass coordinates (see Eq. (3.29)). Indeed, the net force acting on the molecular center of mass is independent on the intramolecular potential, since the latter is invariant under rigid translation of the molecules. When atomic scaling or group (i.e. sub-molecular) scaling is adopted, the virial  $\overleftrightarrow{\mathcal{V}}$  (see Eq. (3.39)) depends also on the fast intramolecular such as stretching motions. In this case the time scale of the barostat coordinate is no longer slow, unless the parameter  $W$  is changed. For standard values of  $W$ , selected to obtain an efficient sampling of the *NPT* phase space [99, 80], the barostat dependent Liouvillians, Eqs. (3.60,3.59), have time scale dynamics comparable to that of the intramolecular Liouvillean  $iG_0$  and therefore must be associated with this term<sup>9</sup>.

Thus, the molecular split of the Liouvillean is hence given by

$$\begin{aligned} iL_1 &= iL_x + iL_y + iL_z + iL_u + iL_s \\ iL_0 &= iG_0 \end{aligned} \quad (3.69)$$

whereas the atomic split is

$$\begin{aligned} iL_1 &= iL_x + iL_y + iL_s \\ iL_0 &= iG_0 + iL_z + iL_u \end{aligned} \quad (3.70)$$

For both scaling, a simple Hermitian factorization of the total time propagator  $e^{iL_t}$  yields the double time discrete propagator

$$e^{iL_1+iL_0} = e^{iL_1\Delta t_1/2} (e^{iL_0\Delta t_0})^n e^{iL_1\Delta t_1/2} \quad (3.71)$$

<sup>9</sup>Similar considerations hold for the thermostat coordinate which in principle depends on the kinetic energy of all degrees of freedom, modulated hence by the fast motion also. In this case, however, the value of the thermostat inertia parameter  $Q$  can be chosen to slow down the time scale of the  $\eta$  coordinates without reducing considerably the sampling efficiency.

where  $\Delta t_0$ , the small time step, must be selected according to the intramolecular time scale whereas  $\Delta t_1$ , the large time step, must be selected according to the time scale of the intermolecular motions. We already know that the propagator (3.71) cannot generate a symplectic. The alert reader may also have noticed that in this case the symmetric form of the multiple time step propagator Eq. (3.71) does not imply necessarily time reversibility. Some operators appearing in the definition of  $L_1$  (e.g.  $iL_z$  and  $iL_s$ ) for the molecular scaling and in the definitions of  $iL_1$  and  $iL_0$  for the atomic scaling are in fact non commuting. We have seen in section 2.2 that first order approximation of non commuting propagators yields time irreversible algorithms. We can render the propagator in Eq. (3.71) time reversible by using second order symmetric approximant (i.e. Trotter approximation) for any two non commuting operators. For example in the case of the molecular scaling, when we propagate in Eq. (3.71) the slow propagator  $e^{iL_1\Delta t/2}$  for half time step, we may use the following second order  $O(\Delta t^3)$  split

$$e^{iL_1\frac{\Delta t_1}{2}} \simeq e^{iL_y\frac{\Delta t_1}{4}} e^{iL_z\frac{\Delta t_1}{2}} e^{iL_y\frac{\Delta t_1}{4}} e^{iL_x\frac{\Delta t_1}{4}} e^{i(L_s+L_u)\frac{\Delta t_1}{2}} e^{iL_x\frac{\Delta t_1}{4}} \quad (3.72)$$

An alternative simpler and equally accurate approach when dealing with non commuting operators is simply to preserve the unitarity by reversing the order of the operators in the first order factorization of the right and left operators of Eq. (3.71) without resorting to locally second order  $O(\Delta t^3)$  approximation like in Eq. (3.72). Again for the molecular scaling, this is easily done by using the approximant

$$\left(e^{iL_1\frac{\Delta t_1}{2}}\right)_{\text{left}} = e^{iL_x\frac{\Delta t_1}{2}} e^{iL_y\frac{\Delta t_1}{2}} e^{iL_z\frac{\Delta t_1}{2}} e^{iL_u\frac{\Delta t_1}{2}} e^{iL_s\frac{\Delta t_1}{2}} \quad (3.73)$$

for the left propagator, and

$$\left(e^{iL_1\frac{\Delta t_1}{2}}\right)_{\text{right}} = e^{iL_s\frac{\Delta t_1}{2}} e^{iL_u\frac{\Delta t_1}{2}} e^{iL_z\frac{\Delta t_1}{2}} e^{iL_y\frac{\Delta t_1}{2}} e^{iL_x\frac{\Delta t_1}{2}} \quad (3.74)$$

for the rightmost propagator. Note that

$$\left(e^{iL_1\frac{\Delta t_1}{2}}\right)_{\text{left}}^{-1} = \left(e^{iL_1\frac{\Delta t_1}{2}}\right)_{\text{right}} \quad (3.75)$$

Inserting these approximations into (3.71) the overall integrator is found to be time reversible and second order. Time reversible integrators are in fact always even order and hence *at least* second order [71, 68]. Therefore the overall molecular and atomic (or group) discrete time propagators are given by

$$\begin{aligned} e^{iL_{\text{mol}}\Delta t_1} &= e^{iL_s\frac{\Delta t_1}{2}} e^{iL_u\frac{\Delta t_1}{2}} e^{iL_z\frac{\Delta t_1}{2}} e^{iL_y\frac{\Delta t_1}{2}} e^{iL_x\frac{\Delta t_1}{2}} (e^{iG_0\Delta t_0})^n \times \\ &\times e^{iL_x\frac{\Delta t_1}{2}} e^{iL_y\frac{\Delta t_1}{2}} e^{iL_z\frac{\Delta t_1}{2}} e^{iL_u\frac{\Delta t_1}{2}} e^{iL_s\frac{\Delta t_1}{2}} \end{aligned} \quad (3.76)$$

$$\begin{aligned} e^{iL_{\text{atom}}\Delta t_1} &= e^{iL_s\frac{\Delta t_1}{2}} e^{iL_y\frac{\Delta t_1}{2}} e^{iL_x\frac{\Delta t_1}{2}} \times \\ &\times (e^{iL_u\Delta t_0/2} e^{iL_z\Delta t_0/2} e^{iG_0\Delta t_0} e^{iL_z\Delta t_0/2} e^{iL_u\Delta t_0/2})^n \times \\ &\times e^{iL_x\frac{\Delta t_1}{2}} e^{iL_y\frac{\Delta t_1}{2}} e^{iL_s\frac{\Delta t_1}{2}} \end{aligned} \quad (3.77)$$

The propagator  $e^{iG_0\Delta t_0}$ , defined in Eq. (3.62), is further split according to the usual velocity Verlet breakup of Eq. (2.22). Note that in case of molecular scaling the “slow” coordinates ( $\mathbf{S}$ ,  $\mathbf{h}$ ,  $\eta$ ) move with constant velocity during the  $n$  small times steps since there is no “fast” force acting on them in the inner integration. The explicit integration algorithm may be easily derived for the two propagators in Eqs. (3.76) and (3.77) using the rule in Eq. (2.23) and its generalization:

$$\begin{aligned} e^{a\mathbf{y}\nabla_{\mathbf{y}}} f(\mathbf{y}) &= f(\mathbf{y}e^a) \\ e^{\overleftrightarrow{\mathbf{a}}\mathbf{y}\nabla_{\mathbf{y}}} f(\mathbf{y}) &= f\left(e^{\overleftrightarrow{\mathbf{a}}}\mathbf{y}\right) \end{aligned} \quad (3.78)$$

Where  $a$  and  $\overleftrightarrow{\mathbf{a}}$  are a scalar and a matrix, respectively. The exponential matrix  $e^{\overleftrightarrow{\mathbf{a}}}$  on the right hand side of Eq. (3.78) is obtained by diagonalization of  $\overleftrightarrow{\mathbf{a}}$ .

As stated before the dynamics generated by Eqs. (3.23-3.27) or (3.35-3.38) in the *NPT* ensemble is not Hamiltonian and hence we cannot speak of symplectic integrators [100] for the  $t$ -flow's defined by Eqs. (3.76, 3.77). The symplectic condition Eq. (2.8) is violated at the level of the transformation (3.14-3.22) which is not canonical. However, the algorithms generated by Eqs. (3.76, 3.77) are time reversible and second order like the velocity Verlet. Several recent studies have shown [26, 25, 27] that these integrators for the non microcanonical ensembles are also stable for long time trajectories, as in case of the symplectic integrators for the NVE ensemble.

### 3.5 Group Scaling and Molecular Scaling

We have seen in section 3.3 that the center of mass or *molecular* pressure is equivalent to the atomic pressure. The atomic pressure is the natural quantity that enters in the virial theorem [12] irrespectively of the form of the interaction potential among the particles. So, in principle it is safer to adopt atomic scaling in the extended system constant pressure simulation. For systems in confined regions, the equivalence between atomic or true pressure and molecular pressure (see sec. 3.3) holds for any definition of the *molecular* subsystem irrespectively of the interaction potentials. In other words we could have defined virtual molecules made up of atoms selected on different *real* molecules. We may expect that, as long as the system, no matter how its unities or *particles* are defined, contains a sufficiently large number of particles, generates a distribution function identical to that generated by using the “correct” atomic scaling. From a computational standpoint molecular scaling is superior to atomic scaling. The fast varying Liouvillean in Eq. (3.70) for the atomic scaling contains the two terms  $iL_z, iL_u$ . These terms are slowly varying when molecular scaling is adopted and are assigned to the slow part of the Liouvillean in Eq. (3.69). The inner part of the time propagation is therefore expected to be more expensive for the multiple time step integration with atomic scaling rather than with molecular scaling. Generally speaking, given the equivalence between the molecular and atomic pressure, molecular scaling should be the preferred choice for maximum efficiency in the multiple time step integration.<sup>10</sup>

For large size molecules, such as proteins, molecular scaling might be inappropriate. The size of the molecule clearly restricts the number of *particles* in the MD simulation box, thereby reducing the statistics on the instantaneous calculated molecular pressure which may show nonphysical large fluctuations. Group scaling [27] is particularly convenient for handling the simulation of macromolecules. A statistically significant number of groups can be selected in order to avoid all problems related to the poor statistics on molecular pressure calculation for samples containing a small number of large size particles. Notwithstanding, for *solvated* biomolecules and provided that enough solvent molecules are included, molecular scaling again yields reliable results. In Ref. [27] Marchi and Procacci showed that the scaling method in the *NPT* ensemble does not affect neither the equilibrium structural and dynamical properties nor the kinetic of non equilibrium MD. For group-based and molecular-based scaling methods in a system of one single molecule of BPTI embedded in a box of about a 1000 water molecules, they obtained identical results for the system volume, the Voronoi volumes of the proteins and for the mean square displacement of both solvent and protein atoms under normal and high pressure.

### 3.6 Switching to Other Ensembles

The *NPT* extended system is the most general among all possible extended Lagrangians. All other ensemble can be in fact obtained within the same computational framework. We must stress [27] that the computational overhead of the extended system formulation, due to the introduction and handling of the extra degrees of freedom of the barostat and thermostat variables, is rather modest and is negligible with respect to a *NVE* simulation for large samples ( $N_f > 2000$ ) [26, 25, 27]. Therefore, a practical, albeit inelegant way of switching among ensembles is simply to set the inertia of the barostat and/or thermostat to a very large number. This must be of course equivalent to decouple the barostat and/or the thermostat from the true degrees of freedom. In fact, by setting  $W$  to infinity<sup>11</sup> in Eqs. (3.23-3.27) we recover the *NVT* canonical ensemble equations of motion. Putting instead  $Q$  to infinity the *NPH* equations of motion are obtained. Finally, setting both  $W$  and  $Q$  to infinity the *NVE* equations of motion are recovered.

Switching to the *NPT* isotropic stress ensemble is less obvious. One may define the kinetic term

<sup>10</sup>There are also other less material reasons to prefer molecular scaling: atomic scaling and molecular scaling yield different dynamical properties because the equations of motions are different. Dynamical data computed via extended system simulations should always be taken with caution. With respect to pure Newtonian dynamics, however, the *NPT* dynamical evolution is slightly modified by a barostat coupled to the molecular center of mass [26] but is brutally damaged when the barostat is coupled to the fast degrees of freedom. For example in liquid flexible nitrogen at normal pressure and 100 K, atomic scaling changes the internal frequency by  $20 \text{ cm}^{-1}$  while no changes are detected when the barostat is coupled to the centers of mass.

<sup>11</sup>The value of  $W$  which works as “infinity” depends on the “force” that is acting on barostat coordinate expressed by the Eq. (3.25), i.e. on how far the system is from the thermodynamic equilibrium. For a system near the thermodynamic equilibrium with  $N_f \simeq 10000$  a value of  $W = 10^{20}$  a.m.u. is sufficient to prevent cell fluctuations.

associated to barostat in the extended Lagrangian as

$$K = \frac{1}{2} \sum_{\alpha\beta} W_{\alpha\beta} s^2 \dot{h}_{\alpha\beta}^2 \quad (3.79)$$

such that a different inertia may in principle be assigned to each of 9 extra degrees of freedom of the barostat. Setting for example

$$W_{\alpha\beta} = W \quad \text{for } \alpha \leq \beta \quad (3.80)$$

$$W_{\alpha\beta} = \infty \quad \text{for } \alpha > \beta \quad (3.81)$$

$$(3.82)$$

one inhibits cell rotations [27].

This trick does not work, unfortunately, to change to isotropic stress tensor. In this case, there is only one independent barostat degrees of freedom, namely the volume of the system. In order to simulate isotropic cell fluctuations a set of five constraints on the  $\mathbf{h}$  matrix are introduced which correspond to the conditions:

$$\begin{aligned} \frac{h_{\alpha\beta}}{h_{11}} - \frac{h_{\alpha\beta}^0}{h_{11}^0} &= 0 \\ \dot{h}_{\alpha\beta} - \frac{h_{\alpha\beta}^0}{h_{11}^0} \dot{h}_{11} &= 0 \quad \text{for } \alpha \leq \beta \end{aligned} \quad (3.83)$$

with  $\mathbf{h}^0$  being some reference  $\mathbf{h}$  matrix. These constraints are implemented naturally in the framework of the multi time step velocity Verlet using the RATTLE algorithm which evaluates iteratively the constraints force to satisfy the constraints on both coordinates  $\mathbf{h}$  and velocities  $\dot{\mathbf{h}}$  [27]. In Ref. [27] it is proved that the phase space sampled by the *NPT* equations with the addition of the constraints Eq. (3.83) correspond to that given by *NPT* distribution function.



## Chapter 4

# Multiple Time Steps Algorithms For Large Size Flexible Systems with Strong Electrostatic Interactions

In the previous sections we have described how to obtain multiple time step integrators *given* a certain potential subdivision and have provided simple examples of potential subdivision based on the inter/intra molecular separation. Here, we focus on the time scale separation of model potentials of complex molecular systems. Additionally, we provide a general potential subdivision applying to biological systems, as well as to many other interesting chemical systems including liquid crystals. This type of systems are typically characterized by high flexibility and strong Coulombic intermolecular interactions. Schematically, we can then write the potential  $V$  as due to two contributions:

$$V = V_{\text{bnd}} + V_{\text{nbnd}}. \quad (4.1)$$

Here, the “bonded” or intramolecular part  $V_{\text{bnd}}$  is fast and is responsible for the flexibility of the system. The “non bonded” or intermolecular (or intergroup) term  $V_{\text{nbnd}}$  is dominated by Coulombic interactions. The aim of the following sections is to describe a general protocol for the subdivision of such forms of the interaction potential and to show how to obtain reasonably efficient and transferable multiple time step integrators valid for any complex molecular system.

### 4.1 Subdivision of the “Bonded” Potential

As we have seen in Sec. 2.3 the idea behind the multiple time step scheme is that of the reference system which propagates for a certain amount of time under the influence of some *unperturbed* reference Hamiltonian, and then undergoes an impulsive *correction* brought by the remainder of the potential. The exact trajectory spanned by the complete Hamiltonian is recovered by applying this impulsive correction onto the “reference” trajectory. We have also seen in the same section that, by subdividing the interaction potential, we can determine as many “nested” reference systems as we wish. The first step in defining a general protocol for the subdivision of the bonded potential for complex molecular systems consists in identifying the various time scales and their connection to the potential. The interaction bonded potential in almost all popular force fields is given as a function of the stretching, bending and torsion internal coordinates and has the general form

$$V_{\text{bnd}} = V_{\text{stretch}} + V_{\text{bend}} + V_{\text{tors}}, \quad (4.2)$$

where

$$\begin{aligned}
V_{\text{stretch}} &= \sum_{\text{Bonds}} K_r (r - r_0)^2 \\
V_{\text{bend}} &= \sum_{\text{Angles}} K_\theta (\theta - \theta_0)^2. \\
V_{\text{tors}} &= \sum_{\text{Dihedrals}} V_\phi [1 + \cos(n\phi - \gamma)].
\end{aligned} \tag{4.3}$$

Here,  $K_r$  and  $K_\theta$  are the bonded force constants associated with bond stretching and angles bending respectively, while  $r_0$  and  $\theta_0$  are their respective equilibrium values. In the torsional potential,  $V_{\text{tors}}$ ,  $\phi$  is the dihedral angle, while  $K_\phi$ ,  $n$  and  $\gamma$  are constants.

The characteristic time scale of a particular internal degrees of freedom can be estimated assuming that this coordinate behaves like a harmonic oscillator, uncoupled from the rest of the other internal degrees of freedom. Thus, the criterion for guiding the subdivision of the potential in Eq. (4.2) is given by the characteristic frequency of this uncoupled oscillator. We now give, for each type of degree of freedom, practical formula to evaluate the harmonic frequency from the force field constants given in Eq. (4.3).

**Stretching:** The stretching frequencies are given by the well known expression

$$\nu_s = \frac{1}{2\pi} \left( \frac{K_r}{\mu} \right)^{(1/2)}, \tag{4.4}$$

where  $\mu$  is reduced mass.

**Bending:** We shall assume for the sake of simplicity that the *uncoupled* bending frequencies depends on the masses of the atom 1 and 3 (see Fig. 4.1), that is mass 2 is assumed to be infinity. This turns out to be in general an excellent approximation for bending involving hydrogen and a good approximation for external bendings in large molecules involving masses of comparable magnitude. The frequency is obtained by writing the Lagrangian in polar coordinates for the mechanical system depicted in Fig. 4.1. The Cartesian coordinates are expressed in terms of the polar coordinates as

$$x_1 = -r_{12} \sin(\alpha/2) \quad y_1 = r_{12} \cos(\alpha/2) \tag{4.5}$$

$$x_3 = r_{32} \sin(\alpha/2) \quad y_3 = r_{32} \cos(\alpha/2) \tag{4.6}$$

where the distance  $r_{32}$  and  $r_{12}$  are constrained to the equilibrium values. The velocities are then

$$\dot{x}_1 = -r_{12} \cos(\alpha/2) \frac{\dot{\alpha}}{2} \quad \dot{y}_1 = -r_{12} \sin(\alpha/2) \frac{\dot{\alpha}}{2} \tag{4.7}$$

$$\dot{x}_3 = r_{32} \cos(\alpha/2) \frac{\dot{\alpha}}{2} \quad \dot{y}_3 = -r_{32} \sin(\alpha/2) \frac{\dot{\alpha}}{2} \tag{4.8}$$

The Lagrangian for the uncoupled bending is then

$$\mathcal{L} = \frac{1}{2} (m_1 \dot{x}_1^2 + m_1 \dot{y}_1^2 + m_3 \dot{x}_3^2 + m_3 \dot{y}_3^2) - V_{\text{bend}} \tag{4.9}$$

$$= \frac{1}{8} (m_1 r_{12}^2 + m_3 r_{32}^2) \dot{\alpha}^2 - \frac{1}{2} k_\theta (\alpha - \alpha_0)^2. \tag{4.10}$$

The equation of motion  $\frac{d}{dt} \frac{\partial \mathcal{L}}{\partial \dot{\alpha}} - \frac{\partial \mathcal{L}}{\partial \alpha} = 0$  for the  $\alpha$  coordinate is given by

$$\ddot{\alpha} + \frac{4K_\theta}{I_b} (\alpha - \alpha_0)^2 = 0. \tag{4.11}$$

Where,  $I_b = m_1 r_{12}^2 + m_3 r_{32}^2$  is the moment of inertia about an axis passing by atom 3 and perpendicular to the bending plane. Finally, the *uncoupled* bending frequency is given by

$$\nu_b = \frac{1}{2\pi} \left( \frac{4K_\theta}{m_1 r_{12}^2 + m_3 r_{32}^2} \right)^{(1/2)} \tag{4.12}$$

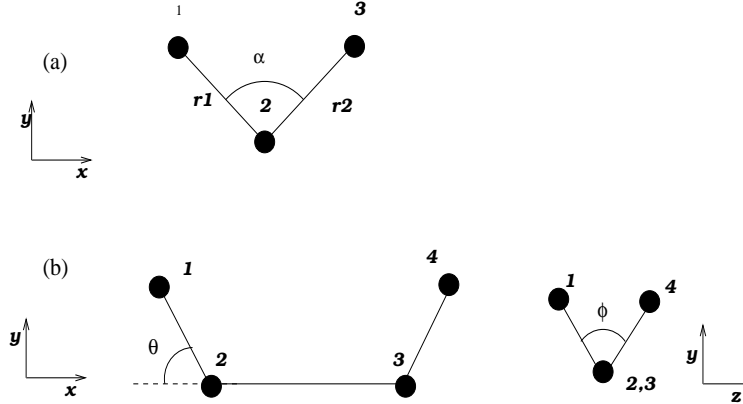


Figure 4.1: Bending and dihedral angles

**Torsion:** We limit our analysis to a purely torsional system (see Fig. 4.1b) where atoms 2 and 3 are held fixed, and all bond distances and the angle  $\theta$  are constrained to their equilibrium values. The system has only one degree of freedom, the dihedral angle  $\phi$  driven by the torsional potential  $V_\phi$ . Again we rewrite the kinetic energy in terms of the bond distances, the dihedral angle and the constant bend angle  $\theta$ . For the kinetic energy, the only relevant coordinates are now those of atoms 1 and 4:

$$\begin{aligned} x_1 &= -d_{12} \cos \theta + \frac{d_{23}}{2} & x_4 &= d_{34} \cos \theta + \frac{d_{23}}{2} \\ y_1 &= d_{12} \sin \theta \cos(\phi/2) & y_4 &= d_{34} \sin \theta \cos(\phi/2) \\ z_1 &= -d_{12} \sin \theta \sin(\phi/2) & z_4 &= d_{34} \sin \theta \sin(\phi/2). \end{aligned} \quad (4.13)$$

The Lagrangian in terms of the dihedral angle coordinate is then

$$\mathcal{L} = \frac{1}{8} I_t \dot{\phi}^2 - V_\phi [1 + \cos(n\phi - \gamma)], \quad (4.14)$$

where

$$I_t = \sin^2 \theta (m_1 d_{12}^2 + m_4 d_{34}^2). \quad (4.15)$$

Assuming small oscillations, the potential may be approximated by a second order expansion around the corresponding equilibrium dihedral angle  $\phi_0$

$$V_{tors} = \frac{1}{2} \left( \frac{\partial^2 V_{tors}}{\partial \phi^2} \right)_{\phi=\phi_0} (\phi - \phi_0)^2 = \frac{1}{2} V_\phi n^2 (\phi - \phi_0)^2 \quad (4.16)$$

Substituting (4.16) into Eq. (4.14) and then writing the Lagrange equation of motion for the coordinate  $\phi$ , one obtains again a differential equation of a harmonic oscillator, namely

$$\ddot{\phi} + \frac{4V_\phi n^2}{I_t} (\phi - \phi_0) = 0. \quad (4.17)$$

Thus, the *uncoupled* torsional frequency is given by

$$\nu_t = \frac{n}{2\pi} \left( 4 \frac{V_\phi}{\sin^2 \theta (m_1 d_{12}^2 + m_4 d_{34}^2)} \right)^{(1/2)}. \quad (4.18)$$

For many all-atom force fields, improper torsions [3, 6] are modeled using a potential identical to that of the proper torsion in Eq. (4.3) and hence in these cases Eq. (4.18) applies also to the improper torsion uncoupled frequency, provided that indices 1 and 4 refer to the *lighter* atoms. In figure (4.2) we report the distribution of frequencies for the hydrated protein Bovine Pancreatin Trypsin Inhibitor (BPTI) using the

AMBER [4] force field. The distributions might be thought as a density of the uncoupled intramolecular states of the system. As we can see in the figure there is a relevant degree of overlap for the various internal degrees of freedom. For example, “slow” degrees of freedom such as torsions may be found up to 600 wavenumber, well inside the “bending” region; these are usually improper or proper torsions involving hydrogen. It is then inappropriate to assign such “fast” torsions involving hydrogen to a slow reference system. We recall that in a multiple time simulation the integration of a supposedly slow degree of freedom with a excessively large time step is enough to undermine the entire simulation. In Fig. 4.2 we also

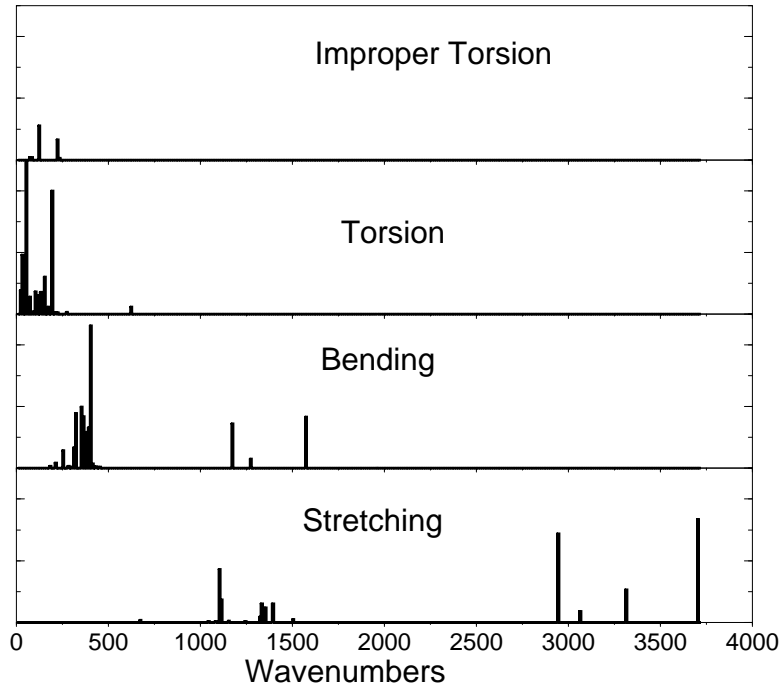


Figure 4.2: density of the uncoupled (see text) states for stretching, bending, proper and improper torsion obtained with the AMBER force field on the protein bovine pancreatic trypsin inhibitor (BPTI). Frequencies were calculated according to Eqs. (4.4,4.12,4.18)

notice that almost all the proper torsions fall below  $350 \text{ cm}^{-1}$ . An efficient and simple separation of the intramolecular AMBER potential [27] assigns all bendings stretching and the improper or proper torsions involving hydrogen to a “fast” reference system labeled  $n0$  and all proper torsions to a slower reference system labeled  $n1$ . The subdivision is then

$$\begin{aligned} V_{n0} &= V_{\text{stretch}} + V_{\text{bend}} + V_{\text{i-tors}} + V_{\text{p-tors}}^{(h)} \\ V_{n1} &= V_{\text{p-tors}} \end{aligned} \quad (4.19)$$

Where with  $V_{\text{p-tors}}^{(h)}$  we indicate proper torsions involving hydrogen. For the reference system  $V_{n0}$ , the hydrogen stretching frequencies are the fastest motions and the  $\Delta t_{n0}$  time step must be set to 0.2–0.3 fs. The computational burden of this part of the potential is very limited, since it involves mostly two or three body forces. For the reference system  $V_{n1}$ , the fastest motion is around  $300 \text{ cm}^{-1}$  and the time step  $\Delta t_{n1}$  should be set to 1–1.5 fs. The computational effort for the reference system potential  $V_{n1}$  is more important because of the numerous proper torsions of complex molecular systems which involve more expensive four body forces calculations. One may also notice that some of the bendings which were assigned to the  $n0$  reference system fall in the torsion frequency region and could be therefore integrated with a time step much larger than  $\Delta t_{n0} \simeq 0.2\text{--}0.3$ . However, in a multiple time step integration, this overlap is just inefficient, but certainly not dangerous. Indeed, no instability may derive for integrating slow degrees of freedom with exceedingly small time steps.

## 4.2 The smooth particle mesh Ewald method

Before we discuss the non bonded multiple time step separation it is useful to describe in some details one of the most advanced techniques to handle long range forces. Indeed, this type of non bonded forces are the most cumbersome to handle and deserve closer scrutiny.

In the recent literature, a variety of techniques are available to handle the problem of long range interactions in computer simulations of charged particles at different level of approximation [30, 31, 12]. In this section, we shall focus on the Ewald summation method for the treatment of long range interactions in periodic systems [32, 33, 101]. The Ewald method gives the *exact* result for the electrostatic energy of a periodic system consisting of an infinitely replicated neutral box of charged particles. The method is the natural choice in MD simulations of complex molecular system with PBC.

The Ewald potential [33] is given by

$$V'_{\text{qd}} = \frac{1}{2} \sum_{ij}^N q_i q_j \sum_n \frac{1}{|\mathbf{r}_{ij} + \mathbf{r}_n|} \text{erfc}(\alpha |\mathbf{r}_{ij} + \mathbf{r}_n|) \quad (4.20)$$

$$V_{\text{qr}} = \left[ \frac{1}{2\pi V} \sum_{\mathbf{m} \neq 0}^{\infty} \frac{\exp(-\pi^2 |\mathbf{m}|^2 / \alpha^2)}{|\mathbf{m}|^2} S(\mathbf{m}) S(-\mathbf{m}) - \frac{\alpha}{\pi^{1/2}} \sum_i q_i^2 \right] - V_{\text{intra}}. \quad (4.21)$$

with

$$S(\mathbf{m}) = \sum_i^N q_i \exp(2\pi i \mathbf{m} \cdot \mathbf{r}_i) \quad (4.22)$$

$$V_{\text{intra}} = \sum_{ij-\text{excl.}} q_i q_j \frac{\text{erf}(\alpha r_{ij})}{r_{ij}}, \quad (4.23)$$

where,  $\mathbf{r}_i$  is the vector position of the atomic charge  $q_i$ ,  $\mathbf{r}_{ij} = \mathbf{r}_i - \mathbf{r}_j$ ,  $\mathbf{r}_n$  is a vector of the direct lattice,  $\text{erfc}(x) = \pi^{-1/2} \int_x^\infty e^{-t^2} dt$  is the complementary error function,  $\text{erf}(x) = 1 - \text{erfc}(x)$ ,  $V$  the unit cell volume,  $\mathbf{m}$  a reciprocal lattice vector and  $\alpha$  is the Ewald convergence parameter. In the direct lattice part, Eq. (4.20), the prime indicates that intramolecular excluded contacts<sup>1</sup> are omitted. In addition, in Eq. (4.21) the term  $V_{\text{intra}}$  subtracts, in direct space, the intra-molecular energy between bonded pairs, which is automatically included in the right hand side of that equation. Consequently, the summation on  $i$  and  $j$  in Eq. (4.23) goes over all the excluded intra-molecular contacts. We must point out that in the Ewald potential given above, we have implicitly assumed the so-called “tin-foil” boundary conditions: the Ewald sphere is immersed in a perfectly conducting medium and hence the dipole term on the surface of the Ewald sphere is zero [33]. For increasingly large systems the computational cost of standard Ewald summation, which scales with  $N^2$ , becomes too large for practical applications. Alternative algorithms which scale with a smaller power of  $N$  than standard Ewald have been proposed in the past. Among the fastest algorithms designed for periodic systems is the particle mesh Ewald algorithm (PME)[34, 35], inspired by the particle mesh method of Hockney and Eastwood [36]. Here, a multidimensional piecewise interpolation approach is used to compute the reciprocal lattice energy,  $V_{\text{qr}}$ , of Eq. 4.21, while the direct part,  $V_{\text{qd}}$ , is computed straightforwardly. The low computational cost of the PME method allows the choice of large values of the Ewald convergence parameter  $\alpha$ , as compared to those used in conventional Ewald. Correspondingly, shorter cutoffs in the direct space Ewald sum  $V_{\text{qd}}$  may be adopted. If  $\mathbf{u}_j$  is the scaled fractional coordinate of the  $i$ -th particle, the charge weighted structure factor,  $S(\mathbf{m})$  in Eq. (4.22), can be rewritten as:

$$S(\mathbf{m}) = \sum_{j=1}^N q_j \exp \left[ 2\pi i \left( \frac{m_1 u_{j1}}{K_1} + \frac{m_2 u_{j2}}{K_2} + \frac{m_3 u_{j3}}{K_3} \right) \right]. \quad (4.24)$$

Where,  $N$  is the number of particles,  $K_1, K_2, K_3$  and  $m_1, m_2, m_3$  are integers. The  $\alpha$  component of the scaled fractional coordinate for the  $i$ -th atom can be written as:<sup>2</sup>

$$u_{i\alpha} = K_\alpha \mathbf{k}_\alpha \cdot \mathbf{r}_i, \quad (4.25)$$

<sup>1</sup>By excluded contacts we mean interactions between charges on atoms connected by bonds or two bonds apart.

<sup>2</sup>The scaled fractional coordinate is related to the scaled coordinates in Eqs (3.1,3.34) by the relation  $s_{i\alpha} = 2u_{i\alpha}/K_\alpha$ .

where  $\mathbf{k}_\alpha$ ,  $\alpha = 1, 2, 3$  are the reciprocal lattice basic vectors.

$S(\mathbf{m})$  in Eq. (4.24) can be looked at as a discrete Fourier transform (FT) of a set of charges placed irregularly within the unit cell. Techniques have been devised in the past to approximate  $S(\mathbf{m})$  with expressions involving Fourier transforms on a regular grid of points. Such approximations of the weighted structure factor are computationally advantageous because they can be evaluated by fast Fourier transforms (FFT). All these FFT-based approaches involve, in some sense, a smearing of the charges over nearby grid points to produce a regularly gridded charge distribution. The PME method accomplishes this task by interpolation. Thus, the complex exponential  $\exp(2\pi i m_\alpha u_{i\alpha}/K_\alpha)$ , computed at the position of the  $i$ -th charge in Eq. (4.24), are rewritten as a sum of interpolation coefficients multiplied by their values at the nearby grid points. In the smooth version of PME (SPME) [35], which uses cardinal B-splines in place of the Lagrangian coefficients adopted by PME, the sum is further multiplied by an appropriate factor, namely:

$$\exp(2\pi i m_\alpha u_{i\alpha}/K_\alpha) = b(m_\alpha) \sum_k M_n(u_{i\alpha} - k) \exp(2\pi i m_\alpha k/K_\alpha), \quad (4.26)$$

where  $n$  is the order of the spline interpolation,  $M_n(u_{i\alpha} - k)$  defines the coefficients of the cardinal B-spline interpolation at the scaled coordinate  $u_{i\alpha}$ . In Eq. (4.26) the sum over  $k$ , representing the grid points, is only over a finite range of integers, since the functions  $M_n(u)$  are zero outside the interval  $0 \leq u \leq n$ . It must be stressed that the complex coefficients  $b(m_i)$  are independent of the charge coordinates  $\mathbf{u}_i$  and need be computed only at the very beginning of a simulation. A detailed derivation of the  $M_n(u)$  functions and of the  $b_\alpha$  coefficients is given in Ref. [35]. By inserting Eq. (4.26) into Eq. (4.24),  $S(\mathbf{m})$  can be rewritten as:

$$S(\mathbf{m}) = b_1(m_1)b_2(m_2)b_3(m_3)\mathcal{F}[Q](m_1, m_2, m_3), \quad (4.27)$$

where  $\mathcal{F}[Q](m_1, m_2, m_3)$  stands for the discrete FT at the grid point  $m_1, m_2, m_3$  of the array  $Q(k_1, k_2, k_3)$  with  $1 \leq k_i \leq K_i$ ,  $i = 1, 2, 3$ . The gridded charge array,  $Q(k_1, k_2, k_3)$ , is defined as:

$$Q(k_1, k_2, k_3) = \sum_{i=1, N} q_i M_n(u_{i1} - k_1) M_n(u_{i2} - k_2) M_n(u_{i3} - k_3) \quad (4.28)$$

Inserting the approximated structure factor of Eq. (4.27) into Eq. (4.21) and using the fact that  $\mathcal{F}[Q](-m_1, -m_2, -m_3) = K_1 K_2 K_3 \mathcal{F}^{-1}[Q](m_1, m_2, m_3)$ , the SPME reciprocal lattice energy can be then written as

$$\begin{aligned} V_{\text{qr}} &= \frac{1}{2} \sum_{m_1=1}^{K_1} \sum_{m_2=1}^{K_2} \sum_{m_3=1}^{K_3} B(m_1, m_2, m_3) C(m_1, m_2, m_3) \times \\ &\times \mathcal{F}[Q](m_1, m_2, m_3) \mathcal{F}[Q](-m_1, -m_2, -m_3) \end{aligned} \quad (4.29)$$

$$\begin{aligned} &= \frac{1}{2} \sum_{m_1=1}^{K_1} \sum_{m_2=1}^{K_2} \sum_{m_3=1}^{K_3} \mathcal{F}^{-1}[\Theta_{\text{rec}}](m_1, m_2, m_3) \mathcal{F}[Q](m_1, m_2, m_3) \times \\ &\times K_1 K_2 K_3 \mathcal{F}^{-1}[Q](m_1, m_2, m_3), \end{aligned} \quad (4.30)$$

with

$$B(m_1, m_2, m_3) = |b_1(m_1)|^2 |b_2(m_2)|^2 |b_3(m_3)|^2 \quad (4.31)$$

$$C(m_1, m_2, m_3) = (1/\pi V) \exp(-\pi^2 \mathbf{m}^2 / \alpha^2) / \mathbf{m}^2 \quad (4.32)$$

$$\Theta_{\text{rec}} = \mathcal{F}[BC]. \quad (4.33)$$

Using the convolution theorem for FFT the energy (4.30) can be rewritten as

$$V_{\text{qr}} = \frac{1}{2} \sum_{m_1=1}^{K_1} \sum_{m_2=1}^{K_2} \sum_{m_3=1}^{K_3} \mathcal{F}^{-1}[\Theta_{\text{rec}} \star Q](m_1, m_2, m_3) \mathcal{F}[Q](m_1, m_2, m_3) \quad (4.34)$$

We now use the identity  $\sum_{\mathbf{m}} F(A)(\mathbf{m})B(\mathbf{m}) = \sum_{\mathbf{m}} A(\mathbf{m})F(B)(\mathbf{m})$  to arrive at

$$V_{\text{qr}} = \frac{1}{2} \sum_{m_1=1}^{K_1} \sum_{m_2=1}^{K_2} \sum_{m_3=1}^{K_3} (\Theta_{\text{rec}} \star Q)(m_1, m_2, m_3) Q(m_1, m_2, m_3) \quad (4.35)$$

We first notice that  $\Theta_{rec}$  does not depend on the charge positions and that  $M_n(u_{i\alpha} - k)$  is differentiable for  $n > 2$  (which is always the case in practical applications). Thus the force on each charge can be obtained by taking the derivative of Eq. (4.35), namely

$$F_{i\alpha}^{(qr)} = -\frac{\partial V_{qr}}{\partial r_{i\alpha}} = \sum_{m_1=1}^{K_1} \sum_{m_2=1}^{K_2} \sum_{m_3=1}^{K_3} \frac{\partial Q(m_1, m_2, m_3)}{\partial r_{i\alpha}} (\Theta_{rec} \star Q)(m_1, m_2, m_3). \quad (4.36)$$

In practice, the calculation is carried out according to the following scheme: i) At each simulation step one computes the grid scaled fractional coordinates  $u_{i\alpha}$  and fills an array with  $Q$  according to Eq. (4.28). At this stage, the derivative of the  $M_n$  functions are also computed and stored in memory. ii) The array containing  $Q$  is then overwritten by  $\mathcal{F}[Q]$ , i.e.  $Q$ 's 3-D Fourier transform. iii) Subsequently, the electrostatic energy is computed via Eq. (4.30). At the same time, the array containing  $\mathcal{F}[Q]$  is overwritten by the product of itself with the array containing  $BC$  (computed at the very beginning of the run). iv) The resulting array is then Fourier transformed to obtain the convolution  $\Theta_{rec} \star Q$ . v) Finally, the forces are computed via Eq. (4.36) using the previously stored derivatives of the  $M_n$  functions to recast  $\partial Q/\partial r_{i\alpha}$ .

The memory requirements of the SPME method are limited.  $2K_1K_2K_3$  double precision real numbers are needed for the grid charge array  $Q$ , while the calculation of the functions  $M_n(u_{i\alpha} - j)$  and their derivatives requires only  $6 \times n \times N$  double precision real numbers. The  $K_\alpha$  integers determines the fineness of the grid along the  $\alpha$ -th lattice vector of the unit cell. The output accuracy of the energy and forces depends on the SPME parameters: The  $\alpha$  convergence parameter, the grid spacing and the order  $n$  of the B-spline interpolation. For a typical  $\alpha \simeq 0.4 \text{ \AA}^{-1}$  a relative accuracies between  $10^{-4} - 10^{-5}$  for the electrostatic energy are obtained when the grid spacing is around  $1 \text{ \AA}$  along each axis, and the order  $n$  of the B-spline interpolation is 4 or 5. A rigorous error analysis and a comparison with standard Ewald summation can be found in Refs. [35] and [102]. For further readings on the PME and SPME techniques we refer to the original papers [34, 102, 29, 35].

#### PME tests on 5CB

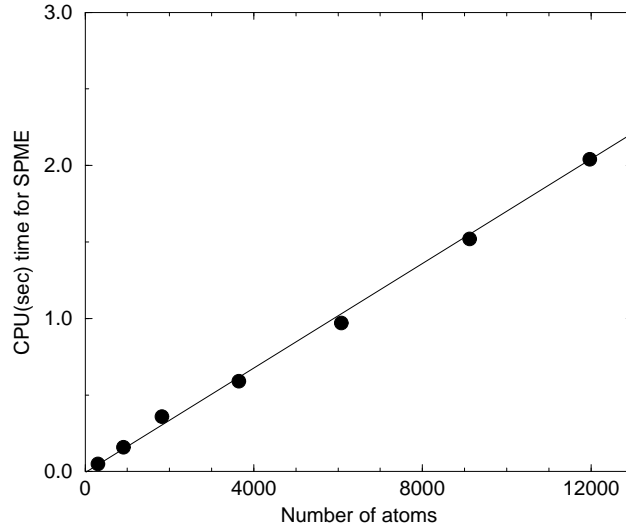


Figure 4.3: CPU time versus number of particles for the SPME algorithm as measured on a 43P/160MH IBM workstation

The power of the SPME algorithm, compared to the straightforward implementation of the standard Ewald method, is indeed astonishing. In Fig. (4.3) we report CPU timing obtained on a low end 43P/160MH IBM workstation for the evaluation of the reciprocal lattice energy and forces via SPME for cyanobiphenil as a function of the number of atoms in the system. Public domain 3-D FFT routines were used. The algorithm is practically linear and for 12,000 particles SPME takes only 2 CPU seconds to perform the calculation. A standard Ewald simulation for a box  $64 \times 64 \times 64 \text{ \AA}^3$  (i.e. with a grid spacing

in  $k$  space of  $k = 2\pi/64 \simeq 0.01 \text{ \AA}^{-1}$ ) for the same sample and at the same level of accuracy would have taken several minutes.

### 4.3 Subdivision the Non Bonded Potential

In addition to the long range electrostatic contributions,  $V_{qr}$  and  $V_{qd}$ , given in Eqs. (4.20,4.21), more short range forces play a significant role in the total non bonded potential energy. The latter can be written as:

$$V_{nbn} = V_{vdw} + V_{qr} + V_{qd} + V_{14}. \quad (4.37)$$

Where,  $V_{vdw}$  is the Lennard-Jones potential, namely

$$V_{vdw} = \sum_{i < j}^{N'} 4\epsilon_{ij} \left[ \left( \frac{\sigma_{ij}}{r_{ij}} \right)^{12} - \left( \frac{\sigma_{ij}}{r_{ij}} \right)^6 \right]. \quad (4.38)$$

Here, the prime on the sum indicates that interactions between atoms separated by less than three consecutive bonds must be omitted. The term  $V_{14}$  is typical for force fields of complex molecular systems [3, 5]. While non bonded forces between atoms involved in the same covalent bond or angle bending interaction are generally excluded, the potential between atoms separated by three covalent bonds is retained and readjusted in various ways. In all cases, the  $V_{14}$  term remains in general a very stiff and, hence, a fast varying term. The computational cost of the  $V_{14}$  contribution is very small compared to other non bonded interactions. Thus, it is safer to assign this potential term to the slowest intramolecular reference system potential  $V_{n1}$  of Eq. (4.19).

The  $V_{qr}$  reciprocal lattice term, *including* the correction due to the excluded or partially excluded (i.e. the electrostatic part of  $V_{14}$ ) interactions cannot be split when using SPME and must be assigned altogether to only one reference system. The time scale of the potential  $V_{qr}$  depends on the convergence parameter  $\alpha$ . Indeed, this constant controls the relative weights of the reciprocal lattice energy  $V_{qr}$ , and of the direct lattice energy  $V_{qd}$ . By increasing  $\alpha$ , one increases the weight of the reciprocal lattice contribution  $V_{qr}$  to the total Coulomb energy. When using SPME the cost of the reciprocal lattice sums is cut down dramatically and, therefore, the use of *large*  $\alpha$ 's becomes helpful to reduce the computational burden of the direct lattice calculation. For a value of  $\alpha$  increased beyond a certain limit, there is no longer a computational gain, since the pair distances must always be evaluated in direct space until convergence of the Lennard-Jones energy (usually occurring at a 10  $\text{\AA}$  cutoff). Furthermore, the larger is  $\alpha$ , the more short-ranged and fast varying becomes the potential  $V_{qr}$ , thus requiring short time steps to integrate correctly the equations of motion. A good compromise for  $\alpha$ , valid for cell of any shape and size, is  $\alpha = 0.4-0.5$ .

The direct space potential is separated [13, 27] in three contributions according to the interaction distance. The overall non bonded potential breakup is therefore

$$\begin{aligned} V_{n1} &= V_{14} \\ V_m &= V_{vdw}^{(1)} + V_{qd}^{(1)} \\ V_l &= V_{vdw}^{(2)} + V_{qd}^{(2)} + V_{qr} \\ V_h &= V_{vdw}^{(3)} + V_{qd}^{(3)} \end{aligned} \quad (4.39)$$

where the superscripts  $m, l, h$  of the direct space term  $V_{vdw}$  and  $V_{qd}$  refer to the short, medium and long range non-bonded interactions, respectively. The  $m$ -th reference system includes non-bonded direct space interactions at short range, typically between 0 to 4.3-5.3  $\text{\AA}$ .  $V_l$  contains both the medium range direct space potential, with a typical range of 4.3-5.3 to 7.3-8.5  $\text{\AA}$ , and the reciprocal space term,  $V_{qr}$ . Finally, the  $h$ -th reference system, which is the most slowly varying contains, the remaining direct space interactions from 7.3-8.5  $\text{\AA}$  to cutoff distance. As the simulations proceeds the particles seen by a target particle may cross from one region to an other, while the number of two body contacts in one distance class [19] or reference system potential must be continuously updated. Instabilities caused by this flow across potential shell boundaries are generally handled by multiplying the pair potential by a group-based switching function [24]<sup>3</sup>. Thus, at any distance  $r$  the direct space potential  $V$  can be written schematically

<sup>3</sup>Here, the word group has a different meaning than in Sec. 3 and stands for sub ensemble of contiguous atoms defined as having a total charge of approximately zero.



as:

$$V = V_1 + V_2 + V_3 \quad (4.40)$$

with

$$V_1 = VS_1 \quad (4.41)$$

$$V_2 = V(S_2 - S_1) \quad (4.42)$$

$$V_3 = V(S_3 - S_2) \quad (4.43)$$

$$(4.44)$$

where  $S_j$  is the switching function for the three shells,  $j = m, l, h$  defined as:

$$S_j(R) = \begin{cases} 1 & R_{j-1} \leq R < R_j \\ S_{3p}^{(j)} & R_j \leq R < R_j + \lambda_j \\ 0 & R_j + \lambda_j < R. \end{cases} \quad (4.45)$$

Here,  $R$  is the intergroup distance and  $\lambda_j$  is the healing interval for the  $j$ -th shell. While  $R_0$  is zero,

Table 4.1: Potential breakup and relative time steps for complex systems with interactions modeled by the AMBER[4] force field and electrostatic computed using the SPME method

Component	Contributions	Spherical Shells	Time step
$V_{n0}$	$V_{\text{stretch}} + V_{\text{bend}} + V_{\text{i-tors}} + V_{\text{p-tors}}^{(h)}$	-	$\Delta t_{n0} = 0.33 \text{ fs}$
$V_{n1}$	$V_{\text{p-tors}} + V_{14}$	-	$\Delta t_{n1} = 1.0 \text{ fs}$
$V_m$	$V_{\text{LJ}}^{(1)} + V_{\text{qd}, \alpha=0.43}^{(1)}$	$0 < r < 4.5 \text{ \AA}$	$\Delta t_m = 2.0 \text{ fs}$
$V_l$	$V_{\text{LJ}}^{(2)} + V_{\text{qd}, \alpha=0.43}^{(2)} + V_{\text{qr}, \alpha=0.43}$	$4.5 \leq r < 7.5 \text{ \AA}$	$\Delta t_l = 4.0 \text{ fs}$
$V_h$	$V_{\text{LJ}}^{(3)} + V_{\text{qd}, \alpha=0.43}^{(3)}$	$7.5 \leq r < 10.0 \text{ \AA}$	$\Delta t_h = 12.0 \text{ fs}$

$R_1 = R_m$ ,  $R_2 = R_l$ , and  $R_3 = R_h$  are the short, medium, long range shell radius, respectively. The switching  $S_{3p}^{(j)}(R)$  is 1 at  $R_j$  and goes monotonically to 0 at  $R_j + \lambda_j$ . Provided that  $S_{3p}^{(j)}$  and its derivatives are continuous at  $R_j$  and  $R_j + \lambda_j$ , the analytical form of  $S_{3p}$  in the healing interval is arbitrary [16, 20, 24, 13]. The full breakup for an AMBER type force field along with the integration time steps, valid for any complex molecular system with strong electrostatic interactions, is summarize in table II. The corresponding five time steps integration algorithm for the NVE ensemble is given by

$$e^{iL\Delta t_h} = \exp \left[ -\frac{\partial V_h}{\partial \mathbf{r}_i} \frac{\partial}{\partial \mathbf{p}_i} \frac{\Delta t_h}{2} \right] \cdot \left\{ \exp \left[ -\frac{\partial V_l}{\partial \mathbf{r}_i} \frac{\partial}{\partial \mathbf{p}_i} \frac{\Delta t_l}{2} \right] \left\{ \exp \left[ -\frac{\partial V_m}{\partial \mathbf{r}_i} \frac{\partial}{\partial \mathbf{p}_i} \frac{\Delta t_m}{2} \right] \right. \right. \\ \left. \left\{ \exp \left[ -\frac{\partial V_{n1}}{\partial \mathbf{r}_i} \frac{\partial}{\partial \mathbf{p}_i} \frac{\Delta t_{n1}}{2} \right] \left\{ \exp \left[ -\frac{\partial V_{n0}}{\partial \mathbf{r}_i} \frac{\partial}{\partial \mathbf{p}_i} \frac{\Delta t_{n0}}{2} \right] \exp \left[ \dot{\mathbf{r}}_i \frac{\partial}{\partial \mathbf{r}_i} \Delta t_0 \right] \right. \right. \right. \\ \left. \left. \exp \left[ -\frac{\partial V_{n0}}{\partial \mathbf{r}_i} \frac{\partial}{\partial \mathbf{p}_i} \frac{\Delta t_{n0}}{2} \right] \right\}^{n_{n0}} \exp \left[ -\frac{\partial V_{n1}}{\partial \mathbf{r}_i} \frac{\partial}{\partial \mathbf{p}_i} \frac{\Delta t_{n1}}{2} \right] \right\}^{n_{n1}} \right. \\ \left. \exp \left[ -\frac{\partial V_m}{\partial \mathbf{r}_i} \frac{\partial}{\partial \mathbf{p}_i} \frac{\Delta t_m}{2} \right] \right\}^{n_m} \exp \left[ -\frac{\partial V_l}{\partial \mathbf{r}_i} \frac{\partial}{\partial \mathbf{p}_i} \frac{\Delta t_l}{2} \right] \right\}^{n_l} \exp \left[ -\frac{\partial V_h}{\partial \mathbf{r}_i} \frac{\partial}{\partial \mathbf{p}_i} \frac{\Delta t_h}{2} \right],$$

where  $n_l = \Delta t_h / \Delta t_l$ ,  $n_m = \Delta t_l / \Delta t_m$ ,  $n_{n1} = \Delta t_m / \Delta t_{n1}$ ,  $n_{n0} = \Delta t_{n1} / \Delta t_{n0}$ . The explicit integration algorithm can be easily derived applying the five-fold discrete time propagator (4.46) to the state vector  $\{\mathbf{p}, \mathbf{q}\}$  at time 0 using the rule Eq. (2.23). The efficiency and accuracy for energy conservation of this r-RESPA symplectic and reversible integrator have been discussed extensively in Refs. [13, 2]. Extension of this subdivision to non NVE simulation is described in Ref. [27].

## 4.4 Electrostatic Corrections for the Multiple Time Step Simulation

In *flexible* molecular systems of large size, the Ewald summation presents computational problems which are crucial to constructing efficient and *stable* multiple time step integrators [103, 2]. We have seen that

intra-molecular Coulomb interactions between bonded atoms or between atoms bonded to a common atom are excluded in most of the standard force fields for protein simulation. In any practical implementation of the Ewald method, the intra-molecular energy  $V_{\text{intra}}$  is automatically included in the reciprocal space summation and is subtracted in *direct space* (see Eqs. (4.23,4.21)). In actual simulations the reciprocal space sum is computed with a finite accuracy whereas the intra-molecular term  $V_{\text{intra}}$ , due to the excluded Coulombic interactions, is computed exactly. This clearly prevents the cancellation of the intra-molecular forces and energies. When the stretching and bending forces are integrated explicitly, the intra-molecular term due to the excluded contacts varies rapidly with time and so does the cancellation error. Consequently, instability may be observed when integrating the reciprocal lattice forces in reference systems with large time steps. The correction due to the truncation can be evaluated by approximating the reciprocal lattice sum for the excluded contacts in Eq. (4.21) to an integral in the 3-dimensional  $k$  space and evaluating this integral from the cutoff  $k_{\text{cut}} \equiv 2\pi|\mathbf{m}|_{\text{max}}$  to infinity in polar coordinates. The neglected reciprocal lattice intra-molecular energy is then [104]

$$V_{\text{corr}} = \frac{\alpha}{\pi^{1/2}} \text{erfc}(k_{\text{cut}}/2\alpha) \sum_i q_i^2 + \sum_{ij-\text{excl.}} q_i q_j \chi(r_{ij}, k_{\text{cut}}, \alpha) \quad (4.46)$$

with

$$\chi(r, k_{\text{cut}}, \alpha) = \frac{2}{\pi} \int_{k_{\text{cut}}}^{\infty} e^{-k^2/4\alpha^2} \frac{\sin(kr)}{kr} dk. \quad (4.47)$$

The first constant term in (4.46) refers to the self energy, while the second accounts for the intra-molecular excluded interactions<sup>4</sup>. This correction must be included in the same reference systems to which  $V_{\text{qr}}$  is assigned, e.g.  $V_l$  in our potential separation (see Table 2).

In principle the correction in Eq. (4.46) applies only to standard Ewald and not to the reciprocal lattice energy computed via SPME. We can still, however, use the correction Eq. (4.46), if a spherical cutoff  $k_{\text{cut}}$  is applied to SPME. This can be done easily by setting  $\exp(-\pi^2 \mathbf{m}^2 / \alpha^2) / \mathbf{m}^2 = 0$  for  $2\pi \mathbf{m} > k_{\text{cut}} \equiv f_f \pi N_f / L$  where  $L$  is the side length of the cubic box and  $N_f$  is the number of grid points in each direction. The factor  $f_f$  must be chosen slightly less than unity. This simple device decreases the effective cutoff in reciprocal space while maintaining the same grid spacing, thus reducing the B-spline interpolation error (the error in the B-spline interpolation of the complex exponential is, indeed, maximum precisely at the tail of the reciprocal sums [35]). In Ref. [104] the effect of including or not such correction in electrostatic systems using multiple time step algorithms is studied and discussed thoroughly.

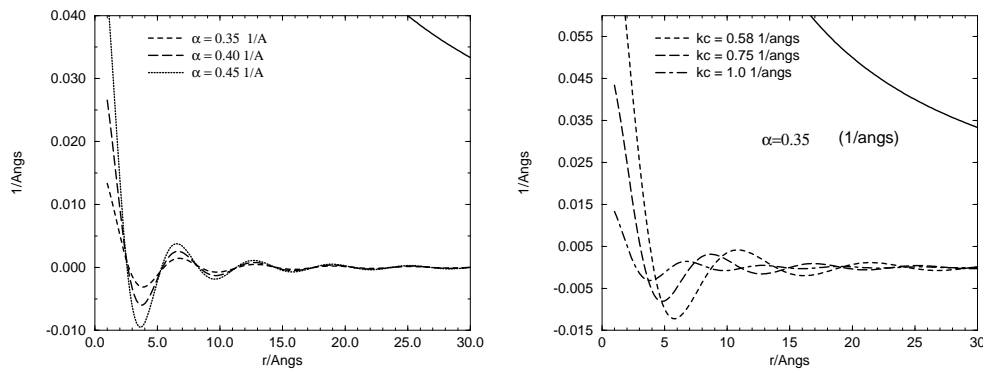


Figure 4.4: The correction potential  $\chi(r, k_c, \alpha)$  as a function of the distance for different values of the parameters  $\alpha$  (left) and  $k_c$  (right). The solid line on the top right corner is the bare Coulomb potential  $1/r$

The potential  $\chi(r, k_{\text{cut}}, \alpha)$  yields, *in direct space*, the neglected reciprocal energy due to the truncation of the reciprocal lattice sums, and must, in principle, be included for each atom pair distance in direct

<sup>4</sup>Note that  $\lim_{k \rightarrow 0} \chi(r, k, \alpha) = \text{erf}(\alpha r)/r$ .

space. Thus, the corrected direct space potential is then

$$V'_{\text{qd}} = \frac{1}{2} \sum_{ij}^N q_i q_j \left[ \sum_n \frac{\text{erfc}\alpha |\mathbf{r}_{ij} + \mathbf{r}_n|}{|\mathbf{r}_{ij} + \mathbf{r}_n|} + \chi(|\mathbf{r}_{ij} + \mathbf{r}_n|, k_{\text{cut}}, \alpha) \right] \quad (4.48)$$

which is then split as usual in short-medium-long range according to (4.39). The correction is certainly more crucial for the excluded intramolecular contacts because  $V_{\text{corr}}$  is essentially a short-ranged potential which is non negligible only for intramolecular short distances. For systems with hydrogen bonds, however, the correction is also important for intermolecular interactions.

In Fig. 4.4 the correction potential is compared to the Coulomb potential (solid line in the top right corner) for different value of the reciprocal space cutoff  $k_c$  and of the convergence parameter  $\alpha$ . For practical values of  $\alpha$  and  $k_c$ , the potential is short ranged and small compared to the bare  $1/r$  Coulomb interaction. In the asymptotic limit  $V_{\text{corr}}$  goes to zero as  $\sin(ar)/r^2$  where  $a$  is a constant. This oscillatory long range behavior of the correction potential  $V_{\text{corr}}$  is somewhat nasty: In Fig. 4.5 we show the integral

$$I(r, k_c, \alpha) = \int_0^r \chi(x, k_c, \alpha) x^2 dx \quad (4.49)$$

as a function of the distance. If this integral converges then the  $\chi(r, k)$  is absolutely convergent in 3D. We

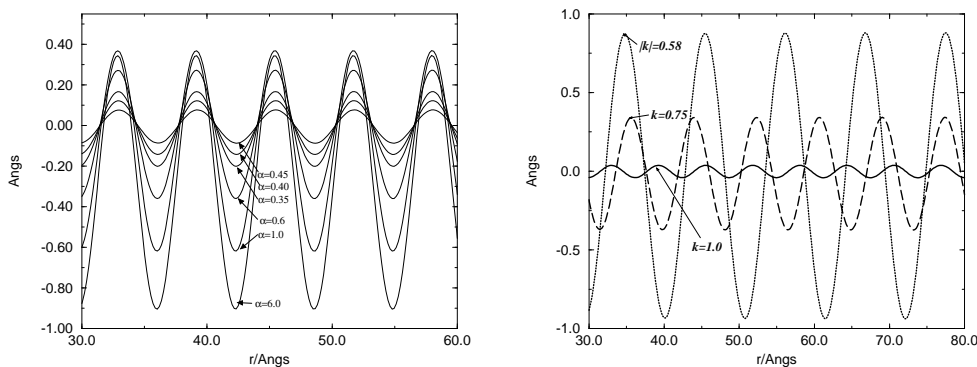


Figure 4.5: The integral  $I(r)$  of Eq. (4.49) as a function of the distance for different values of the parameters  $\alpha$  (left) and  $k_c$  (right)

see that the period of the oscillations in  $I(r)$  increases with  $k_c$  while  $\alpha$  affects only the amplitude. The total energy is hence again conditionally convergent, since the limit  $\lim_{r \rightarrow \infty} I(r)$  does not exist. However, unlike for the  $1/r$  bare potential, the energy integral remains in this case bounded. Due to this, a cutoff on the small potential  $V_{\text{corr}}$  is certainly far less dangerous than a cutoff on the bare  $1/r$  term. In order to verify this, we have calculated some properties of liquid water using the SPC model[105] from a 200 ps MD simulation in the  $NPT$  ensemble at temperature of 300 K and pressure of 0.1 MPa with i) a very accurate Ewald sum (column EWALD in Table 4.2), ii) with inaccurate Ewald but corrected in direct space using Eq. (4.48) (CORRECTED) and iii) with simple cutoff truncation of the bare Coulomb potential and no Ewald (CUTOFF). Results are reported in Table 4.2. We notice that almost all the computed properties of water are essentially independent, within statistical error, of the truncation method. The dielectric properties, on the contrary, appear very sensitive to the method for dealing with long range tails: Accurate and inaccurate Ewald (corrected in direct space through 4.48) yields, within statistical error, comparable results whereas the dielectric constant predicted by the spherical cutoff method is more than order of magnitude smaller. We should remark that method ii) (CORRECTED) is almost twice as efficient as the “exact” method i).

	EWALD	CORRECTED	CUTOFF
Coulomb energy (KJ/mole)	-55.2 $\pm$ 0.1	-55.1 $\pm$ 0.1	-56.4 $\pm$ 0.1
Potential energy (KJ/mole)	-46.2 $\pm$ 0.1	-46.1 $\pm$ 0.1	-47.3 $\pm$ 0.1
Heat Capacity (KJ/mole/K)	74 $\pm$ 24.5	94 $\pm$ 22.0	87 $\pm$ 23.2
Volume (cm <sup>3</sup> )	18.2 $\pm$ 0.1	18.3 $\pm$ 0.1	18.1 $\pm$ 0.1
Volume Fluctuation ( $\text{\AA}^3$ )	136.9 $\pm$ 3.5	147.0 $\pm$ 3.5	138.7 $\pm$ 3.5
$R_{0-0}$ ( $\text{\AA}$ )	2.81 $\pm$ 0.01	2.81 $\pm$ 0.01	2.81 $\pm$ 0.01
Dielectric constant	59 $\pm$ 25.8	47 $\pm$ 27.3	3 $\pm$ 2

Table 4.2: Properties of liquid water computed from a 200 ps simulation at 300 K and 0.1 Mpa on a sample of 343 molecules in PBC with accurate Ewald ( $\alpha = 0.35 \text{ \AA}^{-1}$ ;  $k_c = 2.8 \text{ \AA}^{-1}$ ) and no correction Eq. (4.46) (column EWALD), with inaccurate Ewald ( $\alpha = 0.35 \text{ \AA}^{-1}$ ;  $k_c = 0.9 \text{ \AA}^{-1}$ ) but including the correction Eq. (4.46) and with no Ewald and cutoff at 10.0  $\text{\AA}$ .  $R_{0-0}$  is the distance corresponding to the first peak in the Oxygen-Oxygen pair distribution function.

## Chapter 5

# The Hamiltonian Replica Exchange Method

### 5.1 Temperature REM

The Replica Exchange Method is based on multiple concurrent (parallel) canonical simulation that are allowed to occasionally exchange their configurations. For a system made of  $N$  atoms, by “configuration” we mean a state defined by a  $3N$  dimensional *coordinate* vector, independent of the momenta. Thus, in a replica exchange, only coordinates and not momenta are exchanged. In the standard implementation of the methodology, each replica, bearing a common interaction potential, is characterized by a given temperature and configurations between couple of replicas are tentatively exchanged at prescribed time intervals using a probabilistic criterion. The *target* temperature, i.e. the temperature corresponding to the thermodynamic state of interest, is usually the lowest among all replicas. In this manner, “hot” configurations from hot replicas, i.e. configurations where energy barrier are easily crossed, may be occasionally accepted at the target temperature. The canonical probability of a coordinate configuration  $X$  for  $m$ -th replica is given by

$$P_m(X) = \frac{1}{Z_m} e^{-\beta_m V(X)} \quad (5.1)$$

where  $m$  is the replica index,  $\beta^{-1} = k_B T$ ,  $V(x)$  is the potential of the system, and  $Z_m = \int e^{-\beta_m V(X)} dX$  is the configurational partition function for  $m$ -th replica. Being the  $M$  replicas independent, the probability distribution for a generic configuration of the  $M$ -fold extended system  $\mathbf{X} = (X_1, \dots, X_M)$  is

$$P_{\mathbf{X}} = \prod_m^M P_m(X_m) \quad (5.2)$$

As stated above, the global state  $\mathbf{X}$  of the extended system may evolve in two ways: i) by evolving each replica independently (i.e. via MC or MD simulation protocols) and ii) by exchanging the configurations of two replicas. Regarding the second mechanism, we introduce the transition probability  $W(X, \beta_m; X', \beta_n)$  for the exchange between the configuration  $X$  of replica at  $T_m$  and the configuration  $X'$  for the replica  $T_n$ . The probability for the inverse exchange is clearly given by  $W(X', \beta_m; X, \beta_n)$ . The detailed balance condition on the extended system for this kind of moves is given by

$$P_{\mathbf{X}}(\dots, X, \beta_m, X', \beta_n, \dots) W(X, \beta_m; X', \beta_n) = \quad (5.3)$$

$$P_{\mathbf{X}'}(\dots, X', \beta_m; X, \beta_n, \dots) W(X', \beta_m; X, \beta_n) \quad (5.4)$$

which, using the expressions 5.2 and 5.1 for the global probability, is satisfied if the transition probability satisfies the equation

$$\frac{W(X, \beta_m, X', \beta_n)}{W(X', \beta_m; X, \beta_n)} = e^{-(\beta_m - \beta_n)(E(X') - E(X))}. \quad (5.5)$$

The exchange of configurations of replicas obeying the detailed balance condition 5.5 can be as usual implemented by using the Metropolis algorithm

$$P_{\text{acc}} = \min(1, e^{-\Delta}) \quad (5.6)$$

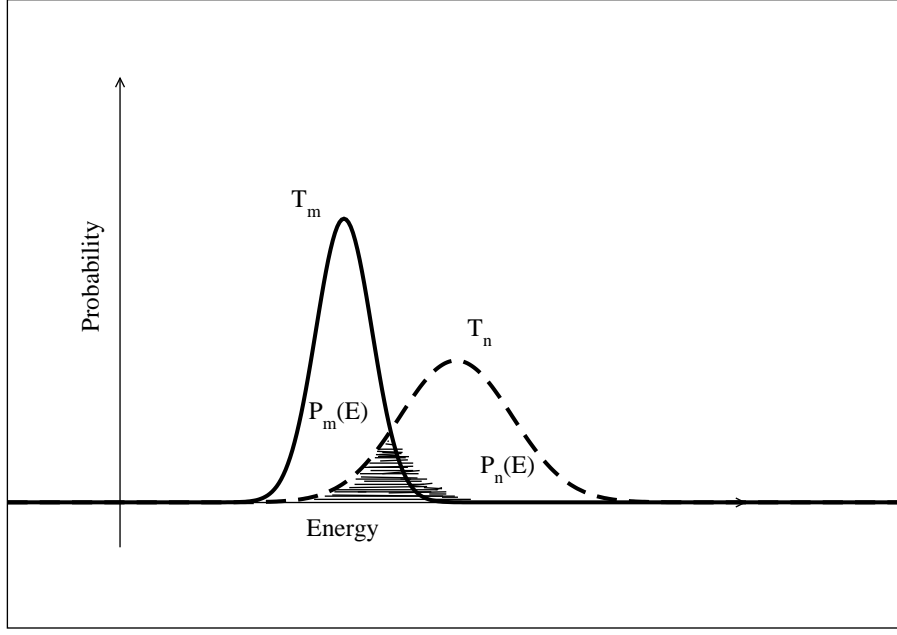


Figure 5.1: Overlapping configurational energy distribution for two replicas. The shaded area is the acceptance probability for the configuration exchange. The overlap between the two distribution is a lower bound for the acceptance probability

with  $\Delta = (\beta_m - \beta_n)(E(X') - E(X))$ . Like in a standard MC technique, because of the detailed balance condition for the extended system, the sampling in the  $\mathbf{X}$  multi-configuration space in REM evolves towards a global equilibrium defined by the multi-canonical probability distribution of the extended system Eq. 5.2.

In principle Eq. 5.6 refers to the probability of an exchange between any two replicas. In practice the exchanges are attempted between replicas that are contiguous in temperature. Let's see why. For any two replicas  $m, n$ , the total number of accepted exchanges between them is given by

$$N^{\text{acc}} = N^{\text{acc}}(\Delta E < 0) + N^{\text{acc}}(\Delta E > 0) \quad (5.7)$$

where  $\Delta E = (E(X') - E(X))$  and  $N^{\text{acc}}(\Delta E < 0)$ ,  $N^{\text{acc}}(\Delta E > 0)$  are the number of accepted exchanges for which  $\Delta E < 0$  and  $\Delta E > 0$ , respectively. When the extended system is at equilibrium, we clearly must have that

$$N^{\text{acc}}(\Delta E < 0) = N^{\text{acc}}(\Delta E > 0) \quad (5.8)$$

Inserting the above equation into Eq. 5.7, we obtain

$$N^{\text{acc}} = 2N^{\text{acc}}(\Delta E < 0) \quad (5.9)$$

Since, according to the prescription 5.6, the probability for accepting the move when  $\Delta E < 0$  is unitary, we may write that

$$\frac{N^{\text{acc}}}{N^{\text{tot}}} = 2P(\Delta E < 0) \quad (5.10)$$

where  $N^{\text{tot}}$  is the total number of attempted exchanges and  $P(\Delta E < 0)$  is the cumulative probability that a  $E(X') < E(X)$ . Eq. 5.10 states that if the two normalized (configurational) energy distribution  $P_m(E)$  of replica  $m$  and  $P_n(E)$  of replica  $n$  are identical, then the probability for a successful exchange between the two replica is equal to the area of the overlap of the two distribution (i.e. the shaded area in Fig. 5.1). If  $P_m(E)$  and  $P_n(E)$  are not identical, we have in general that the overlap of the two distribution is a lower bound for the acceptance probability (the standard deviation  $\delta E$  generally increases with the mean energy  $\bar{E}$ ). Based on the above, and assuming that  $M$ , the total number of replicas, is even, one can then set up

an exchange protocol periodically attempting  $M/2$  simultaneous contiguous replica exchanges  $m \leftrightarrow m+1$  with  $m$  odd, or  $M/2 - 1$  simultaneous contiguous replica exchanges  $m \leftrightarrow m+1$  with  $m$  even, accepting *each* of them with probability given by 5.6.

Given the above scheme, what is the optimal spacing in temperatures for enhanced sampling of the configuration space at the target temperature? First of all, the hottest temperature  $T_M$ , defining the full temperature range  $\Delta T = T_M - T_1$  of the extended system, must be clearly selected such that  $k_B T_M$  is of the order of the maximum height of the free energy barriers that must be overcome at the target temperature  $T_1$ . Concerning the temperature spacing, we have seen that acceptance probability for an exchange is larger, the larger is the overlap of the two energy distributions referring to the two contiguous replica, i.e. the closer are the temperatures. Of course, the closer are the temperatures and the larger is the number of replicas to be simulated, i.e. the heavier is the CPU cost of the simulation. For an optimal choice, we thus set

$$\bar{E}_{m+1} - \bar{E}_m = \sigma_{E_m} \quad (5.11)$$

where  $\bar{E}_m$  and  $\sigma_{E_m}$  are the mean energy and the standard deviation of energy distribution for the  $m$ -th replica. Assuming then that the system can be described by an ensemble of  $N$  harmonic oscillators, we have that  $\bar{E}_m = NkT_m$  and  $\sigma_{E_m} = cN^{1/2}k^{1/2}T_m$ .<sup>1</sup> Substituting these values in Eq. 5.11, we obtain the temperature spacing for optimal superposition:

$$\bar{T}_{m+1} - \bar{T}_m = \left( \frac{c^2}{Nk_b} \right)^{1/2} T_m \quad (5.12)$$

In the parallel implementation of the temperature REM, in order to keep the communication overhead at the lowest possible level, we standardly exchange the temperatures and not the configurations. So the  $m$ -th slave process may explore *the entire range* of temperatures. When the  $m$ -th slave process periodically writes out the coordinates of the configuration (Typically in `pdb` or `xyz` format), one must also keep track of the current temperature (the program does this automatically) in order to be able to reconstruct *a posteriori* the true  $m$ -th temperature configurational space of the  $m$ -th replica. In Fig. 5.2, we show a typical parallel REM simulation for a general system with 8 processes. In the x-axis we report the simulation time, in the left y-axis the process index and in the right y-axis the replica index which is bound to the actual temperature. Each color represents a process running in parallel with other processes with different colors. As it can be seen, on each process the temperature (i.e. the replica index) changes continuously. So, for example the configurational sampling of the replica at the lowest temperature in the given time interval must be reconstructed combining the data for the slave processes 1,2,3,4,6. If the algorithm is working properly, (i.e. if the temperature spacing is chosen correctly and if there are no phase transition between  $T_1$  and  $T_M$ ), the temperature in each parallel process must perform a random walk in the temperature domain  $[T_1, T_M]$ .

Going back to equation 5.12, two important issues must be stressed: i) the temperature spacing for optimal overlap between contiguous replicas while keeping the total number of replicas not too high, is not uniform but grows with the replica temperature; ii) the temperature spacing between contiguous replicas must be decreased with increasing number of degrees of freedom. The latter is indeed a severe limitation of the standard REM technology, since, as the size of the system grows, a larger number of replicas must be employed for preserving a significant exchange acceptance probability. This is due to the inescapable fact that the energy fluctuations grow with  $N^{1/2}$  while the energy grows with  $N$ . Moreover, in many important cases, one has to effectively sample reaction coordinates that are rather localized in the protein, like e.g. in the case of substrate-active site interactions. In the standard temperature REM, the extra heat in the hot replicas is clearly distributed among *all the degrees of freedom* of the system and therefore *most* of this heat is uselessly used for exchanging uninteresting configurations (e.g. solvent configurations).

## 5.2 Hamiltonian REM

In this program we adopt a variant of the replica exchange called Hamiltonian REM, that is far more flexible than the standard temperature REM technique illustrated above. In the Hamiltonian REM, each replica is

---

<sup>1</sup>In the latter equation  $c$  is a constant that depends on the density of states of the  $N$  harmonic oscillators and  $c^2 N = C_v$  with  $C_v$  being the constant volume heat capacity of the system.

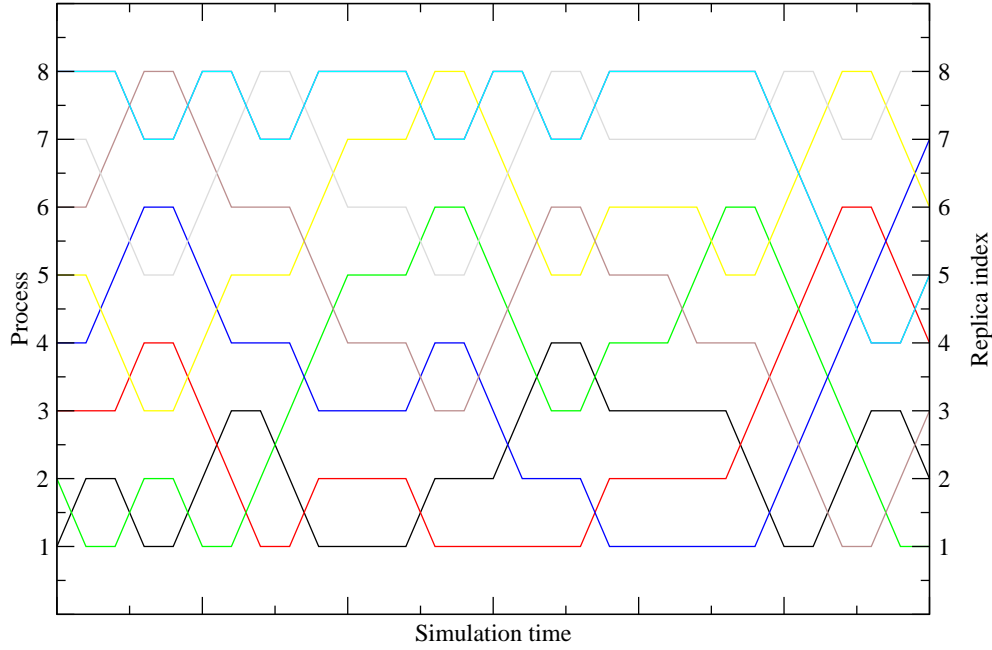


Figure 5.2: Typical REM Simulation with 8 replicas. Each process bear a particular color and the color follows the right scale, i.e. the replica index which is connected to the temperature. To reconstruct a trajectory at a given temperatures, one must combine the data form several processes.

characterized by a different potential energy rather than by a temperature. In its simplest implementation, the potential energies of the replicas differ by a scaling factor  $c_m$ , with  $c_1 = 1$  for the target replica. Clearly, as long as the exchanged states differ only in the coordinates (i.e. momenta are not exchanged), the scaling of the potential energy of a canonical system (NVT) is equivalent to an inverse temperature scaling. Thus, Hamiltonian REM with *full* potential energy scaling and temperature REM are perfectly equivalent in an extended Monte Carlo simulation. When the replica simulations are done by numerically, integrating the Nosé-Hoover equations of motion at constant volume, Hamiltonian REM with full *potential* energy scaling and temperature REM are clearly no longer equivalent. Since momenta are not exchanged, Eq. 5.6 is valid for both full Hamiltonian REM and temperature REM, but in the latter technique *both* the kinetic and the potential energy are scaled, while in the former as implemented in ORAC one scales *only* the potential energy.

The advantage of using the Hamiltonian REM is two-fold: i) as all the replica have the same operating temperature, one does not have, like in temperature REM, to reinitialize the velocities after one successful configuration exchange and ii) since the mean atomic velocities are the same throughout the extended system, one does not have to adapt the time step size for preserving the quality of r-RESPA integrator as it should be done in temperature REM.

Hamiltonian REM can also be applied to *a specific part* of the potential, thereby localizing the effect of the configurational exchanges to specific part of the systems. Given a potential made up of a sum of various  $i = 1, \dots, k$  contributions (e.g. stretching, bending, torsional, solute-solvent solute-solute solvent-solvent non bonded etc.), then one can define in a general way the  $m$ -th replica of the extended system as

$$V_m(X) = \sum_{i=1}^k c_i^{(m)} v_i(X) \quad (5.13)$$

where  $c_i^{(m)}$  is the scaling factor for the  $i$ -th contribution,  $v_i(X)$  of the potential of the  $m$ -th replica. So each replica is characterized by a  $k$ -dimensional scaling vector  $\mathbf{c}_m = (c_1^{(m)}, \dots, c_i^{(m)}, \dots, c_k^{(m)})$  whose component are the scaling factors of  $k$  contributions of the interaction potential for that replica. The target replica,



replica 1, is such that  $V_1(x) = V(x)$ , the unscaled potential corresponding to the target system for which  $\mathbf{c}_m = (1, 1, 1, \dots)$ . In vector notation we may compactly write Eq. 5.13 as

$$V_m(X) = \mathbf{c}_m \cdot \mathbf{v}(X) \quad (5.14)$$

Using this formalism, the probability of a configuration  $X$  in the  $m$ -th replica may be written as

$$P_m(X) = \frac{1}{Z_m} e^{-\beta \mathbf{c}_m \cdot \mathbf{v}(X)}. \quad (5.15)$$

with  $Z_m = \int e^{-\beta \mathbf{c}_m \cdot \mathbf{v}(X)} dX$ . The detailed balance condition for the exchange of configurations between replica  $m$  (characterized by the scaling vector  $\mathbf{c}_m$ ) and replica  $n$  (characterized by the scaling vector  $\mathbf{c}_n$ ) is then given by

$$\frac{W(X, \mathbf{c}_m, X', \mathbf{c}_n, \beta)}{W(X', \mathbf{c}_m; X, \mathbf{c}_n, \beta)} = e^{-\beta(\mathbf{c}_m - \mathbf{c}_n) \cdot [\mathbf{v}(X') - \mathbf{v}(X)]} \quad (5.16)$$

Again, the detailed balance is implemented through Eq. 5.6 with

$$\begin{aligned} \Delta &= \beta(\mathbf{c}_m - \mathbf{c}_n) \cdot [\mathbf{v}(X') - \mathbf{v}(X)] \\ &= \beta \sum_{i=1}^k (c_i^{(m)} - c_i^{(n)}) [V_i(X') - V_i(X)] \end{aligned} \quad (5.17)$$

There is considerable freedom in the splitting of the potential (Eq. 5.13) and in the selection of the corresponding scaling factors. These factors are always positive and can be either smaller or greater than one, meaning that the corresponding potential contributions, for  $m > 1$ , imply a heating and a cooling, respectively, of the involved degrees of freedom. For example we could use  $c < 1$  for torsions and  $c > 1$  for bending, so that, with increasing  $m$ , torsional degrees of freedom are heated up while bending are frozen down.

*Global scaling:* In the present implementation of ORAC, one can do a *global* subdivision (i.e. ignoring the distinction between solvent and solute) of the overall atomistic interaction potential for biomolecular system according to the following:

$$V_m(X) = c_{\text{ba}}^m (V_{\text{Bonds}} + V_{\text{Angle}} + V_{\text{i-tors}}) + c_t^{(m)} (V_{\text{tors}} + V_{14}) + \quad (5.18)$$

$$+ c_{\text{nb}}^{(m)} (V_{\text{vdw}} + V_{\text{qr}} + V_{\text{qd}}) \quad (5.19)$$

where the meaning of the subscripts is given in Sec. 4.1. Typically one then sets  $c_{\text{ba}}^{(m)} = 1 \ \forall m$ , as there is little advantage for conformational sampling in exchanging configurations involving stiff degrees of freedom such as bending, stretching and improper torsion. On the other hand, conformational transitions in proteins are mainly driven by torsional and intraprotein and protein-solvent non bonded interactions. It is thus convenient to heat up these degrees of freedom by scaling with  $c_t^{(m)} < 1$  and  $c_{\text{nb}}^{(m)} < 1$  the corresponding potential functions. With this choice the quantity  $\Delta$  in Eq. 5.17 is given by

$$\begin{aligned} \Delta &= \beta(c_t^{(m)} - c_t^{(n)}) [V_{\text{tors}}(X') + V_{14}(X') - V_{\text{tors}}(X) - V_{14}(X)] + \\ &+ \beta(c_{\text{nb}}^{(m)} - c_{\text{nb}}^{(n)}) [V_{\text{vdw}}(X') + V_{\text{qr}}(X') + V_{\text{qd}}(X') - (V_{\text{vdw}}(X) + V_{\text{qr}}(X) + V_{\text{qd}}(X))] \end{aligned} \quad (5.20)$$

*Local scaling:* Hamiltonian REM in ORAC can work also by tempering only a user defined “solute”. Unlike standard implementation of the solute tempering techniques[106], the “solute” in the present version can be any portion of the system including solvent molecules. Once the solute has been defined, the complementary “non solute” portion of the system is by definition the “solvent”. In this manner, the scaling (i.e. the heating or freezing) can be localized in a specific part of the system with the remainder (the “solvent”) of the system behaving normally (i.e. with the target interaction potential). In order to clarify how local scaling work, we illustrate the technique with a working general example. Suppose to choose a subset of atoms  $n$  in the system that define the “solute”. This subset can be chosen arbitrarily and may include disconnected portions of the protein, as well as selected solvent molecules. The solvent is then made up of the remaining  $N - n$  atoms. According to this subdivision, the global potential of the system may be written as

$$V(X) = V^{(\text{Slt})}(X_n) + V^{(\text{Slt-Slv})}(X_n, X_{N-n}) + V^{(\text{Slv-Slv})}(X_{N-n}) \quad (5.21)$$

where

$$\begin{aligned}
V^{(\text{Slt})}(X_n) &= V_{\text{tors}}(X_n) + V_{14}(X_n) + V_{\text{vdw}}(X_n) + V_{qd}(X_n) \\
V^{(\text{Slt-Slv})}(X_n, X_{N-n}) &= V_{\text{vdw}}(X_n, X_{N-n}) + V_{qd}(X_n, X_{N-n}) \\
V^{(\text{Slv-Slv})}(X_{N-n}) &= V_{\text{vdw}}(X_n, X_{N-n}) + V_{qr}(X_n, X_{N-n}) + V_{qr} + V_{\text{bd}}(X_N)
\end{aligned} \tag{5.22}$$

The solute potential  $V^{(\text{Slt})}(X_n)$  includes all the proper torsions and the 14 non bonded interactions involving the  $n$  atoms of the solute.<sup>2</sup> The solute-solvent interaction involve all non-bonded interactions between the  $N - n$  solvent atoms and the  $n$  solute atoms. The solvent-solvent interaction involve all non-bonded interactions among the  $N - n$  solvent atoms. As one can see, the *global* fast bonded potential  $V_{\text{bd}}(X_N) = (V_{\text{Bonds}} + V_{\text{Angle}} + V_{\text{i-tors}})$  is assimilated to a solvent-solvent contribution. It should also be remarked that the reciprocal lattice contribution  $V_{qr}$ , i.e. the long range electrostatics, is in any case assigned to the solvent-solvent term even if it includes all kinds of non bonded interaction (solute-solute, solvent-solute and solvent-solvent). The reason why  $V_{qr}$  is not split in the solute-solute, solute-solvent and solvent-solvent components is both physical and practical. Firstly, the long-range potential associated to each of three component of this term is expected, in general, to be rather insensitive along arbitrary reaction coordinates, such that a scaling of  $V_{qr}$  do not correspondingly produce a significant heating of any conformational coordinate. Secondly, in the Particle Mesh Approach approach the solute-solute, solvent-solute and solvent-solvent contribution to  $V_{qr}$  can no longer be easily separated, and this term must be thus arbitrarily assigned to one of the three components. Given the subdivision Eq. 5.22, the local scaling for replica  $m$  in ORAC is implemented as

$$V_m(X) = c_{\text{Slt}}^{(m)} V^{(\text{Slt})}(X_n) + c_{(\text{Slt-Slv})}^{(m)} V^{(\text{Slt-Slv})}(X_n, X_{N-n}) + V^{(\text{Slv-Slv})}(X_{N-n}) \tag{5.23}$$

The solvent-solvent interactions, *including the global bonded potential and the long-range electrostatic interactions*, are not scaled in the local approach.

Solute-solute interactions and solute-solvent interactions as defined in Eq. 5.22 are scaled independently, thereby generalizing the so-called solute-tempering approach recently proposed by Liu *et al.*[106] This generality allows a complete freedom in the choice of the scaling protocol. For example, one can choose to set  $c_{(\text{Slt-Slv})}^{(m)} > 1$ , i.e. to progressively “freeze” the solute-solvent interaction as the replica index  $m$  grows, while at the same time setting  $c_{\text{Slt}}^{(m)} = 1$  for all replicas, thereby favouring, at large  $c_{(\text{Slt-Slv})}^{(m)}$  the “solvation” of the solute, i.e., for example, favouring the unfolding.

The global REM algorithm (i.e. uniform scaling of the full interaction potential) as implemented in ORAC works also for constant pressure simulation (see **ISOSTRESS** directive). In that case, the selected external pressure refers to that of the *target* replica ( $m = 1$ ). Since the  $PV$  is a configurational term and *is not* scaled in the current implementation, the non target replicas sample coordinate configurations according to a *higher* external pressure, i.e.  $P_m = P_1/c_m$  where  $c_m$  is the scaling factor of replica  $m$ . This choice is done in order to avoid, through an increase of the external pressure, a catastrophic expansion of the simulation box for low scaling factors (or high temperatures).

### 5.3 Calculating Ensemble Averages Using Configurations from All Ensembles (MBAR estimator)

As recently shown by Shirts and Chodera[107], all the configurations produced by a REM simulation of  $M$  replicas, each characterized by a distribution function  $P_m(X)$ , can be effectively used to obtain equilibrium averages for any target distribution  $P_n(X)$ , using the so-called Multistate Bennett Acceptance Ratio (MBAR) estimator, which is illustrated in the following.

---

<sup>2</sup>With this definition,  $V_{(\text{Slt})}(X_n)$  may also depend on the coordinate of few solvent atoms. Being the definition of the solute atom based rather than potential based, it may be necessary to include in  $V_{\text{slt}}^{bd}(X_n)$ , e.g., torsional terms that involve boundary solvent atoms.

In the ORAC REM implementation, the most general distribution function for replica  $m$  is given by Eq. 5.15. Given that for each replica  $m$  one has saved  $N_m$  configurations of the kind  $\{x_1^m, \dots, x_k^m, \dots\}$ , it can be easily shown that

$$Z_n = \frac{\sum_{m=1}^M Z_m N_m^{-1} \sum_{k=1}^{N_m} \alpha_{nm}(x_k^m) P_n(x_k^m)}{N_n^{-1} \sum_{m=1}^M \sum_{k=1}^{N_n} \alpha_{nm}(x_k^n) P_m(x_k^n)}. \quad (5.24)$$

Eq. 5.24 holds for any arbitrary *bridge function*  $\alpha_{nm}(X)$ , In particular, choosing [107]

$$\alpha_{nm}(X) = \frac{N_m Z_m^{-1}}{\sum_l^M N_l Z_l^{-1} P_l(X)} \quad (5.25)$$

Eq. 5.24 transforms as

$$Z_n = \sum_{k=1}^N \frac{P_n(x_k)}{\sum_{l=1}^M Z_l^{-1} N_l P_l(x_k)} \quad (5.26)$$

where we have collapsed the two indices  $k$ , for the configurations, and  $m$ , for the replicas in one single index  $k$  *running on all the configurations*  $N = \sum_m N_m$  produced by the REMD. Except for an arbitrary multiplicative factor, Eq. 5.26 can be solved iteratively for the partition function  $Z_n$ . At the beginning of the process, one sets  $Z_i = 1$  for all  $i$ . At the iteration  $i + 1$  we have that

$$Z_n(i+1) = \sum_k^N W_n(x_k, i) \quad (5.27)$$

where the weights depend on the  $Z_l$  calculated at the previous iteration

$$W_n(x_k, i) = \frac{e^{-\beta \mathbf{c}_n \cdot \mathbf{v}(x_k)}}{\sum_l N_l e^{-\ln Z_l(i) - \beta \mathbf{c}_l \cdot \mathbf{v}(x_k)}} \quad (5.28)$$

and we have used the definition of 5.15 for the replica distribution in ORAC. Once the  $Z_i$  have been determined,  $Z_*$  for an arbitrary distribution  $P_*(X)$  can be calculated using the configurations sampled in the REMD simulation:

$$Z_* = \sum_k^N \frac{P_*(x_k)}{\sum_l Z_l^{-1} N_l P_l(x_k)} = \sum_k^N W_*(x_k) \quad (5.29)$$

Setting for example  $P_* = P_1(X) * A(X)$ , where  $P_1(X)$  is the *target* distribution  $e^{-\beta V(x)}/Z$  (i.e. that of the replica 1) and  $A(x)$  is an arbitrary configurational property, we obtain

$$\langle A \rangle_1 = \frac{\int P_1(X) A(X) dX}{Z_1} = \frac{\int P_*(X) dX}{Z_1} = \frac{Z_*}{Z_1} \quad (5.30)$$

From Eq. 5.29, we have that  $Z_* = \sum_k^N W_1(x_k) A(x_k)$  and that  $Z_1 = \sum_k^N W_1(x_k)$ . Substituting these results into Eq. 5.30, we obtain

$$\langle A \rangle_1 = \frac{\sum_k^N W_1(x_k) A(x_k)}{\sum_k^N W_1(x_k)} \quad (5.31)$$

where the weights  $W_1$  for *all sampled points* in the REMD simulation are given by

$$W_1(x_k, i) = \frac{e^{-\beta V(x_k)}}{\sum_l N_l e^{-\ln Z_l(i) - \beta \mathbf{c}_l \cdot \mathbf{v}(x_k)}} \quad (5.32)$$

In summary, using the configurational energies from all  $M$  replicas, we first solve iteratively the system 5.26 for all  $Z_n$  (except for a multiplicative factor), with  $1 \leq n \leq M$ . In doing this, the weights  $W_n$  (including  $n = 1$ ) are also determined. Finally configurational averages at, e.g., the target distribution can be determined using *all the REMD configurations* by means of Eq. 5.31.

## Chapter 6

# Serial generalized ensemble simulations

### 6.1 Introduction

A class of simulation algorithms closely related to REM (see Chapter 5) are the so-called *serial generalized-ensemble* (SGE) methods[46]. The basic difference between SGE methods and REM is that in the former no pairs of replicas are necessary to make a trajectory in temperature space and more generally in the generalized ensemble space. In SGE methods only one replica can undergo ensemble transitions which are realized on the basis of a Monte Carlo like criterion. The most known example of SGE algorithm is the simulated tempering (ST) technique[44, 47], where weighted sampling is used to produce a random walk in temperature space. An important limitation of SGE approaches is that an evaluation of free energy differences between ensembles is needed as input to ensure equal visitation of the ensembles, and eventually a faster convergence of structural properties[48]. REM was just developed to eliminate the need to know a priori such free energy differences.

ST and temperature-REM yield an extensive exploration of the phase space without configurational restraints. This allows to recover not only the global minimum-energy state, but also any equilibrium thermodynamic quantity as a function of temperature. The potential of mean force (PMF)[51, 52] along a chosen collective coordinate can also be computed a posteriori by multiple-histogram reweighting techniques[53, 54]. PMF can also be determined by performing generalized-ensemble canonical simulations in the space of the collective coordinate[55] (for example the space of the end-to-end distance of a biopolymer). Comparisons between ST and temperature-REM have been reported[48, 49, 50]. The overall conclusions of these studies are that ST consistently gives a higher rate of delivering the system between high temperature states and low temperature states, as well as a higher rate of transversing the potential energy space. Moreover ST is well-suited to distributed computing environments because synchronization and communication between replicas/processors can be avoided. On the other side, an effective application of ST and, in general, of SGE methods requires a uniform exploration of the ensemble-space. In order to satisfy this criterion, acceptance rates must be not only high but also symmetric between forward and backward directions of the ensemble-space. This symmetry can be achieved by performing weighted sampling, where weights are correlated with the dimensionless free energies of the ensembles. The knowledge of such free energies is not needed in REM because replica exchanges occur between microstates of the same extended thermodynamic ensemble. To achieve rapid sampling of the ensemble-space through high acceptance rates, we need to choose ensembles appropriately so that neighboring ensembles overlap significantly. As stated above, the most critical aspect in SGE schemes is the determination of weight factors (*viz.* dimensionless free energy differences between neighboring ensembles). This issue has been the subject of many studies, especially addressed to ST simulations. The first attempts are based on short trial simulations[47, 108, 109]. The proposed procedures are however quite complicated and computationally expensive for systems with many degrees of freedom. Later, Mitsutake and Okamoto suggested to perform a short REM simulation to estimate ST weight factors[110] via multiple-histogram reweighting[53, 54]. A further approximated, but very simple, approach to evaluate weight factors is based on average energies calculated by means

of conventional molecular dynamics simulations[111]. The weight factors obtained by the average-energy method of Ref. [111] were later demonstrated to correspond to the first term of a cumulant expansion of free energy differences[49]. Huang *et al.* used approximated estimates of potential energy distribution functions (from short trial molecular dynamics simulations) to equalize the acceptance rates of forward and backward transitions between neighboring temperatures, ultimately leading to a uniform temperature sampling in ST[112]. The techniques illustrated above have been devised to determine weight factors to be used without further refinement[110] or as an initial guess to be updated during the simulation[112, 111]. In the former case, these approximate factors should (hopefully) ensure an almost random walk through the ensemble-space. However, as remarked in Ref. [48], the estimate of accurate weight factors may be very difficult for complex systems. Inaccurate estimates, though unaffected the basic principles of SGE methods, do affect the sampling performances in terms of simulation time needed to achieve convergence of structural properties[48].

As discussed above, dimensionless free energy differences between ensembles (*viz.* weight factors) may also be the very aim of the simulation[55] (since they correspond to the PMF along the chosen coordinate). In such cases, accurate determination of weight factors is not simply welcome, but necessary. This can be done a posteriori using multiple-histogram reweighting techniques[53, 54], or with more or less efficient updating protocols applied during the simulation[113, 112, 114, 48, 115].

In the ORAC program we have implemented SGE simulations, either in a ST-like fashion or in the space of bond, bending and torsional coordinates. These simulations exploit the adaptive method to calculate weight factors developed in Ref. [56]. Such method, called BAR-SGE, is based on a generalized expression[116, 117] of the Bennett Acceptance Ratio[118] (BAR) and free energy perturbation[119]. It is asymptotically exact and requires a low computational time per updating step. The algorithm is suited, not only to calculate the free energy on the fly during the simulation, but also as a possible criterion to establish whether equilibration has been reached.

## 6.2 Fundamentals of serial generalized-ensemble methods

SGE methods deal with a set of  $N$  ensembles associated with different dimensionless Hamiltonians  $h_n(x, p)$ , where  $x$  and  $p$  denote the atomic coordinates and momenta of a microstate<sup>1</sup>, and  $n = 1, 2, \dots, N$  denotes the ensemble. Each ensemble is characterized by a partition function expressed as

$$Z_n = \int e^{-h_n(x, p)} dx dp. \quad (6.1)$$

In ST simulations we have temperature ensembles and therefore the dimensionless Hamiltonian is

$$h_n(x, p) = \beta_n H(x, p), \quad (6.2)$$

where  $H(x, p)$  is the original Hamiltonian and  $\beta_n = (k_B T_n)^{-1}$ , with  $k_B$  being the Boltzmann constant and  $T_n$  the temperature of the  $n$ th ensemble. If we express the Hamiltonian as a function of  $\lambda$ , namely a parameter correlated with an arbitrary collective coordinate of the system (or even corresponding to the pressure), then the dimensionless Hamiltonian associated with the  $n$ th  $\lambda$ -ensemble is

$$h_n(x, p) = \beta H(x, p; \lambda_n). \quad (6.3)$$

Here all ensembles have the same temperature. It is also possible to construct a generalized ensemble for multiple parameters[120] as

$$h_{nl}(x, p) = \beta_n H(x, p; \lambda_l). \quad (6.4)$$

In this example two parameters,  $T$  and  $\lambda$ , are employed. However no restraint is actually given to the number of ensemble-spaces. Generalized-ensemble algorithms have a different implementation dependent on whether the temperature is included in the collection of sampling spaces (Eqs. 6.2 and 6.4) or not (Eq. 6.3). Here we adhere to the most general context without specifying any form of  $h_n(x, p)$ .

In SGE simulations, the probability of a microstate  $(x, p)$  in the  $n$ th ensemble [from now on denoted as  $(x, p)_n$ ] is proportional to  $\exp[-h_n(x, p) + g_n]$ , where  $g_n$  is a factor, different for each ensemble, that

---

<sup>1</sup>In Monte Carlo generalized-ensemble simulations, momenta are dropped out.

must ensure almost equal visitation of the  $N$  ensembles. The extended partition function of this “system of ensembles” is

$$Z = \sum_{n=1}^N \int e^{-h_n(x,p)+g_n} dx dp = \sum_{n=1}^N Z_n e^{g_n}, \quad (6.5)$$

where  $Z_n$  is the partition function of the system in the  $n$ th ensemble (Eq. 6.1). In practice, SGE simulations work as follows. A single simulation is performed in a specific ensemble, say  $n$ , using Monte Carlo or molecular dynamics sampling protocols, and after a certain interval, an attempt is made to change the microstate  $(x, p)_n$  to another microstate of a different ensemble,  $(x', p')_m$ . Since high acceptance rates are obtained as the ensembles  $n$  and  $m$  overlap significantly, the final ensemble  $m$  is typically close to the initial one, namely  $m = n \pm 1$ <sup>2</sup>. In principle, the initial and final microstates can be defined by different coordinates and/or momenta ( $x \neq x'$  and/or  $p \neq p'$ ), though the condition  $x = x'$  is usually adopted. The transition probabilities for moving from  $(x, p)_n$  to  $(x', p')_m$  and viceversa have to satisfy the detailed balance condition

$$P_n(x, p)P(n \rightarrow m) = P_m(x', p')P(m \rightarrow n), \quad (6.6)$$

where  $P_n(x, p)$  is the probability of the microstate  $(x, p)_n$  in the extended canonical ensemble (Eq. 6.5)

$$P_n(x, p) = Z^{-1} e^{-h_n(x, p)+g_n}. \quad (6.7)$$

In Eq. 6.6,  $P(n \rightarrow m)$  is a shorthand for the conditional probability of the transition  $(x, p)_n \rightarrow (x', p')_m$ , given the system is in the microstate  $(x, p)_n$  [with analogous meaning of  $P(m \rightarrow n)$ ]. Using Eq. 6.7 together with the analogous expression for  $P_m(x', p')$  in the detailed balance and applying the Metropolis's criterion, we find that the transition  $(x, p)_n \rightarrow (x', p')_m$  is accepted with probability

$$\text{acc}[n \rightarrow m] = \min(1, e^{h_n(x, p)-h_m(x', p')+g_m-g_n}). \quad (6.8)$$

The probability of sampling a given ensemble is

$$P_n = \int P_n(x, p) dx dp = Z_n Z^{-1} e^{g_n}. \quad (6.9)$$

Uniform sampling sets the condition  $P_n = N^{-1}$  for each ensemble ( $n = 1, \dots, N$ ), that leads to the equality

$$g_n = -\ln Z_n + \ln \left( \frac{Z}{N} \right). \quad (6.10)$$

Equation 6.10 implies that, to get uniform sampling, the difference  $g_m - g_n$  in Eq. 6.8 must be replaced with  $f_m - f_n$ , where  $f_n$  is the dimensionless free energy related to the actual free energy of the ensemble  $n$  by the relation  $f_n = \beta F_n = -\ln Z_n$ , where  $\beta$  is the inverse temperature of the ensemble. Here we are interested in determining such free energy differences that will be referred as optimal weight factors, or simply, optimal weights. Accordingly, in the acceptance ratio we will use  $f_n$  instead of  $g_n$ .

### 6.2.1 SGE simulations in temperature-space (simulated tempering) and its implementation in the ORAC program

In SGE Monte Carlo simulations conducted in temperature-space (ST simulations), Eq. 6.2 holds. Specifically, since only configurational sampling is performed, we have

$$h_n(x) = \beta_n V(x), \quad (6.11)$$

where  $V(x)$  is the energy of the configuration  $x$ . Exploiting Eq. 6.11 into Eq. 6.8, we find that transitions from  $n$  to  $m$ -ensemble, realized at fixed configuration, are accepted with probability

$$\text{acc}[n \rightarrow m] = \min(1, e^{(\beta_n - \beta_m)V(x) + f_m - f_n}). \quad (6.12)$$

---

<sup>2</sup>Here, we assume implicitly that the indexes  $n$  and  $m$  belong to an ordered list such that  $T_1 < T_2 < \dots < T_N$  or  $\lambda_1 < \lambda_2 < \dots < \lambda_N$ .



When the system evolution is performed with molecular dynamics simulations, the situation is slightly more complicate. Suppose to deal with canonical ensembles (to simplify the treatment and the notation we consider constant-volume constant-temperature ensembles, though extension to constant-pressure constant-temperature ensembles is straightforward). Usually, constant temperature is implemented through the Nosé-Hoover method[121, 122] or extensions of it[123]. With the symbol  $p_t$ , we will denote the momentum conjugated to the dynamical variable associated with the thermostat. Also in this case Eq. 6.2 holds, but it takes the form

$$h_n(x, p, p_t) = \beta_n H(x, p, p_t). \quad (6.13)$$

In this equation,  $H(x, p, p_t) = V(x) + K(p) + K(p_t)$  is the extended Hamiltonian of the system, where  $V(x)$  is the potential energy, while  $K(p)$  and  $K(p_t)$  are the kinetic energies of the particles and thermostat, respectively. As in Monte Carlo version, transitions from  $n$  to  $m$ -ensemble are realized at fixed configuration, while particle momenta are rescaled as

$$\begin{aligned} p' &= p (T_m/T_n)^{1/2} \\ p'_t &= p_t (T_m/T_n)^{1/2}. \end{aligned} \quad (6.14)$$

As in temperature-REM[124], the scaling drops the momenta out of the detailed balance and the acceptance ratio takes the form of Eq. 6.12. Note that, if more thermostats are adopted[123], then all additional momenta must be rescaled according to Eq. 6.14.

ST is implemented in the ORAC program exactly as it has been done for REM (see Section 5.2). In particular global and local scalings of the potential energy can be realized by keeping fixed the temperature of the system. A generic ensemble  $n$  is therefore defined by a coefficient  $\mathbf{c}_n$  (see Eq. 5.13) that scales the potential energy  $\mathbf{v}(x)$  of the replica (the vectorial form of the potential energy  $V(x)$  is used because of possible local scaling), i.e.,  $V(x) = \mathbf{c}_n \cdot \mathbf{v}(x)$ . In this sort of Hamiltonian tempering, the transition from  $n$  to  $m$ -ensemble is accepted with probability

$$\text{acc}[n \rightarrow m] = \min(1, e^{\beta(\mathbf{c}_n - \mathbf{c}_m) \cdot \mathbf{v}(x) + f_m - f_n}). \quad (6.15)$$

In this approach, since the temperature is the same for all ensembles, momentum rescaling (Eq. 6.14) must not be applied. We will see in Section 6.3 how  $f_m$  and  $f_n$  appearing into Eq. 6.15 are determined.

### 6.2.2 SGE simulations in $\lambda$ -space

In SGE simulations conducted in a generic  $\lambda$ -space at constant temperature, the dimensionless Hamiltonian is given by Eq. 6.3. In the ORAC program we use a Hamiltonian aimed to sample (i) the distance between two target atoms, (ii) the angle formed by three established atoms and (iii) the torsion formed by four established atoms or (iv) combinations of these coordinates. There are several ways to model such a Hamiltonian. Our choice is to use harmonic potential functions correlated to the given collective coordinates:

$$h_n(x, p, p_t) = \beta[H(x, p, p_t) + k(r - \lambda_n)^2], \quad (6.16)$$

where, as usual,  $H(x, p, p_t)$  is the extended Hamiltonian. In Eq. 6.16,  $r$  is the instantaneous collective coordinate (bond, bending, torsion) and  $k$  is a constant. As in ST simulations, transitions from  $n$  to  $m$ -ensemble occur at fixed configuration. However, in this case there is no need of rescaling momenta because they drop out of the detailed balance condition naturally. The resulting acceptance ratio is

$$\text{acc}[n \rightarrow m] = \min(1, e^{\beta k[(r - \lambda_n)^2 - (r - \lambda_m)^2] + f_m - f_n}). \quad (6.17)$$

In this kind of simulations, the free energy as a function of  $\lambda$  corresponds to the biased PMF[51, 52] along the coordinate associated with  $\lambda$ . Biasing arises from the harmonic potential added to the original Hamiltonian (see Eq. 6.16). However, reweighting schemes are available to recover the unbiased PMF along the real coordinate[53, 54, 125, 126]. We will see later how  $f_m$  and  $f_n$  are determined.

## 6.3 The algorithm for optimal weights

### 6.3.1 Tackling free energy estimates

The algorithm used to calculate the optimal weight factors, namely the dimensionless free energy differences between ensembles (see Sec. 6.2), is based on the Bennett acceptance ratio[118, 66] and on the free energy

perturbation formula[119]. We start by showing that the difference between the dimensionless Hamiltonians appearing in the acceptance ratio (see Eq. 6.8) can be viewed as the generalized dimensionless work done on the system during the transition  $(x, p)_n \rightarrow (x', p')_m$ . The concept of generalized dimensionless work in systems subject to mechanical and thermal nonequilibrium changes has been extensively discussed in the literature[116, 127, 117]. In particular it has been shown (see Eq. 45 of Ref. [117]) that, in a nonequilibrium realization performed with extended-Lagrangian molecular dynamics[91], the generalized dimensionless work is

$$W = \beta_\tau H'(\tau) - \beta_0 H'(0) \quad (6.18)$$

where  $\tau$  is the duration of the realization and

$$H'(\tau) = H(x, p, p_t) + k_B T_\tau \mathcal{V}(x_t), \quad (6.19)$$

where  $H(x, p, p_t)$  is defined in Eq. 6.13 and  $\mathcal{V}(x_t)$  is a linear function of the configurational variables  $x_t$  associated with the thermostat (see Eq. 42 of Ref. [117]). For simplicity, in Eq. 6.19 we have only reported the explicit time-dependence of the temperature. Moreover, we have considered to deal with thermal changes alone using constant-volume constant-temperature equations of motion. Extending the treatment to constant-pressure constant-temperature algorithms and to systems subject to generic  $\lambda$ , *e.g.* mechanical, changes is straightforward[117]. Note that, when no changes are externally applied to the system,  $H'$  is exactly the quantity conserved during an equilibrium constant-volume constant-temperature simulation. Accordingly, the work  $W$  is zero. The above definition of generalized dimensionless work is valid for arbitrary values of  $\tau$ . In the special case of instantaneous thermal changes and instantaneous variations of the microstate variables, as it occurs in ST simulations, the times 0 and  $\tau$  in Eq. 6.18 refer to the states instantaneously before and after the  $(x, p)_n \rightarrow (x', p')_m$  transition, respectively. Therefore, according to the notation introduced above, Eq. 6.18 can be rewritten as

$$W[n \rightarrow m] = \beta_m H(x', p', p'_t) - \beta_n H(x, p, p_t) + \mathcal{V}(x'_t) - \mathcal{V}(x_t), \quad (6.20)$$

where  $x_t$  and  $x'_t$  are the values of the configurational thermostat-variables before and after the  $(x, p)_n \rightarrow (x', p')_m$  transition, respectively. In the first two terms of the right-hand side of Eq. 6.20 we can recognize the dimensionless Hamiltonians  $h_m(x', p', p'_t)$  and  $h_n(x, p, p_t)$ . It is important to observe that, in generalized-ensemble simulations, an arbitrary change of  $x_t$  during a transition does not affect the acceptance ratio nor the dynamics of the system. Therefore, by setting  $x'_t = x_t$  and generalizing to  $\lambda$  changes, we recover the equality

$$W[n \rightarrow m] = h_m(x', p', p'_t) - h_n(x, p, p_t). \quad (6.21)$$

Using  $W[n \rightarrow m]$ , the acceptance ratio of Eq. 6.8 becomes

$$\boxed{\text{acc}[n \rightarrow m] = \min(1, e^{\Delta f_{n \rightarrow m} - W[n \rightarrow m]})}, \quad (6.22)$$

where  $\Delta f_{n \rightarrow m} = f_m - f_n$ . The quantity  $W[n \rightarrow m] - \Delta f_{n \rightarrow m}$  can be interpreted as the generalized dimensionless work dissipated in the transition (see Eq. 17 of Ref. [117]).

Until now we have simply restated the acceptance ratio of SGE simulations in terms of the generalized dimensionless work  $W[n \rightarrow m]$ . The truly important aspect of this treatment is that the knowledge of  $W[n \rightarrow m]$  and  $W[m \rightarrow n]$  stored during the sampling gives us the possibility of evaluating the optimal weights  $\Delta f_{n \rightarrow m}$  using the Bennett method[118] reformulated with maximum likelihood arguments[66, 117]. For example, in ST simulations we must take memory of the quantities  $W[n \rightarrow m] = (\beta_m - \beta_n)V_n(x)$  and  $W[m \rightarrow n] = (\beta_n - \beta_m)V_m(x)$ , where the subscripts of the potential energy indicate the ensemble at which sampling occurs. The extension to Hamiltonian tempering implemented in the ORAC program is straightforward

$$\boxed{W[n \rightarrow m] = \beta(\mathbf{c}_m - \mathbf{c}_n) \cdot \mathbf{v}_n(x)} \quad (6.23)$$

with analogous expression for  $W[m \rightarrow n]$ . In the case of SGE simulations in the  $\lambda$ -space we have (substitute Eq. 6.16 into Eq. 6.21 with fixed coordinates and momenta)

$$\boxed{W[n \rightarrow m] = \beta k[(r - \lambda_m)^2 - (r - \lambda_n)^2]}. \quad (6.24)$$



Thus, for each pair of neighboring ensembles  $n$  and  $m$ , we generate two collections of “instantaneous generalized dimensionless works”:  $W_1[m \rightarrow n], W_2[m \rightarrow n], \dots$ , etc. and  $W_1[n \rightarrow m], W_2[n \rightarrow m], \dots$ , etc.. Let us denote the number of elements of such collections with  $N_{m \rightarrow n}$  and  $N_{n \rightarrow m}$ .  $\Delta f_{n \rightarrow m}$  can be calculated by solving the equation (see Eq. 27 of Ref. [117])

$$\left[ \sum_{i=1}^{N_{n \rightarrow m}} \left[ 1 + \frac{N_{n \rightarrow m}}{N_{m \rightarrow n}} e^{W_i[n \rightarrow m] - \Delta f_{n \rightarrow m}} \right]^{-1} - \sum_{j=1}^{N_{m \rightarrow n}} \left[ 1 + \frac{N_{m \rightarrow n}}{N_{n \rightarrow m}} e^{W_j[m \rightarrow n] + \Delta f_{n \rightarrow m}} \right]^{-1} \right] = 0, \quad (6.25)$$

that just corresponds to the Bennett acceptance ratio for dimensionless quantities. It is important to point out that Eq. 6.25 is valid for nonequilibrium transformations, does not matter how far from equilibrium, and is rigorous only if the initial microstates of the transformations are drawn from equilibrium. Therefore care should be taken in verifying whether convergence/equilibrium is reached in the adaptive procedure. It should be noted that Eq. 6.25 is a straightforward generalization of Eq. 8 of Ref. [66] that was specifically derived for systems subject to mechanical changes.

Shirts *et al.*[66] proposed a way of evaluating the square uncertainty (variance) of  $\Delta f_{n \rightarrow m}$  from maximum likelihood methods, by also correcting the estimate in the case of the restriction from fixed probability of forward and backward work measurements to fixed number of forward and backward work measurements. They provided a formula for systems subject only to mechanical work. However, by following the arguments of Ref. [117], it is straightforward to generalize the variance:

$$\sigma^2(\Delta f_{n \rightarrow m}) = 2 \left\{ \sum_{i=1}^{N_{n \rightarrow m}} [1 + \cosh(W_i[n \rightarrow m] - \Delta f')]^{-1} + \sum_{j=1}^{N_{m \rightarrow n}} [1 + \cosh(W_j[m \rightarrow n] + \Delta f')]^{-1} \right\}^{-1} - N_{n \rightarrow m}^{-1} - N_{m \rightarrow n}^{-1}, \quad (6.26)$$

where  $\Delta f' = \Delta f_{n \rightarrow m} + \ln(N_{m \rightarrow n}/N_{n \rightarrow m})$ . The quantity  $\sigma^2(\Delta f_{n \rightarrow m})$  can be calculated once  $\Delta f_{n \rightarrow m}$  is recovered from Eq. 6.25.

It is obvious that, in order to employ Eq. 6.25, both  $n$  and  $m$  ensembles must be visited at least one time. If statistics is instead retrieved from one ensemble alone, say  $n$ , then we have to resort to a different approach. The one we employ is consistent with the previous treatment. In fact, in the limit that only one work collection (specifically, the  $n \rightarrow m$  collection) is available, Eq. 6.25 becomes[66] (compare with Eq. 21 of Ref. [117])

$$e^{-\Delta f_{n \rightarrow m}} = N_{n \rightarrow m}^{-1} \sum_{i=1}^{N_{n \rightarrow m}} e^{-W_i[n \rightarrow m]}, \quad (6.27)$$

thus recovering the well-known fact that the free energy is the expectation value of the work exponential average[63].

### 6.3.2 Implementation of adaptive free energy estimates in the ORAC program: the BAR-SGE method

We now describe how the machinery introduced in Section 6.3.1 can be employed in SGE simulation programs, such as ORAC. Suppose to deal with  $N$  ensembles of a generic  $\Lambda$ -space, be it a temperature-space, a  $\lambda$ -space, or even a multiple-parameter space. Without loss of generality, we order the ensembles as  $\Lambda_1 < \Lambda_2 < \dots < \Lambda_N$ . Thus,  $N - 1$  optimal weights,  $\Delta f_{1 \rightarrow 2}, \Delta f_{2 \rightarrow 3}, \dots, \Delta f_{N-1 \rightarrow N}$ , have to be estimated adaptively.

(1) At the beginning of the simulation we assign the system, *i.e.* the replica, to a randomly chosen ensemble and start the phase space sampling with the established simulation protocol (Monte Carlo or molecular dynamics). Note that several simulations may run in the generalized-ensemble space, each yielding an independent trajectory. Analogously to REM, a single simulated system will be termed “replica”. In the ORAC program, we have arbitrarily decided to use the following criteria to distribute the replicas among the ensembles at the beginning of the SGE simulations. In Hamiltonian tempering simulations, if we deal with  $M$  replicas, we assign them to different ensembles with increasing order, from  $\Lambda_1$  to  $\Lambda_N$ . If  $M > N$  then the  $(N + 1)$ th replica is assigned to  $\Lambda_1$  (as the first replica), the  $(N + 2)$ th replica to  $\Lambda_2$  (as the second replica) and so on. In SGE simulations performed in the  $\lambda$ -space all replicas are assigned to  $\Lambda_1$

(see Section 10.2.11 for the definition of the  $\Lambda$  sequence). For the sake of simplicity, in the following presentation of the method we will take into account one replica alone. A discussion regarding multiple-replica simulations is reported in the final part of this section.

(2) Every  $L_a$  steps and for each ensemble  $n$ , we store into memory the quantities  $W[n \rightarrow n+1]$  and  $W[n \rightarrow n-1]$ , computed as described in Sec. 6.3.1. There is no well-established recipe in choosing  $L_a$ , apart from the requirement that it should ensure (as large as possible) uncorrelation between work values. During the simulation we must also record the number of stored  $W$  elements,  $N_{n \rightarrow n+1}$  and  $N_{n \rightarrow n-1}$ .

(3) Every  $L_b$  steps, such that  $L_b \gg L_a$  (three orders of magnitude at least), we try a free energy update on the basis of Eq. 6.25 or Eq. 6.27. The scheme we propose for  $\Delta f_{n \rightarrow n+1}$  follows.

- (a) First of all we check if the conditions  $N_{n \rightarrow n+1} > N'$  and  $N_{n+1 \rightarrow n} > N'$  are met. In such a case Eq. 6.25 is applied (setting  $m = n+1$ ) using the stored dimensionless works (see point 2). The threshold  $N'$  is used as a control parameter for the accuracy of the calculation. In the ORAC program we have set  $N' = \text{int}(L_b/L_a)$ . Once  $\Delta f_{n \rightarrow n+1}$  is known, its square uncertainty is computed according to Eq. 6.26. Then we set  $N_{n \rightarrow n+1} = 0$  and  $N_{n+1 \rightarrow n} = 0$  and remove  $W[n \rightarrow n+1]$  and  $W[n+1 \rightarrow n]$  from computer memory. Whenever a free energy estimate and the correlated uncertainty are computed, the optimal weight to be used in the acceptance ratio (Eq. 6.22) is determined applying standard formulas from maximum likelihood considerations (see Sec. 6.3.3). This step is realized for  $n = 1, 2, \dots, N-1$ .
- (b) If the criteria needed to apply Eq. 6.25 are not met and no  $\Delta f_{n \rightarrow n+1}$  estimate is still available from point 3a, then we try to apply Eq. 6.27. In particular two independent estimates of  $\Delta f_{n \rightarrow n+1}$  are attempted. One comes from Eq. 6.27 by setting  $m = n+1$ , whereas the other comes from Eq. 6.27 applied in the reverse direction (replace  $n$  with  $n+1$  and  $m$  with  $n$  into Eq. 6.27). The two estimates will be invoked in the acceptance ratio of  $n \rightarrow n+1$  and  $n+1 \rightarrow n$  ensemble transitions, respectively (see next point 4). In the former case we need to resort to additional arrays (denoted as  $N_{n \rightarrow n+1}^{\text{up}}$  and  $W^{\text{up}}[n \rightarrow n+1]$ ) to store  $N_{n \rightarrow n+1}$  and  $W[n \rightarrow n+1]$ . Separate arrays are necessary because they are subject to different manipulation during the simulation. Specifically, if the condition  $N_{n \rightarrow n+1}^{\text{up}} > N'$  is satisfied, then we calculate  $\Delta f_{n \rightarrow n+1}$  via Eq. 6.27. This estimate is employed as such in the acceptance ratio. Then we set  $N_{n \rightarrow n+1}^{\text{up}} = 0$  and remove  $W^{\text{up}}[n \rightarrow n+1]$  from computer memory. The same protocol is used to calculate  $\Delta f_{n+1 \rightarrow n}$  from the quantities  $N_{n+1 \rightarrow n}^{\text{down}}$  and  $W^{\text{down}}[n+1 \rightarrow n]$ . The additional arrays introduced here are updated as described at point 2. Note that in this procedure the arrays of step 3a are neither used nor changed. Note also that the procedure described here corresponds to the way of calculating the finite free energy differences in free energy perturbation method[119].

- (c) If none of the above criteria is met, then optimal weights are not updated and conventional sampling continues. Storage of dimensionless works as described at point 2 continues as well.

We point out that, if equilibrium is reached slowly (case of large viscous systems, or systems with very complex free energy landscape), then the replicas may tend to get trapped in limited regions of the ensemble space at the early stages of the simulation. This is basically due to initially inaccurate determination of  $\Delta f_{n \rightarrow n+1}$  from Eq. 6.25 (point 3a). If such an event occurs, then subsequent free energy estimates from Eq. 6.25 may become very rare or even impossible. However we can prevent this unwanted situation by passing to the updating criteria of point 3b when the criteria of point 3a are not met for a given (prior established) number of consecutive times (10 times in ORAC). When equilibrium will be approached, the criteria of point 3b will favor transitions of the replicas between neighboring ensembles and eventually the conditions to apply again the criteria of point 3a.

(4) Every  $L_c$  steps a transition  $(x, p)_n \rightarrow (x, p)_{n \pm 1}$  is attempted on the basis of the acceptance ratio of Eq. 6.22 and of the current value of  $\Delta f_{n \rightarrow n \pm 1}$  (properly reweighted according to the equations reported in Sec. 6.3.3). If the estimate of  $\Delta f_{n \rightarrow n \pm 1}$  is still not available from the methods described at points 3a and 3b, then the transition is not realized. The upward and downward transitions are chosen with equal probability.

It is worthwhile stressing again that the procedures of point 3b are only aimed to furnish a reliable evaluation of optimal weights when such factors are still not available from the bidirectional algorithm (point 3a) or when the system is get trapped in one or few ensembles (point 3c). Moreover, we remark that the free energy differences estimated via Eq. 6.27 tend to give larger acceptance rates in comparison

to the exact free energy differences, thus favoring the transitions toward the ensemble that has not been visited. This is a well-known (biasing) effect of exponential averaging[128], leading to a mean dissipated (dimensionless) work artificially low. As a matter of fact this is a positive effect since it makes easier ensemble transitions during the equilibration phase of the simulation.

In the above discussion, we do not have mentioned the number  $M$  of (independent) replicas that may run in the space of the  $N$  ensembles. In principle,  $M$  can vary from one to infinity on the basis of our computer facilities. The best performance is obtainable if a one-to-one correspondence exists between replicas and computing processors. A rough parallelization could be obtained performing  $M$  independent simulations and then drawing the data from replicas at the end of the simulation to get an augmented statistics. However, the calculation of the optimal weights would be much improved if they were periodically updated on the fly on the basis of the data drawn from all replicas. This is just what ORAC does. In this respect we notice that our version of multiple-replica SGE algorithm is prone to work efficiently also in distributed computing environments. The phase of the simulation where information is exchanged is that described at point 3 (free energy calculation). It should be noted that, when a free energy estimate is performed, the work arrays stored for each replica/processor (see point 2) do not need to be communicated to all other replicas/processors. Only the sums  $\sum_{i=1}^{N_{n \rightarrow m}} [\cdot]^{-1} - \sum_{j=1}^{N_{m \rightarrow n}} [\cdot]^{-1}$  (case of Eq. 6.25),  $\sum_{i=1}^{N_{n \rightarrow m}} [\cdot]^{-1} + \sum_{j=1}^{N_{m \rightarrow n}} [\cdot]^{-1}$  (case of Eq. 6.26) and  $\sum_{i=1}^{N_{n \rightarrow m}} \exp(-W_i[n \rightarrow m])$  (case of Eq. 6.27), together with  $N_{n \rightarrow m}$  and  $N_{m \rightarrow n}$ , must be exchanged for all  $N - 1$  ensemble transitions. Then each replica/processor “will think by itself” to reassemble the global sums. Exchanging one information implies to send  $M(M - 1)(N - 1)$  real/integer numbers through the net ( $\sim 60$  kB of information using 20 replicas and slightly less than 1 MB of information using 50 replicas). Only in the case of the iterative procedure of Eq. 6.25, one information has to be sent several times per free energy calculation (*i.e.*, the number of iterations needed for solving the equation). The computational cost arising from computer communications can however be reduced updating the free energy rarely. Furthermore, in order to improve the first free energy estimate and hence to speed up the convergence, the  $M$  simulations should be started by distributing the replicas among neighboring ensembles, namely replica 1 to  $\Lambda_1$ , replica 2 to  $\Lambda_2$  and so on (see also the discussion at the beginning of the current section).

### 6.3.3 Free energy evaluation from independent estimates and associated variances

As discussed in Sec. 6.3.2, during a SGE simulation, optimal weights are evaluated using Eq. 6.25, and only temporary values are obtained from Eq. 6.27. Therefore, for each optimal weight, the simulation produces a series of estimates,  $\Delta f_1, \Delta f_2, \dots, \Delta f_P$ . At a given time, the current value of  $P$  depends, on average, on the time and on the update frequency of optimal weights. In this section, for convenience, the subscript in  $\Delta f_i$  labels independent estimates. We also know that each  $\Delta f_i$  value is affected by an uncertainty quantified by the associated variance  $\delta^2(\Delta f_i)$  calculated via Eq. 6.26. We can then write  $\hat{\Delta f}$ , the optimal estimator of  $P^{-1} \sum_{i=1}^P \Delta f_i$ , by a weighted sum of the individual estimates[129]

$$\hat{\Delta f} = \frac{\sum_{i=1}^P [\delta^2(\Delta f_i)]^{-1} \Delta f_i}{\sum_{j=1}^P [\delta^2(\Delta f_j)]^{-1}}. \quad (6.28)$$

Note that independent estimates with smaller variances get greater weight, and if the variances are equal then the estimator  $\hat{\Delta f}$  is simply the mean value of the estimates. The uncertainty in the resulting estimate can be computed from the variances of the single estimates as

$$\delta^2(\hat{\Delta f}) = \left\{ \sum_{j=1}^P [\delta^2(\Delta f_j)]^{-1} \right\}^{-1}. \quad (6.29)$$

The ORAC program allows one to calculate  $\hat{\Delta f}$  using either all available estimates or a fixed number of estimates, taken from the latest ones.

## Chapter 7

# Metadynamics Simulation: history-dependent algorithms in Non-Boltzmann sampling

If we are studying a prototypical elementary reaction, in which two stable states are separated by a high free energy barrier  $\Delta A^* \gg k_B T$  along the reaction coordinate  $s$ , configurations corresponding to the free energy maximum (the transition state  $s^*$ ) can be sampled by adding a restraining potential to the original Hamiltonian of the system, so as to obtain a frequency histogram for the value of the reaction coordinate  $s$  centered around the transition state itself. If we were good enough in locating the transition state and matching the curvature of the potential, this distribution will overlap with the two distributions obtained starting two different simulations from the two metastable states. The free energy difference between the metastable states, as well as the height of the free energy barrier at the transition state, can then be computed using the sampling from this “bridging” distribution. This solution is known as Umbrella Sampling[57]. More generally, if the transition state can be identified and located at some value of the reaction coordinate, the procedure of modifying the energetics of a system in order to balance the activation barrier and flatten the free energy profile is known with the name of Non-Boltzmann sampling. The original free energy can be computed from the free energy of the modified ensemble through the formula

$$A(s) \sim A'(s) - V(s) \quad (7.1)$$

where  $A'(s)$  denotes the free energy computed by simulating the modified ergodic system. As in the Umbrella Sampling algorithm, the hardest part of the Non-Boltzmann sampling approach is the construction of a good biasing potential, since this task can be performed only iteratively. Given a rough (because of some free energy barrier) estimate of  $A(s)$  from an old simulation, the simplest way to know how good this estimate is consists in performing a new simulation using this estimate, inverted in sign, as a bias potential. If the free energy profile of the modified system is flat,  $A' = \text{constant}$ , then  $A(s) \sim -V(s)$  is the free energy inverted in sign. Otherwise, from this simulation we can compute an improved estimate for  $A(s)$  through Eq. 7.1. The effectiveness of this tedious approach is due to the fact that each correction to the biasing potential makes the system more ergodic, and therefore each successive simulation is statistically more accurate than the former.

This iterative approach to the problem[130, 131] led to the development of adaptive biasing potential methods that improve the potential “on the fly” [132, 60, 58, 133], *i.e.*, while the simulation is performed. All these methods share all the common basic idea, namely, “to introduce the concept of memory”[132] during a simulation by changing the potential of mean force perceived by the system, in order to penalize conformations that have been already sampled before. The potential becomes history-dependent since it is now a functional of the past trajectory along the reaction coordinate. Among these algorithms, the Wang-Landau [60] and the metadynamics[58] algorithms have received most attention in the fields of the Monte Carlo (MC) and Molecular Dynamics (MD) simulations, respectively. This success is mainly due to the clearness and the ease of implementation of the algorithm, that is basically the same for the two methods. The Wang-Landau algorithm was initially proposed as a method to compute the density

of states  $g(E)$ , and therefore the entropy  $S(E) = \ln g(E)$ , of a simulated discrete system. During a Wang-Landau MC simulation,  $S(E)$  is estimated as an histogram, incrementing by a fixed quantity the frequency of the visited energy levels, while moves are generated randomly and accepted with a Metropolis probability  $\text{acc}(E \rightarrow E') = \min\{1, \exp(-\Delta S)\}$ , where  $\Delta S = S(E') - S(E)$  is the current estimate of the entropy change after the move. While for a random walk in energy the system would have been trapped in entropy maxima, the algorithm, that can be easily extended to the computation of any entropy-related thermodynamic potential along a generic collective variable, helps the system in escaping from these maxima and reconstructs the entropy  $S(E)$ . The metadynamics algorithm extends this approach to off-lattice systems and to Molecular Dynamics. Metadynamics has been successfully applied in the computation of free energy profiles in disparate fields, ranging from chemical physics to biophysics and material sciences. For a system in the canonical ensemble, metadynamics reconstructs the free energy along some reaction coordinate  $s$  as a sum of Gaussian functions deposited along the trajectory of the system. This sum inverted in sign is used during the simulation as a biasing potential  $V(s, t)$  that depends explicitly on time  $s$ :

$$V(s, t) = \sum_{t'=\tau, 2\tau, \dots, t} \mathcal{G}(s; s_{t'}, h, \sigma) \quad (7.2)$$

where  $\mathcal{G}(s; s_t, h, \sigma) = h \exp(-(s - s_t)^2/2\sigma^2)$  is a Gaussian function centered in  $s_t$  with height  $h$  and variance  $\sigma^2$ . During a metadynamics simulation, the potential  $V(s, t)$  will grow faster for states with an higher probability, pushing out the system from minima in the free energy landscape. If the rate of deposition  $\omega = h/\tau$  is sufficiently slow, the system can be considered in equilibrium with the biased Hamiltonian  $H'(x, t) = H(x) + V(s, t)$ , and therefore the probability of visiting state  $s$  at time  $t$  is the equilibrium canonical distribution  $p(s, t) \propto \exp[-\beta(A(s) + V(s, t))]$ . Once all the free energy minima have been “filled” by the biasing potential, and therefore  $V(s, t) = -A(s)$ , such a probability is uniform along  $s$  and the potential will grow uniformly.

The thermodynamical work spent in changing the potential from the original Hamiltonian  $H(x)$  to  $H'(x, t) = H(x) + V(s, t)$  can be computed through the relation  $W = \int_0^t d\tau \left( \frac{\partial H}{\partial t} \right)_\tau$ . In the limit of an adiabatic transformation, this quantity is equal to the Helmholtz free energy difference  $\Delta A = A' - A_0$  between two systems with energy functions  $H'$  and  $H$ , where  $A' = \int dx \exp(-\beta H')$  and  $A_0 = \int dx \exp(-\beta H)$ [134]. However, if the process is too fast with respect to the ergodic time scale, a part of the work spent during the switching will be dissipated in the system, resulting in an non-equilibrium, non-canonical distribution, and in a systematic error in the free energy estimate. In particular, it is assumed that during a metadynamics simulation all the microscopic variables different from the macroscopic reaction coordinate  $s$  are always in the equilibrium state corresponding to the value of  $s$ [135]. This property is known with the name of Markov property, and it summarizes the main assumption of the algorithm: all the slow modes of the system coupled to the reaction under study have to be known *a priori* and they have to be included in the number of the reaction coordinates. Therefore, at variance with the methods presented in the previous chapters, metadynamics should be considered a quasi-equilibrium method, in which the knowledge about the variables that capture the mechanism of a reaction is exploited to gain insight on the transition states and more generally to compute the free energy landscape along the relevant reaction coordinates.

## 7.1 Implementation in ORAC

From the practical point of view, a metadynamics simulation consists in two steps. In the first one, a set of reaction coordinates is chosen whose dynamics describes the process under study. As we said, such a procedure requires an high degree of chemical and physical intuition for its application to complex molecular system, since these variables are not obviously determined from a molecular structure.

The second step is the metadynamics simulation itself, during which an history-dependent potential is constructed by summing, at regular time intervals, repulsive potential terms centered in the current position of the system in the space of the reaction coordinates. In its standard implementation, the history-dependent potential of metadynamics is given by a sum of small repulsive Gaussian, Eq.7.2. Some variants have been introduced, with the intent of improving the accuracy or the efficiency of the method[136, 137]. In the ORAC program we have used Lucy’s function[138] as a very efficient alternative to the use of Gaussians.

It is defined as <sup>1</sup>

$$\mathcal{L}(s; s_0, h, w) = h \left( 1 + 2 \frac{|s - s_0|}{w} \right) \left( 1 - \frac{|s - s_0|}{w} \right)^2; 0 \text{ if } |s - s_0| > w \quad (7.3)$$

with the origin at  $s_0$ . The symbols  $h$  and  $w$  denote the height and the width, respectively. Such a function is normalizable,  $\int_{-\infty}^{\infty} ds \mathcal{L}(s; s_0, w) = hw$ , has a finite range  $w$ , has a maximum at the origin and it is differentiable everywhere. A Lucy's function can be compared with a Gaussian function with the same value at the origin and at  $|s| = s_0 + w/2$ , such that

$$2\sigma = w/(2 \ln 2)^{1/2} \quad (7.4)$$

A Lucy's function can be regarded as a Gaussian function with  $\sigma$  in Eq.7.4, but without the long tails of the Gaussian, as can be seen in Fig.7.1 where a Lucy's function with  $h = w = 1$  and a Gaussian function with the same height and  $\sigma = w/2(2 \ln 2)^{1/2}$  are shown. The parameters  $h$ ,  $w$  and  $\tau$  affects the accuracy of the free energy reconstruction in a similar manner to the height and the width of Gaussian functions and a comprehensive review on the analysis of the error during a metadynamics run can be found in [62].

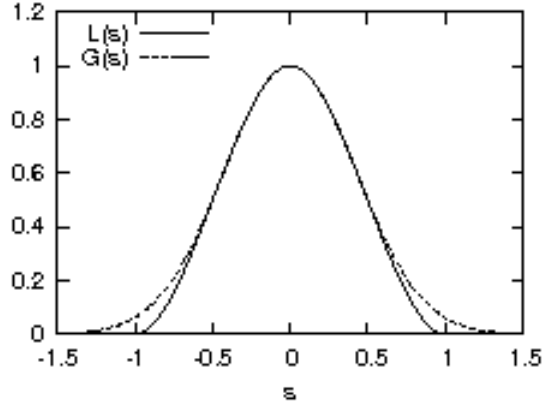


Figure 7.1: Lucy's function  $L$  with  $h = w = 1$ , along with a Gaussian function  $G$  with the same height and  $2\sigma = w/(2 \ln 2)^{1/2}$ .

The history dependent potential used during an ORAC simulation can therefore be written as

$$V(s, t) = \sum_{t'=\tau, 2\tau, \dots} \mathcal{L}(s; s_{t'}, h, w) \quad (7.5)$$

During a simulation, forces from this biasing potential are computed in the shell  $n1$  as a sum of derivatives of  $\mathcal{L}$  functions:

$$\frac{\partial \mathcal{L}(s; s_0, h, w)}{\partial s} = \frac{6h}{w^3} (s - s_0) (|s - s_0| - w); 0 \text{ if } |s - s_0| > w \quad (7.6)$$

Such a derivative is computationally attractive, since it does not require the evaluation of an exponential function as in the case of the derivative of a Gaussian function. Moreover, since  $\mathcal{L}$  has a finite range by

<sup>1</sup> Lucy's function can be defined for a generic order  $n$  such that it has  $n - 1$  continuous derivative everywhere[139]. The original definition[138] was given for  $n = 3$ ; here it is employed with  $n = 2$ .



definition, it does not need to be smoothly truncated[137], as there are no contribution to the forces from hills farther than the width  $w$ .

Using the standard metadynamics approach, during a simulation the algorithm keeps on adding terms to the history-dependent potential (the sum in Eq.7.5) with the same constant rate  $\omega = h/\tau$ . However, the optimal solution would be to use a faster rate at the beginning of the simulation, so as to produce a rough estimate of the free energy, and then to reduce  $\omega$  to refine this estimate[140]. This problem corresponds to finding an optimal protocol for the evolution of the modification factor in the original Wang-Landau algorithm. Various solutions have been proposed[141, 133, 142, 143] in which the energy  $h$  in 7.3 is time-dependent. We propose instead to add a term to the biasing potential with a given probability  $P_t(\text{add})$ , depending parametrically on time. For example, for  $P_t(\text{add}) \propto 1/t$ , the evolution of the rate would be given by  $\omega(t) = P_t(\text{add})\omega_0 \propto \omega_0/t$ . This procedure can be seen on average as an increasing deposition interval  $\tau(t)$ , such that  $\omega(t) = h/\tau(t)$  decreases in time. In the present implementation of ORAC, three different choices are available for the probability  $P(\text{add})$ : the default one is simply  $P(\text{add}) = 1$  and corresponds to the standard metadynamics algorithm. The second one is given by

$$P_t(\text{add}) = e^{-V_{\max}(t)/k_B T'} \quad (7.7)$$

where  $V_{\max}(t)$  is the maximum value of the potential  $V(s, t)$  at time  $t$ . During the simulation, the effective rate  $\omega(t)$  decreases as  $V_{\max}(t)$  increases. As  $V_{\max} \gg k_B T'$ , the deposition rate  $\omega(t)$  is so slow that the transformation can be considered adiabatic, and the biasing potential converges to the free energy inverted in sign,  $A(s) = -V(s, t)$ . The slowdown of  $\omega$  can be tuned through the parameter  $T'$ . Finally, following the well-tempered metadynamics approach[143], the third choice is given by

$$P_{s,t}(\text{add}) = e^{-V(s,t)/k_B T'} \quad (7.8)$$

where the probability depends parametrically both on time  $t$  and on position  $s$  of the system along the reaction coordinate through the biasing potential  $V$ . In this case, the biasing potential does not converge to the free energy inverted in sign as in the previous case, since in general  $\omega$  turns out to be coordinate-dependent even when the potential has flattened the free energy profile. However, as shown in [143], the relation

$$A(s) = -\frac{T + T'}{T} V(s, t) \quad (7.9)$$

can be used to recover the original free energy from the biasing potential.

The multiple walkers version of metadynamics algorithm[144] was implemented in the parallel version of the code through the MPI library. This approach is based on running simultaneously multiple replicas of the system, contributing equally to the same history-dependent potential, and therefore to the same free energy surface reconstruction. For  $N$  replicas,  $V(s, t)$  can be written as a double sum

$$V(s, t) = \sum_{t'=\tau, 2\tau, \dots, t} \sum_{i=1, N} \mathcal{L}(s; s_{i,t'}, h, \sigma) \quad (7.10)$$

where  $s_{i,t'}$  is the position at time  $t'$  of the  $i$ -th replica along  $s$ . In particular, the enhanced efficiency of this algorithm with respect to uncoupled simulations contributes to make the calculation of FESs in high dimensions more accessible.

In the ORAC distribution at <http://www.chim.unifi.it/orac> we provide some example of metadynamics simulations using Lucy's functions on multi-dimensional surfaces of simple molecules in the gas phase along with some ancillary codes for the analysis of the program output.

## Chapter 8

# Steered Molecular Dynamics

Steered molecular dynamics simulation (SMD) is a technique mimicking the principle of the atomic force microscopy (AFM). In practice, one applies a time dependent mechanical external potential that obliges the system to perform some prescribed motion in a prescribed simulation time. SMD has been widely used to explore the mechanical functions of biomolecules such as ligand receptor binding/unbinding and elasticity of muscle proteins during stretching at the atomic level[145]. The SMD has also been used in the past to approximately estimate the potential of mean force (PMF)<sup>1</sup> along a given mechanical coordinate (for example a distance or an angle). The model upon which this technique for estimating the PMF relies was based on the assumption that the driven motion along the reaction coordinate  $z$  could be described by an over-damped one-dimensional Langevin equation of the kind

$$\gamma\dot{z} = -\frac{d\mathcal{W}}{dz} + F_{\text{ext}}(z, t) + \xi(t) \quad (8.1)$$

where  $\gamma$  is the friction coefficient,  $\mathcal{W}$  is the underlying potential of mean force,  $F_{\text{ext}}(z, t)$  is the external force due the driving potential and  $\xi(t)$  is a stochastic force related to the friction through the second fluctuation dissipation theorem. The PMF  $W(z)$  can then be determined only if one knows (or can somehow figure it out) the friction coefficient, so as to evaluate the frictional force that discounts the irreversible work done in the driven process. The method also relies on the strong assumption that the friction along  $z$  is local in time, i.e. the underlying equilibrium process is *Markovian*.

### 8.1 The Crooks theorem

Recent development on non equilibrium thermodynamics have clarified that the PMF along the given reaction coordinate  $z$  can actually be reconstructed *exactly* using an ensemble of steered molecular dynamics simulations without resorting to any assumption on, or having any knowledge of the frictional behaviour of the system along the reaction coordinate. These developments date back to a paper by Evans, Searls[146] where the first example of *transient fluctuation theorem* for a system driven out of equilibrium was formulated, demonstrating the connection between the time integral of the phase compression factor in Liouville space along an arbitrary time interval and the probability ratio of producing the entropy  $A$  and  $-A$  along a deterministic trajectory of a many particles non equilibrium steady state system. Gavin Crooks in his *phd* thesis proposed[64], in the context of Monte Carlo simulations in the canonical ensemble (NVT), a *transient*[146] fluctuation formula (from now on indicated with CT) involving the dissipative work for systems driven out of equilibrium by varying some arbitrary mechanical parameter. The CT is actually even more general than the Evans and Searls fluctuation theorem[146] since in the latter the driven  $z$  coordinate has an underlying zero PMF (i.e. only entropy is produced in the non equilibrium process) while in the former the system can also cross different thermodynamics states (i.e. the underlying PMF can also be non zero such that thermodynamic work can also be done). The Crooks theorem (CT) reads

$$\frac{p(\Gamma(z_0) \rightarrow \Gamma(z_\tau))}{p(\Gamma^*(z_0) \leftarrow \Gamma^*(z_\tau))} = \exp[\beta(W_{\Gamma(z_0) \rightarrow \Gamma(z_\tau)} - \Delta F)], \quad (8.2)$$

---

<sup>1</sup>The potential of mean force is defined as  $\mathcal{W}(z) = -k_B T \ln P(z)$ , where  $P(z) = \langle \delta(z - z(\mathbf{r})) \rangle$  is the probability to find the system at the value of the reaction coordinate  $z(\mathbf{r}) = z$  independently on all the other coordinates.



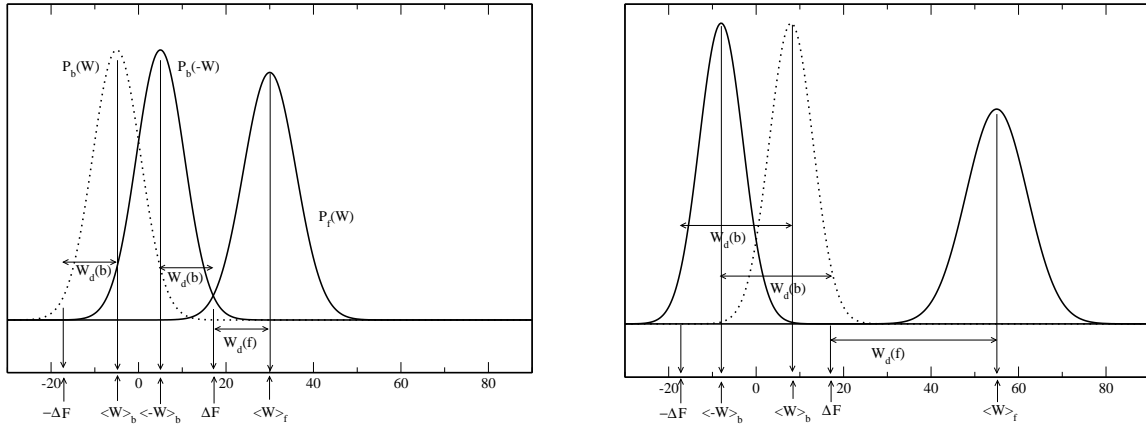


Figure 8.1: Physical significance of the Crooks theorem for a general driven process: for nearly reversible processes (left) the forward  $P_f(W)$  and backward  $P_b(-W)$  work distributions overlap significantly. The dotted line is the the backward work distribution for the inverse process, without changing the sign of the work. The crossing of the two solid distribution occurs at the free energy value for the *forward* process  $\Delta F = 18$ . When the process is done faster (right panel), the dissipation  $W_d$  both in the forward and in the backward process is larger, the overlap is negligible and the crossing point of the two solid distribution can no longer easily identified.

where  $\tau$  is the duration time of the driven non equilibrium process,  $W_{\Gamma(z_0) \rightarrow \Gamma(z_\tau)}$  is the work done on the system during the driven trajectory  $\Gamma(z_0) \rightarrow \Gamma(z_\tau)$ ;  $p(\Gamma(z_0) \rightarrow \Gamma(z_\tau))$  is the joint probability of taking the microstate  $\Gamma(z_0)$  from a canonical distribution with a given initial Hamiltonian  $H(z = z_0)$  and of performing the forward transformation to the microstate  $\Gamma(z_\tau)$  corresponding to a different Hamiltonian  $H(z = z_\tau)$ ;  $p(\Gamma^*(z_0) \leftarrow \Gamma^*(z_\tau))$  is the analogous joint probability for the *time reversal* path, producing the work  $W_{\Gamma(z_\tau) \rightarrow \Gamma(z_0)} = -W_{\Gamma(z_0) \rightarrow \Gamma(z_\tau)}$ .  $\Delta F = F(z = z_\tau) - F(z = z_0)$  is the free energy difference between the thermodynamic states associated to the Hamiltonians  $H(z = z_\tau)$  and  $H(z = z_0)$ . Although the CT can be stated in a more general formulation (see Gavin Crooks, *phd* thesis), here the essential assumptions are that i) the system is deterministic and satisfies the time reversal symmetry and ii) the reverse trajectory is done following a *reversed* time schedule such that  $W_{\Gamma(z_\tau) \rightarrow \Gamma(z_0)} = -W_{\Gamma(z_0) \rightarrow \Gamma(z_\tau)}$ . The first assumption is satisfied by any kind of standard MD equation of motion (Newtonian, Nosé-Hoover, Parrinello-Rahman) while the second condition can be easily imposed in a SMD experiment. A very simple proof of Eq. 8.2 goes as follows: suppose the  $z_0$  is drawn from a canonical distribution, and that the driven trajectory that brings the system to  $z_\tau$  is done adiabatically, i.e. removing the thermal bath. For the reverse trajectory, drawing  $z_\tau$  from a canonical distribution, due to the time reversal symmetry of the Hamilton equations, one ends up adiabatically in  $z_0$ . Under these assumptions, the ratio of the two probabilities on the left hand side of Eq. 8.2 can be written as

$$\begin{aligned}
 \frac{p(\Gamma(z_0) \rightarrow \Gamma(z_\tau))}{p(\Gamma^*(z_0) \leftarrow \Gamma^*(z_\tau))} &= \frac{e^{-\beta H(z=z_0)}}{Z_0} \frac{Z_\tau}{e^{-\beta H(z=z_\tau)}} \\
 &= e^{\beta(H(z=z_\tau) - H(z=z_0) - \Delta F)} \\
 &= \exp \beta(W_{\Gamma(z_0) \rightarrow \Gamma(z_\tau)} - \Delta F)
 \end{aligned} \tag{8.3}$$

equation where we have used the facts that  $\beta F(z = z_0) = \ln Z_0$ ,  $\beta F(z = z_\tau) = \ln Z_\tau$  and that the energy difference  $H_B - H_Z$  in the forward adiabatic trajectory equals to the external work done on the systems. Equation 8.2 refers to the probability of a *single* forward or backward trajectory. Suppose now to perform a large number of forward trajectories all with a give time schedule, but each started from a different initial phase point sampled according to the canonical equilibrium distribution characterized by the Hamiltonian  $H(z = z_0)$  and a large and not necessarily equal number of backward trajectories with reverse time schedule

and starting from initial phase points this time sampled according to the canonical equilibrium distribution characterized by the Hamiltonian  $H(z = z_t)$ .<sup>2</sup> By collecting all trajectories yielding the work  $W$  in (8.2), the CT may compactly be written as:

$$\frac{P_F(W)}{P_R(-W)} = \exp[\beta(W - \Delta F)], \quad (8.4)$$

where  $P_F(W)$  and  $P_R(W)$  are the normalized forward and backward distribution functions (note that, due to the time reversal symmetry, for the backward distribution the work is taken with the minus sign, i.e.  $P_R(-W)$  is the mirror symmetric with respect to  $P_R(W)$ ). According to Eq. 8.4, the  $\Delta F$  may be thus evaluated constructing the two work distribution function:  $\Delta F$  is the work value where the two distribution cross, i.e.  $P_F(W = \Delta) = P_R(-W = \Delta F)$ . We point out in passing that, the famous Jarzynski identity[63] (JI),

$$\langle e^{-\beta W} \rangle = e^{-\beta \Delta F}, \quad (8.5)$$

is actually a trivial consequence of the CT, being derived from the latter by integrating out the work variable and using the fact that the work distribution function  $P_F(W)$  and  $P_R(-W)$  are normalized.

The physical meaning of the Crooks equation sounds indeed very reasonable and can be even be considered as a probabilistic restatement of the second law or of a generalization of the H-Boltzmann theorem: Given a forward *deterministic* non equilibrium trajectory starting from equilibrium and producing a work  $W$ , the probability to observe a trajectory for the reverse process again starting from equilibrium and producing the work  $-W$  is  $e^{\beta W_d}$  small than the former, where  $W_d = W - \Delta F$  is the dissipated work in the forward process. When the dissipated work is zero, i.e. when the driven process is *quasi-static* and is done always at equilibrium, then the two probabilities are identical. With this regard, one important point to stress is that the CT and the JI hold *for all systems* and for any kind of arbitrary non equilibrium process, *no matter how fast is performed*. In particular, if the non equilibrium process is *instantaneous*, i.e. if it is done at infinite speed, then the work done on the system is simply equal to  $W = (H_1 - H_0)$ , with  $H_0$  and  $H_1$  being the Hamiltonian of the initial and final state, respectively. The JI reduces in this case to the famous free energy perturbation Zwanzig[119] formula  $\langle e^{-\beta(H_1 - H_0)} \rangle_0 = e^{-\beta \Delta F}$  with the subscript 0 indicating that the canonical average must be taken according to the equilibrium distribution of the system with Hamiltonian  $H_0$ .

For fast non equilibrium experiments, a large amount of the work, rather than in advancing the reaction coordinate, is dissipated in heat that is in turn (only partly) assimilated by the thermal bath<sup>3</sup> A consequence of this is that the maxima of two work distributions  $P_F(W)$  and  $P_R(W)$  tend to get further apart from each other so that the determination of  $\Delta F$  becomes less accurate. The faster are performed the non equilibrium experiments, the large is the average dissipation and the smaller is the overlap between the two work distributions (see Fig. 8.1) The reason why CT and JI can be so useful in evaluating the free energies along given reaction paths in the molecular dynamics simulation of complex biological system lies on the fact that this methodologies are inherently more accurate the smaller is the sample. Let's see why. As one can see from Fig. 8.1,  $\Delta F$  can be determined with accuracy if the two work distributions overlap appreciably, or stated in other terms, if there are sufficient trajectories that in both directions transiently violate the second law, i.e trajectories for which  $W < \Delta F$ . This is clearly not in contrast with the second law which states that  $\bar{W} \leq \Delta F$  where  $\bar{W} = \int P(W)WdW$  is the *mean* irreversible work. In general, the probability of an overlap of the two work distributions (i.e. the probability of transiently violating the second law) is clearly larger the smaller is the system. Suppose to simultaneously and irreversibly unfold  $N$  identical proteins in a dilute solution starting from their native states. In the assumption that the

<sup>2</sup> The Hamiltonian  $H(z = z_t)$  may be imposed practically in steered molecular dynamics using constraints or adding a stiff harmonic potential that keeps the system at  $z = z_t$ . Both these methods requires small corrections when reconstructing the PMF. In particular, the use of constraints on  $z$  sets also  $\dot{z} = 0$ , a condition that is not present in the definition of the PMF (see previous footnote). The correction to the PMF due this extra artificial condition imposed through a generic constraint is discussed in Ref. [147]. Stiff harmonic potentials, in the sense that the associated stretching motion is decoupled from the degrees of freedom of the system, behaves essentially like constraints.[148] The depuration of the the PMF from the non stiff harmonic driving potential in AFM experiments has been proposed by Hummer and Szabo.[65]

<sup>3</sup> During the non equilibrium experiment, the instantaneous "temperature" of the system as measured by the kinetic energy may well exceed that of the thermal bath. Actually the "temperature" cannot even be defined for a system that is not at equilibrium as part of it, near the reaction path, can be warmer than other parts that are far from the reaction coordinate. This has clearly no consequences whatsoever on the CT, since the temperature in Eq. 8.2 that of the system at the initial points which are drawn by hypothesis at equilibrium

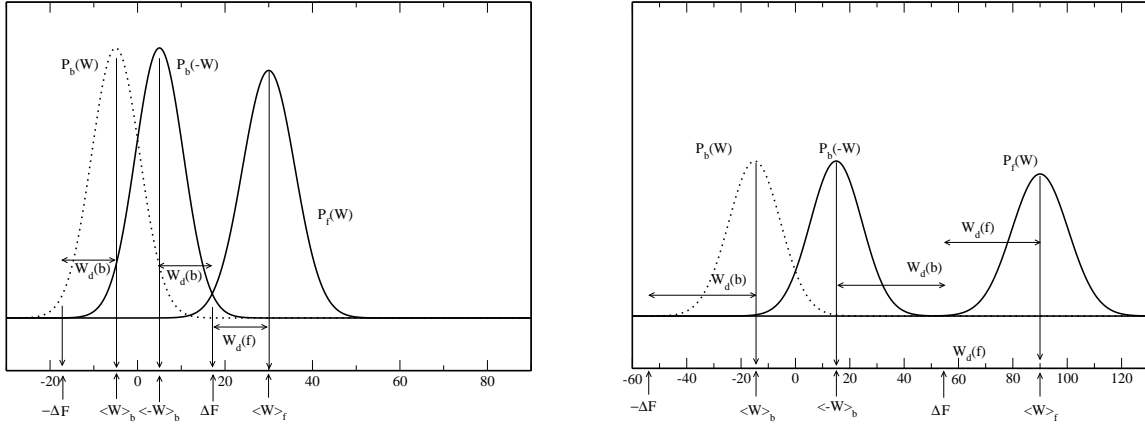


Figure 8.2: Effect of the size of the system on the overlap of the forward and backward work distributions. In the left panel the non equilibrium processes are done in a given time  $\tau$  on a single molecule. In the right panel the processes, as in left panel of duration  $\tau$ , are done independently on three identical molecules. This implies a factor 3 on energies and a factor  $3^{1/2}$  on widths. As a result of the increased size, the overlap between  $P_f(W)$  and  $P_b(-W)$  decreases significantly.

intraprotein interaction are negligible, the mean work for this system will be simply  $N$  times the mean work done on a *single* molecule, while the width of the work distribution for the  $N$  molecule systems will be only  $N^{1/2}$  larger than that of the single molecule system. This effect is illustrated in Fig. 8.2. Now, biomolecular simulation of biosystems are usually done, for computational reasons, on a *single* solvated biomolecule, i.e. in the conditions where the non equilibrium techniques, for the reason explained above, are deemed to be more successful.

## 8.2 Determination of the potential of mean force via bidirectional non equilibrium techniques

The Jarzynski identity is seemingly a better route than the CT to evaluate the full potential of mean force along  $F(z)$  in the interval  $[z_0, z_t]$ , with  $0 < t < \tau$ . However the exponential averages in Eq. 8.5 is known to be strongly biased, i.e. it contains a systematic error[149] that grows with decreasing number of non equilibrium experiments. This can be qualitatively explained with the fact that, for dissipative fast non equilibrium experiments, the forward work distribution  $P(W)$  has its maximum where the exponential factor  $e^{-\beta W}$  is negligibly small, so that the size of the integrand  $P(W)e^{-\beta W}$  is *de facto* controlled by the left tail of the  $P(W)$  distribution.[65] An unfortunate consequence of this, is that the PMF calculated through the JI becomes more and more biased as the reaction  $z$  coordinate is advanced, since the accumulated dissipation work shift the maximum of the  $P(W)$  distribution

The CT is far more precise than the JI to evaluate free energy differences. Shirts and Pande[66] have restated the CT theorem showing that the maximum likelihood estimate (MLE) of the free energy difference exactly correspond to the so-called Bennett acceptance ratio[118]<sup>4</sup>. The MLE restatement of the CT is the following

$$\sum_{i=1}^{n_F} \frac{1}{1 + \frac{n_F}{n_R} e^{\beta(W[\mathbf{F}_i] - \Delta F)}} - \sum_{i=1}^{n_R} \frac{1}{1 + \frac{n_R}{n_F} e^{\beta(W[\mathbf{R}_i] + \Delta F)}} \quad (8.6)$$

<sup>4</sup>Bennett was the first researcher to clearly recognize and formalize through the BAR the superiority of bidirectional methods in the computation of free energy differences. We cite *verbatim* from his paper[118]: “The best estimate of the free energy difference is usually obtained by dividing the available computer time approximately equally between the two ensembles; its efficiency (variance x computer time) is never less, and may be several orders of magnitude greater, than that obtained by sampling only one ensemble, as is done in perturbation theory.”

where the  $n_F$ ,  $n_R$  are the number of forward and backward non equilibrium experiments and  $W[\mathbf{F}_i]$   $W[\mathbf{R}_i]$  indicate the outcome of  $i$ -th forward and backward work measurement. This equation has only one solution for  $\Delta F$ , i.e. the MLE. As such, however, the Crooks theorem allows, through the MLE estimate based on bidirectional work measurements, to compute the free energy difference  $\Delta F$  between the *end points* (i.e. between thermodynamic states at fixed and given reaction coordinates  $z = z_0$  and  $z = z_t$ ). In principle, to reconstruct the full PMF along the reaction coordinate  $z$ , in the spirit of thermodynamics integration, One should provide a series of equilibrium ensembles of configurations at *intermediate* values of  $z_t$ . Here, we briefly sketch out a methodology for reconstructing the full PMF in the segment  $[z_0, z_\tau]$  doing only the two work measurements from  $z_0$  to  $z_\tau$  and back. We first rewrite the Crooks equation, Eq. 8.2, as follows

$$\rho_F(\Gamma) = \rho_R(\hat{\Gamma})e^{\beta(W-\Delta F)}, \quad (8.7)$$

where  $\rho_F$ ,  $\rho_R$  are the probability to observe a particular trajectory  $\Gamma$  in the forward and reverse process, respectively and  $\hat{\Gamma}$  indicate the time trajectory taken with inverted time schedule. Eq. 8.7 trivially implies that

$$\langle \mathcal{F} \rangle_F = \langle \hat{\mathcal{F}} e^{\beta(W-\Delta F)} \rangle_R \quad (8.8)$$

$$\langle \mathcal{F} \rangle_R = \langle \hat{\mathcal{F}} e^{-\beta(W-\Delta F)} \rangle_F \quad (8.9)$$

where  $\mathcal{F} = \mathcal{F}(\Gamma)$ ,  $\hat{\mathcal{F}} = \mathcal{F}(\hat{\Gamma})$  is an arbitrary functional of the trajectory  $\Gamma$  and of its inverted time schedule counterpart  $\hat{\Gamma}$ . Using Eq. 8.7, we thus can combine the direct estimate of  $\rho_F(\Gamma)$  with the indirect estimate of the same quantity obtained from  $\rho_R(\hat{\Gamma})$ . This latter, according to Eq. 8.7, must be unbiased with the weight factor corresponding to the exponential of the dissipated work in the forward measurement. If the direct and indirect (Eq. 8.7) estimates are done with  $n_F$  forward measurements and  $n_R$  reverse measurements, respectively, the optimal (minimum variance) combination of these two estimates of  $\rho_F(\Gamma)$  is done according to the WHAM formula[54]

$$\rho_F(\Gamma) = \frac{n_F \rho_F(\Gamma) + n_R \rho_R(\hat{\Gamma})}{n_F + n_R e^{-\beta(W-\Delta F)}}. \quad (8.10)$$

Here  $W$  is the work done in the full  $\Gamma$  path from the end point at  $t = 0$  to the end point at  $t = \tau$ . We now calculate the average of the trajectory functional  $e^{-\beta W_0^t}$  at intermediate times  $0 < t < \tau$ , using the optimized above density. Taking the average of this functional over forward ( $\Gamma$ ) and reverse ( $\hat{\Gamma}$ ) work measurements, exploiting the Jarzynski identity 8.5 in the form  $\langle e^{-\beta W_0^t} \rangle = e^{-\beta(F(z=z_t) - F(z=z_0))}$ , using the fact that  $W$  is odd under time reversal and that  $W_0^t[\hat{\Gamma}] = -W_{(\tau-t)}^\tau[\Gamma]$ , we obtain the following estimate for the free energy at intermediate  $t$ , with  $0 < t < \tau$ :

$$e^{-\beta(F_t - F_0)} = \left\langle \frac{n_F e^{-\beta W_0^t}}{n_F + n_R e^{-\beta(W-\Delta F)}} \right\rangle_F + \left\langle \frac{n_R e^{\beta W_{(\tau-t)}^\tau}}{n_F + n_R e^{\beta(W+\Delta F)}} \right\rangle_R \quad (8.11)$$

This equation, due to Minh and Adib[125], allows to reconstruct the entire potential of mean force  $F_t - F_0$  along the reaction coordinate spanned during the bidirectional non equilibrium experiments of duration  $\tau$ , *no matter how fast the driven processes are done*. Note that  $\Delta W = F_\tau - F_0$  and  $W$  in Eq. 8.11 are the forward free energy difference and work *relative the end points*, respectively.

For fast pulling experiments, i.e. when the dissipated work is large, it can be shown[150], that Eq. 8.11 reduces to

$$e^{-\beta(F_t - F_0)} = \langle e^{-\beta W_0^t} \rangle_F + e^{-\beta \Delta F} \langle e^{-\beta W_{(\tau-t)}^\tau} \rangle_R \quad (8.12)$$

In both Eq. 8.12 and Eq. 8.11 one needs to know the free energy difference between the end points  $\Delta F$ . An unbiased estimate of  $\Delta F$  is easily available through the Bennett acceptance ratio, Eq. 8.6.

### 8.3 Implementation in ORAC

Steered molecular dynamics in ORAC is implemented by adding an external driving potential depending on user defined internal coordinates in the form of stretching, bending, torsions. The general form of the

time dependent external potential that bring the system from an initial state at  $t = 0$  to a different final state  $t = \tau$  is given by

$$V_{ext}(t) = \frac{1}{2} \left[ \sum_{i=1}^{N_r} K_i (r_i - r_{i0}(t))^2 + \sum_{i=1}^{N_\alpha} K_i (\alpha_i - \alpha_{i0}(t))^2 + \sum_{i=1}^{N_\theta} K_i (\theta_i - \theta_{i0}(t))^2 \right] \quad (8.13)$$

where  $r_i$ ,  $\alpha_i$  and  $\theta_i$  represents the actual  $i$ -th stretching, bending and torsional driven coordinate defined by arbitrarily selecting in the corresponding input definition the involved atoms. So a driven torsion or a stretching may be defined using arbitrarily chosen atoms of the solute that are not connected by any real bond.  $r_{i0}(t)$ ,  $\alpha_{i0}(t)$  and  $\theta_{i0}(t)$  are time dependent parameters that defines the non equilibrium trajectory in the space of the coordinates. In ORAC, each of these parameters, given the duration  $\tau$  of the non equilibrium experiment, is varied *at constant speed* from an initial value at time  $t = 0$  defining the reactants, to a final value at time  $t = \tau$  defining the products :

$$\begin{aligned} r_i(t) &= r_{i0} + \frac{r_{i\tau} - r_{i0}}{\tau} t = r_{i0} + v_{ir} t \\ \alpha_i(t) &= \alpha_{i0} + \frac{\alpha_{i\tau} - \alpha_{i0}}{\tau} t = \alpha_{i0} + v_{i\alpha} t \\ \theta_i(t) &= \theta_{i0} + \frac{\theta_{i\tau} - \theta_{i0}}{\tau} t = \theta_{i0} + v_{i\theta} t \end{aligned} \quad (8.14)$$

As all the steering velocities are constant during the experiments, the above equations define a *line*

$$\mathbf{z}(t) = \{(r_1(t), r_2(t), \dots, \alpha_{1(t)}, \alpha_2(t), \dots, \theta_1(t), \theta_2(t), \dots)\} \quad (8.15)$$

in a reaction coordinate space at  $N_r + N_\alpha + N_\theta$  dimensions

The work done by the external potential, Eq. 8.13, in the time  $\tau$  of the non equilibrium driven process along the coordinate  $\mathbf{z}$  is calculated as

$$W_0^\tau = \int_0^\tau \left[ \sum_{i=1}^{N_r} K_i (r_i - r_{i0}(t)) v_{ir} + \sum_{i=1}^{N_\alpha} K_i (\alpha_i - \alpha_{i0}(t)) v_{i\alpha} + \sum_{i=1}^{N_\theta} K_i (\theta_i - \theta_{i0}(t)) v_{i\theta} \right] dt \quad (8.16)$$

The equilibrium distribution of the starting points for independent work measurements can be determined (either by a standard equilibrium molecular dynamics simulation or by some enhanced simulation technique) by constraining the system with the harmonic constraint

$$V_{ext}(0) = \frac{1}{2} \left[ \sum_{i=1}^{N_r} K_i (r_i - r_{i0})^2 + \sum_{i=1}^{N_\alpha} K_i (\alpha_i - \alpha_{i0})^2 + \sum_{i=1}^{N_\theta} K_i (\theta_i - \theta_{i0})^2 \right] \quad (8.17)$$

for the reactants' state and

$$V_{ext}(\tau) = \frac{1}{2} \left[ \sum_{i=1}^{N_r} K_i (r_i - r_{i\tau})^2 + \sum_{i=1}^{N_\alpha} K_i (\alpha_i - \alpha_{i\tau})^2 + \sum_{i=1}^{N_\theta} K_i (\theta_i - \theta_{i\tau})^2 \right] \quad (8.18)$$

for the products' state. Having produced the work in a series of bidirectional experiments, one can then either apply the Bennett formula, Eq. 8.6, to compute the free energy differences between the reactants and the products states, or, using the intermediate work values  $W_0^t$ , apply Eq. 8.11 or Eq. 8.12 to reconstruct the entire potential of mean force along the the mono-dimensional driven trajectory in a multidimensional reaction coordinate space defined in Eq. 8.14. In order to define a non necessarily linear trajectory in a multidimensional reaction coordinate space (e.g. a putative minimum free energy path), one must be able to assign to a each steered coordinate a different steering time protocol. This can be done in ORAC by providing an auxiliary file defining the path in coordinate space. The file has the general form shown in Table 8.3. The free energy or potential of mean force obtained with the described protocols are not depurated by the jacobian terms arising from the definition of the reaction coordinates. For example, the potential of mean force, calculated with Eq. 8.11 or Eq. 8.12 along a driven *distance* for a freely rotating object includes the *additional* contribution  $J(t) = 2k_b T \ln(r_t/r_0)$  arising from the fact that the

$t_1$	$r_1(t_1)$	...	$r_{N_r}(t_1)$	$\alpha_1(t_1)$	...	$\alpha_{N_\alpha}(t_1)$	$\theta_1(t_1)$	...	$\theta_{N_\alpha}(t_1)$
$t_2$	$r_1(t_2)$	...	$r_{N_r}(t_2)$	$\alpha_1(t_2)$	...	$\alpha_{N_\alpha}(t_2)$	$\theta_1(t_2)$	...	$\theta_{N_\alpha}(t_2)$
	...	...	...						
$t_n$	$r_1(t_n)$	...	$r_{N_r}(t_n)$	$\alpha_1(t_n)$	...	$\alpha_{N_\alpha}(t_n)$	$\theta_1(t_n)$	...	$\theta_{N_\alpha}(t_n)$

Table 8.1: General format of the file defining of an arbitrary time protocol for a curvilinear path in a reaction coordinates space at  $N_r + N_\alpha + N_\theta$  dimensions in ORAC . For a generic coordinate  $\zeta = r, \alpha, \theta$ , the steering velocity between times  $t_k$  and  $t_{k+1}$  is constant and equal to  $v_\zeta(t_k) = (\zeta(t_{k+1}) - \zeta(t_k))/(t_{k+1} - t_k)$

configurational probability  $P(r)$ , for two non interacting particles grows with the square of the distance. Moreover the PMF calculated using the driving potential given in Eq. 8.13 are in principle affected by the so-called stiff spring approximation,[148] i.e. if the constant  $K_r, K_\alpha, K_\theta$  in Eq. 8.13 are not large enough, then one actually computes the free energy associated to the Hamiltonian  $\mathcal{H} = H + V_{ext}(\mathbf{z} - \mathbf{z}_t)$  rather than that associated to the Hamiltonian  $H(\mathbf{z} = \mathbf{z}_t)$ . However the impact of the strength of the force constant on the computed non equilibrium average, especially if the reaction coordinate is characterized by inherently slow dynamics and/or the underlying unbiased potential of mean force is much less stiffer than the harmonic driving potential, is generally rather small even at relatively low values of force constant. With this respect, it has been shown that[148]

$$\phi(\mathbf{z}) = F(\mathbf{z}) + \frac{1}{2k}F'(\mathbf{z}) - \frac{1}{2\beta k}F''(\mathbf{z}) + O(1/k^2) \quad (8.19)$$

where  $\phi(\mathbf{z})$  is PMF of the unbiased system with the Hamiltonian  $H(\mathbf{z})$ , while  $F(\mathbf{z})$  is the PMF that is actually measured in the SMD experiments, i.e. that corresponding to the *biased* Hamiltonian  $\mathcal{H} = H(\mathbf{z}) + V_{ext}(\mathbf{z})$ . From Eq. 8.19, one sees that if the derivatives of  $F$  are not too high or  $k$  is chosen large enough, then one can safely assume that  $\phi(\mathbf{z}) \simeq F(\mathbf{z})$ .

eq:intraq:intra1

## Chapter 9

# Alchemical Transformations

In the following we shall describe in details the theory of continuous alchemical transformations, with focus on the issues and technicalities regarding the implementation in molecular dynamics code using the Ewald method. As we will see, running a simulation using standard implementation of the Ewald methods of a system where atomic charges are varying, implies the insurgence of non trivial terms in the energy and forces that must be considered for producing correct trajectories. In a nutshell, Ewald resummations consists in adding and subtracting to the atomic point charges a spherical Gaussian charge distributions bearing the same charge, so that the electrostatic potential is split in a fast dying term (the **Erfc** term), due to the sum of the point charge and the neutralizing charge distribution and evaluated in the direct lattice, and in a slowly decaying term (the **Erf** term) due to the added Gaussian spherical distributions evaluated in the reciprocal lattice. Thanks to this trick, the conditionally convergent electrostatic energy sum is splitted in two absolutely convergent series. In standard implementations of the Ewald resummation technique, as we will see later on, the electrostatic potential at the atomic position  $\mathbf{r}_i$  is actually not available with mixing of the interactions between alchemical and non alchemical species in the so-called Ewald reciprocal lattice contribution (i.e. the **Erf** part). The Smooth Particle Mesh Ewald method (see Chapter 3) makes no exception, with the additional complication that the atomic point charges (including the alchemical charges) are now smeared over nearby grid points to produce a regularly gridded charge distribution, to be evaluated using Fast Fourier Transform (FFT). Due to the extraordinary efficiency (see Figure 4.3), the Particle Mesh Ewald method is still an unrivaled methodology for the evaluation of electrostatic interactions in complex systems. Moreover, PME can be straightforwardly incorporated in fast multiple time step schemes producing extremely efficient algorithms for, e.g., systems of biological interest. For these reasons, it is therefore highly desirable to devise rigorous and efficient approaches to account for alchemical effects in a system treated with PME.

### 9.0.1 Production of the MD trajectory with an externally driven alchemical process

In a system of  $N$  particles subject to a continuous alchemical transformations, only the non-bonded potential energy function is modified because of the presence of alchemical species. The full non bonded energy of the system is given by

$$\begin{aligned}
 V(\mathbf{r}_1, \dots, \mathbf{r}_N, \lambda, \eta) = & \sum_{ij} [1 - \lambda_{ij}(t)] \frac{Q_i Q_j}{r_{ij}} \text{erfc}(\alpha r_{ij}) - \frac{\alpha}{\pi^{1/2}} \sum_i [1 - \lambda_i(t)]^2 Q_i \\
 & + \frac{1}{2\pi V} \sum_{\mathbf{m} \neq 0} \frac{\exp(-\mathbf{m}^2/\alpha^2)}{\mathbf{m}^2} \sum_{ij} [1 - \lambda_{ij}(t)] Q_i Q_j \exp(-i2\pi \mathbf{m} \cdot \mathbf{r}_{ij}) \\
 & + 4\epsilon_{ij} [1 - \eta_{ij}(t)] \left( \frac{1}{[\gamma \eta_{ij}(t) + (r_{ij}/\sigma_{ij})^6]^2} - \frac{1}{[\gamma \eta_{ij}(t) + (r_{ij}/\sigma_{ij})^6]} \right) \quad (9.1)
 \end{aligned}$$

where  $V$  the unit cell volume,  $\mathbf{m}$  a reciprocal lattice vector and  $\alpha$  is the Ewald convergence parameter related to the width of the Gaussian spherical charge distribution. The first term in the non-bonded energy



Eq. 9.1 is limited to the zero-cell and corresponds to the electrostatic interactions in the direct lattice; the second term refers to the self interactions of the Gaussian charge distributions and the third term corresponds to the interactions between Gaussian distributions in the zero cell as well as in the infinite direct lattice, reformulated as an absolutely convergent summation in the reciprocal lattice. The last term in Eq. 9.1, finally, corresponds to the modified atom-atom Van der Waals interaction introduced in Ref. [151] incorporating a soft-core parameterization, where the infinity in the Lennard-Jones interaction is smoothed to zero as a function of the  $\eta_i$ . The parameter  $\gamma$  is a positive constant (usually set [152] to 0.5) that controls the smoothing to zero of the derivatives Lennard Jones function as  $r$  tends to zero.[153]

$i$	$j$	$\lambda_{ij}(t)$	$\eta_{ij}(t)$
Alchemical	Solvent	$\lambda_i(t)$	$\eta_i(t)$
Solvent	Alchemical	$\lambda_j(t)$	$\eta_j(t)$
Solvent	Solvent	0	0
Alchemical A	Alchemical A	0	0
Alchemical A	Alchemical B	1	1
Alchemical B	Alchemical A	1	1

Table 9.1: Combination rules for alchemical and non alchemical species. The alchemical systems may contains three species: i) alchemical growing subsystems, ii) alchemical annihilating subsystems and iii) the non alchemical solvent. The  $\lambda_i(t), \eta_i(t)$  atomic factors within each of this species are all identical and equal to  $\lambda_{G/A/S}(t), \eta_{G/A/S}(t)$ , where the index  $G, A, S$  label the growing, annihilating and solvent species.

In the present general formulation, according to Eq. 9.1, all atoms of the systems, whether alchemical or not, are characterized by an additional, time dependent and externally driven “coordinate”, the  $\lambda_i(t)$  parameter controlling the charging/discharging of the system and the  $\eta_i(t)$  parameter for switching on or off the atom-atom Lennard-Jones potential. The time dependence of the  $\eta_i(t), \lambda_i(t)$  atomic factors is externally imposed using an appropriately selected time protocol. The non bonded potential energy of Eq. 9.1 coincides with the standard potential energy of a system with no alchemical species when all the alchemical atomic factors  $\lambda_i(t), \eta_i(t)$ , referring to electrostatic and Van der Waals interactions, are constant and equal to zero. At the other extreme, when  $\lambda_i(t) = \eta_i(t) = 1$ , the alchemical species disappears according to the “mixing” rules for  $\lambda_{ij}(t), \eta_{ij}(t)$  factors specified in Table 9.1. These rules are such that the modified alchemical potential is enforced only when one of the two interacting atoms is alchemical while atom-atom interactions within a given alchemical species are accounted for with the standard potential or simply set to zero when they do refer to atoms on different alchemical species. In general, the time protocol for the  $\lambda_i, \eta_i$  Van der Waals and electrostatic atomic parameters may differ from each other and for different alchemical species. A simple and sufficiently flexible scheme [154] would be that, for example, of allowing only two sets of alchemical species, i.e. the species to be annihilated and the species to be created, defining hence two different time protocols for the  $\lambda_i$  and two more for the  $\eta_i$  atomic parameters. Such a scheme allows, for example, the determination of the energy difference when one group in a molecule is replaced by an other group in a single alchemical simulation.

As remarked by others [152], it is convenient in a, e.g., alchemical creation, to switch on first the Van der Waals parameters changing  $\eta$  for the alchemical atoms from one to zero and then charge the system varying  $\lambda$  from one to zero. While for soft-core Lennard Jones term and the direct lattice electrostatic term the combination rules described in Table 1 can be straightforwardly implemented at a very limited computational cost in a standardly written force routine, the same rules cannot be directly applied to the reciprocal lattice part. In common implementation of the Ewald method, for obvious reason of computational convenience, the reciprocal lattice space double sum is rewritten in terms of a squared charge weighted structure factors as

$$V_{rl} = \frac{1}{2\pi V} \sum_{\mathbf{m} \neq 0} \frac{\exp\left(-\pi^2 |\mathbf{m}|^2 / \alpha^2\right)}{|\mathbf{m}|^2} S(\mathbf{m}) S(-\mathbf{m}) \quad (9.2)$$

In a system subject to a continuous alchemical transformation, the charge weighted structure factor becomes



a function of the atomic factors  $\lambda_i(t)$ :

$$S(\mathbf{m}, \lambda) = \sum_i^N (1 - \lambda_i(t)) Q_i \exp(-2\pi i \mathbf{m} \cdot \mathbf{r}_i) \quad (9.3)$$

In the PME method, the sum of Eq. 9.3 is done via FFT by smearing the atomic charges on a regular grid in the direct lattice.[35] In this approach, all charge-charge interactions between alchemical and non alchemical species are almost inextricably mixed in the PME Ewald reciprocal lattice contribution and the application of the rules reported in Table 9.1 requires an extra effort indeed, an effort that has apparently deterred many to use the full Ewald method for computing the work done during continuous alchemical transformations. To this end and with no loss of generality, it is convenient to classify the system in an alchemical “solute” and in a non alchemical “solvent”, with only the former being externally driven. We then label with  $q(t)$  and  $Q$  the time-dependent alchemical charges and the full time-invariant atomic charges of the solute, respectively, and with  $Q_s$  the charges on the solvent. The alchemical  $q(t)$  and full  $Q$  solute charges are related by  $q(t) = (1 - \lambda(t))Q$ . When evaluating the reciprocal lattice energy via Eq. 9.2, the situation for the charge-charge electrostatic interactions is in represented in Table 9.2. In the direct lattice,

Direct Lattice (Erfc)			Reciprocal Lattice (Erf)		
$\frac{EQ}{r}$	$\frac{q(t)Q_s}{r}$	$\frac{Q_s W_s}{r}$	$\frac{q(t)q(t)}{r}$	$\frac{q(t)Q_s}{r}$	$\frac{Q_s e q_s}{r}$
Only interactions $\geq 14$			All interactions		

Table 9.2: Charge-charge interactions in alchemical transformations using the Ewald summation. The atomic charges labeled  $q(t)$ ,  $Q$  and  $Q_s$  refer to the alchemical charge, to the full (time-invariant) solute charge and to the solvent (non alchemical) charge.

the rules reported in table 9.1 can be implemented straightforwardly by excluding in the double atomic summation of Eq. 9.1 all the so-called 12 and 13 contacts. These atom-atom contacts involve directly bonded atoms of atoms bound to a common atom for which no electrostatic charge-charge contribution should be evaluated. In the reciprocal lattice, however, because of the structure of Eq. 9.2, all intra-solute interactions are implicitly of the kind  $q_i(t)q_j(t)\text{erf}(\alpha r)/r$  and 12 and 13 pairs are automatically considered in the sum of Eq. 9.2. The latter terms may be standardly removed in the zero cell by subtracting from the energy the quantity

$$V_{\text{intra}} = \sum_{ij-\text{excl.}} q_i q_j \frac{\text{erf}(\alpha r_{ij})}{r_{ij}}. \quad (9.4)$$

Regarding the 1-4 interactions, these are fully included in the reciprocal lattice sum, while in popular force fields only a portion of them is considered via the so-called fudge factors  $f$ . What must be subtracted in this case is the complementary interaction  $q_i(t)q_j(t)(1 - f)\text{erf}(\alpha r)/r$ .

It should be stressed here that, when the reciprocal lattice sum is computed using Eq. 9.2, the zero cell Erf contribution of the 12, 13 and 14(1 -  $f$ ) interactions must be removed whether the two charges are alchemical or not. So, alchemically driven simulations imply no changes on the subtraction of these peculiar self-interactions with respect to a normally implemented program with no alchemical changes. The routines that implement Eq. 9.4 must be therefore called using the atomic charges  $q_i = (1 - \lambda_i(t))Q_i$  whether alchemical or not (i.e. whether  $\lambda_i$  is different from zero or not). With the same spirit, the self interaction in the zero cell, i.e. the term  $-\frac{\alpha}{\pi^{1/2}} \sum_i [1 - \lambda_i(t)]^2 Q_i$  must be computed using the same charges.

We have seen in Table 9.2 that in the direct lattice the intrasolute non bonded electrostatic interactions are computed using the full time invariant solute charges  $Q$ , as alchemical changes affect only solute-solvent interaction energies. To recover the bare Coulomb potential for intrasolute interaction in a system subject to an alchemical transformation one must then subtract, as done for the 12 13 and 14(1-f) pairs, the Erf  $q(t)q(t)$  contribution, and add a  $QQ$  Erf term to the total energy of the system, producing the alchemical correction to the electrostatic energy

$$V_{\text{alch}} = \sum_{ij>14} Q_i Q_j [1 - (1 - \lambda_i(t))(1 - \lambda_j(t))] \frac{\text{erf}(\alpha r_{ij})}{r_{ij}}. \quad (9.5)$$

where the summation is extended to all non bonded intrasolute interactions. It should be stressed that the energy of Eq. 9.5 is a non trivial additive term that *must* be included in simulations of continuous

alchemical transformations. Such term stems from the time dependent alchemical charges  $q(t)$  and is due to the peculiar implementation of the Ewald method.  $V_{\text{alch}}$  is indeed a large contribution (10-15 kJ mol<sup>-1</sup> per solute atom) and its neglect may lead to severe errors in the electrostatic energies and to incorrect MD trajectories.

We can finally re-write down the total energy of a system subject to an alchemical transformation as

$$V(x, \lambda, \eta) = \sum_{ij} [1 - \lambda_{ij}(t)] \frac{Q_i Q_j}{r_{ij}} \text{erfc}(\alpha r_{ij}) + V_{\text{rl}} - V_{\text{intra}} - \frac{\alpha}{\pi^{1/2}} \sum_i [1 - \lambda_i(t)]^2 Q_i^2 + V_{\text{alch}} \\ + 4\epsilon_{ij} [1 - \eta_{ij}(t)] \left( \frac{1}{[\alpha \eta_{ij}(t) + (r_{ij}/\sigma_{ij})^6]^2} - \frac{1}{[\alpha \eta_{ij}(t) + (r_{ij}/\sigma_{ij})^6]} \right) \quad (9.6)$$

where  $V_{\text{rl}}$ ,  $V_{\text{intra}}$ ,  $V_{\text{alch}}$  are defined in Eqs. 9.2, 9.4 and 9.5, respectively. All terms in Eq. 9.6, except for the self term  $-\frac{\alpha}{\pi^{1/2}} \sum_i [1 - \lambda_i(t)]^2 Q_i^2$ , contribute to the atomic forces that can be standardly computed by taking the derivatives of the energy Eq. 9.6 with respect to the atomic position  $\mathbf{r}_i$  producing the correct trajectories for alchemically driven systems under periodic boundary conditions and treated with the Ewald sum. In the Figure 9.1 we report the time record of the intra-solute electrostatic energy during the discharging of a molecule of ethanol in water in standard conditions. In spite of the huge changes in the contributing energy terms, the total intrasolute energy remains approximately constant during the transformation, modulated by the intramolecular motion, exactly as it should. The changes in the solute self term  $-\frac{\alpha}{\pi^{1/2}} \sum_i [1 - \lambda_i(t)]^2 Q_i$  compensate, at all time steps, the variation of the direct lattice and of Erf intrasolute corrections. This balance does occur provided that *all* terms in the energy of Eq. 9.6 are accounted for, including the intrasolute alchemical Erf correction  $V_{\text{alch}}$  of Eq. 9.5.

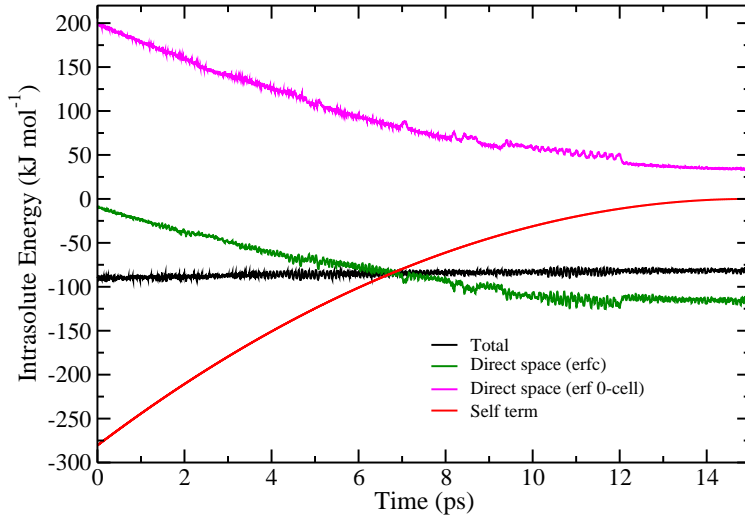


Figure 9.1: Time record for the intrasolute energy arising from electrostatic interactions during the alchemical discharging of ethanol in water at  $T=300$  K and  $P=1$  Atm. The simulation went on for 15 ps. The red curve is due to the self term  $-\frac{\alpha}{\pi^{1/2}} \sum_i [1 - \lambda_i(t)]^2 Q_i^2$ . The green curve is due to the direct lattice contribution. The magenta curve includes the terms  $-V_{\text{intra}}$  (Eq. 9.4) and  $V_{\text{alch}}$  (Eq. 9.5).

In a multiple time scheme, the individual contributions to the non bonded forces evolve in time with disparate time scales and must be hence partitioned in appropriately defined “integration shell” as described in details in Chapter 3. So in condensed phases, the direct lattice term is integrated in the fast short-ranged non bonded shell, while the reciprocal lattice summations (including the Erf intramolecular correction terms in  $V_{\text{intra}}$ ) are usually assigned, with an appropriate choice of the Gaussian parameter  $\alpha$ , to the intermediate non bonded shell. The Lennard-Jones term, finally, is split among the short-ranged, intermediate-range and long-range integration shells. The potential subdivision for condensed phases is basically unaffected by the implementation of alchemical transformation, except for the intrasolute self term  $V_{\text{alch}}$  and for the now time-dependent self term  $\frac{\alpha}{\pi^{1/2}} \sum_i [1 - \lambda_i(t)]^2 q_i$ .<sup>1</sup> The latter can be safely included in the intermediate

<sup>1</sup>This last term does not contribute to the atomic forces but only to the alchemical work and is constant for all non

shell, while the former (a true direct lattice term) must be integrated in the sort-range shell. The  $\lambda_i(t)$  and  $\eta_i(t)$  factors, finally, must be updated, according to the predefined time protocol, before the force computation of the fast short-ranged non bonded shell.

### 9.0.2 Calculation of the alchemical work

The work done on the system by the driven alchemical coordinates during a simulation of length  $\tau$  can be written as

$$W = - \int_0^\tau \frac{\partial H(x, \lambda, \eta)}{\partial \lambda} \dot{\lambda} dt + \int_0^\tau \frac{\partial H(x, \lambda, \eta)}{\partial \eta} \dot{\eta} dt \quad (9.7)$$

In a NVT or NPT extended Lagrangian simulation with an ongoing alchemical process, the alchemical work, Eq. 9.7, could be computed simply by monitoring the changes in the *total* energy of the systems, that includes the real potential and kinetic energy of system and the potential and kinetic energies of the barostat and the thermostats. This energy, if no velocity scaling is implemented (i.e. no heat is artificially transferred to or absorbed from the *extended* system), is a constant of the motion and hence any variation of it must correspond to the work done on the system.[155] Alternatively the work can be computed by analytically evaluating the  $\lambda$  and  $\eta$  derivatives of the non bonded energy Eq. 9.6. Both these methods have counter-indications. The total energy method suffers from the finite precision of energy conservation in the numerical integration of the equations of motion (usually in multiple time step schemes the oscillations of the total energy are the order of 1/50:1/100 of the mean fluctuation of the potential energy of the system)[13]. Also, small drifts in the total energy adds up in the work as a spurious extra dissipation term that may reduce the accuracy in the free energy determination via the Crooks theorem. The method based the derivatives, if alchemical species are annihilated and created within the same process, requires the constant tagging of the *two* creation and annihilation works, as the increments  $\delta\lambda_{G/A}$  or  $\delta\eta_{G/A}$  have opposite signs for creation (*G* species) and annihilation process (*A* species). Besides, while all direct lattice **Erfc** and and reciprocal lattice **Erf** corrections terms pose no difficulties in  $\lambda$  derivation with a moderate extra cost of the force routines, the analytic derivation of reciprocal lattice energy  $V_{rl}$ , Eq. 9.2, with respect to  $\lambda$  implies the calculation of three gridded charge arrays, i.e. one for the whole system and two more for the discharging and for the charging alchemical solutes:

$$\frac{\partial V_{rl}}{\partial \lambda_i} = - \frac{1}{2\pi V} \sum_{\mathbf{m} \neq 0} \frac{\exp\left(-\pi^2 |\mathbf{m}|^2 / \alpha^2\right)}{|\mathbf{m}|^2} (S(\mathbf{m}) S_{a/c \text{ slt}}(-\mathbf{m}) S(-\mathbf{m}) + S_{a/c \text{ slt}}(\mathbf{m})) \quad (9.8)$$

where with the notation  $S_{a/c \text{ slt}}(\mathbf{m})$  we refer to the gridded charge arrays obtained for the discharging ( $0 \leq \lambda \leq 1$ ) and charging alchemical species ( $1 \leq \lambda \leq 0$ ) if they are both present.

The work can also be computed numerically observing that the differential work due to a  $\delta\lambda$  or  $\delta\eta$  increment of the alchemical factors is given by

$$dw = \frac{1}{2} (E(\lambda + \delta\lambda, x) - E(\lambda - \delta\lambda, x) + E(\eta + \delta\eta, x) - E(\eta - \delta\eta, x)) \quad (9.9)$$

which is correct to order  $o(\delta\lambda^2)$  and  $o(\delta\eta^2)$ . Eq. 9.9 requires just one extra calculation of the energy within the direct space force loop using the  $\lambda_i$  values at the previous step with no need for tagging annihilating and creating species. For computing the work arising from the reciprocal lattice sum, Eq. 9.2, the gridded charge array must be computed at every step of the intermediate-range shell using the current charges and those at the previous step with a very limited computational cost. *Both* these array must then undergo FFT. As for the direct lattice, also for the reciprocal term there is no need for tagging creating or annihilating species. The different means to access the alchemical work can be used as a powerful check to test the coherency of the trajectories and of the computed numerical work, Eq. 9.9. The alchemical work indirectly evaluated monitoring the changes of total energy of the system, must follow closely the profile of the numerical work computed using Eq. 9.9. Such test is reported in Figure 9.2 (right) for the discharging of ethanol in water.

In a multiple time step scheme, the alchemical work must be computed exactly as the energy is computed, hence evaluating more often the contributions arising from the fast shells with respect to the terms

---

alchemical species. The work done by an alchemical species through this term is simply given by  $W = \pm \frac{\alpha}{\pi^{1/2}} \sum_i q_i^2$ , depending whether the alchemical species has been charged or discharged.

evolving more slowly. In the scheme reported in the Supporting Information, we succinctly describe the implementation of the alchemical process and the associated work calculation in a molecular dynamics code, highlighting the parts of the code that must be modified because of the presence of alchemical species with respect to a normal MD code. In Figure 9.2 we report the behavior of the various contributions to

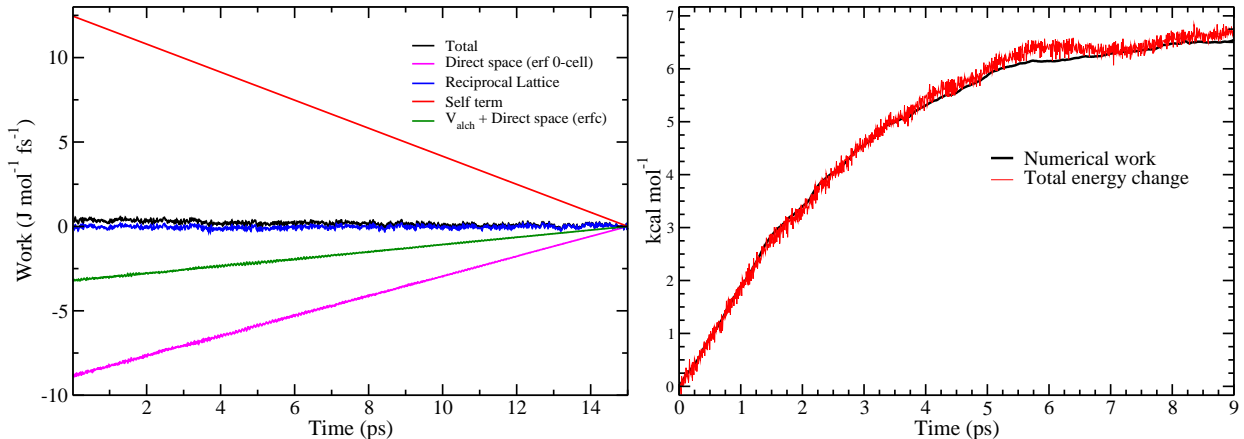


Figure 9.2: Left: Time record for the intrasolute reciprocal lattice contributions to the differential work (Eq. 9.9) arising from electrostatic interactions during the alchemical discharging of ethanol in water at  $T=300$  K and  $P=1$  Atm. The simulation went on for 15 ps. The red curve is due to the self term  $-\frac{\alpha}{\pi^{1/2}} \sum_i [1 - \lambda_i(t)]^2 Q_i^2$ . The green curve is due to the direct lattice contribution and to  $V_{\text{alch}}$ . The magenta curve includes the terms  $-V_{\text{intra}}$  (Eq. 9.4). The blue curve is due to the full reciprocal lattice PME term, Eq. 9.2. Right: Total energy change (red line) and numerical work (black line) computed using Eq. 9.9 for the discharging of ethanol in water in an alchemical trajectory lasting for 9 ps.

the intra-solute differential work computed during the transformation. In the reciprocal lattice term (blue curve) the intrasolute and solute-solvent contributions are mixed. Hence the integrated total differential work (black curve) is, expectedly, slightly positive due to loss of long-range electrostatic energy because of ethanol discharging. Again, paralleling the situation seen for the intrasolute energy, the work due to the self term approximately cancels the end Erfc intrasolute contributions.

We conclude this section with some comments on the time protocol that drives the alchemical transformation. In our implementation, the charges and the Lennard-Jones potential can be switched on and off independently, by setting up different time protocol for  $\eta_i$  and  $\lambda_i$  alchemical coordinates. Such an approach is much more flexible and powerful than that based on the definition of a single alchemical parameter implying the simultaneous variation of Lennard-Jones and electrostatic interactions. If the  $\eta_i$  and  $\lambda_i$  factors are varied coherently (i.e. only *one* type of alchemical coordinate  $\Lambda_i$  is defined), catastrophic numerical instabilities may arise, especially in complex solutes with competing conformational structures. One way to circumvent this problem is to switch electrostatic and Lennard-Jones interactions separately as we do here.

For the evaluation of solvation free energy via alchemical transformations, the target end states are i) the decoupled solute (in the gas phase) and the pure solvent (in the liquid state) and ii) the solution. For the decoupled state i), in principle two independent standard simulations are needed, one for the isolated solute and the other for pure solvent. However the decoupled state can be sampled in one single simulation using the non-bonded energy of Eq. 9.6, by setting the alchemical solute  $\lambda_i$  and  $\eta_i$  factors all equal to one. In fact, according to Eq. 9.6 and to the rules of Table 9.1, when the alchemical solute  $\lambda_i$  and  $\eta_i$  terms are all equal to one, the solute is not felt by any means by the solvent and evolves in time independently, subject only to the intramolecular interactions with no contribution from the solute lattice images. The intrasolute electrostatic energy, in particular, has no contribution from the reciprocal lattice sum as the  $\lambda_i$  referring to the solute are all equal to 1 in Eq. 9.2. It has indeed a direct lattice contribution for non bonded intrasolute evaluated in the zero cell according to the rules specified in Table 9.1 *plus* the alchemic correction term that simply corresponds (with all solute  $\lambda_i$  set to 1) to the complementary Erf part thus recovering the bare intrasolute Coulomb energy. At the other extreme end of the alchemical transformation ( $\lambda_i = 0, \eta_i = 0$ ), according to Eq. 9.6 the solute is fully charged interacting normally with the solvent

and with the solute images via the term Eq. 9.2 We now come to the issue of the efficiency of a code

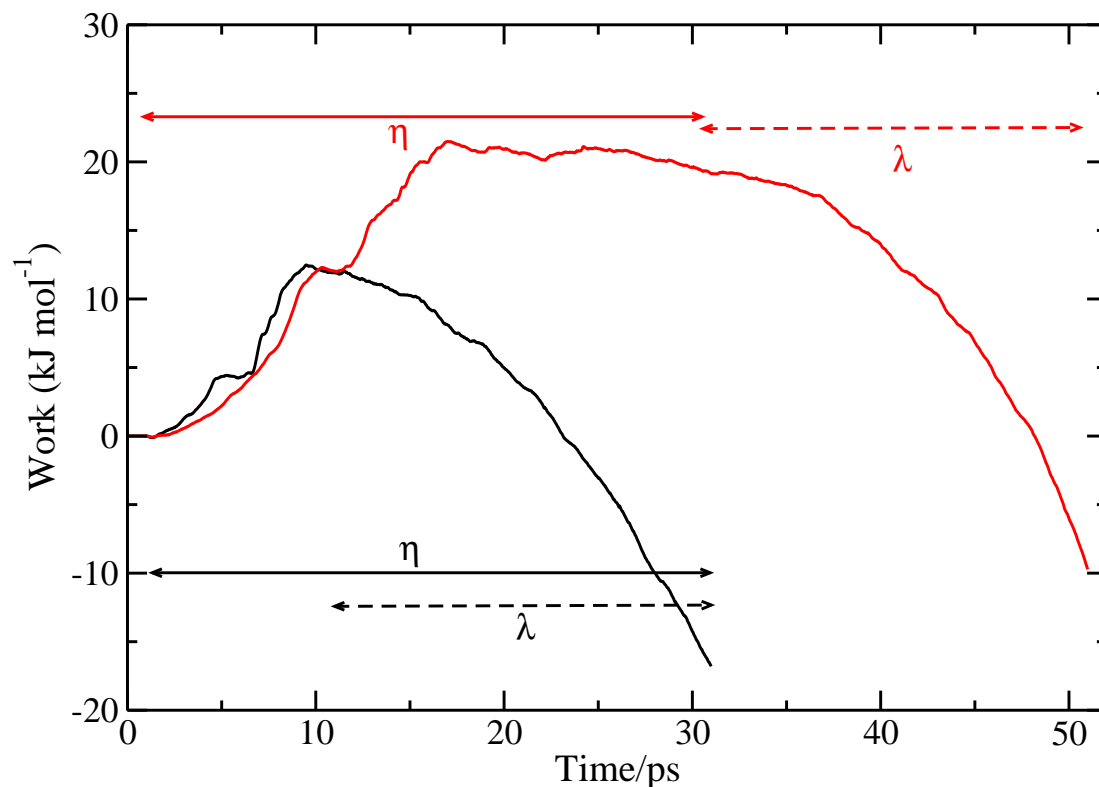
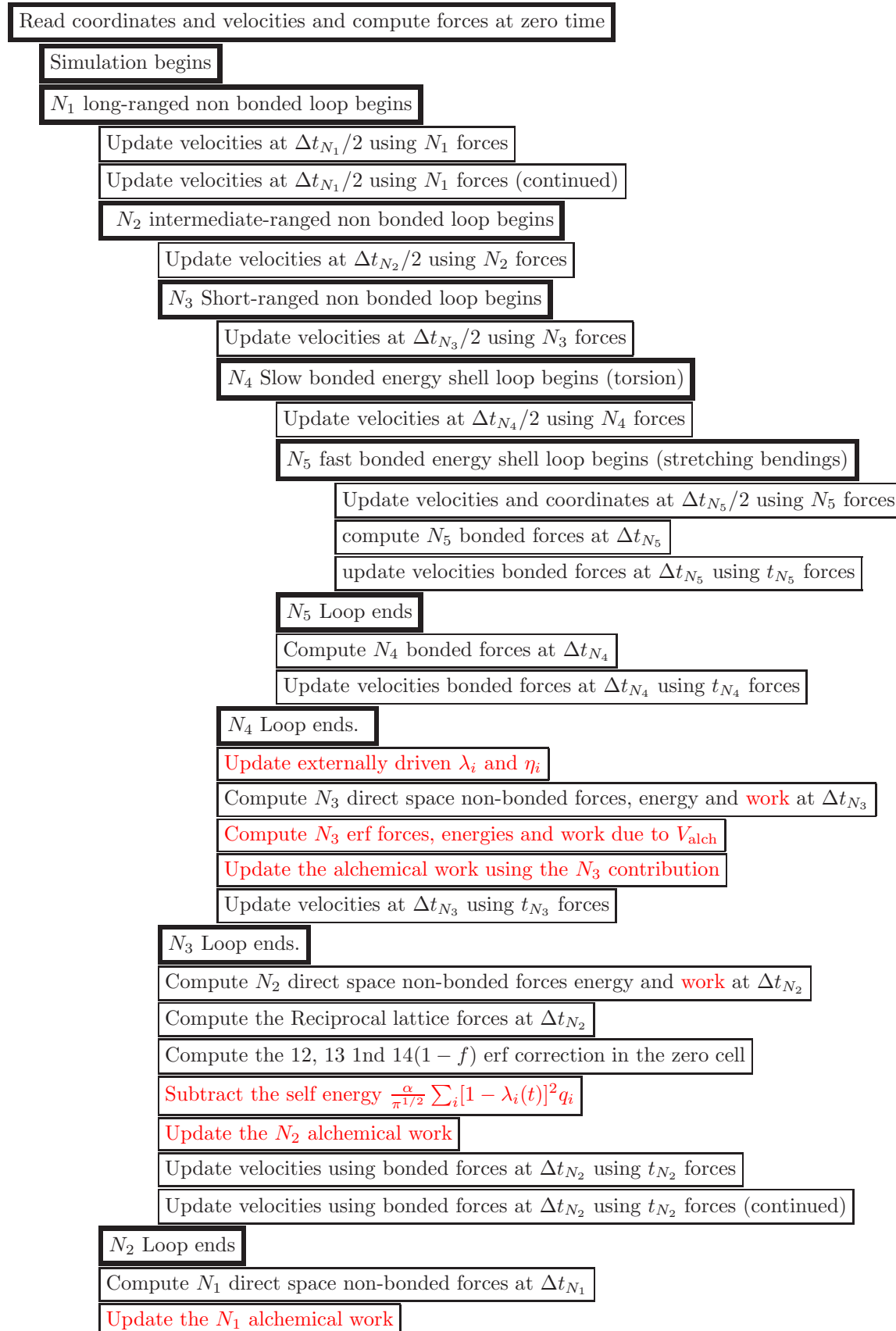


Figure 9.3: Alchemical work produced in the creation of ethanol in water  $T=300$  K and  $P=1$  Atm using two different time protocols represented by the black and red horizontal lines.

with distinct Lennard-Jones and charge alchemical parameters. Of course, also in this case simultaneous switching of  $\lambda_i$  and  $\eta_i$  remains perfectly possible. To avoid numerical instabilities at the early stage of the creation process or at the end of the annihilation, it is sufficient in the first case to slightly delay the charge switching and in last case to anticipate the discharging process. In the Figure 9.3 we report the work computed in the alchemical creation of ethanol in water conducted with two different time protocol. In the red non equilibrium trajectory, the Lennard-Jones  $\eta_i$  parameters for ethanol are prudently brought from 1 to 0 in 30 ps, and in the next 20 ps the solute is charged. In the black trajectories lasting for 30 ps, in the first 10 ps, the  $\eta_i$  coordinates alone are brought from 1 to 0.5 and then, in the last 20 ps, they are brought to zero (fully switched on ethanol) *together* with the charging process that is started at 10 ps. As one can see, both trajectories are regular with no instabilities, yielding negative and comparable works with limited dissipation with respect to the reversible work ( 16-17  $\text{kJ mol}^{-1}$ , see next section) in spite of short duration of the non equilibrium alchemical transformations. We must stress here, that in the fast switching non equilibrium method with determination of the free energy difference between end states via the CFT, once the equilibrium configurations of the starting end states have been prepared, the simulation time per trajectory does correspond indeed to the wall-clock time if the independent non-equilibrium trajectories are performed in parallel. For the creation of ethanol in water, the CPU time amounts to few minutes on a low-end Desktop computer for both time protocols.

In the following scheme, we succinctly describe the implementation of alchemical transformations in a MD driver code with multiple time step (MTS) integrators and Particle Mesh Ewald treatment of long range electrostatics in ORAC. The modification due the alchemical transformations are highlighted in red.

## Alchemical MD pseudo-code



Update velocities bonded forces at $\Delta t_{N_1}$ using $t_{N_1}$ forces
--

$N_1$ Loop ends
-----------------

The computational overhead after the inclusion of the alchemical code in the MD driver is mostly due to the evaluation of the alchemical work during the non equilibrium driven experiment. As the simulation proceeds, the alchemical work must be computed in the direct lattice as well as in the reciprocal lattice with a frequency identical to that of the energy terms. For the reciprocal lattice contribution, one extra Fast Fourier Transform is required in order to evaluate the reciprocal lattice Particle Mesh Ewald energy at the previous step. Moreover, the Erf correction  $V_{\text{alch}}$  (Eq. 9.5) is an entirely new energy term due to the alchemical species. The efficiency loss of the alchemical code with respect to a non alchemical code is around 30%, as measured in a short serial simulation of ethanol in water in standard conditions (see Methods section of the main paper for the simulation parameters),

### 9.0.3 Fast switching Double Annihilation method

Alchemical transformation in ORAC can be effectively used for the determination of ligand-receptor binding free energies via the so-called Fast switching Double Annihilation method (FS-DAM).[1] In this approach, ORAC can be used to produce simultaneously in a parallel application many fast and independent non-equilibrium Molecular Dynamics trajectories with a continuous dynamical evolution of an externally driven alchemical coordinate, completing the decoupling of the ligand in a matter of few tens of picoseconds rather than nanoseconds. In FS-DAM, the requirement of an equilibrium transformation along the entire alchemical path, that is the major stumbling block in obtaining reliable (converged) free energy values via the standard equilibrium approach based on free energy perturbation (FEP/REST),[156] is lifted altogether and the drug-receptor absolute binding free energy can be recovered with reliability from the parallel computation of the annihilation work distribution. To the latter, a unidirectional free energy estimate can be applied, on the assumption that any observed non equilibrium work distribution is given by a mixture of normal distributions, whose components are identical in either direction of the non-equilibrium process, with weights regulated by the Crooks theorem.[157] In contrast to the FEP/REST approach based on the equilibrium simulations of many intermediate alchemical states, in FS-DAM, the equilibrium sampling is required only at the starting fully coupled states (easily attainable using conventional enhanced sampling simulation methods).



# Chapter 10

## Input to ORAC

### 10.1 General Features

**Input File.** At execution time ORAC reads an input file in free format from the standard input. Each line of the input is read as a 80 character string and interpreted. If the first character of the input line is a # the line is ignored. In order to be interpreted the input line is parsed in the composing words which are sequences of characters separated by blanks or commas. Each word represents an instruction which must be interpreted by the program.

**Instructions Set.** The instruction set of ORAC includes *environments*, *commands* and *sub-commands*. An input file is made out of a series of environments. Each environment allows a series of commands which might use a few sub-commands. Environments resembles Fortran NAMELIST, but have not been programmed as NAMELIST. The environment name is a string which always starts with a & followed by capital letters. Each environment ends with the instruction &END. Command names are characters strings all in capital letters. Each command reads a variable set of parameters which can be characters and/or numbers (real or integer). There are also commands (*structured commands*) which are composed of more than one input line. A structured command end with the instruction END and allows a series of sub-commands in its inside. Sub-commands are in lower case and can read sub-string of characters and/or real or integer numbers. In the following section we will describe in details all the supported instruction allow by ORAC .

**Handling External Files.** Many ORAC commands provide instructions to open external files. No unit number needs to be provided as ORAC open sequentially the required files assigning at each file a unit number according to their order of occurrence in the input file. The file units begin at unit 10 and are augmented of one unit for each new file.

### 10.2 Environments, Commands and Sub-commands

The following 10 environments are available:

- 1 &ANALYSIS retrieves the history file.
- 2 &INOUT contains commands concerning input/output operations which can be carried out during run time. The commands allowed within the INOUT environment write history files in different formats and dump the restart files.
- 3 &INTEGRATION includes commands defining the integration algorithms to be used during the simulation run.
- 4 &META includes commands defining the metadynamics simulation.
- 5 &POTENTIAL includes commands which define the general features of the system interacting potentials. These features are common to both solute and solvent and concern only the non-bonded interactions.

- 6 **&PROPERTIES** includes commands which make ORAC compute run time observables. The commands allowed within the **&PROPERTIES** environment can compute on the fly: pair correlation functions, static structure factors and velocity auto-correlation function. This environment is not supported.
- 7 **&REM** setup the Replica Exchange simulation (work only with the parallel version).
- 8 **&RUN** defines run time parameters which concern output printing and run averages.
- 9 **&SETUP** includes commands concerned with the simulation box setup. In this environment, the simulation cell parameters, dimensions and symmetry can be initialized. Moreover, files containing the system coordinates in appropriate format can be provided.
- 10 **&SIMULATION** includes commands which define the type of simulation that is to be carried out. In particular, commands are available to run steepest descent energy minimization, and molecular dynamics simulations in various ensembles.
- 11 **&SOLUTE** includes commands which are concerned with specific aspects of the solute force field and structure.
- 12 **&SOLVENT** includes commands which are concerned with specific aspects of the solvent force field and structure.
- 13 **&ST** setup the Serial Generalized Ensemble simulation (work with both serial and parallel versions).
- 14 **&PARAMETERS** includes commands which read the topology and force field parameter files of the solute. These files contain sufficient information to define the solute topology and to assign potential parameters to the solute molecules.

**Commands' supporting policy.** Since ORAC is free of charge no professional support is provided. Bugs are fixed, upon request to the E-mail address [oracmaster@cedec.cecma.fr](mailto:oracmaster@cedec.cecma.fr), at the authors earliest convenience and support may be requested only for environments, commands or sub-commands which are not marked **unsupported** in this manual. ORAC is simultaneously an ancient code and a new code which is still in the developing stage. ORAC has indeed a stable "core" i.e. the part which is officially maintained, but it also has some obsolete options, some features used for diagnostic or debugging purposes and some other experimental features not yet fully tested, i.e. the unsupported material. Unsupported features are by no means essential to the ORAC functioning and may belong to three categories:

- **Experimental:**  
These features have been generally tested on only one or two unix platform (usually OSF1 or HP-UX), some of them can be used only while running in single time mode, some other can be used only while running with r-RESPA. These features are documented normally and in the WARNINGS section they are referred as  
Experimental - **Unsupported**.
- **Diagnostic:**  
These feature were introduced in the developing stage for diagnostics and debugging purposes. In the current version the diagnostic features are kept since they may turn to be useful to the programmer when modifying the code. These features are documented normally and in the WARNINGS section they are referred as  
Diagnostic - **Unsupported**.
- **Obsolete features:**  
These features are no longer used and will be eliminated in the next ORAC release. They are poorly documented and they are referred as  
Obsolete - **Unsupported**.

---

### 10.2.1 &ANALYSIS

This environment includes commands which define the starting and ending record for reading the trajectory file (see also `TRAJECTORY`, `DUMP(&INOUT)`). The following are allowed commands:

START, STOP, UPDATE

---

#### START

NAME

START

SYNOPSIS

START *nconf*

DESCRIPTION

The trajectory file specified with the command `TRAJECTORY(&INOUT)` is read in starting from configuration *nconf*.

EXAMPLES

START 1

---

#### STOP

NAME

STOP

SYNOPSIS

STOP *nconf*

DESCRIPTION

The trajectory file specified with the command `TRAJECTORY(&INOUT)` is read stopping at configuration *nconf*.

EXAMPLES

STOP 1000

---

#### UPDATE

NAME

UPDATE – Update neighbor list for analysis

SYNOPSIS

UPDATE *nconf* *rcut*

DESCRIPTION

Update the neighbor lists for, e.g., radial distribution function calculations, every *nconf* configurations using a cut-off of *rcut* Å.

EXAMPLES

UPDATE 2 10.0 Å.

WARNINGS

Diagnostics - **Unsupported**

---

---

### 10.2.2 &INOUT

The environment &INOUT contains commands concerning input/output operations which can be carried out during run time. The commands within the INOUT environment allow to write history files in different formats and to dump restart files. The following commands are available:

ASCII, ASCII\_OUTBOX, DCD, DYNAMIC, DUMP, PLOT, RESTART, SAVE, TRAJECTORY

---

#### ASCII

NAME

ASCII – Write solute and solvent coordinates to a history PDB file

SYNOPSIS

ASCII *fplot* OPEN *filename*

DESCRIPTION

This command is active both for solute and solvent molecules. It writes a history PDB file containing the system coordinates. The centers of mass of all molecules are always *inside* the simulations cell. The dumping frequency, in fs, is *fplot*. At each writing the system coordinates in PDB format are appended to the history file *filename*.

EXAMPLES

ASCII 10.0 OPEN test.pdb

Write system coordinates to the history pdb file test.pdb every 10 fs.

WARNINGS

Work only during the acquisition phase (see TIME in environment &RUN).

---

#### ASCII\_OUTBOX

NAME

ASCII – Write solute and solvent coordinates to a history PDB file

SYNOPSIS

ASCII *fplot* OPEN *filename*

DESCRIPTION

This command is active both for solute and solvent molecules. It writes a history PDB file containing the system coordinates. The dumping frequency, in fs, is *fplot*. The centers of mass the molecules are at the position given by the simulation and may be hence also *outside* the simulation box. At each writing the system coordinates in PDB format are appended to the history file *filename*.

EXAMPLES

ASCII\_OUTBOX 10.0 OPEN test.pdb

Write system coordinates to the history pdb file test.pdb every 10 fs.

WARNINGS

Work only during the acquisition phase (see TIME in environment &RUN).

---

## DCD

## NAME

DCD – Write solute and solvent coordinates to a trajectory DCD file

## SYNOPSIS

DCD *fplot* OPEN *filename*

DCD *fplot* OPEN *filename* NOH

## DESCRIPTION

This command is active both for solute and solvent molecules. It writes a trajectory file containing the system coordinates and the simulation box parameters. The centers of mass of all molecules are always *inside* the simulations cell. The dumping frequency, in fs, is *fplot*. At each writing the system coordinates and the simulation box parameters are appended to the trajectory file *filename*. During a REM simulation, this file will automatically be complemented by the file *filename.rem*, where energy terms involved in the REM exchanges, along with the time step and the replica index, will be printed with the same frequency. The file *filename.rem* contains the same information as the one created by the command `PRINT_ENERGY(&REM)`.

## EXAMPLES

DCD 10.0 OPEN `test.dcd`

Write atomic coordinates to the dcd trajectory file `test.dcd` every 10 fs.

DCD 10.0 OPEN `test.dcd` NOH

Write coordinates of non-hydrogen atoms to the dcd trajectory file `test.dcd` every 10 fs.

## WARNINGS

Work only during the acquisition phase (see `TIME` in environment `&RUN`).

---

DYNAMIC

## NAME

DYNAMIC – Write force field parameters in extended format (see also `DEBUG(&RUN)`)

## SYNOPSIS

DYNAMIC OPEN *filename*

## DESCRIPTION

This command prints out to the file *filename* the parameters of the force field *for the solute only* in a verbose format.

## EXAMPLES

DYNAMIC OPEN `ff.out`

---

DUMP

## NAME

DUMP – Write coordinates to a direct access unformatted file with a given frequency. The file is written in a particular format such that it can be easily retrieved at analysis time “by time” and “by atoms”.

## SYNOPSIS

DUMP

....

END

## DESCRIPTION

The DUMP structured command stores the coordinates of the system during a simulation run with a selected frequency. The coordinates are stored in single precision to save disk space. The following subcommands may be specified within DUMP:

atom\_record, occupy, write

- **atom\_record** *natom\_rec*  
Defines the number of atoms per record. Atomic coordinates are dumped to disk as REAL\*4. RecordLength is defined as *lrecl* = *natom* \* 3 \* 4
- **occupy**  
Allocates disk storage for history file *before* the simulation is started. **occupy** fills with zeroes the *entire* direct access history file(s) whose dimensions are controlled by the command MAXRUN(&RUN) and by the number of atoms in the systems. If **occupy** is not specified the history file is expanded at each write request *during* the simulation. This command is useful when sharing disk resources with others, preventing the simulation to die because of sudden lack of disk space.
- **write** *ftime* OPEN *file\_name*  
Defines the dumping frequency and the trajectory auxiliary *file\_name*. Coordinates are dumped to disk every *ftime* femtoseconds. The auxiliary file *file\_name* contains the names for parameters and trajectory files and must be user supported. At execution time this file is rewritten by the program which supports extra information, computed according to input specifications, needed when retrieving the file (see &ANALYSIS). The file *file\_name* looks like

```
system_file_0
traject_file_1
...
traject_file_n
```

**system\_file** is the parameters file where the time steps and the CO matrix are specified. All other files are reserved for the trajectory. Partitioning a very long trajectories in many files allows to overcome, e.g., OS set file size limits or filesystem limits.

## EXAMPLES

```
DUMP
  write 30.0 OPEN alk-1.aux
  occupy
  atom_record 30
END
```

Writes history file and parameters file as specified in auxiliary file **alk-1.aux** every 30.0 fs. After execution the file **alk-1.aux** is rewritten by the program and looks like

# Rewritten by Program

<b>system_file</b>	66	0	0
<b>traject_file_1</b>	1320	20	30

The numbers in columns 1 are the length of the file in records. The numbers in the second columns and second row are the number of records per point (calculated by the program) and the number of atoms per record (given in input: see subcommand **atom\_record**) in the trajectory file **traject\_file\_1**. In the above example the record length is  $30 \times 4 \times 3 = 360$  bytes, the total size of the file of bytes, allocated at simulation start, is given by  $30 \times 3 \times 4 \times 1230 = 442800$ , and the total number of bytes dumped per phase space point is given by  $20 \times 30 \times 3 \times 4 = 7200$ .

## WARNINGS

Work only during the acquisition phase (see TIME in environment &RUN).

## PLOT

## NAME

PLOT – Write solute coordinates and connection table to a history file in Protein Data Bank Format (PDB).

## SYNOPSIS

```
PLOT fplot OPEN filename
PLOT FRAGMENT fplot OPEN filename
PLOT ALCHEMY fplot OPEN filename
PLOT CENTER fplot OPEN filename
PLOT STEER fplot OPEN filename
PLOT STEER_ANALYTIC fplot OPEN filename
PLOT STEER_TEMPERATURE fplot OPEN filename
```

## DESCRIPTION

It writes a history formatted file containing the coordinates of selected part of the solute (and) the solvent coordinates. The dumping frequency in fs is *fplot*.

## EXAMPLES

```
PLOT 10.0 OPEN test.pdb
```

Write coordinates of the backbone atoms of the solute in PDB format every 10 fs to file *test.pdb*

```
PLOT CENTER 10.0 OPEN test.pdb
```

Write coordinates of all atoms of the system in PDB format every 10 fs to file *test.pdb*. Identical to ASCII\_OUTBOX(&INOUT)

```
PLOT FRAGMENT 10.0 OPEN test.xyz
```

Write coordinates of a fragment of the solute (in xyz format) selected according the DEF\_FRAGMENT (&PROPERTIES) directive every 10 fs to file *test.xyz*. The fragment is defined as follows:

## &amp;PROPERTIES

```
...
DEF_FRAGMENT 1 38
...
&END
```

The file *test.xyz* can be animated using the XMOL public domain molecular graphics program.

This defines a fragment consisting of the first 38 atoms of the solute. The numeral order of the atoms corresponds to that specified in the topology file (Sec. 10.3).

```
PLOT STEER 50.0 OPEN wrk.out
```

write the accumulated work (see Eq. 8.16) to the file *wrk.out* every 50 fs. The accumulated work at time *t* is calculated as  $\mathcal{W} = \mathcal{H}(t) - \mathcal{H}(0)$ , where  $\mathcal{H}(t)$  is the total energy of the microcanonical *extended* system, i.e. it includes the energy of the thermostat and/or of the barostat. If the integration time steps are too large and the simulation shows a energy drift, then the accumulated work includes the dissipation due to the energy drift of the integrator.

```
PLOT STEER_ANALYTIC 50.0 OPEN WRK.out
```

Write the accumulated work (see Eq. 8.16) to the file *wrk.out* every 50 fs. The accumulated work at time *t* is calculated analitically according to Eq. 8.16. This option is slightly more computationally demanding than the previous one, but in this case, the accumulated work is not affected by the energy drift. The last two commands are to be used in conjunction with the STEER(&RUN) command and with the commands ADD\_STR\_BONDS, ADD\_STR\_BENDS, ADD\_STR\_TORS (namelist &POTENTIAL) for defining an external steering potential for SMD.



PLOT STEER\_TEMPERATURE 50.0 OPEN WRKTEMP.out

In a steered temperature simulation[150], write the accumulated (adimensional) thermal work every 50 fs to the file WRKTEMP.out. This command must be used in conjunction with the STEER (&RUN) command for steered molecular dynamics simulations and with the THERMOS(&SIMULATION) command for running NVT simulations.

PLOT ALCHEMY 50.0 OPEN alchemic.wrk

Print to the file alchemic.wrk the work done during an alchemical transformation. See also commands DEFINE\_ALCHEMICAL\_ATOM and STEER ALCHEMY.

## RESTART

NAME

RESTART – Write or read an unformatted file from which a simulation might be restarted

SYNOPSIS

RESTART

...

END

DESCRIPTION

The RESTART command may include the following subcommands:

- **read** *filename*  
read restart configuration from file *filename*. When this subcommand is active CONTROL(&RUN) must be non zero and the command READ\_TPGPRM(&PARAMETERS) must have been entered.
- **read\_multiple\_restart** *filename\_prefix* *num*  
This command works only if the code is compiled using the MPI libraries and is not recognized when running in serial. Each of the *nprocs* processor will read a restart file named *filename\_prefix* // *iproc+num* // .rst. So if *filename\_prefix* is /u/foo/restarts/ala and *num* is 0, then process 0 will read the file /u/foo/restarts/ala0000.rst, process 1 will read the file /u/foo/restarts/ala0001.rst and so on. This command is useful when running in parallel multiple steered molecular dynamics trajectories (see also commands ADD\_STR\_BONDS, ADD\_STR\_BENDS, ADD\_STR\_TORS, of namelist &POTENTIAL.)
- **rmr** *filename\_prefix* *num*  
Same as above.
- **write** *fprint* OPEN *filename*  
write restart configuration to file *filename* every *fprint* fs.
- **write** *fprint* SAVE\_ALL\_FILES *filename*  
write restart configuration to files *filename*//i//'''.rst'' every *fprint* fs. (see also command read\_multiple\_restart).

## EXAMPLES

RESTART

read file1.rst

write 1000.0 OPEN file2.rst

END

RESTART

rmr ../RESTARTS/ala 0

END

NB: In the last example valid for parallel runs, the relative path is specified with respect to the **actual** pwd of the parallel processes.

## TRAJECTORY

### NAME

TRAJECTORY – Read history file

### SYNOPSIS

TRAJECTORY *filename*

### DESCRIPTION

The **TRAJECTORY** command instructs the program to read the history file produced at an earlier time (see command **DUMP** in this environment). The auxiliary file *filename* contains the names of the parameters' and history files(s). See also environment **&ANALYSIS** for retrieving the history file and environment **&PROPERTIES** for computing properties from history files.

### EXAMPLES

TRAJECTORY file.aux

---

---

### 10.2.3 &INTEGRATOR

This environment includes commands defining the integration algorithms to be used during the simulation run. The following commands are allowed:

MTS\_RESPA, Timestep.

---

#### MTS\_RESPA

NAME

MTS\_RESPA – Use a multiple time step integrator

SYNOPSIS

MTS\_RESPA

....

END

#### DESCRIPTION

The MTS\_RESPA structured command opens an environment which includes several subcommands used to define a multiple time step integrator. The MTS\_RESPA directive can be specified for NVE simulations and extended system simulations NHP, NPT and NVT. MTS\_RESPA is also compatible with constraints. The following subcommands may be specified within MTS\_RESPA:

step dirty very\_cold\_start energy\_then\_die k-ewald test-times p\_test s\_test

- **step** *type* *n* [*r* [*hl* [*dr*]]] [*reciprocal*]

The command **step** is used to define the potential subdivision and the corresponding time steps. The string *type* can be either “intra” or “nonbond”: in the former case the command defines an intramolecular shell, whereas in the latter a nonbonded shell is defined. If “intra” is specified only one keyword is expected, i.e. the integer *n*. When two subcommand of the type - **step** intra *n* - are entered, the first is assumed to refer to the faster intramolecular subsystem (the  $V_{n0}$  subsystem as defined in eq. 4.3 with  $n = n0$ ) and the second is assumed to define the slower intramolecular subsystem (the  $V_{n1}$  subsystem as defined in eq. 4.3 with  $n = n1$ ). If only one subcommand - **step** intra *n* - is entered then  $n0$  is set to 1 and  $n1 = n$ . If no - **step** intra *n* subcommand is given then  $n1 = n0 = 1$ .

If the first argument of the **step** subcommand is the string “nonbond” then at least an integer and a real are expected. The integer *n* is the time step dividing factor of the nonbonded shell while the real argument equals the shell upper radius. Two more optional real arguments can be defined, i.e. the healing length at the upper shell radius and the corresponding neighbor list offset. The default values of the healing length are As for the intra shell, the more rapidly varying nonbonded shells are entered first. If three - **step nonbond** - subcommands are entered, then the first refers to the  $V_m$ , the second to the  $V_l$  and the third to the  $V_h$  subsystems, with *n* being *m*, *l*, 1 such that  $\Delta t_h = \Delta t$ ,  $\Delta t_l = \Delta t_h/l$ ,  $\Delta t_m = \Delta t_l/m$ , (see Table 4.3). *n* for the last nonbonded shell is set automatically to 1 disregarding its actual value. If two shells are entered then only two intermolecular time steps are used, i.e.  $n = m$  and  $l = 1$ . If one shell is entered only one time step is defined and  $m = l = 1$ . When using Ewald, the  $V_{qr}$  term (Eq. 4.21) in the reciprocal lattice is assigned by entering the string **reciprocal** as the last argument of a - **step nonbond** directive.

- **k-ewald** *kl* *lambdakl* *km* *lambdakm* – Obsolete - **Unsupported**

*kl* and *km* define the shells in reciprocal space. Wave vectors  $k = |\mathbf{k}|$  such that  $rkcut \geq k > kl$ ,  $kl \geq k > km$ , and  $km \geq k > 0$  are assigned to the *h*-shell *l*-shell and *m*-shell, respectively. *lambdakm*, *lambdakl* are the upper healing lengths for the reciprocal space *m* and *l* shells and the lower healing length for the reciprocal space *h* and *l* shells, respectively.

Warning: To be used only when `on` is specified in the directive `EWALD` (environment `&POTENTIAL`); `rkcut` must be defined in the directive `EWALD`). The reciprocal lattice assignment is best done via the keyword `reciprocal` of the command `step nonbond`.

- **test-times** `OPEN filename` – Diagnostic - **Unsupported**

Produce the time record of the potential and kinetic energies at the end of the propagation step (i.e. at intervals of  $\Delta t_h$  fs). The following is the format used for dumping the energies:

```
WRITE(ktest,300) tim,utot,ustot,uptot,upstot,ektot,pottot
300  FORMAT(' TotalEnergy',f12.3,6f15.3)
```

Where `tim,utot,ustot,uptot,upstot,ektot,pottot` are the values of the time, total energy, solvent potential energy, solute potential energy, solvent-solute potential energy, total kinetic energy, total potential energy. Time is given in fs and all energies in *KJ/mole*. The energy conservation ratio  $R \equiv \Delta E / \Delta K$  and the drift  $D = \frac{(E - \langle E \rangle)t}{t(t - \langle t \rangle)}$  are printed periodically (every  $1000 * \Delta t_h$ ) and at the end of the simulation onto the file *filename*.

- **dirty** – Obsolete - **Unsupported**

Scales velocities to the initial total energy  $E(0)$  during production stage. The scaling is done randomly with a Monte Carlo algorithm.

- **p\_test** *n1 n2 n3 n4 n5* – Diagnostic - **Unsupported**

To be used in conjunction with subcommand `test-times`: print out time record of the subsystems potential and forces for the protein for atoms *n1 n2 n3 n4 n5*.

- **s\_test** *n1 n2 n3* – Diagnostic - **Unsupported**

To be used in conjunction with subcommand `test-times`: print out time record of the subsystems potential and forces for the solvent for atoms *n1 n2 n3*.

- **very\_cold\_start** *rmax*

This option is useful when minimizing a protein in a highly unfavorable configuration. The real argument *rmax* is the maximum allowed displacement (in Å) for any atom when integrating the equations of motion irrespectively of the intensity of the force on that atom. This constraint avoid blowing up of the simulation.

- **energy\_then\_die**

Print out energies and then stops.

## EXAMPLES

```
step intra 2
step intra 2
step nonbond 4 4.2
step nonbond 4 7.3  reciprocal
step nonbond 1 9.7
```

Here five time steps are defined, three for nonbonded potentials and two for intramolecular potential. The largest timestep  $\Delta t_h$  is defined by the command `TIMESTEP` in this environment (see above) and refers to the nonbonded subsystem with shell in the range 7.3 – 9.7 Å. We then have  $\Delta t_l = \Delta t_h / 4$  referring to the 4.2 – 7.3 Å shell and  $\Delta t_i = \Delta t_h / 4 / 4$  referring to the 0 – 4.2 Å shell. The reciprocal potential is assigned to the intermediate 4.2 – 7.3 Å shell. The two intramolecular shells have time steps  $\Delta t_{n1} = \Delta t_h / 4 / 4 / 2$  and  $\Delta t_{n0} = \Delta t_h / 4 / 4 / 2 / 2$ .

```
step intra 2
step nonbond 3 6.5  reciprocal
step nonbond 1 9.5
test-times OPEN file-tests
```

Here only one intramolecular and two intermolecular time steps are defined. The reciprocal (PME or standard) contribution is assigned to the fastest intermolecular shell. Energy records are printed onto the file *file-tests* each  $\Delta t_h$  femtoseconds.

## DEFAULTS

```
step intra 1
step intra 1
step nonbond 1 4.1 0.3 0.35
step nonbond 1 7.3 0.3 0.45 reciprocal
step nonbond 1 9.7 0.3 1.5
```

## WARNINGS

- 1 When standard Ewald is used and the reciprocal space contribution is subdivided in **k**-shells, the intramolecular term of Eq. 4.21 is always assigned to the fastest **k**-shell. This may cause instability of the integration. Subdivision of the reciprocal lattice contribution with standard Ewald, although technically possible, is not recommended.
- 2 The directive **dirty** makes fast integrators stable but may severely affect dynamical properties.

---

TIMESTEP

## NAME

TIMESTEP – Define the simulation time step

## SYNOPSIS

TIMESTEP *time*

## DESCRIPTION

The argument *time* represents the integration time step used during the run. As integration of the equations of motion is always done with the r-RESPA algorithm, *time* is the outer most time step. *time* must be given in units of femtoseconds.

## EXAMPLES

TIMESTEP 9.0

---

---

### 10.2.4 &META

Define run time parameters concerning Metadynamics Simulation. The following commands are available:

ADD\_BOND, ADD\_BEND, ADD\_TORS, RATE, READ, SAVE

---

#### ADD\_BOND

##### NAME

ADD\_BOND – Add the distance between two atoms to the list of reaction coordinates.

##### SYNOPSIS

ADD\_BOND      *iat1*      *iat2*      *w*

##### DESCRIPTION

This command adds to the list of the reaction coordinates of a metadynamics simulation the distance between atom *iat1* and *iat2*. The numeric order of the atom indices *iat1*, *iat2* is that specified in the topology file (see 10.3). The repulsive potential terms deposited in the space of the reaction coordinates during the simulation (see 6.3.3) will have a width *w* (in Å) in the direction of this distance.

##### EXAMPLES

ADD\_BOND 1 12 0.2

Add the distance between atom 1 and atom 12 to the list of the reaction coordinates.

---

#### ADD\_BEND

##### NAME

ADD\_BEND – Add the bending angle between three atoms to the list of the reaction coordinates.

##### SYNOPSIS

ADD\_BEND      *iat1*      *iat2*      *iat3*      *w*

##### DESCRIPTION

This command adds to the list of the reaction coordinates of a metadynamics simulation the bending angle between atom *iat1*, *iat2* and *iat3*. The central atom of the bending is *iat2*. The numeric order of the atom indices *iat1*, *iat2*, *iat3* is that specified in the topology file (see 10.3). The repulsive potential terms deposited in the space of the reaction coordinates during the simulation (see 6.3.3) will have a width *w* (in arc degrees) in the direction of this angle.

##### EXAMPLES

ADD\_BEND 1 7 12 4.0

Add the bending angle between atom 1, atom 7 and atom 12 to the list of the reaction coordinates.

---

#### ADD\_TORS

##### NAME

ADD\_TORS – Add the torsional angle between four atoms to the list of the reaction coordinates.

##### SYNOPSIS

ADD\_TORS      *iat1*      *iat2*      *iat3*      *iat4*      *w*

## DESCRIPTION

This command adds to the list of the reaction coordinates of a metadynamics simulation the torsional angle between atom *iat1*, *iat2*, *iat3* and *iat4*. The axis of the torsion is defined by the atoms *iat2* and *iat3*. The numeric order of the atom indices *iat1*, *iat2*, *iat3*, *iat4* is that specified in the topology file (see 10.3). The repulsive potential terms deposited in the space of the reaction coordinates during the simulation (see 6.3.3) will have a width *w* (in arc degrees) in the direction of this angle.

## EXAMPLES

ADD\_TORS 1 5 8 11 4.0

Add the torsional angle between atom 1, atom 5, atom 8 and atom 11 to the list of the reaction coordinates.

---

RATE

## NAME

RATE – Define the deposition rate of a metadynamics run.

## SYNOPSIS

RATE *mtime* [*mheight*]

## DESCRIPTION

This command defines the deposition frequency *mtime* (in fs) and the height *mheight* (in kJ mol<sup>-1</sup>) of the repulsive potential terms deposited during a metadynamics run. If *mheight* is not specified, then a zero height is assumed.

## EXAMPLES

RATE 100.0 0.05

Depose an hill of height 0.05 kJ mol<sup>-1</sup> every 100 fs.

---

READ

## NAME

READ – Read a trajectory from a previous metadynamics run.

## SYNOPSIS

READ *filename*

## DESCRIPTION

When present, the program reads a trajectory *filename* from a previous metadynamics run.

## EXAMPLES

READ old\_traj.out

Read trajectory from file old\_traj.out.

## WARNINGS

The metadynamics parameters of the previous and of the new simulation must be the same in order to obtain meaningful results.

---



## TEMPERED

## NAME

TEMPERED – During a metadynamics simulation, adds an hill to the biasing potential with a decreasing probability.

## SYNOPSIS

TEMPERED  $T'$

## DESCRIPTION

When present, the program adds an hill to the current biasing potential with a probability given by  $P(\text{acc}) = \exp(-V_{\text{max}}(t))/k_B T'$ , where  $V_{\text{max}}(t)$  is the maximum value of the potential  $V(s, t)$  at time  $t$  and  $T'$  is a user-defined temperature.

## EXAMPLES

TEMPERED 1000.0

Run a tempered metadynamics simulation adding new potential terms with a probability that depends on the ratio  $V_{\text{max}}(t)/k_B * 1000.0$ .

## DEFAULTS

$T'$  0.0

## WTEMPERED

## NAME

WTEMPERED – During a metadynamics simulation, adds an hill to the biasing potential with a decreasing probability, following the well-tempered metadynamics algorithm.

## SYNOPSIS

WTEMPERED  $T'$

## DESCRIPTION

When present, the program adds an hill to the current biasing potential with a probability given by  $P(\text{acc}) = \exp(-V(s, t))/k_B T'$ , where  $V(s, t)$  is the value of the biasing potential and  $T'$  is a user-defined temperature.

## EXAMPLES

WTEMPERED 1000.0

Run a tempered metadynamics simulation adding new potential terms with a probability that depends on the ratio  $V(s, t)/k_B * 1000.0$ .

## DEFAULTS

$T'$  0.0

## SAVE

## NAME

SAVE – Save periodically a trajectory file during a metadynamics run.

## SYNOPSIS

SAVE *fprint* [*filename*]

## DESCRIPTION

When present, the program writes the trajectory in the space of the reaction coordinates, sampled with the frequency defined through the command RATE, to file *filename* every *fprint* fs. The first line of the file contains the number of hills deposited when the file was dumped and the height and the

width along each reaction coordinate. If at the beginning of the run a trajectory file from a previous metadynamics simulation was read through the command **READ**, then the program prints the *whole* trajectory.

#### EXAMPLES

**SAVE 10000.0 traj.out**

Print trajectory in file traj.out every 10 ps.

---

### 10.2.5 &PARAMETERS

This environment includes commands which read the topology and force field parameter files of the solute. These files described in Sec. 10.3 contain sufficient information to define the solute topology and to assign potential parameters to the solute molecules. The following commands are allowed:

ADD\_TPG, JOIN, PRINT\_TOPOLOGY, READ\_TPGPRM READ\_PRM\_ASCII, READ\_TPG\_ASCII, REPL\_RESIDUE,  
WRITE\_TPGPRM\_BIN

---

#### ADD\_TPG SOLUTE

NAME

ADD\_TPG SOLUTE – Add topology components to the current solute molecule

SYNOPSIS

ADD\_TPG SOLUTE

...

...

END

#### DESCRIPTION

The structured command **ADD\_TPG SOLUTE** opens an environment including commands which add extra bonds, proper and improper torsions to the topology of the current solute molecule(s). The command is closed by **END**. This command must be used to connect atoms belonging to different residues of the current molecule. For instance to connect through a sulphur bridge two cysteine residues or to bind ligands to a metal atom.

- **bond 1ata 2atb residue num1 num2**

Add a bond to the topology of the current solute molecule which connect atom *ata* of residue number *num1* with atom *atb* of residue number *num2*. The number 1 and 2 refer to residue *num1* and *num2*, respectively. The atom label *ata* and *atb* must be defined in the general formatted topology file as labels of actual atoms of residue number *num1* and *num2*. Here, residue numbers are the sequential numbers of the residues as given in input to command **JOIN**.

- **torsion 1ata 1atb 2atc 2atd residue num1 num2**

Add a proper torsion to the topology of the current solute molecule. The number 1 and 2 refer to residue *num1* and *num2*, respectively. Atom *ata* and *atb* belong to residue number *num1*, while atoms *atc* and *atd* are on residue number *num2*. Additional torsion having three atoms on one residue and one atom on the other residue are also allowed. Here, residue numbers are the sequential numbers of the residues as given in input to command **JOIN**. If the command **AUTO\_DIHEDRAL** of the environment **&SOLUTE** is used, no extra torsions need to be added to the current topology.

- **i.torsion 1ata 1atb 2atc 2atd residue num1 num2**

Add an improper torsion to the topology of the current solute molecule. The number 1 and 2 refer to residue numbers *num1* and *num2*, respectively. Atom *ata* and *atb* belong to residue number *num1*, while atoms *atc* and *atd* are on residue number *num2*. Additional improper torsions having three atoms on one residue and one atom on the other residue are also allowed. Here, residue numbers are the sequential numbers of the residues as given in input to command **JOIN**.

#### EXAMPLES

```

ADD_TPG SOLUTE
    bond 1sg 2sg residue 6 127
    bond 1sg 2sg residue 30 115
    bond 1sg 2sg residue 64 80
    bond 1sg 2sg residue 76 94
END

```

Add extra bonds to the current topology. In this example, the four sulphur bridges of hen egg lysozyme are given.

#### WARNINGS

This command is inactive when used in conjunction with READ\_TPGPRM. To have the desired effect, the ADD\_TPG environment must be used in conjunction with READ\_TPG\_ASCII and READ\_PRM\_ASCII.

## JOIN

### NAME

JOIN – Provide the list of residues forming the current solute or solvent molecule(s).

### SYNOPSIS

```
JOIN [SOLUTE | SOLVENT]
```

```
...
```

```
...
```

```
END
```

### DESCRIPTION

The structured command JOIN reads the sequential list of labels corresponding to the residues forming the solute molecule(s). The list of residues begins at the line following JOIN. The end of this list is signaled by END on the line following the last residue label. Each residue labels must have been defined in the general formatted topology file read by READ\_TPG\_ASCII. See Sec. 10.3 for explanations.

### EXAMPLES

#### JOIN SOLUTE

```

lys-h val phe gly arg cys glu leu ala ala ala met lys
arg hsd gly leu asp asn tyr arg gly tyr ser leu gly
asn trp val cys ala ala lys phe glu ser asn phe asn
thr gln ala thr asn arg asn thr asp gly ser thr asp
tyr gly ile leu gln ile asn ser arg trp trp cys asn
asp gly arg thr pro gly ser arg asn leu cys asn ile
pro cys ser ala leu leu ser ser asp ile thr ala ser
val asn cys ala lys lys ile val ser asp gly asn gly
met asn ala trp val ala trp arg asn arg cys lys gly
thr asp val gln ala trp ile arg gly cys arg leu-o

```

```
END
```

Sequence of residues for hen-egg lysozyme. All labels must have been defined in the general formatted topology file.

#### JOIN SOLVENT

```
hoh
```

```
END
```

Defines the topology of the solvent

## WARNINGS

The command is inactive when used in conjunction with READ\_TPGPRM. To have the desired effect, the JOIN environment must be used in conjunction with READ\_TPG\_ASCII, READ\_PRM\_ASCII and, optionally, the REPL\_RESIDUE environment.

---

PRINT\_TOPOLOGY

## NAME

PRINT\_TOPOLOGY – Print topology components of the current solute molecule.

## SYNOPSIS

```
PRINT_TOPOLOGY
```

```
...
```

```
END
```

## DESCRIPTION

PRINT\_TOPOLOGY is a structured command to be used for printing out part of the topology and potential information for the solute molecule. The following subcommands may be specified within PRINT\_TOPOLOGY:

atoms bendings bonds constraints I-torsions P-torsions sequence

- **bonds**  
Print the bonds list.
- **bendings**  
Print the bendings list.
- **constraints**  
Print the bond constraints list.
- **I-torsions**  
Print the proper torsion list.
- **P-torsions**  
Print the improper torsion list.
- **sequence**  
Print info on the units sequence of both solvent and solute

## EXAMPLES

```
PRINT_TOPOLOGY
```

```
  bonds
```

```
  P-torsions
```

```
END
```

---

## READ\_TPGPRM

## NAME

READ.TPGPRM – Read parameter and topology file

## SYNOPSIS

READ.TPGPRM *filename* [no\_warning]

## DESCRIPTION

The command reads the force field parameters and topology file *filename*. Starting from release 6.0, the parameters and topology file is a text file for ensuring portability. This file contains the topology and force field parameters tables. It is created with the commands WRITE\_TPGPRM\_BIN, READ\_TPG\_ASCII and READ\_PRM\_ASCII. The tables contained in file *filename* are associated only with the current solute molecule(s) and can only be used for that (those) molecule(s). In alternative to the command READ\_TPGPRM, READ\_TPG\_ASCII and READ\_PRM\_ASCII, which read the general formatted topology and parameters files, can be used. Since the use of the latter commands implies the calculation of the topology and parameters tables for the current solute molecule, it is advisable to use them only a first time to create the unformatted file read by READ\_TPGPRM. When READ\_TPGPRM is entered, all the topology of the system is read in from the specified file and the topology commands such as JOIN\_SOLUTE JOIN\_SOLVENT or ADD\_TPG are ignored. Also the environments &SOLUTE, &SOLVENT, &SETUP need not to be specified.

## EXAMPLES

```
&PARAMETERS
  READ_TPGPRM_BIN  benz.prmtpg
&END
&SIMULATION
  ...
&END
&INOUT
  RESTART          50.0    OPEN    benz.rst
&END
&INTEGRATOR
  ...
&END
&POTENTIAL
  ..
&END
&RUN
  CONTROL          1
  ..
&END
```

In this example all topology information and the coordinates of all atoms in the system are taken in care by only three directives: READ\_TPGPRM\_BIN, RESTART, CONTROL. The files **benz.prmtpg** and **benz.rst** which contains the topology and the coordinates, respectively must have been produced with a previous run.

## READ\_PRM\_ASCII

## NAME

READ\_PRM\_ASCII – Read a general formatted parameters file

## SYNOPSIS

READ\_PRM\_ASCII *filename*

## DESCRIPTION

Here *filename* is the ASCII parameter file. The general formatted force field parameters file is described in Sec. 10.3. In this file one must define each potential energy parameter of the given force field defined in Eq. 4.3. It must be consistent with the general topology file read by READ\_TPG\_ASCII. The same parameters file can be used for many different solute molecules. This is the reason of the word “general”.

## EXAMPLES

READ\_PRM\_ASCII forcefield.prm

Read the general formatted parameters file forcefield.prm.

## WARNINGS

Must be used in conjunction with command READ\_TPG\_ASCII.

## READ\_TPG\_ASCII

## NAME

READ\_TPG\_ASCII – Read a general formatted topology file

## SYNOPSIS

READ\_TPG\_ASCII *filename*

## DESCRIPTION

Here *filename* is the ASCII topology file. The general topology file is described in Sec. 10.3. It must define each residue contained in the current solute molecule. The same topology file can be used for many different solute molecules. This is the reason of the word “general”.

## EXAMPLES

READ\_TPG\_ASCII forcefield.tpg

Read the formatted topology file forcefield.tpg.

## WARNINGS

Must be used in conjunction with command READ\_PRM\_ASCII.

## REPL\_RESIDUE

## NAME

REPL\_RESIDUE – Replace or add the topology of a certain residue

## SYNOPSIS

REPL\_RESIDUE

...

...

END

## DESCRIPTION

The command REPL\_RESIDUE opens an environment which includes the same series of commands and subcommands accepted by the general formatted topology file described in Sec. 10.3.

## EXAMPLES



```

REPL_RESIDUE
  RESIDUE gly ( Total Charge = 0.0 )
  atoms
  group
  n      n      -0.41570
  hn     h       0.27190
  group
  ca     ct      -0.02520
  ha1    h1       0.06980
  ha2    h1       0.06980
  group
  c       c       0.59730
  o       o      -0.56790
  end

  bonds
  n      hn      n      ca      o      c      c      ca
  ca     ha1     ca     ha2
  end

  imphd
  -c     ca      n      hn      ca      +n      c      o
  end

  termatom n c
  backbone n ca c
  RESIDUE_END
END

```

Replace or add the topology for residue gly.

## WRITE\_TPGPRM\_BIN

### NAME

WRITE\_TPGPRM\_BIN – Write an unformatted parameter and topology file

### SYNOPSIS

WRITE\_TPGPRM\_BIN *filename*

### DESCRIPTION

This command must be used in combination with READ\_TPG\_ASCII and READ\_PRM\_ASCII. It produces the file *filename* containing the force field and topology tables associated with the current solute molecule(s) which can be reread in subsequent runs by the command READ\_TPGPRM.

### EXAMPLES

WRITE\_TPGPRM\_BIN molecule1.prmtpg

Write the unformatted topology and parameter file for the current solute molecule that can be read by READ\_TPGPRM.

### WARNINGS

Must be used in conjunction with commands READ\_TPG\_ASCII and READ\_PRM\_ASCII.

---

### 10.2.6 &POTENTIAL

The environment &POTENTIAL includes commands which define the general features of the system interacting potentials. These features are common to both solute and solvent and concern both bonded and non-bonded interactions. The following are allowed commands:

ADD\_STR\_BONDS, ADD\_STR\_BENDS, ADD\_STR\_COM, ADD\_STR\_TORS, ADJUST\_BONDS, AUTO\_DIHEDRAL, BENDING, CHECK\_COORD\_OFF CONSTRAINT, CUTOFF, ERF\_CORR, ERFC\_SPLINE, DEFINE\_ALCHEMICAL\_ATOM EWALD, GROUP\_CUTOFF, I-TORSION, JORGENSEN, KEEP\_BONDS, LJ-FUDGE, LINKED\_CELL, QQ\_FUDGE, SELECT\_DIHEDRAL, STEER\_PATH, STRETCHING, UPDATE, VERLET\_LIST

---

#### ADD\_STR\_BONDS

NAME

ADD\_STR\_BONDS – Add a stretching potential between two target atoms.

SYNOPSIS

ADD\_STR\_BONDS      *iat1*      *iat2*      *k*      *r*<sub>0</sub>      [ *r*<sub>τ</sub> ]

DESCRIPTION

This command can be used to impose an additional stretching constraint between atom *iat1* and *iat2* of the solute. The numeric order of the solute atom indices *iat1*, *iat2* is that specified in the topology file (see 10.3). The added stretching potential has force constant *k* (in Kcal/mol/Å<sup>2</sup>) and equilibrium distance *r*<sub>0</sub> (in Å). If *r*<sub>τ</sub> is also specified, then the added stretching potential is time dependent and *r*<sub>τ</sub> is the equilibrium distance after the steering time  $\tau$  (see STEER(&RUN)) command for the definition of the steering time in a SMD simulation)

WARNINGS

If the chosen *r*<sub>0</sub> is very different from the *actual* value of the distance  $|\mathbf{r}_{iat1} - \mathbf{r}_{iat2}|$  at time 0, a very large force is experienced by the atoms involved in the added stretching and the simulation may catastrophically diverge after few steps.

EXAMPLES

– Example 1.

```
ADD_STR_BONDS  1 104  400.  31.5
```

– Example 2.

```
&PARAMETERS
  READ_TPGPRM_BIN  ala10_A.prmtpg
&END

...
&POTENTIAL
  ...
  ADD_STR_BONDS  1 104  400.  31.5  15.5
  ..
&END
....
```

```

...
&RUN
  CONTROL 2
  ...
  REJECT 0.0
  STEER 10000. 50000.
  TIME 50009.0
  ...
&END
..
&INOUT
  RESTART
    rmr ../RESTART/ala10 0
&END

```

In the first example a stretching constraint is imposed between atom 1 and atom 104 of the solute. In the second example a time-dependent driving potential is applied to the same atoms of the solute. The equilibrium distance of such harmonic driving potential moves at constant velocity in  $\tau = 40$  ps (starting at  $t=10$  ps) between  $r_0 = 31.5$  and  $r_\tau = 15.5$ . Since the directive `rmr` (or `read_multiple_restart`) is issued in the `RESTART(&INOUT)` command, the example is assumed to run in parallel. Each process reads a *different* restart file named `ala10iproc.rst` in the `../RESTART` directory. Note that the path of the restart files is specified with respect to the actual value of the `pwd` command when the parallel version is executed (i.e. in the `PARxxxx` directories).

## ADD\_STR\_BENDS

NAME

ADD\_STR\_BENDS – Add a bending potential between three target atoms.

SYNOPSIS

ADD\_STR\_BENDS      *iat1*      *iat2*      *iat2*      *k*       $\alpha_0$       [ *alpha<sub>τ</sub>* ]

DESCRIPTION

This command can be used to impose an additional bending constraint between atom *iat1*, *iat2* and *iat3* of the solute. The numeric order of the solute atom indices *iat1*, *iat2* is that specified in the topology file (see Sec. 10.3). The central atom of the bending is *iat2*. The added bending potential has force constant *k* (in Kcal/mol/rad<sup>2</sup>) and equilibrium bending angle  $\alpha_0$  (in degrees). If  $\alpha_\tau$  is also specified, then the added bending potential is time dependent and  $\alpha_\tau$  is the equilibrium bending angle after the steering time  $\tau$  (see `STEER(&RUN)` command for the definition of the steering time in a SMD simulation)

WARNINGS

If the chosen  $\alpha_0$  is very different from the *actual* value of the bending angle at time 0, a very large force is experienced by the atoms involved in the added bending and the simulation may catastrophically diverge after few steps.

EXAMPLES

– Example 1.

```
ADD_STR_BENDS 1 50 104 400. 180.0
```

– Example 2.

```

&POTENTIAL
...
  ADD_STR_BENDS  1 50 104  400.  180.0 90.0
..
&END
....
...
&RUN
...
  STEER 10000.  50000.
...
&END

```

In the first example a bending constraint is imposed between atom 1, atom 50, and atom 104 of the solute. In the second example a time-dependent driving potential is applied to the same atoms of the solute. The equilibrium bending angle of such harmonic driving potential moves at constant velocity in  $\tau = 40$  ps (starting at  $t=10$  ps) between  $\alpha_0 = 180.0$  and  $\alpha_\tau = 90.0$ .

#### ADD\_STR\_COM

##### NAME

ADD\_STR\_COM – Add a bond potential between the Centers of Mass (COMs) of two selected groups of atoms.

##### SYNOPSIS

```

ADD_STR_COM
  ligand ilig1 ilig2
  target itar1 itar2
  force kcom r0com [r1com]
END

```

##### DESCRIPTION

This command can be used to impose an additional bond restraint potential (with force constant  $kcom$  [ in kcal mol<sup>-1</sup> ] and equilibrium distance  $r0com$ ) ( in Å ) between the COM of a “ligand”, defined by the atoms subset *ilig1-ilig2*, and the COM of a “target”, defined by the atoms subset *itar1-itar2*. If the optional parameter *r1com* is also specified then a steered molecular dynamics is implied (see also **STEER** command).

##### WARNINGS

Experimental - **Unsupported**

##### EXAMPLES

– Example 1

```

&POTENTIAL
...
  ADD_STR_COM
    ligand  1 10
    target  11 1500
    force   10.0 5.0
  END
...
&END

```

– Example 2.

```
&POTENTIAL
...
ADD_STR_COM
  ligand  1 10
  target  11 1500
  force   10.0 5.0  10.0
END
..
&END
....
...
&RUN
...
  STEER 10000.  50000.
...
&END
```

In the first example a COM-COM restraint at  $r = 5.0 \text{ \AA}$  is imposed between the ligand (first 10 atoms as labeled in the output PDB) and a 1489 atoms target with atomic labels going from 11 to 1500. In the second example the restraint potential is steered at constant speed from 5 to 10  $\text{\AA}$  in the time span 10 - 50 ps.

## ADD\_STR\_TORS

### NAME

ADD\_STR\_TORS – Add a harmonic bending potential between three target atoms.

### SYNOPSIS

```
ADD_STR_TORS      iat1      iat2      iat3      iat3      k       $\theta_0$       [  $\theta_\tau$  ]
```

### DESCRIPTION

This command can be used to impose an additional (harmonic) torsional constraint between atoms *iat1*, *iat2*, *iat3* and *iat4* of the solute. The axis of the torsion is defined by the atoms *iat2*, *iat3*. The numeric order of the solute atom indices *iat1*, *iat2*, *iat3*, *iat4* is that specified in the topology file (see Sec. 10.3). The added torsional potential has force constant *k* (in Kcal/mol/rad<sup>2</sup>) and equilibrium dihedral angle  $\theta_0$  (in degrees). If  $\theta_\tau$  is also specified, then the added torsional potential is time dependent and  $\theta_\tau$  is the equilibrium dihedral angle after the steering time  $\tau$  (see STEER(&RUN) command for the definition of the steering time in a SMD simulation)

### WARNINGS

If the chosen  $\theta_0$  is very different from the *actual* value of the dihedral angle at time 0, a very large force is experienced by the atoms involved in the added bending and the simulation may catastrophically diverge after few steps.

### EXAMPLES

– Example 1.

```
ADD_STR_TORS  1 50 70 104  400.  60.0
```

– Example 2.

```

&POTENTIAL
...
ADD_STR_TORS  1 50 70 104  400.  60.0   90.0
..
&END
....
...
&RUN
...
STEER 10000.  50000.
...
&END

```

In the first example a torsional constraint is imposed between atom 1, atom 50, atom 70 and atom 104 of the solute. In the second example a time-dependent driving potential is applied to the same atoms of the solute. The equilibrium dihedral angle of such harmonic driving potential moves at constant velocity in  $\tau = 40$  ps (starting at  $t=10$  ps) between  $\theta_0 = 60$  and  $\theta_\tau = 90$  degrees.

#### ADJUST\_BONDS

NAME  
ADJUST\_BONDS – Constraints bond lengths to starting values.

SYNOPSIS  
ADJUST\_BONDS

#### DESCRIPTION

This command should be specified when bond constraints are imposed to the system (see command STRETCHING and CONSTRAINT in this environment). If specified, all bonds to be constrained are constrained to the lengths specified in the force field parameter file (see sec 10.3.1 PDB file

DEFAULTS  
ADJUST\_BONDS is *.TRUE.*

#### AUTO\_DIHEDRAL

NAME  
AUTO\_DIHEDRAL – Include all the proper torsion angle in the interaction potential

SYNOPSIS  
AUTO\_DIHEDRAL

WARNINGS  
Obsolete - **Unsupported**

#### BENDING

NAME  
BENDING – set constraints on bendings.

SYNOPSIS  
BENDING on  
BENDING off

## DESCRIPTION

With the argument **on**, this command includes harmonic bending potentials in the total solute potential. Conversely, if the argument is **off** all the bending of the solute molecules are constrained.

## DEFAULTS

BENDING **off**

## WARNINGS

Obsolete - **Unsupported**

---

## CHECK\_COORD\_OFF

## NAME

CHECK\_COORD\_OFF

## SYNOPSIS

CHECK\_COORD\_OFF

## DESCRIPTION

This option is used to suppress check on initial atomic coordinates.

---

## CONSTRAINT

## NAME

CONSTRAINT – Constrain bendings.

## SYNOPSIS

CONSTRAINT SHAKE

CONSTRAINT MIM *mimlim*

## DESCRIPTION

Select procedure for fulfilling constraints. With the argument **SHAKE** ORAC uses SHAKE. With argument **MIM** ORAC uses the matrix inversion method (MIM). In the latter case the maximum physical dimension of the constraint matrix *mimlim* must be specified. MIM is best used in conjunction with **STRETCHING HEAVY**

## DEFAULTS

BENDING **off**

---

## CUTOFF

## NAME

CUTOFF

## SYNOPSIS

CUTOFF *rspoff*

## WARNINGS

Used in the minimization routine only.

---

## DEFINE\_ALCHEMICAL\_ATOM

NAME

DEFINE\_ALCHEMICAL\_ATOM

SYNOPSIS

DEFINE\_ALCHEMICAL\_ATOM *iat1* *iat2* on/off

DESCRIPTION

Define an alchemical segment for the solute (N.B. Only solute atoms can be of alchemical types). *iat1* and *iat2* are the index of the first and last atom of the alchemical segment. Alchemical segments can either be switched **on** or switched **off**. The alchemical atoms must be part of the starting PDB file whether they interact or not with the actual atoms. This command is used along with the command STEER\_PATH ALCHEMY (to define the time protocol of the transformation) and the command PLOT ALCHEMY (to printing out the work done during the transformation).

EXAMPLES

– Example 1.

```
DEFINE_ALCHEMICAL_ATOM 1 10 on
... STEER_PATH ALCHEMY alchemy.time.on
```

atoms from 1 to 10 of the solute will be switched **on** with a time protocol specified in the file `alchemy.time.on`

– Example 2.

```
DEFINE_ALCHEMICAL_ATOM 1 10 off
... STEER_PATH ALCHEMY alchemy.time.off
```

atoms from 1 to 10 of the solute will be switched **off** with a time protocol specified in the file `alchemy.time.off`

– Example 3.

```
DEFINE_ALCHEMICAL_ATOM 1 10 on
DEFINE_ALCHEMICAL_ATOM 10 20 off
... STEER_PATH ALCHEMY alchemy.time.on.off
```

atoms from 1 to 10 of the solute will be switched **on** and atoms from 10 to 20 of the solute will be switched **off** each with a time protocol specified in the common file `alchemy.time.on.off`

## ERF\_CORR

NAME

ERF\_CORR – Implements intramolecular Ewald correction

SYNOPSIS

ERF\_CORR *nbin rlow rup*

DESCRIPTION

Adds correction of Eq. 4.47, evaluated only for excluded *intra*-molecular contacts (stretching, bending and “fudged” part of 1-4 interactions) to account for reciprocal space cutoff error. The function  $\chi(r, \alpha)$  is B-splined using *nbin* points in the range  $rlow < r < rup$ .

EXAMPLES

ERF\_CORR 2000 0.8 4.5



## WARNINGS

Choose carefully *r<sub>low</sub>* and *r<sub>up</sub>*. If an intramolecular distance outside the range is found during execution, unpredictable results may occur.

## ERFC\_SPLINE

## NAME

**ERFC\_SPLINE** – Use spline to compute the complementary error function used for electrostatics in direct space

## SYNOPSIS

**ERFC\_SPLINE** *erfc\_bin*

**ERFC\_SPLINE** *erfc\_bin* **corrected** *rcut*

## DESCRIPTION

By default ORAC uses a 5 parameter expansion to compute the complementary error function required by the direct space electrostatic potential ( $V_{qd}$  in Eq. 4.20). With the command **ERFC\_SPLINE** this expansion is replaced by a B-spline. The function  $erfc(x)$  is splined from  $x = 0$  to  $x = 1.1\alpha r_{cut}$ , where  $\alpha$  and  $r_{cut}$  are the Ewald sum parameter and the radial cutoff, respectively. The argument *erfc\_bin* is the bin size of the spline. The usage of the **ERFC\_SPLINE** option is useful when running on workstations where a saving of 10-15 % in CPU time is usually obtained. **ERFC\_SPLINE** may also be used to speed up the Ewald method. By specifying the directive **corrected** ORAC corrects for the reciprocal lattice cutoff for all *intermolecular* interactions in the direct lattice using the same oscillating potential of Eq. (4.47) (see Sec. 4.4) used for correcting the *intra*-molecular potential (see **ERF\_CORR** in this environment). This allows the use shorter cutoffs in reciprocal space (or coarser grids in SPME). The argument *rcut* corresponds to the maximum distance for the spline table. Must be larger than the current cutoff (see examples).

## EXAMPLES

**ERFC\_SPLINE** 0.01

A B-spline is used to evaluate the direct space sum. To evaluate the B-spline the original function is computed on a grid of 0.01 bin size.

**ERFC\_SPLINE** 0.01 **corrected** 14.0

The splined potential is now given by standard the direct lattice Ewald term *plus* the  $\chi(r, \alpha)$  potential defined in Eq. (see also command **ERF\_CORR** in this environment). The B-spline look up table is done for distances  $0 < r < 14$ .

## WARNINGS

*rcut* is an *atomic* cutoff. Always define *rcut* large enough to assure that all atoms are included within *rcut* for any molecular pair. E. g., if  $r_h$  the largest cutoff defined in the structured command **MTS\_RESPA** (&**INTEGRATOR**) and the molecule has a maximum extension in any possible direction of  $\Delta R$ , choose  $rcut = r_h + \Delta R$

## EWALD

## NAME

**EWALD** – Determine if standard Ewald or particle mesh Ewald sum must be used

## SYNOPSIS

**EWALD** **off**

**EWALD** **ON** *alphal* *r<sub>kcut</sub>*

**EWALD** **PME** *alphal* *ftt1* *ftt2* *ftt3* *order*

**EWALD** **REMOVE\_MOMENTUM**

## DESCRIPTION

As described in Sec. 4.1 ORAC can handle the electrostatic interactions by Ewald summation. If the argument to the command is **on** followed by *alphal* and *rkcut*, standard Ewald is used with  $\alpha = \text{alphal}$  in  $\text{\AA}^{-1}$  and the cutoff in k-space  $k_{\text{cut}} = \text{rkcut}$  in  $\text{\AA}^{-1}$ . The output will show what degree of convergence has been reached showing the numerical value of  $\text{erfc}(r_{\text{cut}}\alpha)/r_{\text{cut}}$  and of  $\exp(-k_{\text{cut}}^2/2\alpha)/k_{\text{cut}}$ . To chose instead PME the argument **pme** *alphal* *fft1* *fft2* *fft3* *order* must be chosen. Here, **alphal** has the same meaning as before, while **order** is the order of the spline and *fft1* *fft2* *fft3* define the three dimensional grid in direct space providing the number of bins along the *a*, *b*, *c* crystal axis, i.e. the dimensions of the 3-D FFT used in the PME method. For best efficiency *fft1*, *fft2*, and *fft3* must be multiples of 2, 3 or 5. Of course, if the argument is **off** no Ewald summation is used for the electrostatic interactions. When using PME, Newton third law is not obeyed exactly but to the numerical accuracy of the interpolation. This leads to a small momentum of the MD cell which can be removed by specifying the argument **REMOVE\_MOMENTUM**

## EXAMPLES

1 EWALD on 0.4 2.0

Standard Ewald is used with parameters  $\alpha = 0.4 \text{ \AA}^{-1}$  and  $k_{\text{cut}} = 2.0 \text{ \AA}^{-1}$ .

2 EWALD pme 0.4 45 32 45 6

EWALD REMOVE\_MOMENTUM

The electrostatic interaction is handled by PME with  $\alpha = 0.4 \text{ \AA}^{-1}$ , the order of the spline is 6 and the number of bins for defining the grid are 45,32,45 along the *a*, *b*, *c* crystal axis, respectively. Typically, acceptable relative accuracy ( $10^{-4}$ - $10^{-5}$ ) on electrostatic energies and forces is obtained with a grid spacing of about 1-1.2  $\text{\AA}$  along each dimension. In this example the second invocation of the EWALD command is used in order to remove the linear momentum of the MD cell.

## GROUP\_CUTOFF

NAME

GROUP\_CUTOFF

WARNINGS

Obsolete - **Unsupported**

## H-MASS

NAME

H-MASS – Change the hydrogen mass

SYNOPSIS

H-MASS *hdmass*

DESCRIPTION

The command H-MASS changes the mass of all solute hydrogens to *hdmass* given in a.m.u. This allows to use larger time steps during equilibration.

EXAMPLES

H-MASS 10.0

**I-TORSION****NAME**

**I-TORSION** – Set the type of improper torsion potential

**SYNOPSIS**

**I-TORSION** *itor\_type*

**DESCRIPTION**

This command defines which improper torsion potential must be used. If the argument string *itor\_type* is **HARMONIC** a harmonic CHARMM-like potential functions is chosen. Conversely, if the argument is **COSINE** a sinusoidal AMBER-like potential function is chosen.

**EXAMPLES**

**I-TORSION HARMONIC**

---

**JORGENSEN****NAME**

**JORGENSEN** – Allow Jorgensen-type interaction potentials.

**SYNOPSIS**

**JORGENSEN**

**DESCRIPTION**

If the system is composed of solute molecules of the same type it is sometime useful to use different interaction parameters for intermolecular and intramolecular interactions. The command **JORGENSEN** is designed to handle this situation. Sec. 10.3 describes how the inter and intra-molecular Lennard-Jones parameters are read by ORAC .

**WARNINGS**

Experimental - **Unsupported**

---

**KEEP\_BONDS****NAME**

**KEEP\_BONDS** – Constraints bond lengths to starting values.

**SYNOPSIS**

**KEEP\_BONDS**

**DESCRIPTION**

This command should be specified when bond constraints are imposed to the system (see command **STRETCHING** and **CONSTRAINT** in this environment). If specified, all bonds to be constrained are constrained to the *initial* length found in the starting PDB file

**DEFAULTS**

**KEEP\_BONDS** is *.FALSE.*

---

## LJ-FUDGE

## NAME

LJ-FUDGE – Set the fudge factor of the Lennard–Jones interaction

## SYNOPSIS

LJ-FUDGE *lj-fudge*

## DESCRIPTION

The argument to this command, *lj-fudge*, is the multiplicative factor of the 1-4 Lennard-Jones interaction.

## EXAMPLES

LJ-FUDGE 0.5

## DEFAULTS

LJ-FUDGE 1.0

## LINKED\_CELL

## NAME

LINKED\_CELL - Compute linked cell neighbor lists

## SYNOPSIS

LINKED\_CELL *ncx ncy ncz [nupdte]*

## DESCRIPTION

The LINKED\_CELL command switches to linked cell neighbor lists in place of conventional Verlet lists. The command can be used also for non orthogonal MD boxes. The integers *ncx ncy ncz* define the three dimensional grid by providing the number of bins along the *a, b, c* crystal axis, respectively. The optimum fineness of the cell grid depends on the density of the sample. For normal density a grid spacing of 3.0-3.5 Å along each axis is recommended. The Verlet neighbor list computation depends on  $N^2$  where  $N$  is the number of particle in the system. The linked cell neighbor algorithm [158] scales linearly with  $N$  but it has a large prefactor. The break even point for the two methods is at about 7000 atoms for scalar machines. The frequency of updating of the index cell list is controlled by the argument *nupdate* and by the command UPDATE in this environment. If *fupdate* is the updating time specified in the command UPDATE the updating time for the linked list is *fupdate* × *nupdate*

## EXAMPLES

## &amp;SETUP

```
...
CELL 54.0 72.0 41.0 90.0 102.0 90.0
...
```

## &amp;END

## &amp;POTENTIAL

```
...
LINKED_CELL 15 20 12 1
...
```

## &amp;END

Here a grid spacing of about 3.5 Å along each crystal axis is selected.

## DEFAULTS

*nupdate* = 1

**QQ-FUDGE**

## NAME

QQ-FUDGE – Set the fudge factor of the electrostatic interaction

## SYNOPSIS

QQ-FUDGE *qq-fudge*

## DESCRIPTION

The argument to this command, *qq-fudge*, is the multiplicative factor of the 1-4 electrostatic interaction.

## EXAMPLES

QQ-FUDGE 0.5

## DEFAULTS

QQ-FUDGE 1.0

**SELECT\_DIHEDRAL**

## NAME

SELECT\_DIHEDRAL – Include only selected torsion angles in the potential.

## SYNOPSIS

SELECT\_DIHEDRAL

## DESCRIPTION

In old force field only selected torsion angles were included. This command handles this situation.

## DEFAULTS

The action taken by the command **AUTO\_DIHEDRAL** is the default.

## WARNINGS

Diagnostic - **Unsupported**

**STEER\_PATH**

## NAME

STEER\_PATH – Steer along an arbitrary curvilinear coordinate *or* perform alchemical transformation.

## SYNOPSIS

STEER\_PATH OPEN *filename*

## DESCRIPTION

This command allows to do a MD simulation by steering the system along an arbitrary curvilinear path with arbitrary time protocol in a *n*-dimensional coordinate space (see Sec. 8.3). This curvilinear coordinate and time protocol can be given in terms of time dependent added stretching, bending and torsions external potentials to be specified in the file *filename*. The format of this file is shown in Table 8.3. Refer to Sec. 8.3 for more details.

*or*

STEER\_PATH ALCHEMY *filename*

## DESCRIPTION

This command allows alchemical transformations using a time protocol specified in the file *filename*. See **DEFINE\_ALCHEMICAL\_ATOM** command for details on alchemical transformations.

## STRETCHING

NAME

STRETCHING – Include stretching potentials

SYNOPSIS

STRETCHING [HEAVY]

DESCRIPTION

This command assigns a harmonic stretching potential (see Sec. 10.3.1) between covalently bonded atoms in the solute. Without argument, stretching potentials are assigned to all possible covalently bonded pairs. If the argument **HEAVY** is provided, bonds involving hydrogens are maintained rigid and only stretching potentials for bonded pairs involving non-hydrogen atoms are assigned.

DEFAULT

Constraints on all bonds is the default.

## UPDATE

NAME

UPDATE – Assign parameters for the computation of the Verlet neighbor list

SYNOPSIS

UPDATE *fupdte* *rspcut*

DESCRIPTION

ORAC computes Verlet neighbor lists the atomic groups of both the solvent and solute. There exist three different neighbor lists: a solvent-solvent, a solute-solute and a solvent-solute list. During the run, the calculation is carried out with a frequency equal to *fupdte* fs. All the group-group interactions within a radial cutoff of  $r_{cut} + rspcut$  are included in the neighbor lists. The dimensions of the three lists are printed at run time. In the ORAC output **nnlww**, **nnlpp** and **nnlpw** refers to the solvent-solvent, solute-solute and solute-solvent neighbor list. The current version of ORAC can also use linked cell in place of the conventional Verlet neighbor list (see command **LINKED\_CELL**).

EXAMPLES

UPDATE 65.0 1.4

Update the neighbor lists every 65.0 fs and use a cutoff of  $r_{cut} + 1.4 \text{ \AA}$ .

DEFAULTS

UPDATE 100.0 1.0

WARNINGS

The neighbor list cutoff must not be chosen larger than half of the simulation box size. The calculation of the neighbor list is performed by default. Only for solvent-only simulations, if the radial cutoff is equal to half of the box size, the force calculation is carried out without the use of neighbor list. When using r-RESPA the value of *rspcut* is ignored in the **UPDATE** directive and is taken as an argument of the last **step nonbond** command in the **MTS\_RESPA** structured command.

## VERLET\_LIST

NAME

VERLET\_LIST - Compute Verlet neighbor list

SYNOPSIS

VERLET\_LIST The conventional Verlet List computation is the default.

WARNINGS

Obsolete - **Unsupported**

---

---

### 10.2.7 &PROPERTIES

The &PROPERTIES directive is used to compute statistical properties on the fly or *a posteriori* once the trajectory file has been produced (see command DUMP (&INOUT) and &ANALYSIS environment.) ORAC can compute radial distribution functions, structure factors (GOFR), velocity autocorrelation functions (TIME\_CORRELATIONS). The &PROPERTIES environment is still in the developing stage in the current version of ORAC. Thus, **none of the &PROPERTIES features is officially supported..** Some properties can no longer be computed on the fly in the current version and have to be computed using the &ANALYSIS environment once the trajectory file has been produced.

```
DEF_FRAGMENT DIST_FRAGMENT FORCE_FIELD GOFR, HBONDS PRINT_DIPOLE, STRUCTURES,
TIME_CORRELATIONS, VORONOI, WRITE_GYR
```

---

#### DEF\_FRAGMENT

NAME

DEF\_FRAGMENT – Define a fragment of a solute.

SYNOPSIS

```
DEF_FRAGMENT begin end
```

DESCRIPTION

This command is used in conjunction with the command PLOT FRAGMENT in &INOUT, or in conjunction with the command DIST\_FRAGMENT in this environment. The arguments indicate the ordinal numbers of the first *begin* and the last *end* atom of a solute fragment. These numbers may be deduced by inspection of the PDB file *including* the hydrogens atoms (see command ASCII for generating a PDB file with hydrogens). The command DEF\_FRAGMENT can appear more than one time in the environment. The atoms of different solute molecules defined with this command can overlap.

EXAMPLES

```
DEF_FRAGMENT 1 80
DEF_FRAGMENT 81 90
DEF_FRAGMENT 1001 1256
```

---

#### DIST\_FRAGMENT

NAME

DIST\_FRAGMENT – Print out distances between solute fragments.

SYNOPSIS

```
DIST_FRAGMENT ffragm OPEN filename
```

DESCRIPTION

Write the distances between the centroids of the fragments defined in the command DEF\_FRAGMENT to the file *filename*. This command works only while retrieving the trajectory file by specifying the &ANALYSIS environment.

EXAMPLES

```
DIST_FRAGMENT 10.0 OPEN file_dist.frg
```

WARNINGS

This command has no action while running a simulation.

---



## FORCE\_FIELD

NAME

FORCE\_FIELD – Print force field parameters

SYNOPSIS

FORCE\_FIELD

WARNINGS

Work only in the production/simulation stage. It has no effect when reading the trajectory file.

## GOFR

NAME

GOFR – Compute solvent and/or solute pair correlation function  $g(r)$  and structure factors  $S(k)$ .

SYNOPSIS

GOFR

...

...

END

## DESCRIPTION

The command **GOFR** opens an environment which includes a series of subcommands to define the parameters used in the calculation of the radial distribution functions.

**average** *favg*

Average the  $g(r)$ 's over length *favg* given in units of femtoseconds.

**compute** *fcomp*

Compute the  $g(r)$ 's with a frequency of *fcomp* femtoseconds.

**cutoff** *fcut*

Cut the calculation of the  $g(r)$ 's at distance equal to *fcut* Å.

**delta** *delrg*

Set the bin size of the  $g(r)$ 's to *delrg* Å.

**intra**

Include intramolecular contacts in solvent-solvent  $g(r)$ 's.

**print** *fconf* OPEN *filename*

$g(r)$ 's are printed to the file *filename* every *fconf* fs.

**use\_neighbor**

Use the neighbor list to compute the  $g(r)$ 's.

Radial distribution function can be computed on the fly.

## EXAMPLES

GOFR

```
print 1000.0 OPEN test.gofr
```

```
use_neighbor
```

```
average 1000.0
```

```
compute 10.0
```

```
cutoff 12.0
```

```
delta 0.02
```

END

## WARNINGS

When the the subcommand `use_neighbor` is used `cutoff` cannot exceed the neighbor lists cutoffs.

## HBONDS

NAME

HBONDS – Compute solute H-bonds structural properties

## SYNOPSIS

HBONDS

...

...

END

## DESCRIPTION

The command HBONDS opens an environment which includes a series of subcommands which allow to compute hydrogen bond related properties. The hydrogen bond donor-acceptor pairs *must* be defined in the topological file. (see section 10.3). If these definition where not included when generating the trajectory file, and if READ\_TPGPRM is specified in the &PARAMETERS environment, HBONDS produces no output. These definitions may be provided at analysis time by the READ\_TPG (&PARAMETERS) directive. In the following we indicate with the letters *A* and *D* the donor and acceptor pair.

`angular_cutoff` *cutoff1* [*cutoff2*]

defines two angular cutoffs (in degrees) for  $A...H - D$  and  $A - D...H$ , respectively. If only one argument is specified, the two cutoff are equal.

`histogram` *fbin*

define the bin size (in Å) for hydrogen bonds histograms.

`print` *nprint* OPEN *filename*

print hydrogen bond output to file *filename* every *nprint* configurations. The output format depends on READ\_PDB (&SETUP) directive. If this directive is specified the output contains details concerning atomic types, hydrogen bond distances and angles.

`print_histo` *nprint* OPEN *filename*

print hydrogen histogram to file *filename* every *nprint* configurations

`radial_cutoff` *cutoff*

define the radial cutoff (in Å) for the hydrogen bond.

`residue`

printout hydrogen bonds per residues.

`total`

printout the total number of hydrogen bonds (the default)

`use_neighbor` *nconf* *rcut*

compute neighbor list for hydrogen bonds. *nconf* defines how frequently the neighbor list must be computed; *rcut* defines the radius of the neighbor list sphere.

## EXAMPLES

HBONDS

total

residues

radial\_cutoff 2.5

angular\_cutoff 200.0 200.0

print 10 OPEN test.hbnd

histogram 0.1

```

    use_neighbors 5 5.0
    print_histo 2 OPEN test.hst
END

```

## WARNINGS

residue and total are ineffective when READ\_PDB is also specified. Experimental - **Unsupported**

## PRINT\_DIPOLE

## NAME

PRINT\_DIPOLE – Print out dipole.

## SYNOPSIS

```
PRINT_DIPOLE    fdipole    OPEN filename
```

## DESCRIPTION

Print out the components of the *total* instantaneous dipole **M** (in debye Å ) of the basic cell each *fdipole* fs and the running average of the dielectric constant (relative permittivity).

## EXAMPLES

PRINT\_DIPOLE 10.5 OPEN dipole.out The file dipole.out looks like the following:

```

....
399115.500    0.50455E+02    -0.29885E+02    0.46023E+01    11.330
399126.000    0.48858E+02    -0.40479E+02    0.80527E+01    12.520
399136.500    0.52146E+02    -0.35302E+02    0.70597E+01    13.023
399147.000    0.57283E+02    -0.32666E+02    0.52314E+01    13.372
399157.500    0.62705E+02    -0.36044E+02    -0.76743E+01    13.913
....

```

In the first column, the current simulation time is reported. Column 2-4 contain the instantaneous values of the *x, y, z* component of the cell dipole (in Debye). In column 5 the *running average* of the dielectric constant is reported. The dielectric constant is computed under the assumption of thin-foil boundary conditions[159, 33] (i.e. no surface dipole term at the sphere boundary) using the formula  $\epsilon = 1 + 4\pi(\langle \mathbf{M}^2 \rangle - \langle \mathbf{M} \rangle^2)/(3VRT)$ [159].

## WARNINGS

Diagnostic - **Unsupported**

## STRUCTURES

## NAME

STRUCTURES – Compute the root mean square deviations from a given solute reference structure

## SYNOPSIS

## STRUCTURES

```

    ...
    ...
END

```

## DESCRIPTION

The command **STRUCTURES** opens an environment which includes a series of subcommands which allow to compute average and instantaneous root mean square displacements (rms) *of the solute* for various atomic type ( $\alpha$ -carbon, heavy atoms, backbone atoms etc. ). The reference structure for the solute is entered with the command **TEMPLATE(&SETUP)**

**averaged ca**  
compute average rms of  $\alpha$ -carbons

**averaged heavy**  
compute average rms of non hydrogen atoms

**inst\_xrms** *type\_1 type\_2 ...*  
specifies which instantaneous rms's have to computed. *type\_n* can be any combination of the four keywords **ca** **heavy** **backbone** **allatoms**. The keyword **all** stands for all the the preceding keywords simultaneously. The **inst\_xrms** keyword is mandatory when **print inst\_xrms** is specified.

**print** *type nprint* **OPEN** *filename*  
print rms's calculation as specified by *type* to file *filename* every *nprint* configurations (see also command **DUMP(&INOUT)**) The keyword *type* can be any of the following:

- averaged** - the full protein (solute) coordinates in pdb format are printed to the file *filename* with a constant orientation so that atomic rms's are minimized. Feeding directly the file to **rasmol** gives an pictorial view of the atomic displacements
- avg\_xrms** - The time running averages of the rms's are printed, averaged over *alpha*-carbons, backbone atoms, and all heavy atoms.
- inst\_xrms** - The instantaneous values of the rms's are printed averaged over *alpha*-carbons, backbone atoms, and all heavy atoms. If this subcommand is specified, along with **inst\_xrms** subcommand **orac** also produces the file *filename.atm* which contains the final values of the atomic rms's for the atom types (*alpha* carbon, backbone atoms etc. ) specified in the command **inst\_xrms**.

## EXAMPLES

### STRUCTURES

```
print averaged 2 OPEN test.str
print avg_xrms 3 OPEN test.arms
print inst_xrms 3 OPEN test.irms
inst_xrms ca backbone
averaged ca
print rms 2 OPEN test.rms
END
```

### WARNINGS

**STRUCTURES** commands works only in conjunction with the &ANALYSIS environment. Experimental - **Unsupported**

## TIME\_CORRELATIONS

### NAME

**TIME\_CORRELATIONS** – Compute velocity autocorrelation functions and root mean displacements.

### SYNOPSIS

#### TIME\_CORRELATIONS

```
...
...
END
```

### DESCRIPTION

The command **TIME\_CORRELATIONS** opens an environment which includes a series of subcommands to define the parameters used in the calculation.

```
diffusion    OPEN    filename
compute the mean square displacements  $|r(t) - r(0)|^2$ 

divide_step  nspline
provide a number equal to nspline of interpolated points between data points.

vacf         OPEN    filename
Compute velocity autocorrelation functions and print out results to file filename
```

## EXAMPLES

## TIME\_CORRELATIONS

```
vacf OPEN vacf.test2
divide_step 2
diffusion OPEN diff.test2
END
```

## WARNINGS

When the the subcommand `use_neighbor` is used `cutoff` cannot exceed the neighbor lists cutoffs.  
 Experimental - **Unsupported**

## VORONOI

## NAME

VORONOI – Compute the Voronoi polihedra of atoms, residues and molecules

## SYNOPSIS

## VORONOI

```
...
...
END
```

## DESCRIPTION

The command VORONOI opens an environment which includes a series of subcommands which allow to compute average and instantaneous properties related to the Voronoi polihedra of the solute and of the solvent.

**compute accessibility**

Compute the area of the Voronoi polihedron for all residues of the solute (computed as the sum of the voronoi volumes of the individual atoms) and evaluate for each residue the fraction of the surface that is accessible to the solvent (solute and solvent as defined in the command JOIN(&PARAMETERS))

**compute contact\_solute** *int1 int2*

Compute the contact surface among selected solute residues with residue number *int1* and *int2* as in the the PDB file.

**compute neighbors**

Compute the Voronoi coordination number relative to the whole solute-solute, solvent-solvent and solute-solvent contacts.

**compute volume**

Compute the Voronoi volumes of all residues in the solute.

**cutoff** *value*

*values* the cutoff (Å) for

**heavy\_atoms**

Use only non hydrogen atoms for evaluating Voronoi polihedra

```
print nprint OPEN filename
Print all output as to file filename every nprint configurations
```

## EXAMPLES

## VORONOI

```
print 5 OPEN 6.vor
cutoff 8.0
heavy_atoms
compute contact_solute 1 2
compute contact_solute 5 6
compute volume
compute neighbors
compute accessibility
END
```

In this example we compute the voronoi volumes, areas and accessibility and neighbors for the residues of a proteins every 5 configurations. Also the contact surfaces between residues 1 and 2 and residue 5 and 6 are evaluated. All output are printed to the file 6.vor.

## WARNINGS

VORONOI commands works only in conjunction with the &ANALYSIS environment. Experimental - **Unsupported**

## WRITE\_GYR

## NAME

WRITE\_GYR – Print gyration radius.

## SYNOPSIS

```
WRITE_GYR ngyr OPEN filename
```

## EXAMPLES

```
WRITE_GYR 10.0 OPEN test.gyr
```

## WARNINGS

Work only at single time step. Experimental - **Unsupported**

---

### 10.2.8 &REM

Define run time parameters concerning Replica Exchange Simulation. Work only with the parallel version (see Chapter 11), i.e. this namelist is not recognized when the serial program is compiled. The following commands are allowed:

BATTERIES, PRINT, PRINT\_DIAGNOSTIC, PRINT\_ENERGY, SEGMENT, SETUP, STEP

---

#### BATTERIES

NAME

BATTERIES – produces simulation multiplets

SYNOPSIS

BATTERIES *nbatt*

DESCRIPTION

Produces *nbatt* independent simulations of the same generalized ensemble system. This option can be used to augment the statistics of a REM simulation. In case of multiple REM simulations, the option BATTERIES expand the total number of MPI instances to  $nbatt \times nreplicas$ . The number of replicas in each independent simulation processes is given by the integer  $NPROC/nbatt$  where NPROC is specified in the `mpirun` command.

EXAMPLES

– Example 1.

```
&REM
..
SETUP      1.0          0.3          0.3          1
BATTERIES 32
...
&END
```

When this input is launched on, e.g. exactly 320 MPI instances, 32 independent H-REM simulations are produced, each scaling torsional and non bonded potential from 1.0 (target state) to 0.3 (hottest state).

– Example 2.

```
&REM
..
SETUP      1.0          1.0          1.0          1
BATTERIES 32
...
&END
```

When this input is launched on exactly 32 MPI instances, 32 independent standard simulations are produced.

DEFAULTS

`nbatt=1`

---

## PRINT

NAME

PRINT – print out info on REM.

SYNOPSIS

PRINT *iprint*

DESCRIPTION

Controls intermediate printing of the acceptance ratio between adjacent replicas.

EXAMPLES

PRINT 1000

Print info on the current acceptance ratios every 1000 fs.

DEFAULTS

No info is printed.

## PRINT\_DIAGNOSTIC

NAME

PRINT\_DIAGNOSTIC – print out info on REM.

SYNOPSIS

PRINT\_DIAGNOSTIC *fprint*

DESCRIPTION

Controls the frequency of intermediate printings for diagnostic data in the file REM\_DIAGNOSTIC.

EXAMPLES

PRINT\_DIAGNOSTIC 1000.0

Print info on the current acceptance ratios every 1000.0 fs.

DEFAULTS

Printed at every outermost time step.

## PRINT\_ENERGY

NAME

PRINT\_ENERGY – print out (unscaled) energies terms

SYNOPSIS

PRINT\_ENERGY *fplot* OPEN *filename*

DESCRIPTION

Controls intermediate printing of the unscaled energy terms: (1) stretching+bending+improper torsions, (2) proper torsions+1-4, (3) real space electrostatic+lennard-jones. The energy terms are appended to the history file *filename*, along with the time step and the replica index. The dumping frequency, in fs, is *fplot*.

EXAMPLES

PRINT 60.0 OPEN test.ene

Print energies to the file file test.ene every 60 fs.

DEFAULTS

No info is printed.



## SEGMENT

## NAME

SEGMENT – Define the “solute” in solute tempering simulations.

## SYNOPSIS

```
SEGMENT
```

```
....
```

```
END
```

## DESCRIPTION

This structured command is used to define the “solute” in the a solute/tempering REM simulation and to assign the scaling factors for the Hamiltonian REM simulation (see Sec. 5.2) to the intrasolute, solute-solvent and solvent-solvent interactions. The following subcommands may be specified within SEGMENT:

```
define, kind
```

- **define**      *n1*      *n2*

The **define** command is used to crop a piece of solute for Hamiltonian scaling in a REMD simulation. One can use up to a maximum of 10 *define* commands, cropping 10 disconnected (non overlapping) part of the solute. *n1* and *n2* are the atom indices of the selected solute parts, The numeric order of the atoms is that specified in the topology file (see Sec. 10.3).

- **kind**      *inter\_type*

Once the “solute” has been defined using the **define** subcommand, the subcommand **kind** is used to scale the solute-solute, solute-solvent interactions. Possible choices for the string *inter\_type* are **intra** and **inter**. **intra** means that the non-bonded energy scaling (see **SETUP** command ) is applied to the *intrasolute* non-bonded interactions only, i.e. solute-solvent interactions are not scaled where by “solvent” we mean the actual solvent and the solute atoms which were not selected using the **define** subcommand. *inter* scales only solute-non solute (i.e. solvent) non bonded interactions. Intrasolute interactions are NOT scaled if **inter** is specified. If the subcommand **kind** is not specified, the ORAC assumes that *both* solute-solvent and solute-solute interactions are scaled.

## EXAMPLES

```
SEGMENT
```

```
define 1 10
```

```
define 1300 1325
```

```
kind inter
```

```
END
```

## SETUP

## NAME

SETUP – Define the scaling in a REM simulation.

## SYNOPSIS

```
SETUP scale1 [scale2 scale3] irest
```

## DESCRIPTION

The **SETUP** command is used to define the lowest scaling factor(s) (i.e the highest temperature) of the last replica. The number of replicas in the REMD simulations are equal to the number of processors passed to the MPI routines (nprocs). The spacing bewteen the replicas is controlled by the *irest* integer. If only the *scale*<sub>1</sub> real parameter is specified, an equal scaling is applied to all parts of the potential. If the three parameters *scale*<sub>1</sub>, *scale*<sub>2</sub>, *scale*<sub>3</sub> are specified, then *scale*<sub>1</sub> refers to the bending, stretching and improper torsional potential, *scale*<sub>2</sub> to the (proper) torsional potential and

to the 14 non-bonded interactions and finally  $scale_3$  refers to the non bonded potential. NB: when the Ewald summation is used together with the command `SEGMENT(&REM)`,  $scale_3$  scales only the *direct* (short-ranged) part of the electrostatic interactions and the (long-ranged) reciprocal part has a scaling factor of 1.0 (i.e. these interaction are not scaled). If  $irest=0$ , the run is restarted from a previous one. This implies that the directories PARXXXX are present and are equal in number to  $nprocs$  as specified in the `mpiexec/mpiexec` command.

If  $irest \neq 0$  then the run refers to a cold start from scratch and

- if  $irest=1$ , then the scaling factors of the intermediate replicas are derived according to a geometric progression, namely  $scale_i(m) = scale_i^{m/(nprocs-1)}$ , where  $scale_i(m)$  is the scaling factor for the potential  $i$  of the replica  $m$  with  $0 \leq m \leq nprocs-1$ . For example, if  $scale_i = 0.6$  and  $nprocs=4$ , then replica  $m=0$  has  $scale_i(0) = 1$ , replica  $m=1$  has  $scale_i(1) = 0.843433$ , replica  $m=2$  has  $scale_i(2) = 0.711379$  and the replica  $m=3$  has  $scale_i(3) = scale_i = 0.6$ .
- if  $irest=2$ , the scaling factors are read from an auxiliary file called “REM.set” that must be present in the directory from which the program is launched using the `mpiexec/mpiexec` command. This ASCII file has as many lines as parallel processes and on each line the three (or one) scale factors must be specified.

#### EXAMPLES

SETUP 1.0 1.0 0.6 1

Scales only the non bonded potential (direct part) using a geometric progression.

#### DEFAULTS

SETUP 1.0 1.0 1.0 1

#### STEP

##### NAME

STEP – exchange time for REM

##### SYNOPSIS

STEP *rtime*

##### DESCRIPTION

Define the time (in fs) for attempting an exchange between adjacent replicas.

##### EXAMPLES

STEP 5.0

Attempt replica exchanges every 5 fs.

##### DEFAULTS

STEP 0

##### WARNINGS

If STEP is not set, *rtime* is set to the time step of the  $m$ -th intermolceular shell,

---

### 10.2.9 &RUN

Define run time parameters which concern output printing and run averages. The following commands are allowed:

CONTROL, DEBUG, OPTION, MAXRUN, PRINT, PROPERTY, REJECT, STEER, TIME

---

#### CONTROL

##### NAME

CONTROL – Indicate initial conditions

##### SYNOPSIS

CONTROL *icontrol*

##### DESCRIPTION

ORAC can run simulations or minimization reading the system initial momenta and/or coordinates from different sources. If the integer argument *icontrol* is zero, the simulation run must commence from coordinates either stored entirely in a PDB file or generated by ORAC itself from some initial configuration (see CELL or SPACE\_GROUP in &SETUP). CONTROL 0 implies that all system momenta are initialized from the Boltzmann distribution at the wanted temperature. When CONTROL 2, the run is started from the restart file defined by the command SAVE or RESTART in &INOUT. With CONTROL 2 all system averages are zeroed. The same action is taken if CONTROL 1, but the averages are **not** initialized to zero.

##### EXAMPLES

CONTROL 2

Run a simulation from a restart file and set all averages to zero.

##### DEFAULTS

CONTROL 0

##### WARNINGS

When restarting a run with a different integration scheme from the one used in the restart file, CONTROL should be set to 2. If not, unpredictable behavior may occur.

---

#### DEBUG

##### NAME

DEBUG – Print debug information

##### SYNOPSIS

DEBUG **all**

DEBUG *debug-type*

##### DESCRIPTION

Print various arrays to the standard output for debugging. Information regarding the solute topology and force field is written only if the solute topology and parameter list is actually computed and **not** read from a binary file (i.e. READ\_TPGPRM\_BIN in &PARAMETERS must be inactive). The *debug-type* string can be

**residue\_sequence**

The residue sequence is printed.

**bond\_table**

Details about bonds and corresponding stretching parameters are printed.

**bend\_table**

Details about bending and corresponding parameters are printed.

**ptors\_table**

Details about proper torsions and corresponding parameters are printed.

**pitors\_table**

Details about improper torsions and corresponding parameters are printed.

**EXAMPLES**

**DEBUG all**

print out all tables.

**DEBUG bond\_table**

**DEBUG bend\_table**

**DEBUG residue\_sequence**

print out the bond and bending table and the residue sequence.

**MAXRUN****NAME**

**MAXRUN** – Provide the maximum simulation length (in fs)

**SYNOPSIS**

**MAXRUN** *fmaxrun*

**DESCRIPTION**

This command controls the total length of the direct access file. The number of records initialized by the **DUMP(&INOUT)** command is given by  $nrec = fmaxrun * natoms / atom\_rec$  where *natoms* and *atom\_rec* are the total number of atoms in the system and the atoms per record, respectively. *fmaxrun* cannot be less than *ftime* (see command **TIME** in this environment).

**EXAMPLES**

**MAXRUN 500000.0**

**PRINT****NAME**

**PRINT** – Print instantaneous results

**SYNOPSIS**

**PRINT** *fprint*

**DESCRIPTION**

ORAC writes the instantaneous energies of the system to standard output. The real argument *fprint* indicates the chosen printing frequency in fs.

**EXAMPLES**

**PRINT 5.0**

## PROPERTY

## NAME

PROPERTY – Print averages with a given frequency

## SYNOPSIS

PROPERTY *fprop*

## DESCRIPTION

ORAC writes to the standard output the running averages of the current run. The real argument *fprop* is the frequency of printing in femtoseconds.

## EXAMPLES

PROPERTY 500.0

Write averages every 500.0 fs.

## WARNINGS

- An error condition will occur if this command is not included in the input to ORAC or if the argument, *fprop* is zero.
- The command is not active only in the rejection phase (see command REJECT).

## REJECT

## NAME

REJECT – Provide the length of the rejection phase

## SYNOPSIS

REJECT *freject*

## DESCRIPTION

During the equilibration or rejection phase only instantaneous results are printed, while averages are discarded. The real argument *freject* indicates the time lag, in femtoseconds, of the rejection phase.

## EXAMPLES

REJECT 1000.0

Does not accumulate averages during the initial 1000.0 fs of the run.

## WARNINGS

This command is inactive during a minimization run (see command MDRUN in &SIMULATION).

## STEER

## NAME

STEER – Provide the starting and final time (in fs) for a steered molecular dynamics. The time dependent harmonic potential is defined in the namelist &POTENTIAL using the command ADD\_STR\_BONDS, ADD\_STR\_BENDS, ADD\_STR\_TORS.

## SYNOPSIS

STEER *tiniz* *tfinal*

STEER **temperature** *temp0* *tempt* *tiniz* *tfinal*

## DESCRIPTION

Steer the system with the time dependent mechanical potential defined in the namelist &POTENTIAL, starting the SMD at time *tiniz* and ending at time *tfinal*. This command can also be used to gradually change the temperature in conjunction with the command PLOT STEER\_TEMPERATURE(&INOUT) where

the adimensional thermal work done on the thermostat is printed at regular time intervals (see the PLOT (&INOUT) command). Steered molecular dynamics can be automatically restarted. In order to do this, one sets once for all the steering time ( *t<sub>final</sub>*) to the desired value, updating, at each restart, *only* the simulation time given by the TIME(&RUN) directive.

## EXAMPLES

```
&RUN
...
STEER 1000.0 10000.0
..
&END
&INOUT
..
PLOT STEER_ANALYTIC 100.0 OPEN WRK.out
..
&END
```

Start to apply the time dependent potential (see Eq. 8.13) at 1 ps and switch it off at 11 ps. Print out the accumulated work every 100 fs to the file WRK.out. The accumulated work is calculated according to Eq. 8.16.

```
&RUN
...
STEER temperature 300. 1500. 1000.0 11000.0
..
&END
&INOUT
..
PLOT STEER_TEMPERATURE 100.0 OPEN WRKTEMP.out
..
&END
```

rise the temperature from 300 to 1500 K starting at 1 ps and ending at 11 ps, with the constant speed of 120 K /ps. The thermal work is printed every 100 fs to the file WRKTEMP.out.

```
&RUN
CONTROL 1
STEER 0.0 18000.0
TIME 10000.0
..
&END
&INOUT
..
PLOT STEER_ANALYTIC 100.0 OPEN WRK.out
..
&END
..
&INOUT
  RESTART
    read file.rst
    write 30.0 OPEN new.rst
  END
&END
```

In this example, the simulation starts from the restart file `file.rst` and goes from the time found in that file to 10000.0 fs. The total steering time is 18000.0 fs. In the next restarted run the configuration of the system at  $t = 10000$  fs is found in the file `new.rst`. The next restarted simulation could be thus of the kind:

```
&RUN
  CONTROL 1
  STEER  0.0 18000.0
  TIME 18000.0
  ..
&END
&INOUT
  ..
  PLOT STEER_ANALYTIC 100.0 OPEN WRK_10000_18000.out
  ..
&END
  ..
&INOUT
  RESTART
    read new.rst
  END
&END
```

In this example, the steering is complete and in the output file `WRK_10000_18000.out`, the work is calculated from  $t = 10000$  fs to  $t = 18000$  fs.

---

## TIME

### NAME

TIME – Length of the simulation not including the rejection phase

### SYNOPSIS

TIME *f<sub>time</sub>*

### DESCRIPTION

This command gives the length of the acquisition run which is to be carried out after the rejection (equilibration) phase. The unit of its real argument *f<sub>time</sub>* is femtoseconds. During the acquisition run averages are accumulated.

### EXAMPLES

TIME 100000.0

---

---

### 10.2.10 &SETUP

The environment &SETUP includes commands concerned with the simulation box setup. In this environment, the simulation cell parameters, dimensions and symmetry can be initialized. Moreover, files containing the system coordinates in appropriate format can be provided. The following commands are incorporated in &SETUP:

CRYSTAL, READ\_PDB, RECONSTRUCT, REPLICATE, TEMPLATE

---

#### CHANGE\_CELL

##### NAME

CHANGE\_CELL – Recomputes the atomic coordinates according to input.

##### SYNOPSIS

CHANGE\_CELL

##### DESCRIPTION

This command has an effect only when the run is restarted (see commands RESTART(&INOUT) and CONTROL(&RUN)). This command must be specified, in case one wishes to change the MD cell parameters, with respect to those dumped in the available restart file, to those specified in the CRYSTAL directive in this environment. If CHANGE\_CELL is not specified and the run is restarted, the CRYSTAL directive is ignored and the cell parameters are taken from the last configuration of the restart file. If CONTROL 0 is entered in the environment &RUN, this command has no effect.

##### EXAMPLES

CHANGE\_CELL

---

#### CRYSTAL

##### NAME

CRYSTAL – Read the cell parameters defining the shape of the simulation box

##### SYNOPSIS

CRYSTAL  $a$   $[b \quad c \quad [\alpha \quad \beta \quad \gamma]]$

##### DESCRIPTION

The arguments  $\alpha$ ,  $\beta$  and  $\gamma$  to this command are defined using the usual crystallographic conventions:  $\alpha$  is the angle between the  $b$  and  $c$  axis,  $\beta$  is the angle between  $a$  and  $c$ , and  $\gamma$  is the angle between  $a$  and  $b$ .

##### EXAMPLES

CRYSTAL 12.3 14.5 12.3 90.0 95.0 90.0

CRYSTAL 15.0

##### DEFAULTS

$\alpha = \beta = \gamma = 90.0$

---



## READ\_PDB

## NAME

READ\_PDB – Read input system coordinates from a PDB file

## SYNOPSIS

READ\_PDB *filename*

## DESCRIPTION

This command indicates the name of a file in the protein data bank format which contains the solute and/or solvent coordinates. The name of this file, *filename*, must be provided. The coordinates of the solvent molecules, if present, must follow those of the solute in the PDB file. The atom labels for solute and/or solvent must correspond with those defined in the topology file (see description in Sec. 10.3). The order of the atoms, within a solute residue or a solvent molecule, specified in the PDB file is unimportant (the “ORAC order” corresponds to that specified in the topology file). If the system contains hydrogens, the PDB file ought not to include the hydrogens coordinates. If hydrogens atoms are not present in the PDB file, but they are included in the topological specification of residue or solvent, their coordinates are generated by ORAC according to geometry considerations.

## EXAMPLES

READ\_PDB test.pdb

## WARNINGS

This command has no action if CONTROL in &RUN is different from zero, i.e. if the system coordinates are read from a restart file (see RESTART in &INOUT).

## REPLICATE

## NAME

REPLICATE – Replicate the unit cell generated by SPACE\_GROUP(&SOLUTE)

## SYNOPSIS

REPLICATE *icl icm icn*

## DESCRIPTION

The integer arguments *icl*, *icm*, *icn* indicate how many times along the three axis the unit cell must be replicated. The cell parameters of the replicated structure are input to the command CRYSTAL.

## EXAMPLES

REPLICATE 4 4 5

Replicate the unit cell 4, 4 and 5 times along the *a*, *b* and *c* crystal axis, respectively.

## WARNINGS

This command has no action if CONTROL in &RUN is different from zero, i.e. if the system coordinates are read from a restart file (see RESTART in &INOUT).

## RESET\_CM

## NAME

RESET\_CM – Reset to zero the position of the center of mass of the solute atoms.

## SYNOPSIS

RESET\_CM

## DESCRIPTION

This command is active only if the solute coordinates are read from a PDB file. Before the run starts RESET\_CM set the center of mass of the solute to zero.

## READ\_CO

## NAME

READ\_CO – Read Crystal to Orthogonal (CO) matrix.

## SYNOPSIS

```

READ_CO
  ax  bx  cx
  ax  by  cy
  ax  by  cz
END

```

## DESCRIPTION

This command is active only the simulation is restarted and overwrites the CO matrix retrieved from the restart file.

## SOLUTE

## NAME

SOLUTE – assume solute

## SYNOPSIS

SOLUTE [ON] SOLUTE [OFF]

## DESCRIPTION

This command is active only if the solute coordinates are read from a PDB file. If ON is specified, ORAC assumes that a solute is present and its coordinates are read in from the file PDB specified by the directive READ\_PDB in this environment. When SOLUTE [ON] is specified, the namelist &SOLUTE may be omitted. When SOLUTE OFF is specified, the namelist &SOLUTE *must* be omitted.

## EXAMPLES

```

&SETUP
  READ_PDB solute.pdb
  SOLUTE ON
&END

```

A solute is present and the coordinates are read in from the file PDB. The “residue” sequence found in the PDB must match that given in the JOIN SOLUTE (&PARAMETERS) directive. If the environment &SOLUTE is entered, solute is assumed anyway, this command has no effect.

## SOLVENT

## NAME

SOLVENT – Reset to zero the position of the center of mass of the solvent atoms.

## SYNOPSIS

SOLVENT [ON] SOLVENT [OFF]

## DESCRIPTION

If ON is specified, ORAC assumes that a solvent is present and its coordinates are read in from the file PDB specified by the directive READ\_PDB in this environment. This command is not mandatory as, if the solvent is present the environment &SOLVENT (which has the same effect of SOLVENT [ON]) must be entered anyway in order to specify how to generate the solvent or the number of solvent molecules in the PDB file. When SOLVENT OFF is specified, the namelist &SOLVENT *must* be omitted.

## EXAMPLES

```

&SETUP
  READ_PDB solvent.pdb
  SOLVENT ON
&END
...
&SOLVENT
  ADD_UNITS 432
&END
...
&PARAMETERS
  ...
  JOIN SOLVENT
    hoh
  END
&END
...

```

A solvent (432 molecules) is present and the coordinates are read in from the file PDB. The “residue” sequence for the solvent found in the PDB must match that given in the JOIN SOLVENT (&PARAMETERS) directive. If a solute is also present and its coordinates are given in the PDB file specified by the READ\_PDB command, then the coordinates of the solvent molecules *must* follow those of the solute in the PDB file. An example is the following

```

&SETUP
  READ_PDB solute+solvent.pdb
  SOLVENT ON
  SOLUTE ON
&END
...
&SOLVENT
  ADD_UNITS 432
&END
...
&PARAMETERS
  ...
  JOIN SOLVENT
    hoh
  END
  JOIN SOLUTE
    ala-h ala ala ala-o
  END
&END
...

```

---

 TEMPLATE

NAME

TEMPLATE – Define a template or reference structure

SYNOPSIS

TEMPLATE *filename*

#### DESCRIPTION

This command defines a template PDB file *filename* which contains reference solute coordinates used during run time analysis for computing root mean square displacements (see command **X\_RMS** in **&PROPERTIES** for instance).

#### EXAMPLES

TEMPLATE test\_template.pdb

---

---

### 10.2.11 &SGE

Define run time parameters concerning Serial Generalized Ensemble simulations (see Chapter 6). It works with both serial and parallel versions of the ORAC program (see Chapter 11). When reporting SGE simulations obtained by BAR-SGE method, please cite Ref. [56].

#### OUTPUT FILES:

**SGE\_DF** – In the serial version of ORAC, this file is written in the working directory. In the parallel version it is written in the PAR0001 directory. The file reports the average dimensionless free energy differences between ensembles (see Eq. 6.28) along with the errors calculated by Eq. 6.29 (see top of the file). The file is updated in time intervals defined by the parameter  $L_b$  of the command **STEP** (see below).

**SGE\_ENERGY** – In the serial version of ORAC, this file is written in the working directory. In the parallel version it is written in the PARXXXX directories. The file reports the energies of the system (see top of the file) including the ensemble index corresponding to the current replica (*e.g.* the number  $n$  if the current ensemble of the replica is  $\Lambda_n$ ). The file is updated in time intervals defined by the parameter  $L_c$  of the command **STEP** (see below).

**SGE\_HISTOG** – In the serial version of ORAC, this file is written in the working directory. In the parallel version it is written in the PAR0001 directory. The file reports a histogram related to the (replica) population of the various ensembles. The file is updated in time intervals defined by the parameter  $L_b$  of the command **STEP** (see below).

The following commands are allowed in the &SGE environment:

```
FIX_FREE_ENERGY, PRINT_ACCEPTANCE_RATIO, PRINT_WHAM, SEGMENT, SETUP, STEP,
TRANSITION_SCHEME, ZERO_FREE_ENERGY
```

---

#### FIX\_FREE\_ENERGY

##### NAME

**FIX\_FREE\_ENERGY** – Set up input for performing a SGE simulation with fixed weight factors.

##### SYNOPSIS

**FIX\_FREE\_ENERGY** OPEN *PATH/filename*

##### DESCRIPTION

The presence of this command in the input establishes that user-defined weight factors (the  $\Delta g_{n \rightarrow m} = g_m - g_n$  difference factors in Eq. 6.8) instead of self-updating free energy differences (the  $\Delta f_{n \rightarrow m} = f_m - f_n$  free energy difference in Eq. 6.22) must be used in the SGE simulation. Such factors are kept constant during the simulation run. They are defined in the file named *filename*. The absolute path (*PATH*) must be specified to localize *filename*. If one needs to use the relative path in a many-replica SGE simulation (parallel run) then the working directories of the replicas must be considered the PARXXXX ones. The weight factors  $\Delta g_{n \rightarrow m} = g_m - g_n$  are dimensionless and, in *filename*, must be reported one per line, from  $g_{2 \rightarrow 1}$  to  $g_{nstates \rightarrow nstates-1}$ .

##### EXAMPLES

**FIX\_FREE\_ENERGY** OPEN ../weight\_factors.dat

A SGE simulation is performed with fixed weight factors read from file ../weight\_factors.dat.

##### DEFAULTS

The absence of the **FIX\_FREE\_ENERGY** command in the input implies the use of the BAR-SGE method (see Section 6.3.2) to update the weight factors during the simulation.

---

**PRINT\_ACCEPTANCE\_RATIO****NAME**

**PRINT\_ACCEPTANCE\_RATIO** – Print out the acceptance ratio of the SGE simulation.

**SYNOPSIS**

**PRINT\_ACCEPTANCE\_RATIO** *iprint*

**DESCRIPTION**

Print the acceptance ratio between adjacent ensembles of the SGE simulation every *iprint* fs. The ratio is printed in the standard output.

**EXAMPLES**

**PRINT\_ACCEPTANCE\_RATIO** 1000.

Print the acceptance ratios every 1000 fs.

**DEFAULTS**

The acceptance ratio is printed with a frequency corresponding to that of free energy updating (see  $L_b$  in command **STEP**).

**PRINT\_WHAM****NAME**

**PRINT\_WHAM** – Print out data needed for reweighting the configurations of all ensembles on a target state.

**SYNOPSIS**

**PRINT\_WHAM** *freq\_print*

**DESCRIPTION**

Save data necessary for reweighting by “weighted histogram analysis method” [107] (WHAM) every *freq\_print* fs in the file **SGE\_WHAM**. In the serial version of ORAC, this file is written in the working directory. In the parallel version it is written in the **PARXXXX** directories. If a Hamiltonian SGE simulation is performed, then the file reports the 3 unscaled potential energy terms ( $\mathbf{v}(x)$  vector of Eq. 6.15) that are subject to scaling (see command **SETUP** above). In a SGE simulation in the space of collective coordinates, instead of  $\mathbf{v}(x)$ , the file reports the index of (bond, bending, torsion) coordinate, the equilibrium value corresponding to the current ensemble ( $\lambda_n$  in Eq. 6.16) and the current value of the coordinate ( $r$  in Eq. 6.16).

**EXAMPLES**

**PRINT\_WHAM** 1000

Print data every 1000 fs.

**DEFAULTS**

No data are printed.

**SEGMENT****NAME**

**SEGMENT** – Define the “solute” in Hamiltonian SGE simulations.

**SYNOPSIS**

**SEGMENT**

....

**END**

## DESCRIPTION

This structured command is used to define the “solute” in a Hamiltonian SGE simulation and to assign the scaling factors to the intrasolute, solute-solvent and solvent-solvent interactions. The following subcommands may be specified within **SEGMENT**:

**define, kind**

- **define** *n1 n2*

The **define** command is used to crop a piece of solute for Hamiltonian scaling in a SGE simulation. One can use up to a maximum of 10 *define* commands, cropping 10 disconnected (non overlapping) part of the solute. *n1* and *n2* are the atom indices of the selected solute parts. The numeric order of the atoms is that specified in the topology file (see Section 10.3).

- **kind** *inter\_type*

Once the “solute” has been defined using the **define** subcommand, the subcommand **kind** is used to scale the solute-solute, solute-solvent interactions. Possible choices for the string *inter\_type* are **intra** and **inter**. **intra** means that the non-bonded energy scaling (see **SETUP** command) is applied to the *intrasolute* non-bonded interactions only, i.e. solute-solvent interactions are not scaled, where by “solvent” we mean the actual solvent and the solute atoms which were not selected using the **define** subcommand. **inter** scales only solute-non solute (i.e. solvent) non bonded interactions. Intrasolute interactions are NOT scaled if **inter** is specified. If the subcommand **kind** is not specified, the **ORAC** assumes that *both* solute-solvent and solute-solute interactions are scaled.

## EXAMPLES

**SEGMENT**

**define** 1 10

**define** 1300 1325

**kind** *inter*

**END**

## SETUP

## NAME

**SETUP** – This is the basic command to decide which kind of simulation, *Hamiltonian SGE simulation* or *SGE simulation in the space of collective coordinates*, one wants to carry out. This command also defines the number of ensembles, the scaling options and the restart option.

## SYNOPSIS

**SETUP** *nstates* [*scale<sub>1</sub> scale<sub>2</sub> scale<sub>3</sub>*] *irest*

## DESCRIPTION

*Hamiltonian SGE simulations.*

If the parameters *scale<sub>1</sub>*, *scale<sub>2</sub>* and *scale<sub>3</sub>* (real numbers) are specified in the **SETUP** command, then a Hamiltonian SGE simulation with total or partial scaling of the potential energy is performed (simulated-tempering and solute-tempering like simulations, respectively). In such a case the **SETUP** command is used to define the number of ensembles (*nstates*; integer number) and the lowest scaling factor (i.e the highest temperature) of the last ensemble. The number of replicas in the SGE simulations is equal to the number of processors passed to the MPI routines (*nprocs*). At variance with REM, *nprocs* may be not equal to *nstates*. The restart option of a SGE simulation is controlled by *irest* (integer number). The three parameters, *scale<sub>1</sub>*, *scale<sub>2</sub>* and *scale<sub>3</sub>*, can be different and refer to scaling features of different parts of the potential energy. *scale<sub>1</sub>* refers to the bending, stretching and improper torsional potentials, *scale<sub>2</sub>* to the (proper) torsional potential and to the 1-4 non-bonded interactions and *scale<sub>3</sub>* refers to the non bonded potential. IMPORTANT NOTE: when the Ewald summation is used together with the command **SEGMENT(&SGE)**, *scale<sub>3</sub>* scales only the

*direct* (short-ranged) part of the electrostatic interactions and the (long-ranged) reciprocal part has a scaling factor of 1 (i.e. these interactions are not scaled). If  $scale_1 = scale_2 = scale_3$ , then an equal scaling is applied to all parts of the potential (it corresponds to a simulated tempering simulation). If  $irest = 0$ , the run is restarted from a previous one. This implies that the directories PARXXXX are present and are equal in number to  $nprocs$ , i.e. the number of replicas. If  $irest \neq 0$  then the run refers to a cold start from scratch and

- $irest = 1$ : the scaling factors associated with the intermediate ensembles are derived according to a geometric progression, namely  $scale_i(m) = scale_i^{(m-1)/(nstates-1)}$ , where  $scale_i(m)$  is the scaling factor for the potential  $i$  of the ensemble  $m$  with  $1 \leq m \leq nstates$ . For example, if  $scale_i = 0.6$  and  $nstates = 4$ , then  $scale_i(1) = 1$ ,  $scale_i(2) = 0.843433$ ,  $scale_i(3) = 0.711379$  and  $scale_i(4) = scale_i = 0.6$ . The  $nprocs$  replicas are initially distributed as described in Section 6.3.2 (note: we assume  $\Lambda_1$  to correspond to  $m = 1$ , i.e., to the unscaled ensemble).
- $irest = 2$ : the scaling factors are read from an auxiliary file called “SGE.set” that must be present in the directory from which the program is launched using the `mpiexec/mpirun` command. This ASCII file has two comment lines on the top and then as many lines as the number of ensembles ( $nstates$ ). On each line there are four numbers in the following order: (1) the number of the ensemble; (2) the scaling factor for bonding and bending potential related to that ensemble; (3) the scaling factor for torsions and 1-4 interaction potentials related to that ensemble; (4) the related scaling factor for non-bonding potential related to that ensemble.

#### SGE simulations in the space of collective coordinates.

If the parameters  $scale_1$ ,  $scale_2$  and  $scale_3$  are not specified in the `SETUP` command, then a SGE simulation in the space of collective coordinates is performed. In such a case the `SETUP` command is used to define the number of ensembles ( $nstates$ ) and the restart option ( $irest$ ). Their meaning has been explained above. The collective coordinates are defined using the `ADD_STR_BONDS` (bond coordinates), `ADD_STR_BENDS` (bending coordinates) and `ADD_STR_TORS` (torsional coordinates). These commands are defined in the `&POTENTIAL` environment and must be used in the following form

`ADD_STR_BONDS iat1 iat2  $k_s$   $r_i$   $r_f$`

`ADD_STR_BENDS iat1 iat2 iat3  $k_b$   $\alpha_i$   $\alpha_f$`

`ADD_STR_TORS iat1 iat2 iat3 iat4  $k_t$   $\theta_i$   $\theta_f$`

These expressions define the additional harmonic potential entering into Eq. 6.24. For example, if we perform a SGE simulation in the space of a distance between two atoms, then `ADD_STR_BONDS` must be used. The parameters  $iat1$  and  $iat2$  are the atom numbers,  $k_s$  corresponds to  $k$  of Eq. 6.24 and  $r_i$  and  $r_f$  define the intermediate ensembles as follows:  $\lambda_n = r_i + (n-1)(r_f - r_i)/(nstates - 1)$ , where  $\lambda_n$  is the parameter characteristic of the ensemble  $n$  with  $n = 1, 2, \dots, nstates$  (see Eq. 6.24).

#### EXAMPLES

`SETUP 5 1. 1. 0.6 1`

A Hamiltonian SGE simulation is performed. The non bonded potential (direct part) is scaled using a geometric progression, while the other potential terms are unscaled. The number of ensembles is 5.

`SETUP 4 1`

`ADD_STR_BONDS 22 143 1. 10. 14.5`

`ADD_STR_BENDS 25 33 67 2. 100. 130.`

A SGE simulation in the space of collective coordinates is performed using 4 ensembles. The collective coordinates are one bond and one bending. The bond is related to the atoms 22 and 143. The bending is defined by the atoms 25, 33 and 67. The ensembles are defined by 2 parameters,  $\Lambda_n = (\lambda_n^{bond}, \lambda_n^{bend})$ , where the bond related parameters are  $\lambda_1^{bond} = 10$ ,  $\lambda_2^{bond} = 11.5$ ,  $\lambda_3^{bond} = 13$ ,  $\lambda_4^{bond} = 14.5$  (in Å) and the bending related parameters is  $\lambda_1^{bend} = 100$ ,  $\lambda_2^{bend} = 110$ ,  $\lambda_3^{bend} = 120$ ,  $\lambda_4^{bend} = 130$  (in degrees). Therefore the transition of a replica from the ensemble  $\Lambda_n$  to the ensemble  $\Lambda_{n+1}$  involves a synchronous change of both parameters, i.e.  $\lambda_n^{bond} \rightarrow \lambda_{n+1}^{bond}$  and  $\lambda_n^{bend} \rightarrow \lambda_{n+1}^{bend}$ . Finally, the harmonic force constants (see Eq. 6.24) are 1 and 2 kcal mol<sup>-1</sup> for bond and bending, respectively.



## STEP

## NAME

STEP – Set up input information on the frequency of the ensemble transitions and on the free energy updating options.

## SYNOPSIS

STEP  $L_c$   $L_a$   $L_b$  [ $n_{av}$ ]

## DESCRIPTION

This command defines the following parameters.  $L_c$  (real number): time interval (in fs) used to attempt a transition of a replica between adjacent ensembles [see point (4) in Section 6.3.2];  $L_a$  (real number): time interval (in fs) used to store the dimensionless works  $W[n \rightarrow n+1]$  and  $W[n \rightarrow n-1]$  [see point (2) in Section 6.3.2];  $L_b$  (real number): time interval (in fs) used to try a free energy update [see point (3) in Section 6.3.2];  $n_{av}$  (integer number): number of independent free energy estimates used to update the weighted free energy averages [see Section 6.3.3]. The parameter  $n_{av}$  is optional. If  $n_{av} = 0$  or not reported in the input, then all free energy estimates stored during the run are used. IMPORTANT NOTE: it is also possible to change  $n_{av}$  “on-the-fly” during the simulation. In such a case a file called SGE\_DF\_FLY.set must be created by the user in the working directory (when using the serial version of ORAC ) or in the parent directory of PARXXXX directories (when using the parallel version of ORAC ). Such a file must contain an integer number alone, which corresponds to  $n_{av}$  (additional characters will be ignored). Note also that if this option is employed then an additional working file, called SGE\_DF\_FLY.dat, will be created by the program in the same directory. This file contains information related to the single estimates of free energy differences (do not remove it when restarting from a previous run). If the file SGE\_DF\_FLY.set is removed after a simulation and a new simulation is restarted, then this latter simulation continues as if the former simulation had been launched with the STEP command specified in the input file.

## EXAMPLES

STEP 5. 10. 2000. 40

Ensemble transitions are attempted every 5 fs; dimensionless works are stored every 10 fs; free energy updates are attempted every 2000 fs; the last 40 free energy estimates are used in the weighted free energy average of Eq. 6.28.

## DEFAULTS

The only allowed default value is related to  $n_{av}$  ( $n_{av} = 0$ ). In such a case, all free energy estimates are used in the weighted free energy average.

## WARNINGS

If STEP is not set in the input, then default values are employed. Default values are  $L_c = tstep$ ,  $L_a = tstep$ ,  $L_b = 1000 \times tstep$  and  $n_{av} = 0$ , where  $tstep$  is the simulation time step (in fs) of the  $h$ th intermolecular shell (see Section 4.3).

## TRANSITION\_SCHEME

## NAME

TRANSITION\_SCHEME – Choose scheme for replica transitions

## SYNOPSIS

TRANSITION\_SCHEME *scheme*

## DESCRIPTION

This command defines the replica transition scheme used during an SGE simulation. The allowed values of the keyword *scheme* are:

- **SEO**  
Use the so-called “Stochastic Even/Odd” (SEO) transition scheme. At each transition step the trajectory in ensemble  $n$  attempts a transition towards ensemble  $(n + 1)$  or  $(n - 1)$  with equal probability.
- **DEO**  
Use the so-called “Deterministic Even/Odd” (DEO) transition scheme. If at the  $s$ -th transition step the trajectory is in ensemble  $n$ , a transition is attempted towards ensemble  $n + (-1)^{n+s}$ ; that is, toward ensemble  $(n + 1)$  at even steps and to ensemble  $(n - 1)$  at odd steps, if  $n$  is even; the opposite if  $n$  is odd. This scheme is the same as the coupling scheme used in Replica Exchange, and is expected to give better diffusion in temperature space than SEO [114].

**EXAMPLE**

```
TRANSITION_SCHEME SEO
```

**DEFAULTS**

The default for *scheme* is DEO

**ZERO\_FREE\_ENERGY****NAME**

**ZERO\_FREE\_ENERGY** – Set up input for zeroing the accumulated free energy averages.

**SYNOPSIS**

```
ZERO_FREE_ENERGY
```

**DESCRIPTION**

The presence of this command in the input establishes that the weighted averages of the free energy differences (see Eq. 6.28) are reset, *i.e.*, the averages accumulated in a previous simulation are discarded in the new one.

**EXAMPLES**

```
ZERO_FREE_ENERGY
```

A SGE simulation is performed by resetting the averages of the free energy differences (weight factors).

**DEFAULTS**

The absence of the **ZERO\_FREE\_ENERGY** command in the input implies that the estimates of the free energy differences performed during the simulation are accumulated to those of a previous simulation.

---

### 10.2.12 &SIMULATION

The environment includes commands which define the type of simulation that is to be carried out. In particular, commands are available to run steepest descent energy minimizations, and molecular dynamics simulations in various ensembles. The environment &SIMULATION allows the following commands:

ANDERSEN, ANNEALING, BUSSI, ISEED, ISOSTRESS, ISOSTRESSXY, MINIMIZE, MDSIM, SCALE,  
STRESS, TEMPERATURE, WRITE\_PRESSURE

---

#### ANDERSEN

##### NAME

ANDERSEN – The simulation is performed in the NVT Ensemble using the stochastic collision method by Andersen.

##### SYNOPSIS

ANDERSEN *time*

##### DESCRIPTION

Implement Andersen thermostat with a period for random collision of *time* femtoseconds.

##### EXAMPLES

ANDERSEN 1000.0

##### WARNINGS

Diagnostic - **Unsupported**

---

#### ANNEALING

##### NAME

ANNEALING – Velocities are multiplied by factor to speed up

##### SYNOPSIS

ANNEALING *scale\_factor*

##### DESCRIPTION

Velocities are multiplied by *scale\_factor*.

##### EXAMPLES

ANNEALING 2.0

##### WARNINGS

Diagnostic - **Unsupported**

---

#### BUSSI

##### NAME

BUSSI – The simulation is performed at constant temperature using the rescaling/stochastic method by G. Bussi *et al.* [J. Chem. Phys. 126, 014101 (2007)].

##### SYNOPSIS

BUSSI [*taut*]

## DESCRIPTION

Implement the Bussi thermostat with an adimensional friction factor of *taut* (default value is 0.1). The Bussi thermostat can be used also in conjunction with a barostat (see ISOSTRESS, STRESS, NPT ensemble).

## EXAMPLES

BUSSI 0.5

## WARNINGS

Experimental - **Unsupported**.

## ISEED

## NAME

ISEED – Provide a seed for the random number generator.

## SYNOPSIS

ISEED *seed*

## EXAMPLES

ISEED 34567

## DEFAULTS

ISEED 12345667

## WARNINGS

Diagnostic - **Unsupported**

## ISOSTRES

## NAME

ISOSTRESS – Run MD simulations at constant pressure with an isotropic volume variable

## SYNOPSIS

ISOSTRESS [PRESS-EXT *pext*] [BARO-MASS *wpr*] [COMPR *compressibility*]

## DESCRIPTION

This command allows to run simulations and minimizations at a given pressure with isotropic volume changes. If the command is used alone ORAC runs simulations in the NPH ensemble. Simulations in the NPT ensemble can instead be carried out if ISOSTRESS is used in conjunction with the command THERMOS. The external pressure in MPa is read in by the keyword PRESS-EXT. Also, the keyword BARO-MASS expects the mass of the barostat in  $\text{cm}^{-1}$ . [80] The system compressibility in  $\text{MPa}^{-1}$  is read in as input to keyword *compr*. According to the relation given in Ref. [80] compressibility and frequency should be consistent. If *compr* is not specified the default value is used.

## EXAMPLES

ISOSTRESS PRESS-EXT 0.1 BARO-MASS 10.0 COMPR 5.3e-4

Run a simulation at pressure 0.1 MPA (atmospheric pressure) with a barostat mass corresponding to  $10.0 \text{ cm}^{-1}$ . The compressibility is set to  $5.3 \times 10^{-4} \text{ MPa}^{-1}$ .

## DEFAULTS

ORAC uses the water compressibility at 300 K (i.e.  $5.3 \times 10^{-4} \text{ MPa}^{-1}$ ) as the default compressibility.

## WARNINGS

- 1 ORAC can carry out constant pressure runs with isotropic volume changes only for orthogonal cells.

- 2 Make sure that when simulations at constant pressure are run ORAC has been compiled with the appropriate `PRESSURE` option in the `config.h` file (see Chapter 11)

## ISOSTRESSXY

## NAME

**ISOSTRESS** – Run MD simulations at constant pressure with an isotropic surface variation ( $a, b$  cell parameters) and independent  $c$  cell parameter variation. This protocol is engineered for membrane simulations.

## SYNOPSIS

ISOSTRESSXY [`PRESS-EXT` *pext*] [`BARO-MASS` *wpr*] [`COMPR` *compressibility*]

## DESCRIPTION

See command ISOSTRESS.

## EXAMPLES

...

&SETUP

CRYSTAL 40.0 40.0 60.0 90.0 90.0 90.0

&END

...

ISOSTRESSXY `PRESS-EXT` 0.1 `BARO-MASS` 10.0 `COMPR` 5.3e-4

...

The  $a, b$  cell parameters vary isotropically independent of the  $c$  cell parameter under atmospheric pressure.

## DEFAULTS

ORAC uses the water compressibility at 300 K (i.e.  $5.3 \times 10^{-4} \text{ MPa}^{-1}$ ) as the default compressibility.

## WARNINGS

- 1 ORAC can carry out constant pressure runs with isotropic surface changes only for orthogonal cells.
- 2 Make sure that when simulations at constant pressure are run ORAC has been compiled with the appropriate `PRESSURE` option in the `config.h` file (see Chapter 11)

## FREQUENCIES

## NAME

**FREQUENCIES** – Compute harmonic frequencies of the system. All atoms (solute and solvent) are included in the dynamical computation.

## SYNOPSIS

FREQUENCIES

...

END

## DESCRIPTION

The following subcommands may be specified within `FREQUENCIES`:

`dist_max`, `no_step`, `print`

- **dist\_max**        *hdist*  
The differential increment (in Å) for numerical computation of the dynamical matrix. The default is 0.03 Å, which is OK for most systems and force fields.
- **no\_step**        *steps*  
Order of Chebyshev polynomial for numerical computation of the dynamical matrix. The default is 6 which is OK for most systems and force fields
- **print OPEN**    *filename*  
Write frequencies and eigenvectors to file filename. If not specified frequencies are written to the main output file.

## EXAMPLES

## FREQUENCIES

```
print OPEN  myfreq.out
END
```

## MINIMIZE

## NAME

MINIMIZE – Run steepest descent-like or conjugate gradient minimization at constant volume or at a given pressure

## SYNOPSIS

```
MINIMIZE
...
END
```

## DESCRIPTION

Run energy minimization using a method of choice (steepest descent or conjugate gradient). After minimization is done, the dynamical matrix is computed and diagonalized and the normal frequencies are listed along with eigenvectors. The following subcommands may be specified within MINIMIZE:

CG, SD, WRITE\_GRADIENT, AGBNP

- **GC**        *eps\_energy*  
Use conjugate gradient with energy tolerance *eps\_energy*.
- **SD**        *eps\_energy*  
Use steepest descent with energy tolerance *eps\_energy*.
- **WRITE\_GRADIENT**  
Write final gradient at each atom.
- **AGBNP**  
Minimization is done using an AGBNP model[160] for implicit solvent. A file named **agbnp.param** file must be in the current directory. Dielectric constant of the solvent continuum is set in that file. In the present release AGBNP works only for constant volume minimization and with no &SOLVENT specification.

## EXAMPLES

## MINIMIZE

```
CG 0.00001
WRITE_GRADIENT
END
```

**MDSIM****NAME****MDSIM** – Run molecular dynamics simulations**SYNOPSIS****MDSIM****DESCRIPTION**

Use this command to run molecular dynamics simulation in any ensembles. It has no argument.

**DEFAULTS****MDSIM** is the default.

---

**SCALE****NAME****SCALE** – Periodic temperature scaling**SYNOPSIS****SCALE** *fscale***DESCRIPTION**Use this command for periodically re-scale the temperature with frequency *fscale* in units of femtoseconds. Scaling stands here for random initialization of the system velocities at temperature *temp* according to a Gaussian distribution.**EXAMPLES****SCALE** 100.0

Reinitialize the system velocities every 100 fs.

**WARNINGS**Work only during the rejection phase (see **REJECT** in environment **&RUN**).

---

**SCALING****NAME****SCALING** – Choose scaling methods for constant pressure simulations**SYNOPSIS****SCALING** MOLECULAR**DESCRIPTION**This command sets the scaling method when running with a barostat (see **STRESS** and **ISOSTRESS** directive in this environment).**EXAMPLES****SCALING** MOLECULAR

Run with molecular scaling.

**SCALING** GROUP

This specification has no effect. Starting from release 6.0, only molecular scaling can be done for NPT runs.

## STRESS

NAME

STRESS – Run MD simulations at constant pressure with a non-isotropic volume changes

SYNOPSIS

STRESS [PRESS-EXT *pext*] [BARO-MASS *wpr*] [COMPR *compressibility*]

DESCRIPTION

This command allows to run simulations and minimizations at a given pressure with non-isotropic volume changes according to the Parrinello-Rahman equation of motion. If the command is used alone ORAC runs simulations in the NPH ensemble. Simulations in the NPT ensemble can instead be carried out if STRESS is used in conjunction with the command THERMOS. The external pressure in MPa is read in by the keyword PRESS-EXT. Also, the keyword BARO-MASS expects the mass of the barostat in  $\text{cm}^{-1}$  (see ISOSTRESS). The system compressibility in  $\text{MPa}^{-1}$  is read in as input to keyword COMPR (see ISOSTRESS)

EXAMPLES

&amp;SIMULATION

MDSIM

TEMPERATURE 300.0 25.0

STRESS PRESS-EXT 0.1 BARO-MASS 10.0 COMPR 1.0e-4

&amp;END

Run a simulation in the NHP ensemble at pressure 0.1 MPa (atmospheric pressure) with a barostat mass corresponding to  $10.0 \text{ cm}^{-1}$ . The compressibility is set to  $1.0 \times 10^{-4} \text{ MPa}^{-1}$ . Velocities are initialized and (optionally scaled) according to a temperature of 300 K.

&amp;SIMULATION

MDSIM

TEMPERATURE 300.0 25.0

STRESS PRESS-EXT 0.1 BARO-MASS 10.0 COMPR 1.0e-4

THERMOS

...

END

&amp;END

Same as before but with a Nosé thermostat. The simulation is hence in the NPT ensemble with  $T=300 \text{ K}$ .

DEFAULTS

ORAC uses the water compressibility at 300 K (i.e.  $5.3 \times 10^{-4} \text{ MPa}^{-1}$ ) as the default compressibility.

WARNINGS

Make sure that when simulations at constant pressure are run ORAC has been compiled with the appropriate PRESSURE option in the `config.h` file (see Chapter 11)

## TEMPERATURE

NAME

TEMPERATURE – Set the system temperature for the run

SYNOPSIS

TEMPERATURE *temp* *dt*



## DESCRIPTION

The argument *temp* is the target temperature for the simulation run. *dt* is used only during the rejection phase (see command **REJECT** of environment **&RUN**) and indicates the temperature window in Kelvin outside which temperature scaling occurs. Scaling stands here for random initialization of the system velocities at temperature *temp* according to a Gaussian distribution. System scaling in rejection phase occurs also during constant temperature simulations (see command **THERMOS** in **&SIMULATION**).

## EXAMPLES

TEMPERATURE 300.0 50.0

## WARNINGS

Work only during the rejection phase (see **REJECT** in environment **&RUN**).

## THERMOS

## NAME

**THERMOS** – Run with Nosé thermostats for NVT or NPT simulations.

## SYNOPSIS

**THERMOS**

...

**END**

## DESCRIPTION

For a faster and better energy equipartition, **ORAC** uses three thermostats. The first, coupled to the center of mass momenta of all molecules in the system, the second coupled to the momenta of the atoms of the solute (if present) and the third coupled to the momenta of solvent atoms (if present). The following subcommands may be specified within **THERMOS**:

cofm, defaults, solute, solvent, temp\_limit

- **cofm**      *freq\_mass*  
Specify the mass of the barostat coupled to the centers of mass of the molecules. This mass is also assigned to the barostat coupled to the box momenta in NPT simulation, in case **STRESS** or **ISOSTRESS** have been specified. Actually, what is entered with the variable *freq\_mass* is the (approximate) frequency of oscillation of the thermostat. The actual “mass” *W* (in units of mass times a length to the power of two) of the barostat may be recovered according to the relation  $\text{freq\_mass} = (2Nk_B T/W)^{1/2}$ . [80]
- **defaults**  
Use defaults value for “mass” variables. The defaults are *freq\_mass\_solute* = *freq\_mass\_solvent* *freq\_mass* = 30.0.
- **solute**      *freq\_mass\_solute*  
Specify mass (units of cm<sup>-1</sup>) of the barostat coupled to the momenta of the solute atoms.
- **solvent**      *freq\_mass\_solvent*  
Specify mass (units of cm<sup>-1</sup>) of the barostat coupled to the momenta of the solvent atoms.
- **temp\_limit**      *maxtemp*  
Specify maximum temperature allowed for all Nosé thermostat when the argument of the command **REJECT(&RUN)** is different from zero. In principle, for a system out of equilibrium, no temperature scaling should be enforced when using Nosé thermostating. Actually, when equilibrating systems in the NVT or NPT ensembles, it is strongly recommended to specify the subcommand **temp\_limit** along with a rejection time **REJECT(&RUN)** as normally done for conventional scaling in NVE dynamics. In a NV(P)T system out of equilibrium, while the temperature of the system remains close to the selected temperature, the temperature of the thermostat coordinates (which are not themselves thermostatted) may raise dramatically, if not scaled.

## EXAMPLES

```
&SIMULATION
  TEMPERATURE 300.0 25.0
  MDSIM
  THERMOS
    cofm 30.0
    solute 30.0
    solvent 30.0
  END
&END
```

Run a simulation in the NVT ensemble at  $T = 300$  K.

---

**WRITE\_PRESSURE****NAME**

WRITE.PRESSURE – Write the pressure of the system during a simulation

**SYNOPSIS**

WRITE.PRESSURE

**DESCRIPTION**

This command is used to print the system pressure and stress tensor to the simulation output. It has no argument.

**WARNINGS**

Make sure that when simulations at constant pressure are run ORAC has been compiled with the appropriate **PRESSURE** option in the `config.h` file (see Chapter 11)

---

---

### 10.2.13 &SOLUTE

The &SOLUTE environment includes commands which are concerned with specific aspects of the solute force field and structure. The following commands are allowed:

COORDINATES, DEF\_SOLUTE, SCALE\_CHARGES, SPACE\_GROUP

---

#### COORDINATES

NAME

COORDINATES – Define the coordinates of a solute.

SYNOPSIS

COORDINATES *filename*

DESCRIPTION

Read the coordinates of the solute (in PDB format) from file *filename*. This command is best used when also the solvent atoms must be read in.

EXAMPLES

&SETUP

CRYSTAL 20.00 20.00 20.00 90.0 90.0 90.0

# REPLICATE 2 2 2

&END

&SOLUTE

COORDINATES solute.pdb

# SPACE\_GROUP OPEN benz.group P 2/c

&END

&SOLVENT

CELL SC

INSERT 1.5

COORDINATES solvent.pdb

GENERATE RANDOMIZE 4 4 4

# GENERATE RANDOMIZE 8 8 8

&END

In this example the coordinates of the solute are read in from the file `solute.pdb` while the coordinates of the solvent molecule (see &SOLVENT) are read in from the file `solvent.pdb`. As is now, this input would produce in a box of  $20 \times 20 \times 20 \text{ \AA}^3$ , 1 solute along with 64 replicas (see command GENERATE(&SOLVENT)) of the solvent molecule. Of this 64 molecule, those that overlap with the solute molecule (see command INSERT(&SOLVENT)) are discarded. If the second line in the environment &SOLUTE is uncommented, the solute is assumed to be arranged in the MD box according to the space group specified by the SPACE\_GROUP directive. In the present example the group contains 4 molecules per unit cell. So 4 molecules of solute are arranged in the box according to the P 2/c space group along with 64 replicas of solvent molecules. Again the overlapping solvent molecules (say  $n_o$ ) will be discarded. If we comment the line GENERATE RANDOMIZE 4 4 4 and uncomment the lines # GENERATE RANDOMIZE 8 8 8 and # REPLICATE 2 2 2 we double the size of the sample: we will have 8 cell of  $20 \times 20 \times 20 \text{ \AA}^3$  each with 4 molecules of solute and  $8 \times 8 \times 8 = 512$  solvent molecules minus  $8 \times n_o$  overlapping molecules.

---

## DEF\_SOLUTE

NAME

DEF\_SOLUTE – Define a solute molecule

SYNOPSIS

DEF\_SOLUTE *begin end*

DESCRIPTION

This command is used in conjunction with the command **STRUCTURES** in **&PROPERTIES** and **TEMPLATE** in **&INOUT**. It defines the solute atoms from which mean square displacements are to be computed. The arguments indicate the ordinal numbers of the first *begin* and the last atom *end* of a solute molecule. These numbers may be deduced by inspection of the Template file. The command **DEF\_SOLUTE** can appear more than one time in the environment. The atoms of different solute molecules defined with this command may overlap.

EXAMPLES

&amp;SETUP

```
...
DEF SOLUTE 1 10
DEF SOLUTE 31 57
END
```

&amp;ANALYSIS

```
UPDATE 3 2.0
START 1
STOP 199
```

&amp;END

&amp;PROPERTIES

```
STRUCTURES
inst_xrms heavy
print inst_xrms 1 OPEN isnt.xrms
END
&END
```

Computes instantaneous mean square displacements for heavy atoms for the solute chunks 1-10 and 31-57. ...

WARNINGS

This command has no action while running a simulation. It works only during analysis stage (see **&ANALYSIS**)

## SCALE\_CHARGES

NAME

SCALE\_CHARGES – Scale the total charge on the solute to zero

SYNOPSIS

SCALE\_CHARGES *nmol i<sub>1</sub> i<sub>2</sub> ...i<sub>nmol</sub>*

DESCRIPTION

If  $Q$  is the excess charge on the solute, electro-neutrality is imposed by equally distributing  $-Q$  charge over the atoms of *nmol* disconnected molecules of solute specified by the indices  $i_1, \dots, i_{nmol}$ . Disconnected molecules are ordered according to the sequence given in the structured command **JOIN**.

## EXAMPLES

SCALE\_CHARGES 4 1 5 7 11

The excess charge is distributed over 4 molecules: the 1-st, the 5-th, the 7-th and the 11-th molecule as specified in the sequence give in JOIN.

## WARNINGS

This command is active only if the solute topology and parameter list is actually computed and **not** read from a binary file (i.e. READ\_TPGPRM in &PARAMETERS must be inactive).

## SPACE\_GROUP

## NAME

SPACE\_GROUP – Generate a simulation box applying symmetry operations to an input asymmetric unit

## SYNOPSIS

SPACE\_GROUP OPEN *filename* *group*

## DESCRIPTION

Read the space group *group* parameters (inequivalent molecules and corresponding interchange matrices and fractional translations) from the ASCII file *filename*. The file *filename* is a user database which may contain many entries corresponding to different space groups. The following is an example of an entry of this file:

Space Group Symmetry P 2\_1

```

2
1.00      .00      .00
.00      1.00      .00
.00      .00      1.00
.00      .00      .00
-1.00     .00      .00
.00      1.00      .00
.00      .00     -1.00
.00      .50      .00
```

Space Group Symmetry P 2/c

```

4
1.00      .00      .00
.00      1.00      .00
.00      .00      1.00
.00      .00      .00
-1.00     .00      .00
.00     -1.00      .00
.00      .00      0.00
.50      .00      .50
-1.00     .00      .00
.00      1.00      .00
.00      .00     -1.00
.00      .50      .50
1.00      .00      .00
.00     -1.00      .00
.00      .00     -1.00
.50      .50      .00
```

The space group file is parsed by ORAC as usual by interpreting the composing tokens of each line string. The space group name is taken to begin after the third word **Symmetry** in the first line and

may be composed of more than one word. The number of inequivalent molecules *nmol* in the cell is read in the immediately following line. Then, for each molecule, four lines must be provide where the interchange matrix and the fractional translations are read in. No comment lines may be included. In the present example, for the first molecule the identity matrix and the zero translation are given from line 3-6, while in, e.g., the  $P2_1$  group, for the second molecule a  $C_{2y}$  (line 7-9) rotation and a 0.5 fractional translation (line 10) along the same axis are given. The coordinates of the asymmetric unit must be provided in input through the command **READ\_PDB**. The command **REPLICATE** is used to generate a simulation box larger than the unitary cell. Note that the cell parameters of the simulation box are input to the command **CRYSTAL**.

#### EXAMPLES

**SPACE.GROUP** sgroup.dat P 2\_1

The symmetry transformations of the space group  $P2_1$  are applied to the asymmetric unit in order to generate the coordinates of the other molecules contained in the unit cell.

---

---

### 10.2.14 &SOLVENT

The &SOLVENT environment includes commands which are concerned with specific aspects of the solvent structure. In the present version of ORAC force field and topology specifications are given in the same Force fields and topology files used for the solute. The following commands are allowed:

ADD\_UNITS CELL COORDINATES GENERATE INSERT READ\_SOLVENT REDEFINE

---

#### ADD\_UNITS

NAME

ADD\_UNITS – Add solvent molecules

SYNOPSIS

ADD\_UNITS *nmol*

DESCRIPTION

Reads *nmol* molecules from PDB file specified in the READ\_PDB(&SETUP) command. This command must be entered when starting from a PDB file which includes *both* solute and solvent coordinates.

EXAMPLES

&SETUP

CRYSTAL 20.00 20.00 20.00 90.0 90.0 90.0

READ\_PDB solute+342solvent.pdb

&END

&PARAMETERS

READ\_TPG\_ASCII ../tpg-prm/amber95.tpg

READ\_PRM\_ASCII ../tpg-prm/amber95.prm

JOIN SOLUTE

ala-h ala ala ala ala-o

END

JOIN SOLVENT

hoh

END

&END

&SOLVENT

ADD UNITS 342

&END

...

The file `solute+342solvent.pdb` contains the coordinates of a penta-alanine along with 342 water molecules.

---

#### CELL

NAME

CELL – Define the initial lattice for the solvent

SYNOPSIS

CELL *type*

## DESCRIPTION

This command defines the Bravais lattice type to be used when generating a solvent lattice with GENERATE. *type* may be BCC, FCC, or SC, corresponding to Body Centered Cubic, Face Centered Cubic, and Simple Cubic lattices, respectively.

## EXAMPLES

```
&SOLVENT
  CELL SC
  GENERATE RANDOMIZE 4 4 4
  . . . .
&END
```

## COORDINATES

## NAME

COORDINATES – Define the coordinates of a solvent molecule

## SYNOPSIS

COORDINATES *filename*

## DESCRIPTION

Read the coordinates of the solvent molecule (in PDB format) from file *filename*.

## EXAMPLES

```
&SETUP
  CRYSTAL 20.00 20.00 20.00 90.0 90.0 90.0
&END
&SOLVENT
  CELL SC
  INSERT 1.5
  COORDINATES solvent.pdb
  GENERATE RANDOMIZE 4 4 4
&END
```

In this example the coordinates of the solvent are read in from the file `solvent.pdb` (see &SOLVENT). This input would produce 64 solvent molecules in a box of  $20 \times 20 \times 20 \text{ \AA}^3$ . For generating solvent in presence of the solute see COORDINATES(&SOLUTE)

## GENERATE

## NAME

GENERATE – Replicate solvent molecules.

## SYNOPSIS

GENERATE [RANDOMIZE] *ia ib ic*

## DESCRIPTION

This command is used to generate a lattice of  $ia \times ib \times ic$  cells belonging to the Bravais lattice specified in the command CELL. The optional string RANDOMIZE is used for assigning a random rotation to each solvent molecule in the lattice.

## EXAMPLES



```

&SOLVENT
  CELL SC
  GENERATE RANDOMIZE  4 4 4
  . . . .
&END

```

The elementary cell is simple cubic with one molecule per unit cell. 64 cells are generated (four in each direction).

## INSERT

NAME

INSERT – Insert solute molecules in the solvent

SYNOPSIS

INSERT *radius*

DESCRIPTION

This command is designed to insert solute molecules in a simulation box containing solvent molecules. The solvent molecules which overlap with the solute are discarded. ORAC assumes that two molecules overlap if their distance is less than the sum of their respective Lennard–Jones radii multiplied by *radius*. There is no optimal value for *radius*, however reasonable values are within 0.6 and 0.8.

EXAMPLES

INSERT 0.6

WARNINGS

This command has no action if CONTROL in &RUN is different from zero, i.e. if the system coordinates are read from a restart file (see RESTART in &INOUT).

## READ\_SOLVENT

NAME

READ\_SOLVENT – Read solvent molecules

SYNOPSIS

READ\_SOLVENT *nmol*

DESCRIPTION

This command is a synonymous of ADD\_UNITS

## REDEFINE

NAME

REDEFINE – Read solvent molecules

SYNOPSIS

REDEFINE *unit\_name*

DESCRIPTION

This command is used for deleting the unit *unit\_name* from the solute list and assigning it to the solvent molecules. As long as energies and properties are concerned, the unit *unit\_name* will pertain to the solvent.

## EXAMPLES

```
&PARAMETERS
  READ_TPGPRM_BIN  benz.prmtpg
&END
...
&SOLVENT
  REDEFINE po4
&END
```

We redefine the *solute* unit po4 as a *solvent* unit

---

## 10.3 Input to ORAC : Force Field and Topology Files

Compared to molecular liquids, simulating any complex macromolecule, poses additional problems due to the covalent structure of the systems and to the related complexity of the potential force fields. ORAC builds the covalent topology needed to evaluate the potential energy from the structure of its constituents. In case of a protein the constituents are the amino acids. Also, ORAC tries to minimize the size and the complexity of the actual input needed to construct this topology.

In practice, the minimal information to be provided in order to describe the residue topology is the constituent atoms, the covalent bonds and, in case of polymers or biopolymers, the terminal atoms used to connect the unit to the rest of the chain. In addition, in order to assign the correct potential parameters to the bonds, bending and torsions of the residue, the type of each atom needs to be specified. Finally, to each atom type must correspond a set of non-bonded parameters.

When the bonding topology of the different residues contained in the solute molecule(s) is known, the units are linked together according to their occurrence in the sequence. In this fashion the total bonding topology is obtained. From this information, all possible bond angles are collected by searching for all possible couples of bonds which share one atom. Similarly, by selecting all couples of bonds linked among each other by a distinct bond, torsions can be obtained.

The following sections describe the format of the topology and force field parameters files read by ORAC . The reading of the two files is carried out immediately after the command `READ_TPF_ASCII` and `READ_PRM_ASCII` in the environment `&PARAMETERS` are encountered in the input file. The topology and force field parameters files are strongly dependent from each other and together fully define the molecular force field of the solute molecule(s). In the ORAC distribution archive the most recent AMBER[4] force field and topology files are provided.

### 10.3.1 Force Field Parameters

The force field parameters must be placed in the file defined by the command `READ_PRM_ASCII` of the environment `&PARAMETERS`. This file can contain the directives defining the stretching, angle bending, proper and improper torsion, Lennard-Jones potential parameters. Each directive is terminated by the keyword `END` subsequent to the last line of input. The allowed commands are the followings:

```
BENDINGS, BOND, NONBONDED [MIXRULE, NOMIXRULE], TORSION [ PROPER, IMPROPER ]
```

#### BENDING

NAME

BENDINGS – Read angle bending potential parameters

SYNOPSIS

BENDINGS

...

*typ1 typ2 typ3*  $K_{angle}$   $\theta_0$

...

END

DESCRIPTION

The command reads a sequence of angle bending potential parameters. *typ1*, *typ2* and *typ3* are three character strings, not to exceed 7 characters, indicating the atom types of the three atoms involved in the angle bending interaction.  $K_{angle}$  and  $\theta_0$  are the angle bending force constant and the equilibrium angle, respectively. The units used for the  $K_{angle}$  and  $r_0$  are Kcal mol<sup>-1</sup> rad<sup>-2</sup> and degree.

EXAMPLES

BENDINGS

```
cb    c    na    70.00    111.30
```

```

cb   c   o      80.00   128.80
cm   c   o      80.00   125.30
n*   c   na     70.00   115.40
END

```

---

## BOND

NAME

BOND – Read stretching potential parameters

SYNOPSIS

BOND

...

*typ1 typ2 K<sub>stretch</sub> r<sub>0</sub>*

...

END

DESCRIPTION

The command reads a sequence of stretching potential parameters. *typ1* and *typ2* are two character strings, not to exceed 7 characters, indicating the atom types of the two atoms involved in the stretching interaction. *K<sub>stretch</sub>* and *r<sub>0</sub>* are the stretching force constant and the stretching equilibrium distance, respectively. The units used for the *K<sub>stretch</sub>* and *r<sub>0</sub>* are Kcal mol<sup>-1</sup> Å<sup>-2</sup> and Å.

EXAMPLES

BOND

```

c     ca      469.00    1.409
c     cb      447.00    1.419
c     cm      410.00    1.444
END

```

---

## NONBONDED

NAME

NONBONDED – Read Lennard-Jones parameters

SYNOPSIS

NONBONDED [MIXRULE, NOMIXRULE]

...

END

DESCRIPTION

The command reads the Lennard-Jones parameters for the solute non-bonded interactions:

$$\frac{A}{r^{12}} - \frac{B}{r^6} = 4\epsilon \left[ \left( \frac{\sigma}{r} \right)^{12} - \left( \frac{\sigma}{r} \right)^6 \right] \quad (10.1)$$

Arguments MIXRULE and NOMIXRULE to the command indicate if Lennard-Jones mixing rules are to be used by ORAC or, conversely, explicit mixed Lennard-Jones potentials are to be expected in input. The format of the nonbonded potential is different in the two alternative cases. If mixing rules are to be found the input to NONBONDED looks like:

NONBONDED MIXRULE

...

```
typ1 r_min  $\epsilon$   $\gamma$  mass
```

```
...
```

```
END
```

Here, *typ1* is a character string, not to exceed 7 characters, labeling the atom type for the atom;  $r_{min}$  is the radius corresponding to the minimum of the Lennard-Jones potential;  $\epsilon$  the Lennard-Jones well depth;  $\gamma$  is reserved for later usage and should be set to zero; *mass* is the atom mass. The non-bonded potential format changes if different Lennard-Jones potentials must be used for the 1-4 interactions in which atom type *typ1* is involved:

```
NONBONDED MIXRULE
```

```
...
```

```
typ1 r_min  $\epsilon^{14}$   $\epsilon^{14}$  mass
```

```
...
```

```
END
```

Here, parameters  $r_{min}^{14}$   $\epsilon^{14}$  are used only for 1-4 interactions. In case the argument *NOMIXRULE* is used, the input to *NONBONDED* looks like:

```
NONBONDED NOMIXRULE
```

```
...
```

```
typ1 r_min  $\epsilon$   $\gamma$  mass
```

```
...
```

```
END
```

```
...
```

```
 $B_{ij}$   $A_{ij}$ 
```

```
...
```

First the sequence of the  $N_{type}$  force field atom types and Lennard-Jones parameters is read interrupted by the keyword *END* at the beginning of a new line. Second, a list of the  $N_{type}(N_{type} + 1)/2$  interaction potential parameters *B* and *A* must be provided in input. For most of the biomolecular force fields non-bonded mixing rules are commonly used.

#### EXAMPLES 1

```
NONBONDED MIXRULE
```

```
h4      1.409   0.015   0.000   1.008
```

```
o       1.661   0.210   0.000  16.000
```

```
ca      1.908   0.086   0.000  12.010
```

```
END
```

#### EXAMPLES 2

```
NONBONDED NOMIXRULE
```

```
h       0.000   0.000   0.000   1.008
```

```
o       1.700   0.120   0.000  15.999
```

```
c       2.000   0.110   0.000  12.011
```

```
END
```

```
0.0      0.0           Interaction type [h -- h]
```

```
0.0      0.0           Interaction type [h -- o]
```

```
0.0      0.0           Interaction type [h -- c]
```

```
1200.0   600700.0      Interaction type [o -- o]
```

```
1000.0   800000.0      Interaction type [o -- c]
```

```
2000.0   500100.0      Interaction type [c -- c]
```

#### WARNINGS

If the 1-4 interaction parameters are not provided in input to *NONBONDED MIXRULE*, the regular non-bonded parameters multiplied by the 1-4 factor *LJ-FUDGE* (see environment *&POTENTIAL*) are used instead. For interactions involving one atom for which the 1-4 parameters are given and another for which they are not, regular non-bonded parameters for the interaction are used multiplied by the eventual *LJ-FUDGE* factor.

## TORSION PROPER

NAME

TORSION – Read proper torsion potential

SYNOPSIS

TORSION PROPER

...

*typ1 typ2 typ3 typ4 K<sub>phi</sub> n γ*

...

END

DESCRIPTION

*typ1*, *typ2*, *typ3* and *typ4* are four character strings, not to exceed 7 characters, indicating the atom types of the four atoms involved in the torsion interaction (a *x* string is taken to be as a wild card indicating *any* atom). The torsional axis, according to the ORAC convention is the one connecting the *type2* and *type3*. The parameters  $K_\phi$  and  $n$  and  $\gamma$  are defined in Eq. 4.3.  $K_{phi}$  is in unit of Kcal mol<sup>-1</sup>;  $n$  is an integer indicating the number of minima(maxima) for 360 degree rotation about the torsional axis;  $\gamma$  is given in degrees and can be either 0.0 or 180.0.

EXAMPLE

TORSION PROPER

x	c	ca	x	3.6250	2.0	180.0
x	cw	na	x	1.5000	2.0	180.0
ct	ct	os	ct	0.3830	3.0	0.0
ct	ct	os	ct	0.1000	2.0	180.0

END

## TORSION IMPROPER

NAME

TORSION IMPROPER – Read proper torsion potential

SYNOPSIS

– AMBER form [cosine]

TORSION IMPROPER

...

*typ1 typ2 typ3 typ4 K<sub>phi</sub> n γ [cosine]*

...

END

– CHARMM form [harmonic]

TORSION IMPROPER

...

*typ1 typ2 typ3 typ4 K<sub>phi</sub> angle [harmonic]*

...

END

DESCRIPTION

*typ1*, *typ2*, *typ3* and *typ4* are four character strings, not to exceed 7 characters, indicating the atom types of the four atoms involved in the torsion interaction (a *x* string is taken to be as a wild card indicating *any* atom) For improper torsions, ORAC allows both the CHARMM-like form (a simple harmonic potential) or the AMBER-like form (a torsional potential):

For the CHARMM form  $K_{phi}$  must be given in Kcal mol<sup>-1</sup> rad<sup>-2</sup>, while *angle* is the equilibrium angle of the improper torsion in degree.

For the AMBER form the meaning of the symbol are identical to those described in the TORSION PROPER directive.

#### EXAMPLE

```
TORSION IMPROPER
x    x    ca  h4      1.1000  2.0  180.0 cosine
x    x    ca  h5      1.1000  2.0  180.0
ck   cb   n*  ct      1.0000  2.0  180.0 cosine
cm   c    n*  ct      1.0000  2.0  180.0 cosine
ha   cpa  cpa  cpm     29.40   0.0  harmonic
ha   cpb  c    c      20.00   0.0  harmonic
ha   ha   c    c      20.00  180.0  harmonic
END
```

### 10.3.2 Topology

ORAC is instructed to read the topology file by the command

```
READ_TPG_ASCII field.tpg
```

of the &PARAMETERS environment. File **field.tpg** contains information on the series of residues needed to define the topology of the actual solute molecules. This information is provided through a series of free format keywords and their corresponding input data as done in the main input file **sys.mddata**. In this way, ORAC reads the solute connectivity, the atomic charges, the atomic labels corresponding to those found in the PDB file, and the atomic types according to the chosen force field (i.e. AMBER, CHARMM or others). Moreover, the atomic groups and the improper torsions are also defined.

As for the mail input file, the file **field.tpg** is parsed and the composing substrings of each line are interpreted. Comment lines must have the “#” character in column 1. Each residue or unit definition starts with the keyword

```
RESIDUE residue_name
```

where *residue\_name* is a character label which *must* match labels found in the command JOIN of the environment &PARAMETERS, and must end with the keyword RESIDUE\_END. These residue delimiting keywords are the only one in capital letters in *field.tpg* (see the valine example later on in this section)

Atom type definitions and charges are read in between the keywords **atom** and **end**. For each atom three strings must be entered: the PDB atom label, the potential type according to the selected force field as specified in parameter file (see Sec.10.3.1) and the point charge in electron units. Groups are composed of all atoms entered between two successive **group** keywords. The PDB labels must be all *different* from each others since they are used to establish the topology and connectivity of the solute.

The bond connectivity is specified between the keywords **bond** and **end** by providing the series of bonds present in the residue. Each bond is specified by two atom labels corresponding to the atoms participating to the bond.

All possible bendings and proper torsions are computed by ORAC from bond connectivity and need not to be specified. Improper torsions must instead be provided. Improper torsion are used to impose geometrical constraints to specific quadruplets of atoms in the solute. In modern *all-atoms* force fields, improper torsions are generally used to ensure the planarity of an *sp*<sub>2</sub> hybridized atom. The convention in ORAC to compute the proper or improper torsion dihedral angle is the following: If **r**<sub>1</sub>, **r**<sub>2</sub>, **r**<sub>3</sub>, **r**<sub>4</sub> are the position vectors of the four atoms identifying the torsion, the dihedral angle  $\chi$  is defined as

$$\chi = \arccos \left[ \frac{(\mathbf{r}_2 - \mathbf{r}_1) \times (\mathbf{r}_3 - \mathbf{r}_2)}{|\mathbf{r}_2 - \mathbf{r}_1| |\mathbf{r}_3 - \mathbf{r}_2|} \bullet \frac{(\mathbf{r}_3 - \mathbf{r}_2) \times (\mathbf{r}_4 - \mathbf{r}_3)}{|\mathbf{r}_3 - \mathbf{r}_2| |\mathbf{r}_4 - \mathbf{r}_3|} \right] \quad (10.2)$$

## RESIDUE

## NAME

RESIDUE – Read covalent topology of the residue

## SYNOPSIS

RESIDUE *res1*

...

END

## DESCRIPTION

The command **RESIDUE** read the covalent topology for the residue labeled *res1*. *res1* must be a character string not to exceed 8 characters. The environment generated by this command can accept the following keywords:

atoms, bonds, rigid, dihed, imphd, omit\_angle, backbone termatom, acc, don

This are described in the following paragraphs.

## EXAMPLES

Residue topology of amino acid valine.

RESIDUE val ( Total Charge = 0.0 )

## atoms

## group

n	n	-0.41570
hn	h	0.27190
ca	ct	-0.08750
ha	h1	0.09690

## group

cb	ct	0.29850
hb	hc	-0.02970

## group

cg1	ct	-0.31920
hg11	hc	0.07910
hg12	hc	0.07910
hg13	hc	0.07910

## group

cg2	ct	-0.31920
hg21	hc	0.07910
hg22	hc	0.07910
hg23	hc	0.07910

## group

c	c	0.59730
o	o	-0.56790

end

## bonds

cb	ca	cg1	cb	cg2	cb	n	hn		
n	ca	o	c	c	ca	ca	ha		
cb	hb	cg1	hg11	cg1	hg12	cg1	hg13	cg2	hg21
cg2	hg22	cg2	hg23						

end

## imphd

-c	ca	n	hn	ca	+n	c	o
----	----	---	----	----	----	---	---

end



```

termatom n c
backbone n ca c
END

```

#### atoms

##### NAME

**atoms** – Read the list of atoms forming the residue.

##### SYNOPSIS

```

atoms
group
...
lab1 typ1 charge
...
group
...
end

```

##### DESCRIPTION

The command read the list of atoms and corresponding charges *charge* in electron forming the residue. The list can (and must!) contain the keyword **group** to define atomic groups and is terminated by **end**. *lab1* and *typ1* are both character strings, not to exceed 7 characters, and correspond to the atom label and type, respectively. While, each atom type listed by **atoms** must be defined in the parameters file, each atom label defines uniquely a particular atom of the residue. ORAC expects that labels found in **atoms** be consistent with those used in the input coordinates (i.e. in the PDB file). Atoms in between two consecutive **group** (or between a **group** and the final **end**) form the atomic group.

##### EXAMPLES

```

atoms
group
n      n      -0.41570
hn     h       0.27190
ca     ct     -0.08750
ha     h1      0.09690
group
cb     ct      0.29850
hb     hc     -0.02970
end

```

##### WARNINGS

The keyword **atoms** must appear at the beginning of the **RESIDUE** environment.

#### rigid

##### NAME

**rigid** – Define a rigid unit

##### SYNOPSIS

```
rigid
```

##### DESCRIPTION

Not supported

**bonds**

## NAME

**bonds** – Read list of bonds

## SYNOPSIS

**bonds**

...

*lab1 lab2    lab3 lab4 ...*

...

**end**

## DESCRIPTION

The keyword is used to define a list of covalent bonds among the atoms forming the residue. The list is terminated by **end**. On the lines following **bonds** a series of pairs of atom labels is expected. In the synopsis, atom *lab1* is covalently bound to atom *lab2* and *lab3* to *lab4*. The labels appearing in input to **bonds** must be defined in the atom list given with the command **atoms**.

## EXAMPLES

**bonds**

n    ca    o    c    c    ca    ca    ha

cg2 hg22    cg2 hg23

**end**

## WARNINGS

The keyword **atoms** must appear before **bonds**.

**omit\_angles**

## NAME

**omit\_angles** – Provide a list of angle bendings to omit

## SYNOPSIS

**omit\_angles**

...

*lab1 lab2 lab3    lab4 lab5 lab6 ...*

...

**end**

## DESCRIPTION

Given the list of bonds for the solute molecule(s) ORAC generates all possible angle bendings. The keyword **omit\_angles** allows the deletion of any angle bendings from the residue angle bendings list. Following the line with **omit\_angles** a series of triplets of atom labels is expected. In the synopsis, *lab1*, *lab2* and *lab3* are the three atoms involved in one angle bending to be deleted from the residue list. Labels starting with a - or a + correspond to atoms belonging to the preceding and following residue in the solute sequence.

## EXAMPLES

**omit\_angles**

n ca c    c ca ha

**end**

## WARNINGS

The keyword **bonds** must appear before **omit\_angles**.

**dihed**

## NAME

**dihed** – Define proper torsions list for the residue. Obsolete **Unsupported**

## SYNOPSIS

**dihed**

...

*lab1 lab2 lab3 lab4      lab5 lab6 lab7 lab8 ...*

...

**end**

## DESCRIPTION

In more modern biomolecular force fields all possible torsion angles are included in the interaction potential (see **AUTO\_DIHEDRAL** of the environment **&SOLUTE**). **dihed** includes only selected proper torsions in the potential as it was required by earlier force fields. Each proper torsion is defined by a quadruplet of atom labels (see synopsis). Labels starting with a - or a + refer to atoms belonging to the preceding and following residue in the solute sequence.

## EXAMPLES

**dihed**

-c n ca cb      n ca cb cg1      n ca c +n

**end**

## WARNINGS

The keyword **bonds** must appear before **dihed**. If **AUTO\_DIHEDRAL** of the environment **&SOLUTE** is selected, the keyword **dihed** has no effect.

**imphd**

## NAME

**imphd** – Define improper torsions list for the residue

## SYNOPSIS

**imphd**

...

*lab1 lab2 lab3 lab4      lab5 lab6 lab7 lab8 ...*

...

**end**

## DESCRIPTION

The keyword includes only selected improper torsions. Following **imphd** a list of improper torsions ended by the keyword **end** must be provided. Each improper torsion is defined by a quadruplet of atom labels (see synopsis). Labels starting with a - or a + refer to atoms belonging to the preceding and following residue in the solute sequence.

## EXAMPLES

**imphd**

-c    ca    n      hn    ca    +n    c      o

**end**

## WARNINGS

The keyword **bonds** must appear before **imphd**.

**backbone**

## NAME

**backbone** – Define the backbone atoms for the residue

## SYNOPSIS

**backbone**    *lab1 lab2 lab3 ...*

## DESCRIPTION

With **backbone** a list of atom labels (*lab1*, *lab2*, *lab3*) is provided which belong to the biomolecule backbone. The corresponding atoms are uniquely identified. The backbone atoms are only used by ORAC in the calculation of run time properties. The command can be repeated as many times as necessary.

## WARNINGS

The keyword **bonds** must appear before **backbone**.

**termatom**

## NAME

**termatom** – Define a pair of atoms which are covalently bound to other residues

## SYNOPSIS

**termatom** *lab1 lab2*

## DESCRIPTION

**termatom** is used to define two atoms, whose labels are *lab1* and *lab2*, which are connecting the residue to the rest of the biopolymer. If the residue has only one connecting atom or has none, one of the labels or both must be replaced by a **\***.

## EXAMPLES 1

Connecting atoms for an amino acid:

**termatom** n c

## EXAMPLES 2

Connecting atoms for a residue not covalently connected with the others residues of any solute sequence: **termatom** \* \*

## WARNINGS

This keywords must be always present in any **RESIDUE** environment.

**acc**

## NAME

**acc** – List the hydrogen bond acceptor atoms. Experimental - **Unsupported**

## SYNOPSIS

**acc** *lab1 lab2*

## DESCRIPTION

The labels *lab1*, *lab2* are string character indicating the atom types (see command **atom**). If only one label is specified, *label1* refers to the hydrogen bond acceptor. If also *label2* is specified, the latter is the acceptor and *label1* while refers to the conjugate acceptor bonded atom (e.g. N and H (acceptor) in the C-O bond)

don

NAME

don – List the hydrogen bond donor atoms. Experimental - **Unsupported**

SYNOPSIS

don *lab1 lab2*

DESCRIPTION

The labels *lab1*, *lab2* are string character indicating the atom types (see command **atom**). If only one label is specified, *label1* refers to the hydrogen bond donor. If also *label2* is specified, the latter is the donor and *label1* while refers to the conjugate acceptor bonded atom (e.g. C (acceptor) and O (donor) in the C-O bond)

---

## Chapter 11

# Compiling and Running ORAC

### 11.1 Compiling the Program

#### 11.1.1 Serial version

ORAC has been written *mostly* in FORTRAN. ORAC 6.0 can be compiled with `gfortran`, the Gnu FORTRAN compiler for GCC, the Gnu Compiler Collection. ORAC 6.0 is currently supported only for Linux operating systems. The code does not require any library to run except for the standard mathematical libraries. ORAC can use the efficient FFTW suite[161] for Fourier Transform in the evaluation of the PME contribution to reciprocal lattice forces, but has its own built-in FFT libraries. You must have the Gnu version of `make` to make the executable. Starting from this release, a `configure` script is provided for generating the Makefile from a Makefile.in template. The ORAC distribution file is a tar archive containing the ORAC source code and a few examples which illustrate most of the important features of the program.

The untarring of the distribution file using the command `tar -xvf orac.tar6.0.gz` will create a directory with the following sub-directories:

```
./ORAC
./ORAC/doc
./ORAC/etc
./ORAC/lib
./ORAC/pdb
./ORAC/src
./ORAC/tests
./ORAC/tools
```

The directory `./ORAC/doc` contains this manual in pdf and HTML format.

The directory `./ORAC/etc` contains material for developers

The directory `./ORAC/lib` contains the force field parameters (AMBER03) and topology files (see sec. 10.3)

The directory `./ORAC/pdb` contains The Protein Data Bank format coordinate files for running the input examples in `./ORAC/tests`

The directory `./ORAC/src` contains the source code. Read the copyright agreement `COPYRIGHT_NOTICE` before modifying or distributing the code.

The directory `./ORAC/tools` contains ancillary codes for analyzing MD data.

To compile ORAC just do

```
% ./configure [options]
% make
```

This will create an executable ORAC in the target directory as specified in [options]. When no options are specified, the default target GNU [no MPI/OpenMP/fftw support] is created.

In order to see the list of the available `configure` options cd into the `./ORAC/src` directory and do

```
% ./configure -help
```

The program is known to compile and run with gcc 4.8 and Intel Fortran Compiler (10.1 to 14) both in 32- and 64- bit architecture; XL Fortran for AIX (V12.1-V14.1) and XL C/C++ for AIX (V10.1-V12.0); PGI Fortran 2003. To compile ORAC with the Intel FORTRAN compiler do

```
% cd $HOME/ORAC/src
% ./configure -Intel
% make
```

This will produce the executable in the `./ORAC/src/INTEL` directory. To compile ORAC with the Intel FORTRAN compiler, MPI support and FFTW libraries do

```
% cd $HOME/ORAC/src
% ./configure -Intel -FFTW -MPI
% make
```

A directory `$HOME/src/INTEL-FFTW-MPI` will be created. *Nota Bene:* you must have the FFTW libraries installed in your system. For parallel execution, `libfftw3`, `libfftw3_omp`, `libfftw3_threads` are needed. In Debian/Ubuntu systems these libraries are provided in the packages `fftw3` and `fftw3-dev`. An alternative path for fftw libraries can be specified in the `-FFTW` configure option `[-FFTW=alt_path]`. For example

```
% cd $HOME/ORAC/src
% ./configure -Intel -FFTW=alt_path -MPI
% make
```

To compile ORAC with the Intel FORTRAN compiler, MPI and OpenMP support and FFTW libraries do

```
% cd $HOME/ORAC/src
% ./configure -Intel -FFTW -MPI -OMP
% make
```

This will generate a directory `./ORAC/src/INTEL-FFTW-OMP-MPI`.

### 11.1.2 Parallel version

ORAC implements a weak scaling parallel algorithm via MPI calls in H-REM/SGE generalized ensemble simulations or driven simulations technologies based on the Crooks theorem. and a strong scaling parallel approach on the OpenMP layer based on particle decomposition for the computation of the forces. The nature of the executable (serial, MPI only and MPI/OpenMP with or without FFTW libraries) is straightforwardly controlled by the specification of the options of the `configure` command, as described above. Parallel execution can therefore be done on either MPI or OpenMP level or on the two combined levels using the appropriate target executable. ORAC is designed to maximize the sampling efficiency of a single MD simulation job on a NUMA multicore platforms using advanced highly parallel techniques, such as H-REM or SGE, or even zero-communication embarrassingly parallel approach like FS-DAM. We deem as “thermodynamic” the parallelism related to such weakly scaling algorithms. Thermodynamic parallelism in ORAC is handled only at the distributed memory MPI level, with a minimal incidence of the inter-replica (for H-REM and SGE simulations) communication overhead or no overhead at all for the NE independent trajectories in FS-DAM simulations. Therefore, the number of MPI threads in ORAC (defined via the `mpiexec` command) simply equals the number of replica/walkers in H-REM/SGE simulations or the number of independent NE trajectories in a FS-DAM job.

By default, ORAC uses a fixed (static) number of OpenMP threads, `nthr`, for all asynchronous force computations. This number, returned by a standard run time library routine, corresponds to the number of cores found on the compute node. This is true also when on the same compute node are running more than one MPI instance related, so that the node gets overloaded with more OpenMP threads than cores.

In order to tame the loss of parallel efficiency due thread overloading and/or granularity issues produced by the default behavior, ORAC can handle the disparate granularity of the various force computation in the nested MTS levels using an end-user controlled dynamic adjustment of the OpenMP threads numbers. Intramolecular forces, implementation of constraints, step-wise advancement of velocities/coordinates and computation of non bonded forces in the direct and reciprocal lattice can each be computed with a user controlled number of threads by switching on dynamic threading. From the end user point of view, dynamic

```
# ORAC MAIN input file
#####OPENMP HEADER #####
#&T NTHREADS      8  CACHELINE      8
#&T NT-LEVEL1     4  CACHELINE      8
#&T NT-LEVEL2     6  CACHELINE      8
#####OPENMP HEADER #####

#.... orac input file follows

..
..
```

Figure 11.1: Orac input header for dynamic threading and cache line size control. Cache line size is expressed in units of 8 bytes words. The ‘‘T’’ following the shebang-like sequence ‘‘#&’’ is optional. When provided, the program produces detailed timing of the various parallel computations.

threading can be specified by supporting the optional heading reported in the figure 11.1 in the main input file. In this heading, the shebang-like character sequence ‘‘#&’’ instructs an OpenMP compiled executable to implement dynamic threading with up to three OpenMP levels: main level, for non bonded forces and fast Fourier transform of the gridded charge array in PME computation; level-1, for fast forces (improper torsion and bending) and step-wise advancement in all MTS levels; level-2 for bond constraints, proper torsion and direct lattice Ewald intramolecular corrections. In the same heading, the user can also control the cache-line size to be used in the various previously defined OpenMP levels. Cache line size control in OpenMP applications is essential in minimizing the impact of cache misses due to “false-sharing”. The latter may occur in the reduction operation of the force arrays involved in particle decomposition parallel algorithm, when threads on different processors modify variables that reside on the same cache line, thus invalidating the cache line for all processors (cache misses) and hurting the parallel performances. Cache misses clearly depends on the length of the cache line that is architecture dependent. Common cache line sizes are 32, 64 and 128 bytes. To keep up with the rapidly evolving multicore architectures, in the compact main input heading reported in Figure 11.1, ORAC provides the possibility of specifying the actual cache line size on the underlying compute node, thus guaranteeing cache coherence of force reduction operations. The OpenMP optional heading is interpreted as a simple comment by executables that were compiled for serial execution, thus preserving the retro-compatibility of the input file for the non OpenMP past releases.

When launched in an MPI environment, ORAC creates in the directory from which it was launched, *nprocs* PARXXXX new directories where the main input file is copied and all output of the replicas are written. The only two files that *need* to be in the directory from which ORAC is launched are the main input and the REM.set file (only if the a REM simulation is started from scratch and the scaling factors of the replicas are assigned manually and not automatically (see SETUP(&REM)).

## 11.2 How to set dimensions in ORAC : The config.h file

Being written mostly in fortran77 language, the ORAC program does not dynamically allocate the required memory. Memory allocation is done statically and dimensions throughout the code are given in a single file named `config.h`. To adapt the size of the program to other problems the `config.h` file need to be changed and the program recompiled. In the current distribution an ancillary `awk` script that builds the `config.h` file has been provided. This script is called `configure` and can be found in the `tests` directory. `configure` parses a general input file for ORAC and produces, to the standard output, the corresponding



`config.h` file.

A certain number of ORAC routines contains `INCLUDE` statements. The corresponding include files, which may contain `PARAMETER`, `COMMON` and general dimension statements (`REAL`, `INTEGER` etc.), have by convention a `.h` suffix and are generated by the standard preprocessor (`/lib/cpp`) from `.inc` files and the `config.h` file. The `.inc` files are templates of include files, where constants are initialized to character symbols (some are listed below). When making the executable, these character symbols are replaced by the standard preprocessor with their numeric values assigned in the `config.h` file.

The meaning of most of the character symbols contained in the `config.h` is explained in the file itself. Here, it is worth mentioning a few:

- **PRESSURE**

The statement `#define PRESSURE` is found in the distribution `config.h` file. It implies that the single time step non-bonded force routines will be generated including the pressure computation section. Since force routines not including the pressure calculation are faster of about 10-20 %, it might be useful in simulation at constant volume to replace the statement with:

```
#undef PRESSURE
```

With the current version of ORAC, after this change all the `*.CPP.f` files must be removed by hand and the program recompiled.

- **\_SIT\_SOLU\_**

This is the maximum number of atoms in the system (it includes the solvent and solute atoms. The highly misleading name is due to historical reasons.

- **\_TYP\_SOLU\_**

This is the maximum number of possible *different* units type as coded in the topology database.

- **\_NRES\_**

This is the maximum number of possible units in the solute (i.e. the number of entries in the `JOIN` structured command).

- **\_TGROUP\_**

This is the maximum number of groups in the system.

- **\_LMAX\_    \_MMAX\_    \_NMAX\_**

These parameters controls the dimension of the sine/cosine work in the standard Ewald Method. In the `config.h` provided in the ORAC distribution archive, written for SPME simulations, these parameters are all defined to be 1

- **\_NAT\_WW\_    \_NAT\_WP\_    \_NAT\_PP\_**

These parameters control the neighbor list dimensions. E.g. the three neighbor lists for the solvent (since a maximum of three shell for r-RESPA are allowed) are integer arrays of dimensions `_NAT_WW_×_MOL_SOLV_`.

- **\_FFT1\_    \_FFT2\_    \_FFT2\_    MORD**

These parameters control the dimensions of the  $Q$  charge array and of the  $M$  polynomials for PME computation (see section 4.1)

The total size of the code depends on the number of particles in the system and on the kind of calculation to be carried out. To give an idea, an 8000 atoms system, running with PME, linked cell and computing e.g. the VACF, requires about 25 Mb of memory. The equilibration of the solvated reaction center (33000 atoms) requires around 85 Mb.

# Index

- alpha*-carbon, 117
- acc**, 165
- acceptance ratio, 89, 90, 121
- ADD\_BEND**, 89
- ADD\_BOND**, 89
- ADD\_STR\_BENDS**, 100
- ADD\_STR\_COM**, 101
- ADD\_STR\_BONDS**, 99
- ADD\_STR\_TORS**, 102
- ADD\_TORS**, 89
- adding a bending, 100
- adding a COM-COM stretching, 101
- adding a harmonic distance constraint, 99
- adding an harmonic torsion, 102
- ADD\_TPG SOLUTE**, 93
- ADD\_UNITS**, 152
- ADJUST\_BONDS**, 103
- AGBNP**, 143
- Alchemical transformations, 104, 110
  - definition of the alchemical portion of the solute, 105
  - printout of the work done, 84
- alchemical transformations, 67
- alkanes, 16
- AMBER force field, 33
- &ANALYSIS**, 79
- ANDERSEN**, 140
- Andersen, H.C., 140
- angular\_cutoff**, 115
- angular cutoff, 115
- animation
  - using ORAC generated file, 83
- animation from xyz file, 113
- ANNEALING**, 140
- UPDATE**, 79
- ASCII**, 80
- DCD**, 81
- asymmetric unit, 151
- atom\_record**, 82
- atomic charges
  - subtracting excess charge, 149
- atomic scaling, 23
  - Liouvillean split for, 26
- atoms**, 162
- AUTO\_DIHEDRAL**, 103
- average**, 114
- averaged**, 116
- B-spline interpolation, 35
- backbone, 117
  - writing the coordinates of  $\square$  atoms, 83
- backbone**, 165
- barostat, 20
- BATTERIES**
  - replica exchange method, 120
- bending
  - printing out, 95
- BENDING**, 103
- bending potential, 31, 124
- BENDINGS**, 156
- Bennett acceptance ratio, 47, 65
- Berendsen H., 24
- Berne B. J., 5
- BOND**, 157
- bonded potential, 30
  - subdivision of, 30
- bonds**, 163
- BPTI**, 28
- B-spline
  - of the direct lattice potential, 106
- BUSSI**, 140
- Bussi, G., 140
- canonical transformations, 9
- CELL**, 152
- center of mass, 130
- CG**, 143
- CHANGE\_CELL**, 129
- CHECK\_COORD\_OFF**, 104
- Ciccotti G., 24
- cofm**, 146
- COM-COM added bond , 101
- compiling ORAC , 167
- compute accessibility**, 118
- compute contac\_solute**, 118
- compute neighbors**, 118
- compute volume**, 118
- config.h**, 169
- config.h** file, 170
- configure file, 170
- conjugate gradient, 143, 146
- constant pressure
  - scaling, 144

constant pressure simulation, 19, 142  
 constant temperature simulation, 19, 146  
**CONSTRAINT**, 104  
 constraints, 103, 104  
     printing out, 95  
     with r-RESPA, 15  
**CONTROL**, 124  
 coordinates  
     of the solvent, 152, 154  
**COORDINATES**, 148, 153  
 Crooks theorem, 61  
**CRYSTAL**, 129  
 crystal structure, 130  
 crystal symmetry, 150  
 crystal to orthogonal matrix, 131  
 crystallographic parameters, 129  
 cutoff, 5, 34, 37, 106  
     for hydrogen bonds, 115  
     in the reciprocal lattice, 40  
     reciprocal lattice, 106  
**CUTOFF**, 104  
**cutoff**, 114, 118  
  
**DCD**  
     generating a file, 81  
**DEBUG**, 124  
 decaalanine, 7  
**defaults**, 146  
**DEF\_FRAGMENT**, 113  
**DEFINE\_ALCHEMICAL\_ATOM**, 105  
**DEF\_SOLUTE**, 149  
 density of states, 33  
 dielectric constant, 5, 40, 116  
**diffusion**, 117  
 diffusion coefficient, 113  
**dihed**, 164  
 dihedral angle, 32  
 dihedral angle in torsions, 160  
 dimensions  
     changing the, in ORAC , 169  
 dipole, 113  
 direct lattice potential, 34  
 direct potential  
     subdivision of, 37  
**dirty**, 87  
 discrete time propagator, 11, 13, 38  
**DIST\_FRAGMENT**, 113  
**dist\_max**, 143  
**dived\_step**, 118  
**don**, 166  
 driven thermal changes, 84, 127  
 driving external potential, 99  
**DUMP**, 81  
 dumping the restart file, 84  
**DYNAMIC**, 81

dynamical matrix, 142  
  
 eigenvectors, 142  
 electrostatic correction, 106  
 electrostatic corrections, 38  
 electrostatic potential, 35  
     subdivision of, 37  
 energy equipartition, 146  
**energy\_then\_die**, 87  
 enhanced sampling, 6  
 equations of motion, 9  
     for Parrinello-Rahman-Nosé Hamiltonian, 20  
 equilibration, 128  
**ERF\_CORR**, 105  
**ERFC\_SPLINE**, 106  
 error function, 34, 106  
**EWALD**, 106  
 Ewald method, 6, 34  
     electrostatic corrections, 38  
     in multiple time scales integrators, 86  
     intramolecular correction, 105  
     intramolecular self term, 34  
     self energy, 39  
     setting work array dimensions, 170  
     smooth particle mesh, 35  
 excess charge, 149  
 extended Lagrangian, 19  
  
 Fast switching Double Annihilation method, 76  
**FIX\_FREE\_ENERGY(&SGE)**, 134  
 fluctuation theorem, 61  
 force breakup, 14  
 force field, 30, 156  
     input parameters from ASCII file, 96  
     input parameters from tpgprm file , 96  
 force field printout, 81  
**FORCE\_FIELD**, 114  
 fractional translations, 150  
 fragment  
     writing coordinates of, 83  
 free energy, 6  
**FREQUENCIES**, 142  
**FS-DAM**, 76  
 fudge factor, 109  
  
 generalized Born solvent model, 143  
**GENERATE**, 153  
 glycine, 98  
**GOFR**, 114  
 group scaling, 22, 23, 27, 144  
     Liouvillean split for, 26  
**GROUP\_CUTOFF**, 107  
  
 Hamilton  
     equations, 9, 11  
 harmonic constraints, 99, 100

- on the center of mass, 101
- harmonic frequencies, 142
- HBONDS, 115
- heavy\_atoms, 118
- Hermitian operator, 12
- histogram, 115
- history file, 81, 82, 85, 113
  - auxiliary file, 82
- H-MASS, 107
- hydrogen bond, 115, 165
  - acceptor and donor, 166
- imphd, 164
- implicit solvent, 143
- improper torsion, 32, 95, 125, 164
  - definition of, in the parameter file, 160
- &INOUT, 80
- INSERT, 154
- inst\_xrms, 117
- &INTEGRATOR, 86
- integrator
  - reversible, 12
  - symplectic, 8, 11
- interchange matrix, 150
- ISEED, 141
- ISOSTRESS, 141, 142
- isothermal-isobaric ensemble, 18
- I-TORSION, 108
- jacobian, 10
- Jarzynski identity, 63
- JOIN, 94
- JORGENSEN, 108
- KEEP\_BONDS, 108
- k-ewald, 86
- leap frog algorithm, 12
- Legendre transformation, 21
- Lennard-Jones, 15, 158
  - cutoff, 37
  - parameters, 158
- Lennard-Jones potential
  - Soft-core variant for alchemical transformations, 68
- linked cell, 109, 111
- LINKED\_CELL, 109
- Liouville
  - formalism, 11
- Liouvillean, 5, 13, 38
  - split of Parrinello-Rahman-Nosé, 25
- liquid water, 40
- LJ-FUDGE, 109
- Lucy's functions, 59
- lysozyme, 94
- Markovian process, 61
- Martyna G, 5
- mass
  - of the Nosé thermostat, 146
  - specifying the type atomic, 158
- maximum likelihood, 65
- MAXRUN, 125
- MBAR, 47
- MDSIM, 144
- mean square displacement, 117
- membrane
  - simulation at constant pressure in the NPT ensemble, 142
- memory demand in ORAC, 169
- Message Passing library interface, 168
- &META, 89
- metadynamics, 7, 57, 89
  - Gaussian and Lucy's function, 59
  - multiple walkers, 7
  - well-tempered metadynamics, 60
- minimization
  - with dielectric continuum, 143
- MINIMIZE, 143
- mixing rules, 157
- molecular scaling, 27, 28, 144
  - Liouvillean split for, 26
- MPI, 168
- MTS\_RESPA, 86
- multiple Bennett acceptance ratio, 47
- multiple restarts in parallel simulation, 84
- multiple time steps, 5, 29
  - for Parrinello-Rahman-Nosé Hamiltonian, 20
- neighbor list, 109, 111
  - for hydrogen bonds, 115
  - setting work arrays dimensions, 170
- non bonded potential
  - subdivision of, 37
- non-bonded potential, 30
- Nosé thermostat, 20, 146
- no\_step, 143
- NPT ensemble, 19, 146
- NPT simulation, 142
- NVT ensemble, 19, 28, 84, 146
- occupy, 82
- omit\_angles, 163
- OpenMP, 168
- pair correlation function, 114
- parallel job
  - Launching multiple independent simulations, 120
- parallel version
  - compiling, 169
  - REM algorithm, 123
  - steered molecular dynamics simulations, 100

- `&PARAMETERS`, 93
- Parrinello-Rahman-Nosé Extended Lagrangian, 19, 144
- PARXXXX directories, 123, 134, 169
- PDB, 130, 131
  - generating a file, 80
  - writing the `□` file to disk, 83
- PLOT, 83
- PLOT\_FRAGMENT, 113
- PMF, 61
- position Verlet, 12
- potential
  - bending, 31
  - bonded, 30
  - non-bonded, 30
  - of mean force, 61
  - stretching, 30
  - subdivision of, 12
- `&POTENTIAL`, 99
- potential of mean force
  - determination of via the Crooks theorem, 64
- potential subdivision, 30, 38
  - for the AMBER force field, 33, 38
- pressure
  - control for membrane simulation, 142
  - simulation with isotropic and anisotropic stress tensor, 19, 142
- PRESSURE
  - parameter in the `config.h` file, 170
- PRINT\_ENERGY
  - replica exchange method, 121
- PRINT, 125
  - replica exchange method, 121
- print
  - for harmonic calculations, 143
- print, 115
- PRINT\_DIAGNOSTIC
  - replica exchange method, 121
- PRINT\_DIPOLE, 116
- print\_histo, 115
- printing the force field parameters, 81, 124
- printing topology information, 124
- PRINT\_ACCEPTANCE\_RATIO(&SGE), 135
- PRINT\_WHAM(&SGE), 135
- PRINT\_TOPOLOGY, 95
- propagator, 11
  - discrete time, 11
  - stepwise, 11
- proper torsion, 31, 95, 125
  - definition of, in the parameter file, 159
  - frequency range, 33
- `&PROPERTIES`, 113
- PROPERTY, 126
- protein
  - printing out the sequence, 95
  - giving the input sequence in ORAC, 94
- `p_test`, 87
- QQ-FUDGE, 110
- r-RESPA, 15
  - energy conservation, 16
  - for NPT ensemble, 25
  - input examples, 87
  - performances, 16
  - use in ORAC, 86
  - with Parrinello-Rahman-Nosé Hamiltonian, 20
- `radial_cutoff`, 115
- radial distribution function, 113
- RATE, 90
- RATTLE, 15
- reaction coordinate, 7, 61
- reaction field, 5
- READ, 90
- READ\_CO, 131
- reading the restart file, 84, 124
- READ\_PDB, 130
- READ\_PRM\_ASCII, 96
- READ\_SOLVENT, 154
- READ\_TPG\_ASCII, 97
- READ\_TPGPRM, 96
- reciprocal lattice, 37
- reciprocal lattice potential, 34
- REDEFINE, 154
- reference system, 12, 37
- REJECT, 126
- `&REM`, 120
- REM\_DIAGNOSTIC, 121
- replica exchange method, 40, 49, 120–122
  - Hamiltonian REM, 44
  - local scaling and global scaling, 123
  - temperature REM, 42
- REPLICATE, 130
- REPL\_RESIDUE, 97
- RESET\_CM, 130
- RESIDUE, 161
- residue, 97, 161
  - definition of, in the `tpg` file, 161
  - sequence, 94
- residue, 115
- residue sequence, 124
- RESTART, 84, 124
- restart file, 84, 124, 129
  - parallel simulation, 84
- restricted canonical transformation, 9
- reversible integrator, 12
- rigid, 162
- root mean square displacement, 115, 116, 133, 149
- `&RUN`, 124
- Ryckaert J.-P., 24

- SAVE, 91
- saving coordinates to disk, 82
- SCALE, 144
- SCALING, 144
- SCALE\_CHARGES, 149
- scaling
  - equivalence of atomic and group, 23
- SD, 143
- SEGMENT, 122
- SEGMENT(&SGE), 135
- SELECT\_DIHEDRAL, 110
- Serial Generalized Ensemble simulations, 49
  - BAR-SGE method, 52, 54, 56
  - General theory, 50
  - Input of (see also &SGE), 134
  - Simulated tempering, 51
  - Simulations in collective coordinate space, 52
- SETUP(&REM)
  - replica exchange method, 122
- &SETUP, 129
- SETUP(&SGE), 136
- &SGE, 134
  - FIX\_FREE\_ENERGY, 134
  - PRINT\_ACCEPTANCE\_RATIO, 135
  - PRINT\_WHAM, 135
  - SEGMENT, 135
  - SETUP, 136
  - STEP, 138
  - TRANSITION\_SCHEME, 138
  - ZERO\_FREE\_ENERGY, 139
- Description of the method (see also Serial Generalized Ensemble simulations), 134
- SHAKE, 5, 15, 104
- Simulated tempering (see also Serial Generalized Ensemble simulations), 49
- &SIMULATION, 140
- simulation box, 129
- smooth particle mesh Ewald (see also SPME), 35
- Soft-core Lennard-Jones potential, 68
- solute
  - defining a fragment of, 113
  - input examples, 131
  - input topology from ASCII file, 97
  - input topology from tpgprm file, 96
  - inserting in solvent, 154
  - pair correlation function, 114
  - setting up the unit cell, 148
  - topology, 129
  - total charge, 149
- SOLUTE, 131
- &SOLUTE, 148
- solute
  - thermostatting solute atoms, 146
- solvent
  - thermostatting solvent atoms, 146
- solute tempering, 122
- SOLVENT, 131
- solvent
  - generating the coordinates, 148, 153, 154
  - input examples, 131
  - reading the coordinates of, 152, 154
  - setting up the unit cell, 153
- &SOLVENT, 152
- space group, 130, 148, 150
- SPACE\_GROUP, 150
- spherical cutoff, 37
- SPME, 6, 33, 35, 107
  - accuracy, 36
  - B-spline interpolation, 35
  - in multiple time scales integrators, 86
  - memory demand, 36
  - performances, 36
  - setting work arrays dimensions., 170
- START, 79
- STOP, 79
- steepest descent, 143
- STEER, 126
- steered molecular dynamics, 8, 61
  - adding a time dependent bending, 100, 101
  - adding a time dependent stretching, 99
  - adding a time dependent torsion, 102
  - along a curvilinear coordinate, 110
  - printing out the work, 84
  - restart, 127
  - thermal changes, 84
- STEER\_PATH, 110
- step, 86
- STEP(&REM), 123
- STEP(&SGE), 138
- s\_test, 87
- STRESS, 145
- stress tensor, 19, 142
- stretching, 157
  - printing out, 95
- STRETCHING
  - for the solute, 111
- stretching potential, 30, 124
- structure factor, 35, 113, 114, 117
- structured commands
  - definition of, 77
- STRUCTURES, 116
- VORONOI, 118
- symplectic
  - building integrators, 11
  - condition, 12
  - condition for canonical transformations, 10
  - integrators, 8
  - notation of the equations of motion, 9
- TEMPERATURE, 145

- temperature scaling
  - with Nosé thermostats, 146
- TEMPERED, 91
- TEMPLATE, 132
- termatom, 165
- test-times, 87
- thermal changes, 127
- thermal work, 127
- thermalization, 128
- THERMOS, 146
- thermostat, 20, 146
  - Andersen, 140
  - Bussi, 141
  - Nosé-Hoover, 146
- TIME, 128
- time dependent bending, 100, 101
- time dependent stretching, 99
- time dependent torsion, 102
- TIME\_CORRELATIONS, 117
- TIMESTEP, 88
- topology, 97, 156, 160
  - adding extra topology, 93
  - from ASCII file, 97
  - from tpgprm file, 96
  - printing, 95
- torsion
  - definition of dihedral angle, 160
  - improper, 164
  - TORSION IMPROPER, 160
  - printing out, 95
  - proper, 159
- torsional potential, 16, 31, 124
- TORSION IMPROPER, 159
- TORSION PROPER, 159
- total, 115
- TRAJECTORY, 85
- trajectory file, 79, 81, 82, 113
  - auxiliary file, 82
- TRANSITION\_SCHEME(&SGE), 138
- Trotter formula, 11
- Tuckerman M., 5
- unit cell, 148, 153
  - replicating along selected directions, 130, 148, 153
- unitary transformation, 12
- UPDATE, 111
- use\_neighbor, 114
- use\_neighbors
  - for hydrogen bonds, 115
- vacf, 118
- valine, 161
- velocity
  - rescaling, 144
- velocity autocorrelation function, 113, 117
- velocity Verlet, 12
- Verlet
  - neighbor list, 111
- VERLET\_LIST, 111
- very\_cold\_start, 87
- virtual variables, 21
- Volume calculation, 118
- Voronoi, 28
- Voronoi Polihedra, 118
- Wang-Landau algorithm, 57
- water, 28
  - properties of, 40
- work
  - in a SMD simulation, 84
  - in alchemical tranformation, 72
- write, 82
- WRITE\_GRADIENT, 143
- WRITE\_GYR, 119
- WRITE\_PRESSURE, 147
- WRITE\_TPGPRM\_BIN, 98
- WTEMPERED, 91
- Xmol animation, 113
- X\_RMS, 149
- xyz format, 83
- ZERO\_FREE\_ENERGY(&SGE), 139

# Bibliography

- [1] Robert B. Sandberg, Martina Banchelli, Carlo Guardiani, Stefano Menichetti, Gabriella Caminati, and Piero Procacci. Efficient nonequilibrium method for binding free energy calculations in molecular dynamics simulations. *Journal of Chemical Theory and Computation*, 11(2):423–435, 2015.
- [2] P. Procacci, T. Darden, E. Paci, and M. Marchi. *J. Comput. Chem.*, 18:1848, 1997.
- [3] S. J. Wiener, P. A. Kollmann, D. T. Nguyen, and D. A. Case. *J. Comput. Chem.*, 7:230, 1986.
- [4] W. D. Cornell, P. Cieplak, C. I. Bavy, I. R. Gould, K. M. Merz Jr., D. M. Ferguson, D. C. Spellmeyer, T. Fox, J. W. Caldwell, and P. Kollmann. *J. Am. Chem. Soc.*, 117:5179, 1995.
- [5] B. R. Brooks, R. E. Bruccoleri, B. D. Olafson, D.J. States, S. Swaminathan, and M. Karplus. *J. Comput. Chem.*, 4:187, 1983.
- [6] W.F. van Gunsteren and H. J. C. Berendsen. *Groningen Molecular Simulation (GROMOS) Library Manual*. Biomos, Groningen, 1987.
- [7] A. D. MacKerrel, J. Wirkiwicz-Kuczera, and M. Karplus. *J. Am. Chem. Soc.*, 117:11946, 1995.
- [8] J. J. Pavelites, P. A. Gao, and A. D. MacKerrel. *Biophysical J.*, 18:221, 1997.
- [9] A. D. MacKerell Jr., D. Bashford, M. Bellott, R. L. Dunbrack, J. D. Evanseck, M. J. Field, S. Fischer, J. Gao, H. Guo, S. Ha, D. Joseph-McCarthy, L. Kuchnir, K. Kuczera, F. T. K. Lau, C. Mattos, S. Michnick T., Ngo, D. T. Nguyen, B. Prodhom, W. E. Reiher III, B. Roux, M. Schlenkrich, J. C. Smith, R. Stote, J. Straub, M. Watanabe, J. Wierkiewicz-Kuczera, D. Yin, and M. Karplus. *J. Phys. Chem. B*, 102:3586, 1998.
- [10] J. P. Ryckaert, G. Ciccotti, and H. J. C Berendsen. *J. Comput. Phys.*, 23:327, 1977.
- [11] G. Ciccotti and J. P. Ryckaert. *Comp. Phys. Report*, 4:345, 1986.
- [12] M. P. Allen and D. J. Tildesley. *Computer Simulation of Liquids*. Oxford University Press, Walton Street, Oxford OX2 6DP, 1989.
- [13] P. Procacci, T. Darden, and M. Marchi. *J. Phys. Chem*, 100:10464, 1996.
- [14] W. B. Street, D.J. Tildesley, and G. Saville. *Mol. Phys.*, 35:639, 1978.
- [15] O. Teleman and B. Joensson. *J. Comput. Chem.*, 7:58, 1986.
- [16] M. E. Tuckerman, G. J. Martyna, and B. J. Berne. *J. Chem. Phys.*, 94:6811, 1991.
- [17] M. E. Tuckerman and B. J. Berne. *J. Chem. Phys.*, 95:8362, 1991.
- [18] M. E. Tuckerman, B. J. Berne, and A. Rossi. *J. Chem. Phys.*, 94:1465, 1990.
- [19] H. Grubmüller, H. Heller, A. Winemuth, and K. Schulten. *Mol. Simul.*, 6:121, 1991.
- [20] M. E. Tuckerman, B.J. Berne, and G.J. Martyna. *J. Chem. Phys.*, 97:1990, 1992.
- [21] M. E. Tuckerman, B. J. Berne, and G. J. Martyna. *J. Chem. Phys.*, 99:2278, 1993.



- [22] D. D. Humphreys, R. A. Friesner, and B. J. Berne. *J. Phys. Chem.*, 98:6885, 1994.
- [23] P. Procacci and B. J. Berne. *J. Chem. Phys.*, 101:2421, 1994.
- [24] P. Procacci and M. Marchi. *J. Chem. Phys.*, 104:3003, 1996.
- [25] G. J. Martyna, M. E. Tuckerman, D. J. Tobias, and M. L. Klein. *Mol. Phys.*, 87:1117, 1996.
- [26] P. Procacci and B. J. Berne. *Mol. Phys.*, 83:255, 1994.
- [27] M. Marchi and P. Procacci. *J. Chem. Phys.*, 109:5194, 1998.
- [28] M. Saito. *J. Chem. Phys.*, 101:4055, 1994.
- [29] H. Lee, T. A. Darden, and L. G. Pedersen. *J. Chem. Phys.*, 102:3830, 1995.
- [30] J. A. Barker and R. O. Watts. *Mol. Phys.*, 26:789, 1973.
- [31] J. A. Barker. The problem of long-range forces in the computer simulation of condensed matter. volume 9, page 45. NRCC Workshop Proceedings, 1980.
- [32] P. Ewald. *Ann. Phys.*, 64:253, 1921.
- [33] S.W. deLeeuw, J. W. Perram, and E. R. Smith. *Proc. R. Soc. London A*, 373:27, 1980.
- [34] T. Darden, D. York, and L. Pedersen. *J. Chem. Phys.*, 98:10089, 1993.
- [35] U. Essmann, L. Perera, M. L. Berkowitz, T. Darden, H. Lee, and L. G. Pedersen. *J. Chem. Phys.*, 101:8577, 1995.
- [36] R. W. Hockney. *Computer Simulation Using Particles*. McGraw-Hill, New York, 1989.
- [37] H.G. Petersen, D. Soelvanson, and J. W. Perram. *J. Chem. Phys.*, 101:8870, 1994.
- [38] L. Greengard and V. Rokhlin. *J. Comput. Phys.*, 73:325, 1987.
- [39] J. Shimada, H. Kaneko, and T. Takada. *J. Comput. Chem.*, 15:28, 1994.
- [40] R. Zhou and B. J. Berne. *J. Chem. Phys.*, 103:9444, 1996.
- [41] Y. Duan and P. A. Kollman. Pathways to a protein folding intermediate observed in a 1-microsecond simulation in aqueous solution. *Science*, 282:740–744, 1998.
- [42] R. H. Swendsen and J. S. Wang. *Phys. Rev. Lett.*, 57:2607, 1986.
- [43] C. G. Geyer. in *Computing Science and Statistics, Proceedings of the 23rd Symposium on the Interface*, edited by E. M. Keramidis, page 156, 1991.
- [44] E. Marinari and G. Parisi. *Europhys. Lett.*, 19:451, 1992.
- [45] K. Hukushima and K. Nemoto. *J. Phys. Soc. Jpn.*, 65:1604, 1996.
- [46] Y. Okamoto. *J. Mol. Graphics Modell.*, 22:425, 2004.
- [47] A. P. Lyubartsev, A. A. Martsinovski, S. V. Shevkunov, and P. N. Vorontsov-Velyaminov. *J. Chem. Phys.*, 96:1776, 1992.
- [48] S. Rauscher, C. Neale, and R. Pomès. *J. Chem. Theory Comput.*, 5:2640, 2009.
- [49] S. Park. *Phys. Rev. E*, 77:016709, 2008.
- [50] C. Zhang and J. Ma. *J. Chem. Phys.*, 129:134112, 2008.
- [51] J. G. Kirkwood. *J. Chem. Phys.*, 3:300, 1935.
- [52] D. A. McQuarrie. *Statistical Mechanics*. HarperCollinsPublishers, New York, USA, 1976.

- [53] S. Kumar, D. Bouzida, R. H. Swendsen, P. A. Kollman, and J. M. Rosenberg. *J. Comput. Chem.*, 13:1011, 1992.
- [54] A. M. Ferrenberg and R. H. Swendsen. *Phys. Rev. Lett.*, 63:1195, 1989.
- [55] C. J. Woods, J. W. Essex, and M. A. King. *J. Phys. Chem. B*, 107:13703, 2003.
- [56] R. Chelli. *J. Chem. Theory. Comput.*, 6:1935, 2010.
- [57] G. M. Torrie and J. P. Valleau. *Chem. Phys. Lett.*, 28:578–581, 1974.
- [58] A. Laio and M. Parrinello. Escaping free-energy minima. *Proc. Natl. Acad. Sci. USA*, 99:12562–12566, 2002.
- [59] S. Marsili, A. Barducci, R. Chelli, P. Proccaci, and V. Schettino. *J. Phys. Chem. B*, 110:14011–14014, 2006.
- [60] F. Wang and D. P. Landau. *Phys. Rev. Lett.*, 86:2050–2053, 2001.
- [61] J. Henin and C. Chipot. *J. Chem. Phys.*, 121:2904–2914, 2004.
- [62] A. Laio, A. Rodriguez-Forte, F. L. Gervasio, M. Ceccarelli, and M. Parrinello. Assessing the accuracy of metadynamics. *J. Phys. Chem. B*, 109:6714–6721, 2005.
- [63] C. Jarzynski. Nonequilibrium equality for free energy differences. *Phys. Rev. Lett.*, 78:2690–2693, 1997.
- [64] G. E. Crooks. *J. Stat. Phys.*, 90:1481–1487, 1998.
- [65] G. Hummer and A. Szabo. *Proc. Natl. Acad. Sci. USA*, 98:3658–3661, 2001.
- [66] M. R. Shirts, E. Bair, G. Hooker, and V. S. Pande. *Phys. Rev. Lett.*, 91:140601, 2003.
- [67] D. Chandler. *Introduction to Modern Statistical Mechanics*. Oxford University Press, 1987.
- [68] J. M. Sanz-Serna. *Acta Numerica*, 1:243, 1992.
- [69] S. K. Grey, D. W. Noid, and B. G. Sumpter. *J. Chem. Phys.*, 101:4062, 1994.
- [70] J. J. Biesiadecki and R. D. Skeel. *J. Comp. Physics.*, 109:318, 1993.
- [71] P. J. Channel and C. Scovel. *Nonlinearity*, 3:231, 1990.
- [72] H. Goldstein. *Classical Mechanics*. Addison-Wesley, Reading MA, 1980.
- [73] V. I. Arnold. *Mathematical Methods of Classical Mechanics*. Springer-Verlag, Berlin, 1989.
- [74] H. F. Trotter. *Proc. Am. Math Soc.*, 10:545, 1959.
- [75] H. de Raedt and B. De Raedt. *Phys. Rev. A*, 28:3575, 1983.
- [76] H. Yoshida. *Phys. Letters A*, 150:262, 1990.
- [77] S. J. Toxvaerd. *J. Chem. Phys.*, 87:6140, 1987.
- [78] H.C Andersen. *J. Comput. Phys.*, 52:24, 1983.
- [79] M. E. Tuckerman and M. Parrinello. *J. Chem. Phys.*, 101:1302, 1994.
- [80] S. Nose and M. L. Klein. *Mol. Phys.*, 50:1055, 1983.
- [81] G. Herzberg. *Spectra of Diatomic Molecules*. Van Nostrand, New York, 1950.
- [82] M. Watanabe and M. Karplus. *J. Phys. Chem.*, 99:5680, 1995.
- [83] J. K. Kjems and G. Dolling. *Phys. Rev. B*, 11:16397, 1975.

- [84] F. D. Medina and W. B. Daniels. *J. Chem. Phys.*, 64:150, 1976.
- [85] G. Cardini and V. Schettino. *Chem. Phys.*, 146:147, 1990.
- [86] D. Frenkel and B. Smit. *Understanding Molecular Simulations*. Academic Press, San Diego, 1996.
- [87] D. C. Rapaport. *The Art of Molecular Dynamics Simulation*. Cambridge University Press, Cambridge (UK), 1995.
- [88] S. Nosé. In M. Meyer and V. Pontikis, editors, *Computer Simulation in Materials Science*, page 21. Kluwer Academic Publishers, 1991.
- [89] S. Nosé. *Prog. Theor. Phys. Supp.*, 103:1, 1991.
- [90] M. Ferrario. In M.P.Allen and D.J.Tildesley, editors, *Computer Simulation in Chemical Physics*, page 153. Kluwer Academic Publishers, 1993.
- [91] G. J. Martyna, D. J. Tobias, and M. L. Klein. *J. Chem. Phys.*, 101:4177, 1994.
- [92] H. C. Andersen. *J. Chem. Phys.*, 72:2384, 1980.
- [93] M. Parrinello and A. Rahman. *Phys. Rev. Letters*, 45:1196, 1980.
- [94] S. Nose. *Mol. Phys.*, 52:255, 1984.
- [95] M. Ferrario and J.-P. Ryckaert. *Mol. Phys.*, 78:7368, 1985.
- [96] M. E. Tuckerman, C. J. Mundy, and M. L. Klein. *Phys. Rev. Letters*, 78:2042, 1997.
- [97] S. Melchionna, G. Ciccotti, and B. L. Holian. *Mol. Phys.*, 78:533, 1993.
- [98] H.J.C.Berendsen. Lectures notes unpublished; reported by G. Ciccotti and J.P. Ryckaert, Comp. Physics Report 4 (1986) 345, 1986.
- [99] E. Paci and M. Marchi. *J. Phys. Chem.*, 104:3003, 1996.
- [100] S. Toxvaerd. *Phys. Rev. B.*, 47:343, 1993.
- [101] J.-P. Hansen. Molecular-dynamics simulation of coulomb systems in two and three dimensions. In *Molecular Dynamics Simulation of Statistical-Mechanics Systems*, Proceedings of the International School of Physics "Enrico Fermi". North Holland Physics, 1986.
- [102] H.G. Petersen. *J. Chem. Phys.*, 103:3668, 1995.
- [103] S. J. Stuart, R. Zhou, and B. J. Berne. *J. Chem. Phys.*, 105:1426, 1996.
- [104] P. Procacci, M. Marchi, and G. J. Martyna. *J. Chem. Phys.*, 108:8799, 1998.
- [105] A. Rahman and F. H. Stillinger. *J. Chem. Phys.*, 55:3336, 1971.
- [106] P. Liu, B. Kim., R. A. Friesner, and B. J. Berne. *Proc. Acad. Sci.*, 102:13749–13754, 2005.
- [107] M. R. Shirts and J. D. Chodera. *J. Chem. Phys.*, 129:124105, 2008.
- [108] U. H. E. Hansmann and Y. Okamoto. *J. Comput. Chem.*, 18:920, 1997.
- [109] A. Irbäck and F. Potthast. *J. Chem. Phys.*, 103:10298, 1995.
- [110] A. Mitsutake and Y. Okamoto. *Chem. Phys. Lett.*, 332:131, 2000.
- [111] S. Park and V. S. Pande. *Phys. Rev. E*, 76:016703, 2007.
- [112] X. Huang, G. R. Bowman, and V. S. Pande. *J. Chem. Phys.*, 128:205106, 2008.
- [113] C. Zhang and J. Ma. *Phys. Rev. E*, 76:036708, 2007.

- [114] R. Denschlag, M. Lingenheil, P. Tavan, and G. Mathias. *J. Chem. Theory Comput.*, 5:2847, 2009.
- [115] S. Park, D. L. Ensign, and V. S. Pande. *Phys. Rev. E*, 74:066703, 2006.
- [116] R. Chelli, S. Marsili, A. Barducci, and P. Procacci. *Phys. Rev. E*, 75:050101, 2007.
- [117] R. Chelli. *J. Chem. Phys.*, 130:054102, 2009.
- [118] C. H. Bennett. *J. Comp. Phys.*, 22:245, 1976.
- [119] R. W. Zwanzig. *J. Chem. Phys.*, 22:1420, 1954.
- [120] A. Mitsutake and Y. Okamoto. *J. Chem. Phys.*, 130:214105, 2009.
- [121] W. G. Hoover. *Phys. Rev. A*, 31:1695, 1985.
- [122] W. G. Hoover. *Phys. Rev. A*, 34:2499, 1986.
- [123] G.L. Martyna, M.L. Klein, and M. E. Tuckerman. *J. Chem. Phys.*, 97:2635, 1992.
- [124] Y. Sugita and Y. Okamoto. *Chem. Phys. Lett.*, 314:141, 1999.
- [125] D. D. Minh and A. B. Adib. *Phys. Rev. Lett.*, 100:180602, 2008.
- [126] P. Nicolini, P. Procacci, and R. Chelli. *J. Phys. Chem. B*, 114:9546, 2010.
- [127] S. R. Williams, D. J. Searles, and D. J. Evans. *Phys. Rev. Lett.*, 100:250601, 2008.
- [128] J. Gore, F. Ritort, and C. Bustamante. *Proc. Natl. Acad. Sci. USA*, 100:12564, 2003.
- [129] G. Cowan. *Statistical data analysis*. Oxford University Press, 1998.
- [130] M. Mezei. *J. Comput. Phys.*, 68:237, 1987.
- [131] G. H. Paine and H. A. Scheraga. *Biopolymers*, 24:1391, 1985.
- [132] T. Huber, A. E. Torda, and W. F. van Gunsteren. *J. Comput.-Aided Mol. Des.*, 8:695, 1994.
- [133] S. Marsili, A. Barducci, R. Chelli, P. Procacci, and V. Schettino. *J. Phys. Chem. B*, 110:14011, 2006.
- [134] M. Watanabe and W. P. Reinhardt. *Phys. Rev. Lett*, 65:3301, 1990.
- [135] N. G. Van Kampen. *Stochastic Processes in Physics and Chemistry*. North-Holland, 1992.
- [136] M. Iannuzzi, A. Laio, and M. Parrinello. *Phys. Rev. Lett.*, 90:238302, 2003.
- [137] V. Babin, C. Roland, T. A. Darden, and C. Sagui. *J. Chem. Phys.*, 125:204909, 2006.
- [138] L. B. Lucy. *Astronom. J.*, 82:1013, 1977.
- [139] W. G. Hoover. and C. G. Hoover. *Phys. Rev. E*, 73:016702, 2006.
- [140] D. J. Earl and M. W. Deem. *J. Phys. Chem. B*, 109:6701, 2005.
- [141] C. Zhou and R. N. Bhatt. *Phys. Rev. E*, 72:0205701(R), 2005.
- [142] R. E. Belardinelli and V. D. Pereira. *Phys. Rev. E*, 75:046701, 2007.
- [143] A. Barducci, G. Bussi, and M. Parrinello. *Phys. Rev. Lett.*, 100:020603, 2008.
- [144] P. Raiteri, F. L. Gervasio, C. Micheletti, and M. Parrinello. *J. Phys. Chem. B*, 110:3533, 2006.
- [145] B. Isralewitz, M. Gao, and K. Schulten. *Curr. Op. Struct. Biol.*, 11:224–230, 2001.
- [146] D. J. Evans and D. J. Searls. *Phys. Rev. E*, 50:1645–1648, 1994.
- [147] M. Sprik and G. Ciccotti. *J. Chem. Phys.*, 109:7737–7744, 1998.

- [148] S. Park and K. Schulten. *J. Chem. Phys.*, 120:5946–5961, 2004.
- [149] R. H. Wood and W. C. F. Muehlbauer. *J. Phys. Chem.*, 95:6670–6675, 1991.
- [150] R. Chelli and P. Procacci. *Phys. Chem. Chem. Phys.*, 11:1152–1158, 2009.
- [151] M.R. Shirts and V.S. Pande. Solvation free energies of amino acid side chain analogs for common molecular mechanics water models. *J. Chem. Phys.*, page 134508, 2005.
- [152] M.R. Shirts, J.W. Pitner, W.C. Swope, and V.S. Pande. Extremely precise free energy calculations of amino acid side chain analogs: Comparison of common molecular mechanics force fields for proteins. *J. Chem. Phys.*, 119:5740–5761, 2003.
- [153] In the formulation of Eq. 9.1, we have implicitly assumed the so-called ”tin-foil” boundary conditions: the Ewald sphere is immersed in a perfectly conducting medium and hence the dipole term on the surface of the Ewald sphere is zero [S.W. deLeeuw, J. W. Perram, and E. R. Smith. *Proc. R. Soc. London A*, 373:27, 1980].
- [154] See for example the GROMACS manual and the tutorial for alchemical calculations: *Hands-on tutorial Solvation free energy of ethanol* available at <http://www.gromacs.org>. For NAMD, See the tutorial: *In silico alchemy: A tutorial for alchemical free-energy perturbation calculations with NAMD* available at <http://www.ks.uiuc.edu>.
- [155] P. Procacci, S. Marsili, A. Barducci, G. F. Signorini, and R. Chelli. *J. Chem. Phys.*, 125:164101, 2006.
- [156] Lingle Wang, Yujie Wu, Yuqing Deng, Byungchan Kim, Levi Pierce, Goran Krilov, Dmitry Lupyan, Shaughnessy Robinson, Markus K. Dahlgren, Jeremy Greenwood, Donna L. Romero, Craig Masse, Jennifer L. Knight, Thomas Steinbrecher, Thijs Beuming, Wolfgang Damm, Ed Harder, Woody Sherman, Mark Brewer, Ron Wester, Mark Murcko, Leah Frye, Ramy Farid, Teng Lin, David L. Mobley, William L. Jorgensen, Bruce J. Berne, Richard A. Friesner, and Robert Abel. Accurate and reliable prediction of relative ligand binding potency in prospective drug discovery by way of a modern free-energy calculation protocol and force field. *Journal of the American Chemical Society*, 137(7):2695–2703, 2015.
- [157] Piero Procacci. Unbiased free energy estimates in fast nonequilibrium transformations using gaussian mixtures. *The Journal of Chemical Physics*, 142(15):154117, 2015.
- [158] C. Broth B. Quentrec. *J. Comp. Phys*, 13:430, 1975.
- [159] M. P. Allen and D. J. Tildesley. *Computer Simulation of Liquids*. Oxford University Press, Walton Street, Oxford OX2 6DP, 1989.
- [160] R. M. Levy E. Gallicchio. Agbnp: An analytic implicit solvent model suitable for molecular dynamics simulations and high-resolution modeling. *J. Comput. Chem.*, 25:479–499, 2004.
- [161] Matteo Frigo and Steven G. Johnson. The design and implementation of FFTW3. *Proceedings of the IEEE*, 93(2):216–231, 2005. Special issue on ”Program Generation, Optimization, and Platform Adaptation”.